MODELING FRAMEWORK FOR SIMULATING HYDRODYNAMICS AND WATER QUALITY IN THE PRETTYBOY AND LOCH RAVEN RESERVOIRS, GUNPOWDER RIVER BASIN, MARYLAND

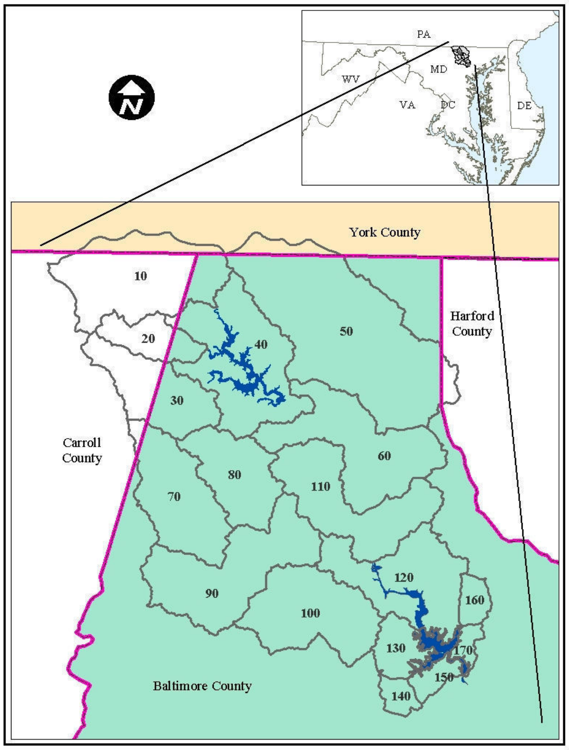

Prepared by:

Interstate Commission on the Potomac River Basin

51 Monroe Street

Suite PE-08

Rockville, MD 20850

Prepared for:

Maryland Department of the Environment

1800 Washington Boulevard, Suite 540

Baltimore, MD 21230

ICPRB Report 06-7

August 31, 2006

Acknowledgments

As explained in Section1, the project documented in this report is built upon previous work at Maryland Department of the Environment (MDE), under the direction of Angelica Gutierrez-Magness (currently U. S. Geological Survey) and the University of Virginia, under the direction of Dr. Winston Lung. Section 3 of this report borrows extensively from draft reports documenting earlier work by MDE staff, though it must be said that the responsibility for this report rests with the staff of the Interstate Commission on the Potomac River Basin (ICPRB) alone.

The project could not be completed without the guidance and direction of Mr. Tim Rule, the project officer at MDE, and Mr. Nauth Panday. The contribution of Mr. Sajan Pokharel of MDE, who collaborated with us on the technical work, was essential to our efforts.

We gratefully acknowledge the cooperation of the City of Baltimore Department of Public Works (DPW) and their constructive comments on the project. In particular we would like to thank Mr. Bill Stack, and his colleagues Mr. Robert McAuley, Mr. Eugene Scarpulla, and others who provided us with the necessary information for the project. We also would like to thank Mr. Stack and DPW's consultant, Mr. Paul Jacobson, for sharing the results of their analysis of reservoir monitoring data with us. Mr. Steve Stewart of Baltimore County Department of Environmental Protection and Resource Management (DEPRM) also provided us with essential information on the County's monitoring program and his interpretation of the results. There are probably many others who contributions to earlier phases of the project should be acknowledged but are unknown to us directly.

We would like to thank Mr. Edward Buchak and the staff of J. E. Edinger Associates (currently of Environmental Resource Management, Inc.) for their helpful instruction and general advice on using the CE-QUAL-W2 model during a workshop which ICPRB staff attended April 12-14, 2005.

We also would like to thank Mr. Gould Charshee of the Baltimore Metropolitan Council and other Reservoir Technical Group (RTG) members for providing a forum for us to present the project at critical stages to an engaged and informed audience. We appreciated the intelligent discussion and friendly criticism and hope the results of this project will be useful to the RTG in the future.

***

This report has been prepared by the staff of the Interstate Commission on the Potomac River Basin. Support was provided by the Maryland Department of the Environment. The opinions expressed are those of the authors and should not be construed as representing the opinions or policies of the United States or any of its agencies, the several states, or the Commissioners of the Interstate Commission on the Potomac River Basin.

TABLE OF CONTENTS

EXECUTIVE SUMMARY ... xii
E.1. Introduction ... xii
E.2. Water Quality Analysis ... xiii
E.3. The Gunpowder Falls HSPF Model ... xiv
E.4. Prettyboy and Loch Raven Reservoir CE-QUAL-W2 Models ... xx
E.5. Sensitivity of Reservoir Models to Loading Rates ... xxv
E.6. Summary ... xxx
Section 1. **INTRODUCTION** ... 1
1.1. INTRODUCTION ... 1
Section 2. DESCRIPTION OF THE GUNPOWDER WATERSHED 4
2.1. BASIN CHARACTERISTICS ... 5
2.2. CLIMATE ... 6
2.3. GEOLOGY, TOPOGRAPHY AND SOILS ... 7
Section 3. **MODEL DESCRIPTION AND STRUCTURE OF THE GUNPOWDER WATERSHED** 10
3.1. INTRODUCTION ... 10
3.2. OVERVIEW OF THE HYDROLOGIC SIMULATION PROGRAM FORTRAN (HSPF) ... 10
3.3. MODEL ASSUMPTIONS ... 11
3.4. WATERSHED SEGMENTATION ... 12
3.5. LAND USE ... 13
3.5.1. Developed Land ... 14
3.5.2. Undeveloped Land ... 14
3.5.3. Agricultural Land ... 16
3.6. NON-POINT SOURCES INFORMATION ... 20
3.6.1. Animal Counts ... 21
3.6.2. Manure Acres ... 21
3.6.3. Nutrient Applications ... 22
3.6.4. Atmospheric Deposition ... 25
3.6.5. Septic Information ... 26
3.7. POINT SOURCES ... 27
3.8. METEOROLOGIC INFORMATION AND CALIBRATION DATA ... 31
3.8.1. Meteorologic Data ... 31
3.8.2. Calibration Data ... 31
Section 4. **HSPF MODEL CALIBRATION/VERIFICATION IN THE GUNPOWDER WATERSHED** ... 36
4.1. INTRODUCTION ... 36
4.2. HYDROLOGY CALIBRATION ... 36
4.3. TEMPERATURE CALIBRATION ... 42
4.4. CALIBRATION TARGETS FOR THE SEDIMENT AND NUTRIENT CALIBRATIONS ... 43
4.4.1. ESTIMATOR and Monthly Load Calibration Targets ... 43
4.4.2. Edge-of-Field and Edge-of-Stream Calibration Targets ... 45
4.5. IMPLEMENTATION OF SEDIMENT AND NUTRIENT DYNAMICS IN THE GUNPOWDER WATERSHED HSPF MODEL ... 49
4.6. SEDIMENT CALIBRATION ... 52
4.7. NUTRIENT CALIBRATION ... 56
4.7.1. Edge of Stream (EOS) Nutrient Loads ... 56
4.7.2. Calibration of In-stream Nutrient Processes ... 58
4.7.3. Calibration Results ... 59
4.8. DIRECT COMPARISON OF OBSERVED AND SIMULATED CONCENTRATIONS ... 67
4.9. LOADINGS TO THE PRETTYBOY AND LOCH RAVEN RESERVOIRS ... 70
4.9.1. Comparison of Gunpowder Falls HSPF Model Loads To Other Load Estimates ... 70
Section 5. **WATER QUALITY SIMULATION OF PRETTYBOY AND LOCH RAVEN RESERVOIRS** ... 79

5.1. WATER QUALITY MONITORING DATA AND ANALYSIS ... 79
5.1.1. The Application of Water Quality Standards to Stratified Reservoirs ... 79
5.1.2. Baltimore City DPW Monitoring Program ... 82
5.1.3. Temperature Stratification ... 86
5.1.4. Dissolved Oxygen ... 87
5.1.5. Total Phosphorus ... 93
5.1.6. Ammonia and Nitrate ... 95
5.1.7. Secchi Depth ... 96
5.1.8. Algae and Chlorophyll a ... 99
5.1.9. Trophic Indices ... 104
5.1.10. Sedimentation ... 104
5.2. OVERVIEW OF THE CE-QUAL-W2 MODEL ... 105
5.3. IMPLEMENTATION OF THE CE-QUAL-W2 MODEL FOR PRETTYBOY AND LOCH RAVEN RESERVOIRS ... 110
5.3.1. Segmentation and Model Cell Properties ... 110
5.3.2. Inflows, Meteorological Data and Boundary Conditions ... 119
5.3.3. Configuration of Water Quality Constituents ... 119
5.4. WATER BALANCE CALIBRATION ... 122
5.5. TEMPERATURE CALIBRATION ... 124
5.6. Water Quality Calibration ... 127
5.6.1. Calibration of Total Phosphorus Concentrations ... 127
5.6.2. Simulation of Algae and Chlorophyll a ... 140
5.6.3. Simulation of Dissolved Oxygen ... 151
5.6.4. Simulation of Ammonia and Nitrate ... 163
Section 6. LOAD REDUCTION SCENARIOS AND SENSITIVITY ANALYSIS ... 176
6.1. Scenario Descriptions ... 177
6.1.1. TMDL Scenario ... 177
6.1.2. All Forest Scenario ... 177
6.1.3. Comparison of Scenario Loading Rates ... 177
6.2. Criteria Tests ... 178
6.2.1. Chlorophyll Tests ... 178
6.2.2. Dissolved Oxygen Tests ... 179
6.3. Response of Chlorophyll Concentrations to Reductions in Phosphorus Loads ... 183
6.4. The Response of DO Concentrations to Load Reductions ... 187
6.4.1. The Response of Simulated Bottom DO Concentrations to Load Reductions ... 187
6.4.2. The Response of Simulated Surface DO Concentrations to Load Reductions ... 194
Section 7. CONCLUSIONS AND RECOMMENDATIONS ... 199
7.1. Summary and Conclusions ... 199
7.2. Recommendations ... 200
7.2.1. Additional Monitoring Data ... 200
7.2.2. Enhancements to the Simulation of Sediment Diagenesis ... 201
REFERENCES ... 203
LIST OF ABBREVIATIONS 206

TABLES

Table E-1. Hydrology Calibration Stations and Associated Active USGS Gages ... xvii
Table E-2. Hydrology Calibration Results ... xvii
Table E-3. Average Annual Loads by Segment (tons/yr) ... xix
Table 1.1-1. Reservoir and Dam Characteristics ... 4
Table 1.1-2. Water Quality Impairments in Prettyboy and Loch Raven Reservoirs ... 4
Table 2.1-1. Distribution of Watershed Area By County (in square miles) ... 5
Table 2.2-1. Summary Statistics Meteorological Data Baltimore-Washington International Airport, 1971 – 2000 ... 7
Table 2.2-2. Summary Statistics Meteorological Data Millers 4NE, 1971 – 2000 ... 7
Table 2.3-1. Distribution of Hydrologic Soil Groups in Baltimore County Portion of Prettyboy and Loch Raven Reservoir Watersheds (DEPRM, 2000) ... 9
Table 3.5-1. Gunpowder Basin Land Use by Model Segment (in acres) ... 16
Table 3.5-2. Pervious and Impervious Developed Land by Model Segment (in acres) ... 17
Table 3.6.2-1. Constants Used to Calculate Animal Units and Confinement by Animal Type ... 22
Table 3.6.3-1. Manure Constants ... 23
Table 3.6.3-2. Runoff Losses and Volatilization Factors ... 23
Table 3.6.3-3. Mass Fractions Per Animal Type ... 23
Table 3.6.3.1-1. Manure Applications to Crops ... 25
Table 3.6.5-1. Number of Septic Systems and Nitrogen Loads (Lbs/Day) by County and Model Segment ... 27
Table 3.7-1. Municipal Point Source Facilities ... 28
Table 3.7-2. Industrial Point Source Facilities ... 28
Table 3.7-3. Annual Sediment Point Source Loads by Model Segment ... 29
Table 3.7-4. Annual Point Source Loads by Model Segment and by Constituent ... 29
Table 3.8-1. Active USGS Gages in the Gunpowder Falls Watershed above Loch Raven Reservoir . 34
Table 3.8-2. Sample Collection Period for Monitoring Programs ... 34
Table 3.8-3. Constituents Sampled by Monitoring Program ... 35
Table 3.8-4. Number of Samples Collected 1992-1997 at Major Monitoring Stations In Gunpowder Falls Watershed ... 35
Table 4.2-1. Correlation Coefficient between Flow at Little Falls and Prettyboy Reservoir Tributaries, May 2000-Septmber 2003 ... 37
Table 4.2-2. Key Hydrology Calibration Parameters ... 39
Table 4.2-3. Ratio of Cropland Parameters to Those for Other Land Uses ... 39
Table 4.2-4. Monthly Hydrology Parameters ... 40
Table 4.2-5. Coefficient of Determination for Hydrology Calibration with Alternative Precipitation Time Series ... 41
Table 4.2-6. Hydrology Calibration Parameter Values ... 41
Table 4.2-7. Hydrology Calibration Results ... 41
Table 4.2-8. Comparison of Coefficients of Determination from Original and Current Calibrations 42
Table 4.3-1. Temperature Calibration Parameters ... 42
Table 4.3-2. Temperature Calibration Parameter Results ... 42
Table 4.4-1. Coefficients of Regression Equation and Regression Statistics, Western Run ... 46
Table 4.4-2. Coefficients of Regression Equation and Regression Statistics, Beaverdam Run ... 46
Table 4.4-3. Average Annual EOF Erosion Rates by Land Use ... 47
Table 4.4-4. Sediment Delivery Ratios ... 48
Table 4.4-5. Average EMCs Derived From Maryland NPDES Stormwater Permits ... 48
Table 4.5-1. Description of HSPF Subroutines ... 49
Table 4.5-2 HSPF Subroutines Used in the HSPF Model by Land Use and Constituent ... 50
Table 4.6-1. Summary Statistics for Sediment Calibration ... 53
Table 4.7-1. Average Monthly Baseflow TP Concentrations by Segment ... 58
Table 4.7-2. Summary Statistics for Total ... 60
Table 4.7-3. Summary Statistics for Ammonia-N Calibration ... 60
Table 4.8-1. Summary Statistics Comparing Observed and Simulated Concentrations ... 68
Table 4.9-1. Average Annual Loads by Segment (ton/yr) ... 73

Table 4.9-2. Edge-of-Stream Total Phosphorus Loading Rates (lbs/ac/yr) 74
Table 4.9-3. Edge-of-Stream Sediment Loading Rates (ton/ac/yr) 75
Table 4.9-4. Edge-of-Stream Ammonia-N Loading Rates (lbs/ac/yr) 76
Table 4.9-4. Edge-of-Stream Ammonia-N Loading Rates (lbs/ac/yr) 76
Table 4.9-5. Edge-of-Stream Nitrate-N Loading Rates (lbs/ac/yr) 77
Table 4.9.1-1. Constituent Loads By Land Use, CBP Phase 4.3 Watershed Model, Segment 480 (Gwynn Falls) 78
Table 4.9.1-2. Constituent Loads From Loch Raven SWMM Model (Tetra Tech,1997) 78
Table 4.9.1-3. Average Annual Constituent Loads (lbs/ac/yr) from Loch Raven Reservoir Watershed Below Prettyboy Reservoir SWMM Model (Tetra Tech, 1997) 78
Table 4.9.1-4. Baltimore City Estimates of Average Annual Constituent Loads for Selected Watersheds. 78
Table 5.1.2-1. Characterization of Reservoir Monitoring Locations 83
Table 5.1.4-1. Observed Low Dissolved Oxygen in the Surface Layer, Loch Raven Reservoir 90
Table 5.1.4-2. Observed Low Dissolved Oxygen in the Surface Layer, Prettyboy Reservoir 91
Table 5.1.5-1. Summary Statistics for TP Concentrations in Prettyboy Reservoir, 1992-2004 93
Table 5.1.7-1. Prettyboy Reservoir Water Clarity Correlations 98
Table 5.1.7-2. Loch Raven Reservoir Water Clarity Correlations 99
Table 5.1.7-3. Secchi Depth vs. Cholorophyll a, Color and Turbidity 99
Table 5.1.8-1. Maximum Chlorophyll A Concentration (Mg/L) in Surface Layer by Month, Loch Raven Reservoir 101
Table 5.1.8-2. Maximum Chlorophyll A Concentration (Mg/L) in Surface Layer by Month, Prettyboy Reservoir 102
Table 5.1.10-1. Sedimentation Rates in Prettyboy and Loch Raven Reservoirs 105
Table 5.3.1-1. Percent of Flows and Loads from HSPF Model Segments Entering CE-QUAL-W2 Model Segments, Prettyboy Reservoir 114
Table 5.3.1-2. Percent of Flows and Loads from HSPF Model Segments Entering CE-QUAL-W2 Model Segments, Loch Raven Reservoir 114
Table 5.3.1-3. Prettyboy Reservoir Model Bathymetry 115
Table 5.1.3-4. Loch Raven Reservoir Model Bathymetry 117
Table 5.3.3-1. Water Quality State Variables in CE-QUAL-W2 and their Realization in the Gunpowder Reservoir Models 122
Table 5.5-1. Parameters Used in W2 Temperature Calibration 124
Table 5.5-2. Temperature Calibration Parameter Values, Prettyboy Reservoir 125
Table 5.5-3. Temperature Calibration Parameter Values, Loch Raven Reservoir 126
Table 5.6.1-1. Simulated Settling Rates 128
Table 5.6.1-2. Average Annual and Median TP Concentration in Loch Raven Reservoir, Compared to Average Annual Flow and Baseflow TP Concentrations in its Tributaries 129
Table 5.6.2-1. Algal Season Characteristics in Prettyboy Reservoir 142
Table 5.6.2-2. Algal Season Characteristics in Loch Raven Reservoir 142
Table 5.6.2-3. Algal Temperature Parameters in Prettyboy Reservoir 143
Table 5.6.2-4. Algal Temperature Parameters in Loch Raven Reservoir 143
Table 5.6.2-5. Maximum Chlorophyll Concentration (µg/l) by Season 144
Table 5.6.3-1. DO Calibration Parameter Values 153
Table 5.6.4-1 Average Nitrogen Species Concentration Statistics, Prettyboy Reservoir 165
Table 5.6.4-2 Average Nitrogen Species Concentration Statistics, Loch Raven Reservoir 165
Table 6.1-1. Scenario Annual Phosphorus Load (lbs/yr) By Species and Forest Scenario Percent of Calibration Load 178
Table 6.2-1 Monthly Average Daily Temperature Gradient (°C/m) Determining Relative Position of Epilimnion and Metalimnion in Prettyboy Reservoir 181
Table 6.2-2 Monthly Average Daily Temperature Gradient (°C/m) Determining Relative Position of Epilimnion and Metalimnion in Loch Raven Reservoir 182
Table 6.3-1. Scenario Summary Statistics for the Simulated Average Surface Concentrations (mg/l) of Total Phosphorus at Sampling Locations in Prettyboy and Loch Raven Reservoirs 184

FIGURES

Figure E-1. Location of Prettyboy and Loch Raven Reservoirs ... xiii
Figure E-2. Gunpowder Watershed Model Segmentation ... xv
Figure E-3. Land Use in Prettyboy Reservoir Watershed ... xvi
Figure E-4. Land Use in Loch Raven Reservoir Watershed ... xvi
Figure E-5. Percent Contribution of Sources to Total Phosphorus Loads to Prettyboy Reservoir ... xix
Figure E-6. Percent Contribution of Sources to Total Phosphorus Loads to Loch Raven Reservoir ... xx
Figure E-7. Observed and Simulated Maximum Chlorophyll Concentrations by Date, Calibration Scenario, Prettyboy Reservoir ... xxiii
Figure E-8. Observed and Simulated Maximum Chlorophyll Concentrations by Date, Calibration Scenario, Loch Raven Reservoir ... xxiii
Figure E-9. Cumulative Distribution of Observed and Simulated Maximum Chlorophyll Concentrations By Station and Date, Calibration Scenario, Prettyboy Reservoir ... xxiv
Figure E-10. Cumulative Distribution of Observed and Simulated Maximum Chlorophyll Concentrations by Station and Date, Calibration Scenario, Loch Raven Reservoir ... xxv
Figure E-11. Observed and Simulated Average Bottom DO Concentrations, Lower Stations, Calibration Scenario, Prettyboy Reservoir ... xxvi
Figure E-12. Observed and Simulated Average Bottom DO Concentrations, Lower Station, Calibration Scenario, Loch Raven Reservoir ... xxvii
Figure E-13. Observed and Simulated Maximum Chlorophyll Concentrations by Date, TMDL Scenario, Prettyboy Reservoir ... xxvii
Figure E-14. Observed and Simulated Maximum Chlorophyll Concentrations by Date, TMDL Scenario, Loch Raven Reservoir ... xxviii
Figure E-15. Observed and Simulated Average Bottom DO Concentrations, Lower Stations, All-Forest Scenario, Prettyboy Reservoir ... xxx
Figure E-16. Observed and Simulated Average Bottom DO Concentrations, Lower Station, All-Forest Scenario, Loch Raven Reservoir ... xxx
Figure 1.1-1. Location of Prettyboy and Loch Raven Reservoirs ... 3
Figure 2.1-1. Gunpowder Watersheds and Counties ... 6
Figure 3.4-1. Gunpowder Watershed Model Segmentation ... 13
Figure 3.5.1. Gunpowder Watershed Land Use ... 15
Figure 3.5.2-2. Gunpowder Watershed Model Segments Overlaid by the FSA Grid ... 18
Figure 3.7-1. Point Source Facilities in the Gunpowder Watershed ... 28
Figure 3.8.2-1. Monitoring Stations in the Gunpowder Basin ... 33
Figure 4.6-1. Time Series of ESTIMATOR and HSPF Monthly Sediment Loads (tons), Western Run ... 54
Figure 4.6-2. Scatter Plot of ESTIMATOR and HSPF Monthly Sediment Loads (tons), Western Run ... 55
Figure 4.6-3. Time Series of ESTIMATOR and HSPF Monthly Sediment Loads (tons), Beaverdam Run ... 55
Figure 4.6-4. Scatter Plot of ESTIMATOR and HSPF Monthly Sediment Loads (tons), Beaverdam Run ... 56
Figure 4.7-1. Time Series of ESTIMATOR and HSPF Monthly Phosphorus Loads (tons), Western Run ... 61
Figure 4.7-2. Scatter Plot of ESTIMATOR and HSPF Monthly Phosphorus Loads (tons), Western Run ... 62
Figure 4.7-3. Time Series of ESTIMATOR and HSPF Monthly Phosphorus Loads (tons), Beaverdam Run ... 62
Figure 4.7-4. Scatter Plot of ESTIMATOR and HSPF Monthly Phosphorus Loads (tons), Beaverdam Run ... 63
Figure 4.7-5. Time Series of ESTIMATOR and HSPF Monthly Ammonia Nitrogen Loads (tons), Western Run ... 63
Figure 4.7-6. Scatter Plot of ESTIMATOR and HSPF Monthly Ammonia Nitrogen Loads (tons), Western Run ... 64

Figure 4.7-7. Time Series of ESTIMATOR and HSPF Monthly Ammonia Nitrogen Loads (tons), Beaverdam Run 64
Figure 4.7-8. Scatter Plot of ESTIMATOR and HSPF Monthly Ammonia Nitrogen Loads (tons), Beaverdam Run 65
Figure 4.7-9. Time Series of ESTIMATOR and HSPF Monthly Nitrate Loads (tons), Western Run 65
Figure 4.7-10. Scatter Plot of ESTIMATOR and HSPF Monthly Nitrate Loads (tons), Western Run 66
Figure 4.7-11. Time Series of ESTIMATOR and HSPF Monthly Nitrate Loads (tons), Beaverdam Run........ 66
Figure 4.7-12. Scatter Plot of ESTIMATOR and HSPF Monthly Nitrate Loads (tons), Beaverdam Run........ 67
Figure 5.2.1-1. Sampling Locations in Prettyboy Reservoir (from DPW)........ 84
Figure 5.2.1.-2. Sampling Locations, Loch Raven Reservoir (from DPW)........ 85
Figure 5.1.3-1 Isothermal Temperature Contours, Loch Raven Reservoir, Middle Stations, 1993.... 87
Figure 5.1.4-1. DO Contour, Loch Raven Reservoir, Middle Locations, 1993........ 92
Figure 5.1.4-2. Surface Water Elevation in Prettyboy Reservoir, 1994-2004........ 92
Figure 5.1.5-1. Observed TP Concentrations, Loch Raven Reservoir, Upper Stations, with Western Run monthly TP loading rates from ESTIMATOR........ 95
Figure 5.1.7-1. Average Monthly Secchi Depth, 1992-2004, Lower Stations in Prettyboy Reservoir . 97
Figure 5.1.5-2 Average Monthly Secchi Depth, 1992-2004, Lower Station in Loch Raven Reservoir 98
Figure 5.1.8-1. Relative Abundance of Algal Taxa by Month, Loch Raven Reservoir GUN0142..... 103
Figure 5.1.8-2. Relative Abundance of Algal Taxa by Month, Prettyboy Reservoir GUN0401......... 103
Figure 5.2-1. 107
THE BASIC EQUATIONS OF CE-QUAL-W2 107
Figure 5.3.1-1. Model Segmentation of Prettyboy Reservoir........ 112
Figure 5.3.1-2. Model Segmentation of Loch Raven Reservoir 113
Figure 5.3.1-3. Volume vs. Elevation Curves, Prettyboy Reservoir 118
Figure 5.3.1-4. Volume vs. Elevation Curves, Loch Raven Reservoir........ 118
Figure 5.6.1-1. Observed and Simulated Average Surface Total Phosphorus Concentrations, Middle Station, Calibration Scenario, Prettyboy Reservoir 131
Figure 5.6.1-2. Observed and Simulated Average Surface Total Phosphorus Concentrations, Lower Station, Calibration Scenario, Prettyboy Reservoir 131
Figure 5.6.1-3. Observed and Simulated Total Average Surface Phosphorus Concentrations, Upper Station, Calibration Scenario, Loch Raven Reservoir 132
Figure 5.6.1-4. Observed and Simulated Total Average Surface Phosphorus Concentrations, Middle Station, Calibration Scenario, Loch Raven Reservoir 132
Figure 5.6.1-5. Observed and Simulated Total Average Surface Phosphorus Concentrations, Lower Station, Calibration Scenario, Loch Raven Reservoir 133
Figure 5.6.1-6. Observed and Simulated Average Surface Total Phosphorus Concentrations, Calibration Scenario, Prettyboy Reservoir 133
Figure 5.6.1-7. Observed and Simulated Total Average Surface Phosphorus Concentrations, Calibration Scenario, Loch Raven Reservoir........ 134
Figure 5.6.1-8. Cumulative Distribution of Observed and Simulated Average Surface Total Phosphorus Concentrations, Calibration Scenario, Prettyboy Reservoir 134
Figure 5.6.1-9. Cumulative Distribution of Observed and Simulated Average Surface Total Phosphorus Concentrations, Calibration Scenario, Loch Raven Reservoir 135
Figure 5.6.1-10. Observed and Simulated Average Bottom Total Phosphorus Concentrations, Middle Station, Calibration Scenario, Prettyboy Reservoir 135
Figure 5.6.1-11. Observed and Simulated Average Bottom Total Phosphorus Concentrations, Lower Station, Calibration Scenario, Prettyboy Reservoir 136
Figure 5.6.1-12. Observed and Simulated Total Average Bottom Phosphorus Concentrations, Upper Station, Calibration Scenario, Loch Raven Reservoir 136
Figure 5.6.1-13. Observed and Simulated Total Average Bottom Phosphorus Concentrations, Middle Station, Calibration Scenario, Loch Raven Reservoir 137
Figure 5.6.1-14. Observed and Simulated Total Average Bottom Phosphorus Concentrations, Lower Station, Calibration Scenario, Loch Raven Reservoir 137

Figure 5.6.1-15. Observed and Simulated Total Average Bottom Phosphorus Concentrations, Calibration Scenario, Prettyboy Reservoir 138
Figure 5.6.1-16. Observed and Simulated Total Average Bottom Phosphorus Concentrations, Calibration Scenario, Loch Raven Reservoir 138
Figure 5.6.1-17. Cumulative Distribution of Observed and Simulated Total Average Bottom Phosphorus Concentrations, Calibration Scenario, Prettyboy Reservoir 139
Figure 5.6.1-18. Cumulative Distribution of Observed and Simulated Total Average Bottom Phosphorus Concentrations, Calibration Scenario, Loch Raven Reservoir 139
Figure 5.6.2-1. Observed and Simulated Maximum Chlorophyll Concentrations By Date, Calibration Scenario, Prettyboy Reservoir 145
Figure 5.6.2-2. Observed and Simulated Maximum Chlorophyll Concentrations, Calibration Scenario, Prettyboy Reservoir 145
Figure 5.6.2-3. Cumulative Distribution of Observed and Simulated Maximum Chlorophyll Concentrations, Calibration Scenario, Prettyboy Reservoir 146
Figure 5.6.2-4. Observed and Simulated Maximum Chlorophyll Concentrations, Middle Station, Calibration Scenario, Prettyboy Reservoir 146
Figure 5.6.2-5. Observed and Simulated Maximum Chlorophyll Concentrations, Lower Stations, Calibration Scenario, Prettyboy Reservoir 147
Figure 5.6.2-6. Observed and Simulated Maximum Chlorophyll Concentrations By Date, Calibration Scenario, Loch Raven Reservoir 147
Figure 5.6.2-7. Observed and Simulated Maximum Chlorophyll Concentrations, Calibration Scenario, Loch Raven Reservoir 148
Figure 5.6.2-8. Cumulative Distribution of Observed and Simulated Maximum Chlorophyll Concentrations, Calibration Scenario, Loch Raven Reservoir 148
Figure 5.6.2-9. Observed and Simulated Maximum Chlorophyll Concentrations, Upper Stations, Calibration Scenario, Loch Raven Reservoir 149
Figure 5.6.2-10. Observed and Simulated Maximum Chlorophyll Concentrations, Middle Stations, Calibration Scenario, Loch Raven Reservoir 149
Figure 5.6.2-11 Observed and Simulated Maximum Chlorophyll Concentrations, Lower Station, Calibration Scenario, Loch Raven Reservoir 150
Figure 5.6.3-1. Observed and Simulated Average Bottom DO Concentrations, Middle Station, Calibration Scenario, Prettyboy Reservoir 154
Figure 5.6.3-2. Observed and Simulated Average Bottom DO Concentrations, Lower Stations, Calibration Scenario, Prettyboy Reservoir 154
Figure 5.6.3-3. Observed and Simulated Average Bottom DO Concentrations, Upper Stations, Calibration Scenario, Loch Raven Reservoir 155
Figure 5.6.3-4. Observed and Simulated Average Bottom DO Concentrations, Middle Stations, Calibration Scenario, Loch Raven Reservoir 155
Figure 5.6.3-5. Observed and Simulated Average Bottom DO Concentrations, Lower Station, Calibration Scenario, Loch Raven Reservoir 156
Figure 5.6.3-6. Observed and Simulated Average Bottom DO Concentrations, Calibration Scenario, Prettyboy Reservoir 156
Figure 5.6.3-7. Observed and Simulated Average Bottom DO Concentrations, Calibration Scenario, Loch Raven Reservoir 157
Figure 5.6.3-8. Cumulative Distribution of Observed and Simulated Average Bottom DO Concentrations, Calibration Scenario, Prettyboy Reservoir 157
Figure 5.6.3-9. Cumulative Distribution of Observed and Simulated Average Bottom DO Concentrations, Calibration Scenario, Loch Raven Reservoir 158
Figure 5.6.3-10. Observed and Simulated Average Surface DO Concentrations, Middle Station, Calibration Scenario, Prettyboy Reservoir 158
Figure 5.6.3-11. Observed and Simulated Average Surface DO Concentrations, Lower Stations, Calibration Scenario, Prettyboy Reservoir 159
Figure 5.6.3-12. Observed and Simulated Average Surface DO Concentrations, Upper Stations, Calibration Scenario, Loch Raven Reservoir 159
Figure 5.6.3-13. Observed and Simulated Average Surface DO Concentrations, Middle Stations, Calibration Scenario, Loch Reservoir 160

Figure 5.6.3-14. Observed and Simulated Average Surface DO Concentrations, Lower Station, Calibration Scenario, Loch Reservoir 160
Figure 5.6.3-15. Observed and Simulated Average Surface DO Concentrations, Calibration Scenario, Prettyboy Reservoir........ 161
Figure 5.6.3-16. Observed and Simulated Average Surface DO Concentrations, Calibration Scenario, Loch Raven Reservoir........ 161
Figure 5.6.3-17. Cumulative Distribution of Observed and Simulated Average Surface DO Concentrations, Calibration Scenario, Prettyboy Reservoir 162
Figure 5.6.3-18. Cumulative Distribution of Observed and Simulated Average Surface DO Concentrations, Calibration Scenario, Loch Raven Reservoir........ 162
Figure 5.6.4-1. Observed and Simulated Average Surface Ammonia Concentrations, Middle Station, Calibration Scenario, Prettyboy Reservoir 166
Figure 5.6.4-2. Observed and Simulated Average Bottom Ammonia Concentrations, Middle Station, Calibration Scenario, Prettyboy Reservoir 166
Figure 5.6.4-3. Observed and Simulated Average Surface Ammonia Concentrations, Lower Station, Calibration Scenario, Prettyboy Reservoir 167
Figure 5.6.4-4. Observed and Simulated Average Bottom Ammonia Concentrations, Lower Station, Calibration Scenario, Prettyboy Reservoir 167
Figure 5.6.4-5. Observed and Simulated Average Surface Nitrate Concentrations, Middle Station, Calibration Scenario, Prettyboy Reservoir 168
Figure 5.6.4-6. Observed and Simulated Average Bottom Nitrate Concentrations, Middle Station, Calibration Scenario, Prettyboy Reservoir 168
Figure 5.6.4-7. Observed and Simulated Average Surface Nitrate Concentrations, Lower Station, Calibration Scenario, Prettyboy Reservoir 169
Figure 5.6.4-8. Observed and Simulated Average Bottom Nitrate Concentrations, Lower Station, Calibration Scenario, Prettyboy Reservoir 169
Figure 5.6.4-9. Observed and Simulated Average Surface Ammonia Concentrations, Upper Station, Calibration Scenario, Loch Raven Reservoir........ 170
Figure 5.6.4-10. Observed and Simulated Average Bottom Ammonia Concentrations, Upper Station, Calibration Scenario, Loch Raven Reservoir........ 170
Figure 5.6.4-11. Observed and Simulated Average Surface Ammonia Concentrations, Middle Station, Calibration Scenario, Loch Raven Reservoir........ 171
Figure 5.6.4-12. Observed and Simulated Average Bottom Ammonia Concentrations, Middle Station, Calibration Scenario, Loch Raven Reservoir........ 171
Figure 5.6.4-13. Observed and Simulated Average Surface Ammonia Concentrations, Lower Station, Calibration Scenario, Loch Raven Reservoir........ 172
Figure 5.6.4-14. Observed and Simulated Average Bottom Ammonia Concentrations, Lower Station, Calibration Scenario, Loch Raven Reservoir........ 172
Figure 5.6.4-15. Observed and Simulated Average Surface Nitrate Concentrations, Upper Station, Calibration Scenario, Loch Raven Reservoir........ 173
Figure 5.6.4-16. Observed and Simulated Average Bottom Nitrate Concentrations, Upper Station, Calibration Scenario, Loch Raven Reservoir........ 173
Figure 5.6.4-17. Observed and Simulated Average Surface Nitrate Concentrations, Middle Station, Calibration Scenario, Loch Raven Reservoir........ 174
Figure 5.6.4-18. Observed and Simulated Average Bottom Nitrate Concentrations, Middle Station, Calibration Scenario, Loch Raven Reservoir........ 174
Figure 5.6.4-19. Observed and Simulated Average Surface Nitrate Concentrations, Lower Station, Calibration Scenario, Loch Raven Reservoir........ 175
Figure 5.6.4-20. Observed and Simulated Average Bottom Nitrate Concentrations, Lower Station, Calibration Scenario, Loch Raven Reservoir........ 175
Figure 6.2-1. Position of the Interface between Epilimnion and Metalimnion, Prettyboy Reservoir 182
Figure 6.2-2. Position of the Interface Between Epilimnion and Metalimnion, Loch Raven Reservoir 183
Figure 6.3-1. Observed and Simulated Maximum Chlorophyll Concentrations by Date, TMDL Scenario, Prettyboy Reservoir........ 185

Figure 6.3-2. Observed and Simulated Maximum Chlorophyll Concentrations by Date, TMDL Scenario, Loch Raven Reservoir 185
Figure 6.3-4. Simulated Maximum Chlorophyll Concentrations By Date, Calibration, TMDL, and Forest Scenarios, Loch Raven Reservoir. 186
Figure 6.4-1. Observed and Simulated Average Bottom DO Concentrations, Middle Station, TMDL Scenario, Prettyboy Reservoir 189
Figure 6.4-2. Observed and Simulated Average Bottom DO Concentrations, Lower Stations, TMDL Scenario, Prettyboy Reservoir 189
Figure 6.4-3. Observed and Simulated Average Bottom DO Concentrations, Upper Stations, TMDL Scenario, Loch Raven Reservoir 190
Figure 6.4-4. Observed and Simulated Average Bottom DO Concentrations, Middle Stations, TMDL Scenario, Loch Raven Reservoir 190
Figure 6.4-5. Observed and Simulated Average Bottom DO Concentrations, Lower Station, TMDL Scenario, Loch Raven Reservoir 191
Figure 6.4-6. Observed and Simulated Average Bottom DO Concentrations, Middle Station, All-Forest Scenario, Prettyboy Reservoir 191
Figure 6.4-7. Observed and Simulated Average Bottom DO Concentrations, Lower Stations, All-Forest Scenario, Prettyboy Reservoir 192
Figure 6.4-8. Observed and Simulated Average Bottom DO Concentrations, Upper Stations, All-Forest Scenario, Loch Raven Reservoir 192
Figure 6.4-9. Observed and Simulated Average Bottom DO Concentrations, Middle Stations, All-Forest Scenario, Loch Raven Reservoir 193
Figure 6.4-10. Observed and Simulated Average Bottom DO Concentrations, Lower Station, All-Forest Scenario, Loch Raven Reservoir 193
Figure 6.4-11. Percent of Sampling Dates on which DO < 2 mg/l at Sampling Locations as a function of Load Reductions from All-Forest Scenario 194
Figure 6.4-12. Minimum DO Concentration at the Middle Sampling Location on Sampling Dates in the Simulated Surface Layer, Prettyboy Reservoir 196
Figure 6.4-13. Minimum DO Concentration at the Lower Sampling Locations on Sampling Dates in the Simulated Surface Layer, Prettyboy Reservoir 197
Figure 6.4-14. Minimum DO Concentration at the Upper Sampling Location on Sampling Dates in the Simulated Surface Layer, Loch Raven Reservoir 197
Figure 6.4-15. Minimum DO Concentration at the Middle Sampling Location on Sampling Dates in the Simulated Surface Layer, Loch Raven Reservoir 198
Figure 6.4-16. Minimum DO Concentration at the Lower Sampling Location on Sampling Dates in the Simulated Surface Layer, Loch Raven Reservoir 198

EXECUTIVE SUMMARY

E.1. Introduction

Prettyboy Reservoir and Loch Raven Reservoir are two public water supply reservoirs operated by the City of Baltimore in the Gunpowder Falls Watershed. Figure E-1 shows the location of the reservoirs. In addition to the reservoirs being used for public water supply, COMAR regulations classify both Prettyboy and Loch Raven Reservoirs, as well as their tributaries, as Class III-P Nontidal Cold Water and Public Water Supply. The Maryland Department of the Environment (MDE) placed both reservoirs on Maryland's 303 (d) List of impaired waters. Excess nutrients are one cause of the impairments in both reservoirs. Loch Raven Reservoir is also listed as impaired by sediment. The Clean Water Act specifies that a Total Maximum Daily Load (TMDL) must be determined for waterbodies not meeting water quality standards. A TMDL is the maximum amount of a pollutant a waterbody can receive and still meet water quality standards. This report documents the development of a modeling framework for determining TMDLs in Prettyboy and Loch Raven Reservoirs for nutrients, and, in the case of Loch Raven, sediment.

Figure E-1. Location of Prettyboy and Loch Raven Reservoirs

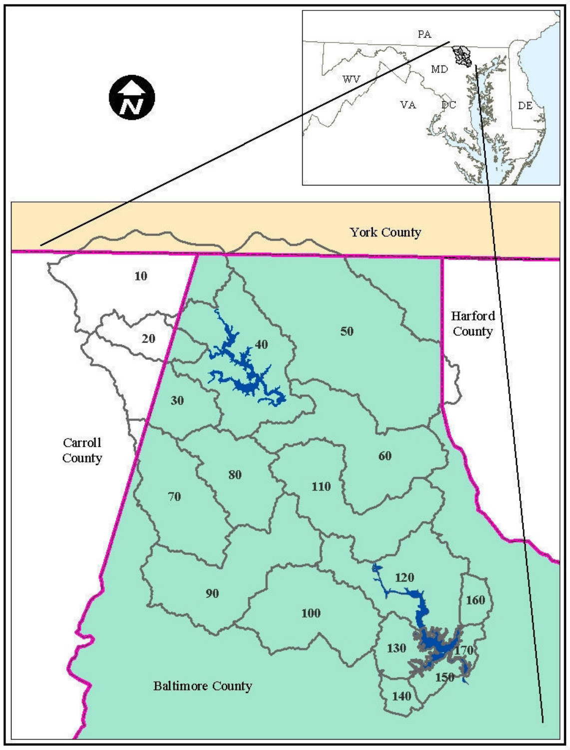

E.2. Water Quality Analysis

Prettyboy and Loch Raven Reservoirs both regularly exhibit temperature stratification starting in April or May and lasting until November. The differential heating of the water column, combined with wind-driven mixing of the surface layers, leads to the establishment of three regions of temperature and density differences in the spring and summer: the epilimnion, or well-mixed surface layer with relatively homogeneous temperature; the hypolimnion, or bottom-layers, which are also relatively homogeneous in temperature; and the metalimnion or thermocline connecting these two regions, which is characterized by a steep gradient in temperature and density. In Prettyboy and Loch Raven Reservoirs, stratification can also occur in winter but without significant consequences for water quality.

During the summer and fall under stratified conditions, bottom waters in both reservoirs can become hypoxic, because stable density differences inhibit the turbulent mixing which transports oxygen from the surface. Both reservoirs regularly experience seasonal hypoxia in the hypolimnion which begins in later spring or early summer and lasts into late fall.

Both Prettyboy and Loch Raven Reservoirs are considered eutrophic. Eutrophication is the over-enrichment of aquatic systems by excessive inputs of nutrients (nitrogen and/or phosphorus). The nutrients act as a fertilizer leading to the excessive growth of algae and aquatic plants. The algae eventually die and decompose, leading to bacterial consumption of dissolved oxygen (DO). Chlorophyll concentrations above 10 µg/l occur frequently but not regularly in both reservoirs. Concentrations above 30 µg/l are infrequent but not unusual.

In both Prettyboy and Loch Raven Reservoirs, phosphorus is the limiting nutrient. In the vast majority of water quality monitoring samples taken, the N:P ratio is much greater than 10:1 ratio that marks the lower boundary of phosphorus limitation. The nutrient TMDL for the reservoirs is therefore expressed in terms of total phosphorus.

E.3. The Gunpowder Falls HSPF Model

A computer simulation model of the Gunpowder Falls watershed draining into Prettyboy and Loch Raven Reservoirs was developed using the Hydrological Simulation Program—Fortran (HSPF). The model builds on an earlier HSPF model of the Gunpowder Watershed developed by MDE. The simulation period is 1992-1997, the same as the original model. Figure E.2 shows the segmentation of the watershed used in the model.

Figure E-2. Gunpowder Watershed Model Segmentation

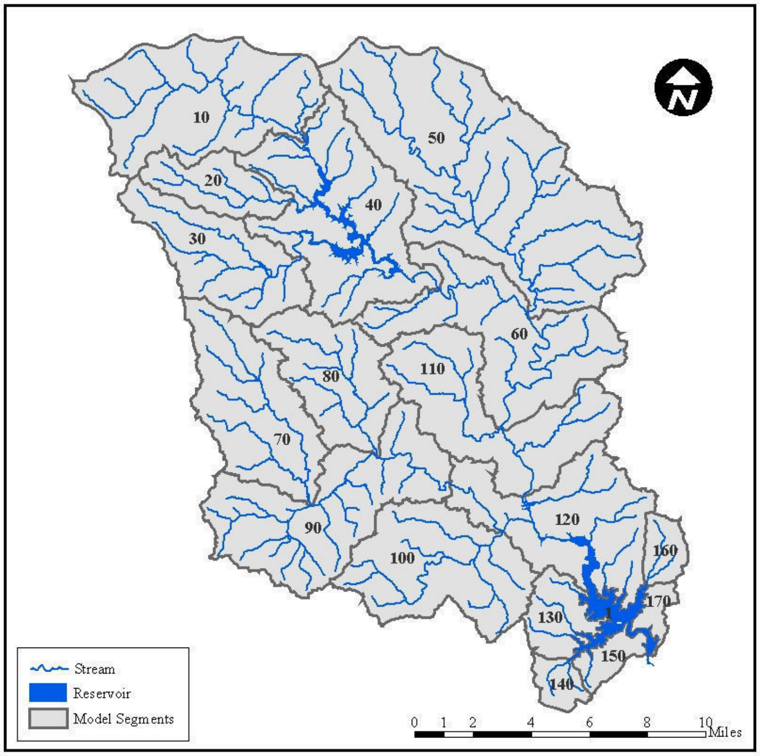

Twelve land uses were represented in the model: forest, pasture, pervious developed land, impervious land, mixed open land, confined animal areas, and five crop land uses. Figures E-3 and E-4 show the percent of each general land use type in the Prettyboy and Loch Raven watersheds.

Hydrology and river routing were calibrated using PEST, a parameter optimization software, at three locations in the Loch Raven watershed. Flows were also calibrated at three locations in the Prettyboy watershed where there currently are gages which were not operating during the simulation period. Synthetic flows were generated for these locations to facilitate calibration. Table E -1 shows the calibration locations and Table E-2 shows the hydrology calibration results.

Figure E-3. Land Use in Prettyboy Reservoir Watershed

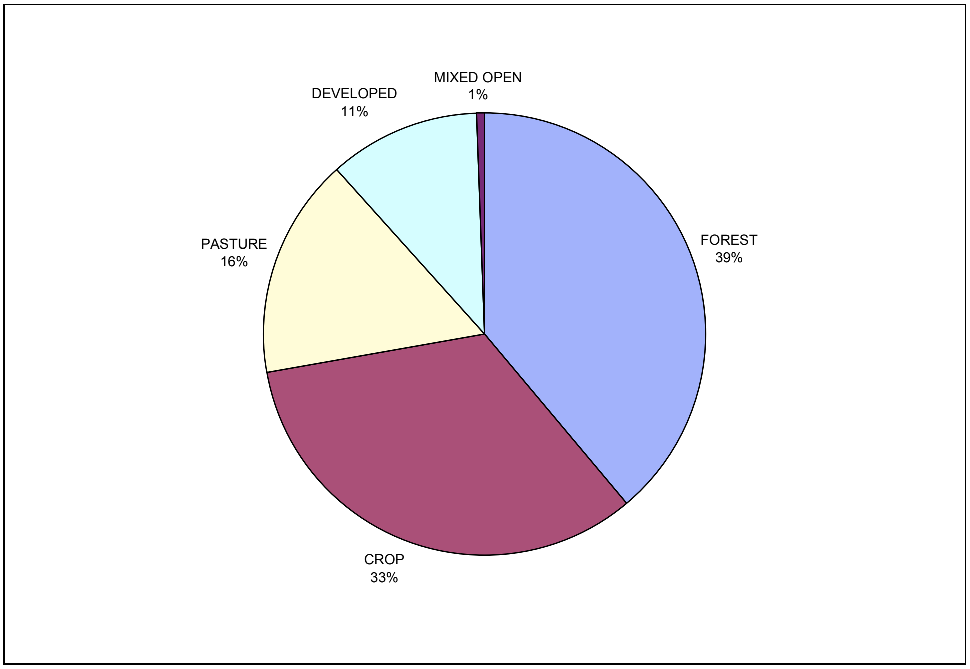

Figure E-4. Land Use in Loch Raven Reservoir Watershed

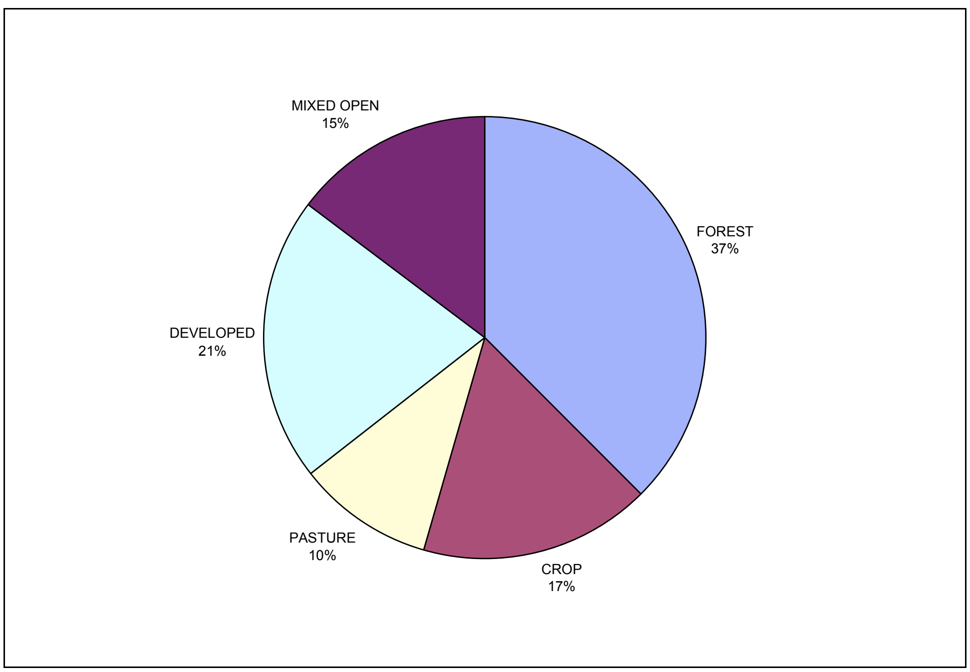

Table E-1. Hydrology Calibration Stations and Associated Active USGS Gages

Gage Number	Name	Watershed Area (mi.2)	Mean Flow (cfs)	HSPF Segment
01581810	Gunpowder Falls near Hoffmanville, MD	27.0	29.6	10
01581830	Grave Run near Bekleysville, MD	7.68	8.85	20
01581870	Georges Run near Beckleysville, MD	15.8	18.1	30
01582000	Little Falls at Blue Mount, MD	52.9	68.1	50
01583500	Western Run at Western Run, MD	59.8	68.9	90
01583600	Beaverdam Run at Cockleysville, MD	20.9	29.8	100

Table E-2. Hydrology Calibration Results

Statistic	Segments					
	10	20	30	50	90	100
Water Balance	100%	100%	101%	99%	100%	95%
Flows < 50th Percentile	116%	115%	116%	114%	119%	105%
Flows > 90th Percentile	92%	93%	96%	86%	89%	94%
Daily R2	0.73	0.72	0.67	0.72	0.72	0.71
Monthly R2	0.89	0.89	0.93	0.91	0.90	0.84

Two types of calibration targets were used to calibrate the HSPF model: edge-of-stream (EOS) targets and in-stream targets. EOS targets were derived from the following sources:

- EOS annual sediment loads for cropland and pasture were set based upon Baltimore County erosion rates determined by the National Resource Inventory (NRI) following the approach used in the Chesapeake Bay Watershed Models.
- EOS nutrient and sediment loads for developed and impervious land were based on statewide average concentrations from monitoring data collected for NPDES stormwater permits.
- Baseflow nutrient loads for forests were based on the Gunpowder Study (DEPRM, 2000) of the predominately-forested Mingo Run.
- Runoff loads of phosphorus from pasture and forest were based on soil phosphorus concentrations for the Maryland Piedmont.

EOS nutrient loads for agricultural land were not explicitly calibrated but were determined by (1) fertilizer applications, (2) manure applications, (3) soil nutrient concentrations, and (4) crop uptake.

Average monthly baseflow total phosphorus concentrations from developed land and pasture were set based on monitored average monthly TP concentrations. Monthly nutrient and sediment loads for Western Run and Beaverdam Run, two key watersheds where storm monitoring data were available, were calculated using the USGS's ESTIMATOR software. The HSPF models of these watersheds were calibrated against the monthly loads from ESTIMATOR. Other portions of the Gunpowder Model were then parameterized based on the results of the calibration of Western Run and Beaverdam Run.

Since phosphorus is the primary constituent of interest, all organic material in the HSPF model was accounted for in terms of phosphorus, so that a mass balance of total phosphorus was preserved in the modeling framework.

Table E-3 shows the average annual constituent loads by segment and reservoir. Figures E-5 and E-6 show the breakdown of the total phosphorus load by major land use.

Table E-3. Average Annual Loads by Segment (tons/yr)

Segment	Ammonia	Nitrate	Total Phosphorus	Suspended Solids
10	1.69	120.99	9.76	9,415
20	0.32	32.81	2.99	2,971
30	2.04	84.13	6.52	6,341
40	4.73	70.07	5.95	5,442
50	7.57	122.61	14.37	9,658
60	2.40	22.68	4.66	3,188
70	2.42	74.31	4.57	4,175
80	1.64	42.60	3.01	2,697
90	2.59	73.27	5.66	4,513
100	4.13	54.41	5.33	3,874
110	1.28	78.99	5.45	6,040
120	5.80	21.85	2.77	2,392
130	2.53	4.77	0.77	376
140	1.61	2.86	0.44	142
150	1.04	1.25	0.35	244
160	1.36	6.89	0.80	444
170	0.34	2.04	0.26	236
Prettyboy	8.78	308.00	25.21	24,167
Prettyboy Outflow	2.47	245.10	6.50	587
Loch Raven	37.18	753.63	54.94	38,567

Figure E-5. Percent Contribution of Sources to Total Phosphorus Loads to Prettyboy Reservoir

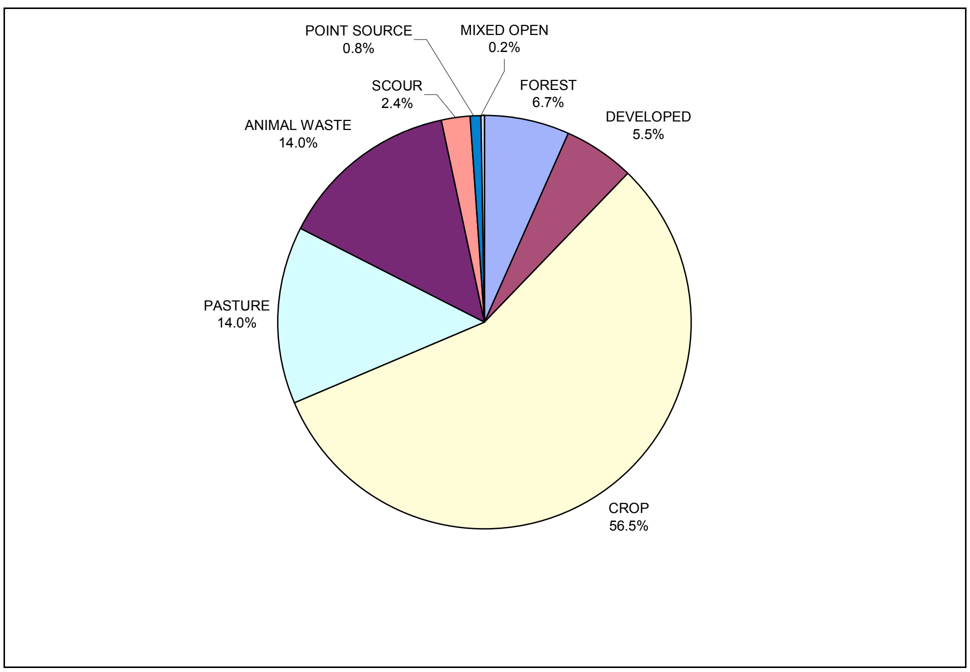

Figure E-6. Percent Contribution of Sources to Total Phosphorus Loads to Loch Raven Reservoir

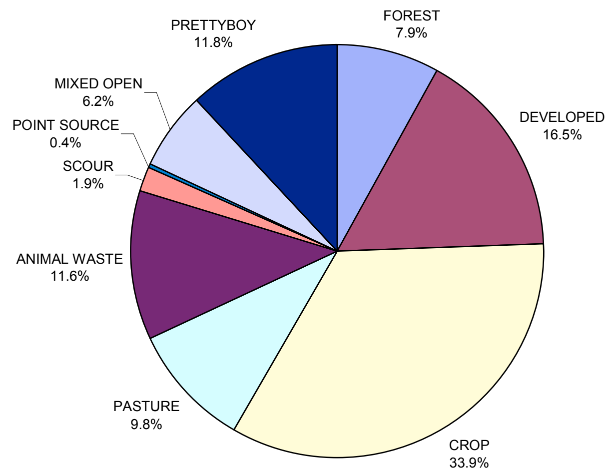

E.4. Prettyboy and Loch Raven Reservoir CE-QUAL-W2 Models

CE-QUAL-W2 is a laterally-averaged two-dimensional computer simulation model capable of representing the hydrodynamics and water quality of rivers, lakes, and estuaries. It is particularly suited for representing temperature stratification that occurs in reservoirs like Prettyboy and Loch Raven. An earlier pair of reservoir models used W2 to simulate the hydrodynamics of the reservoirs, but used WASP to simulate water quality (Leung and Zou, 2000). The current models build upon the earlier versions but simulate not only hydrodynamics and temperature but also dissolved oxygen and eutrophication dynamics as well.

Prettyboy Reservoir was represented by 18 active longitudinal segments in two branches. Each segment contains from four to 30 one-meter thick layers. Loch Raven Reservoir is represented by a single branch of 16 segments, each with four to 16 one-meter thick layers. The simulation period was set to 1992-1997 to coincide with the Gunpowder HSPF Model. Each year was simulated separately, and observed data, where available, were used to set the initial conditions for the simulation.

State variables in the CE-QUAL-W2 model include dissolved oxygen, ammonia, nitrate, dissolved inorganic phosphorus, and both dissolved and particulate organic matter (POM) in labile and refractory forms. Any number of inorganic solids, CBOD variables or algal species can be represented in the model. Organic nitrogen and phosphorus, however, are only implicitly represented through CBOD, organic matter, and algal biomass state variables. In order to preserve a mass balance of all species of phosphorus, the state variables in the W2 models were configured as follows:

1. Inorganic phosphorus attached to silt and clay was modeled as distinct inorganic solids. Sorption between sediment and the water column was not simulated in the model.
2. Three CBOD variables were used to represent allochthanous organic matter inputs to the reservoirs: (1) labile dissolved CBOD, (2) labile particulate CBOD, and (3) refractory particulate CBOD. The concentration of these CBOD inputs were calculated based on the concentration of organic phosphorus determined by the HSPF model, using the stoichiometric ratio between phosphorus and oxygen demand in the reservoir models.
3. The organic matter state variables were reserved to represent the recycling of nutrients within the reservoir between algal biomass and reservoir nutrient pools. No organic matter, as represented by these variables, was input into the reservoirs. They were used to track nutrients released from algal decomposition.

To use the W2 model in this configuration, several minor changes had to be made to the W2 code. Most importantly, the code was altered so that (1) CBOD species could be assigned a settling velocity and (2) labile particulate CBOD contributed to sediment organic matter and sediment oxygen demand (SOD), configured as a first-order reaction based on the quantity of labile organic matter which has settled to the bottom of a segment. Each year's simulation was initialized with the final concentrations of sediment organic matter from the previous year's simulation, because no observations of sediment organic matter were available.

The primary function of the CE-QUAL-W2 models of Prettyboy and Loch Raven Reservoirs is to link algae biomass concentrations, as represented by chlorophyll a concentrations, to total phosphorus loads. The models were calibrated conservatively, to ensure that simulated chlorophyll concentrations were at least as large as observed concentrations, even if maximum seasonal concentrations were shifted in the simulation upstream or downstream, or occurred a month earlier or later than the corresponding observed concentrations.

Figures E-7 and E-8 compare simulated and observed maximum chlorophyll concentrations in the surface layer of Prettyboy and Loch Raven Reservoirs by sampling date. The models capture the observed peaks seasonal average chlorophyll concentrations though sometimes the maximum chlorophyll concentration is shifted spatially or temporally.

Figure E-7. Observed and Simulated Maximum Chlorophyll Concentrations by Date, Calibration Scenario, Prettyboy Reservoir

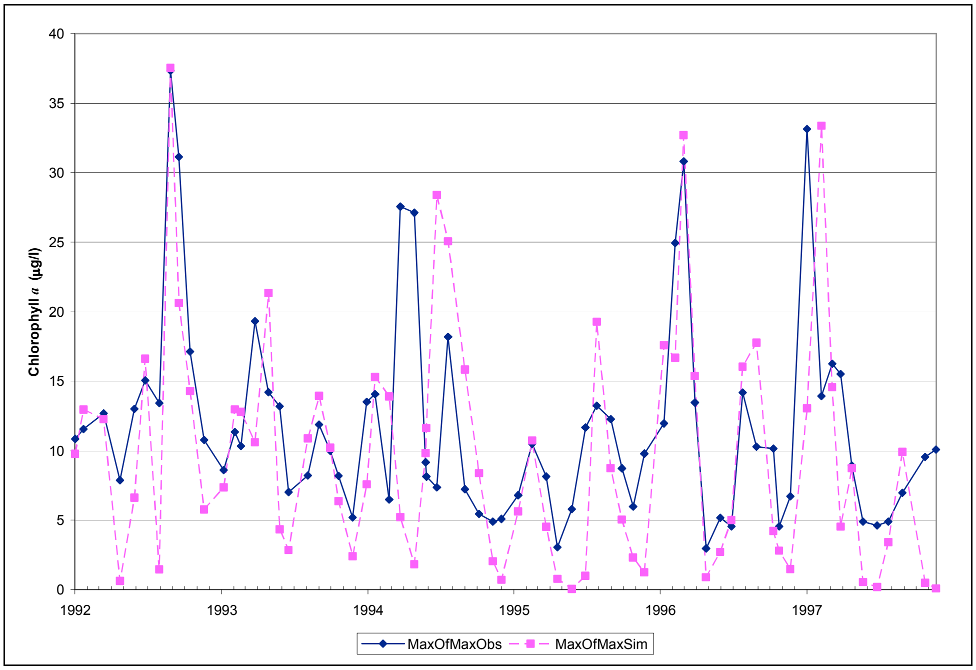

Figure E-8. Observed and Simulated Maximum Chlorophyll Concentrations by Date, Calibration Scenario, Loch Raven Reservoir

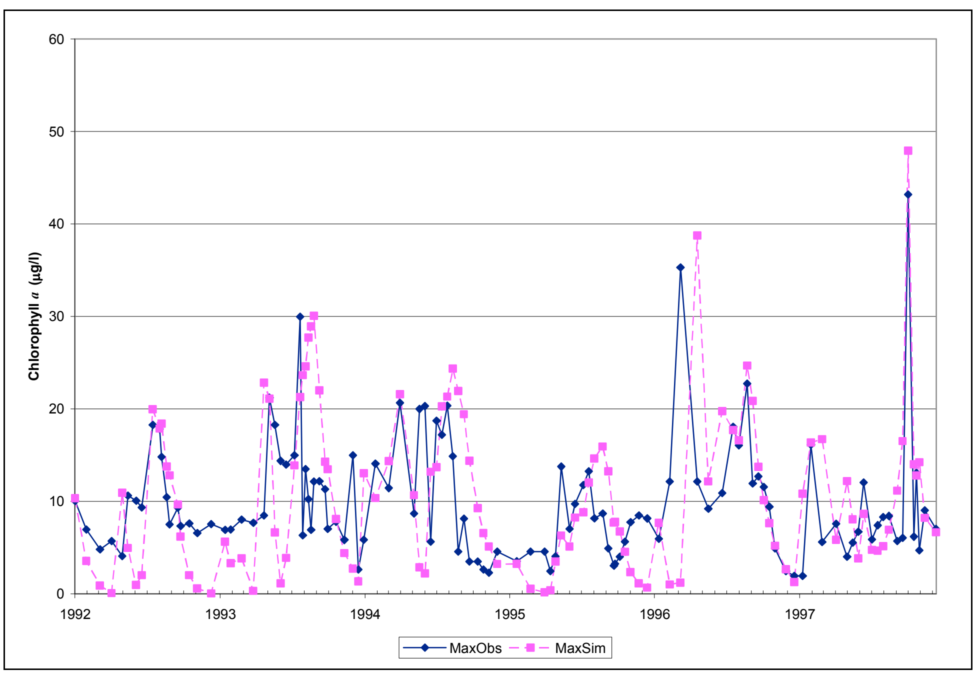

Figures E-9 and E-10 show the cumulative distribution of simulated and observed maximum chlorophyll concentrations by date and location in Prettyboy and Loch Raven Reservoirs, respectively. In both reservoirs simulated concentrations dominate observed concentrations when concentrations are above10 µg/l. This again demonstrates the conservative character of the calibration.

Figure E-9. Cumulative Distribution of Observed and Simulated Maximum Chlorophyll Concentrations By Station and Date, Calibration Scenario, Prettyboy Reservoir

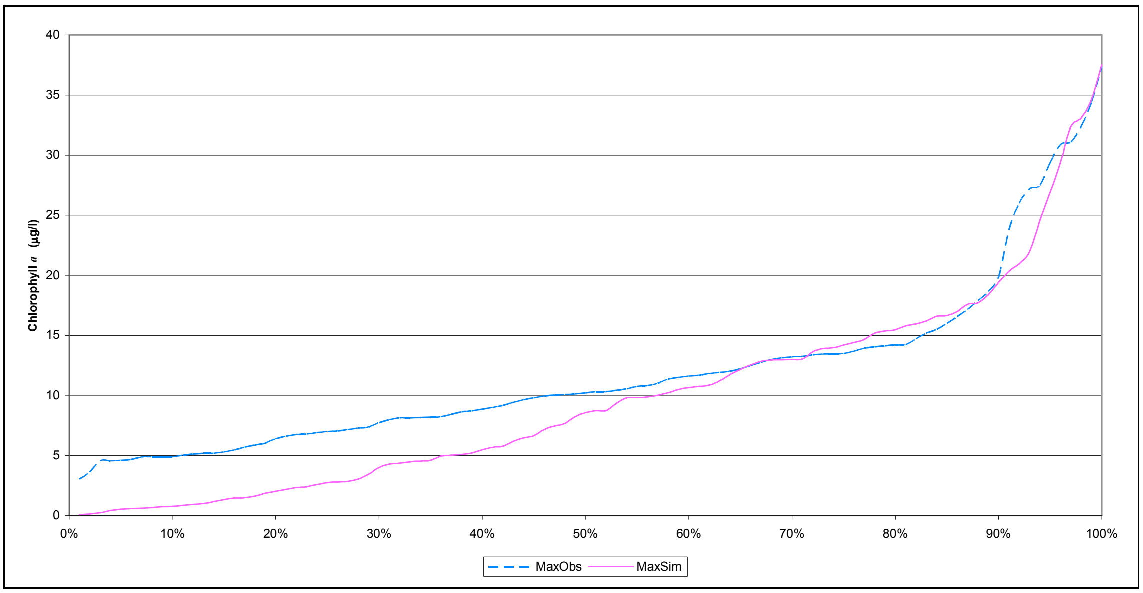

Figure E-10. Cumulative Distribution of Observed and Simulated Maximum Chlorophyll Concentrations by Station and Date, Calibration Scenario, Loch Raven Reservoir

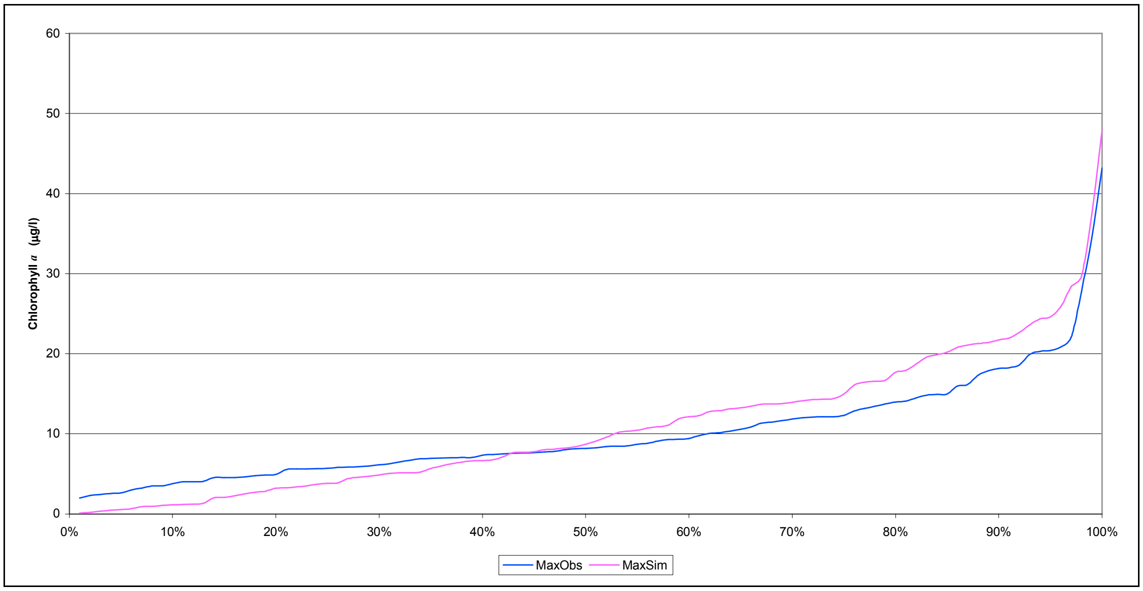

A second function of the CE-QUAL-W2 models was to simulate the seasonal hypoxia in the hypolimnia of the reservoirs and to determine whether it is primarily due to eutrophic conditions or whether it is primarily a function of stratification and reservoir morphology. Hypolimnetic DO concentrations were calibrated by adjusting temperature coefficients and decay rates and by determining the labile fraction of external organic matter that could contribute to sediment oxygen demand. Figures E-11 and E-12 compare observed and simulated average DO concentrations in the hypolimnion of the Prettyboy and Loch Raven Reservoirs. The models capture the seasonal trends in DO very well. The coefficient of determination between observed and simulated concentrations is in 0.80 in Prettyboy Reservoir and 0.81 in Loch Raven Reservoir.

E.5. Sensitivity of Reservoir Models to Loading Rates

The primary purpose of the W2 models is to determine nutrient TMDLs for Prettyboy and Loch Raven Reservoirs. Because phosphorus is the limiting nutrient, the nutrient TMDLs address total phosphorus (TP). Figures E-13 and E-14 demonstrate that the models are sensitive to reductions in TP. They compare the maximum observed chlorophyll *a* concentrations at sampling locations by date, and contrast the observations with both the calibrated simulation and proposed TMDL Scenario, in which TP loads are reduced by 54% and 50% in Prettyboy and Loch Raven Reservoirs, respectively. Under the TMDL Scenario, the reservoirs meet the TMDL endpoints for chlorophyll *a*, which call for no chlorophyll *a* concentration to be above 30 µg/l and for the 30-day moving average chlorophyll *a* concentration to be no more than 10 µg/l. These endpoints were chosen to meet Maryland's General Water Quality Criteria, which prohibit pollution of waters of the state by any material in amounts sufficient to create a nuisance or interfere directly or indirectly with designated uses (See COMAR 26.08.02.03G(1)).

Figure E-11. Observed and Simulated Average Bottom DO Concentrations, Lower Stations, Calibration Scenario, Prettyboy Reservoir

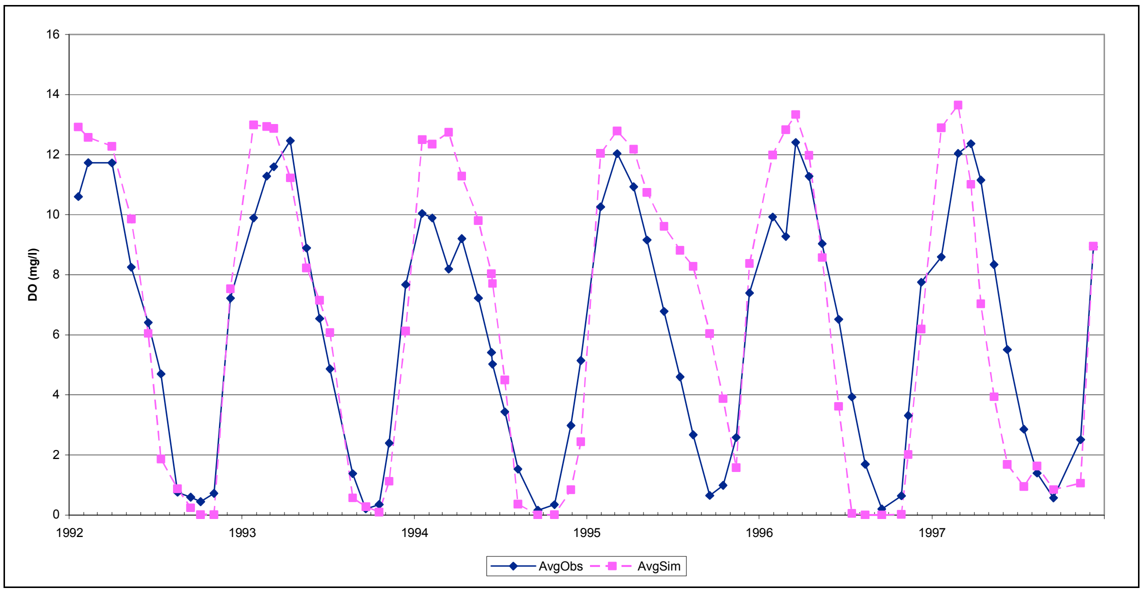

Figure E-12. Observed and Simulated Average Bottom DO Concentrations, Lower Station, Calibration Scenario, Loch Raven Reservoir

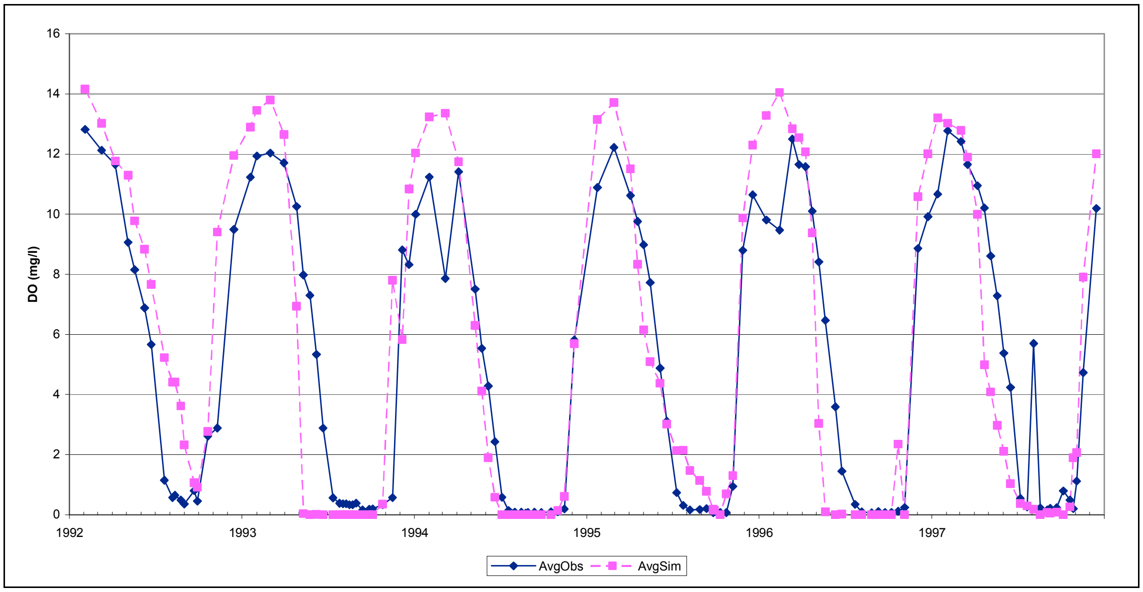

Figure E-13. Observed and Simulated Maximum Chlorophyll Concentrations by Date, TMDL Scenario, Prettyboy Reservoir

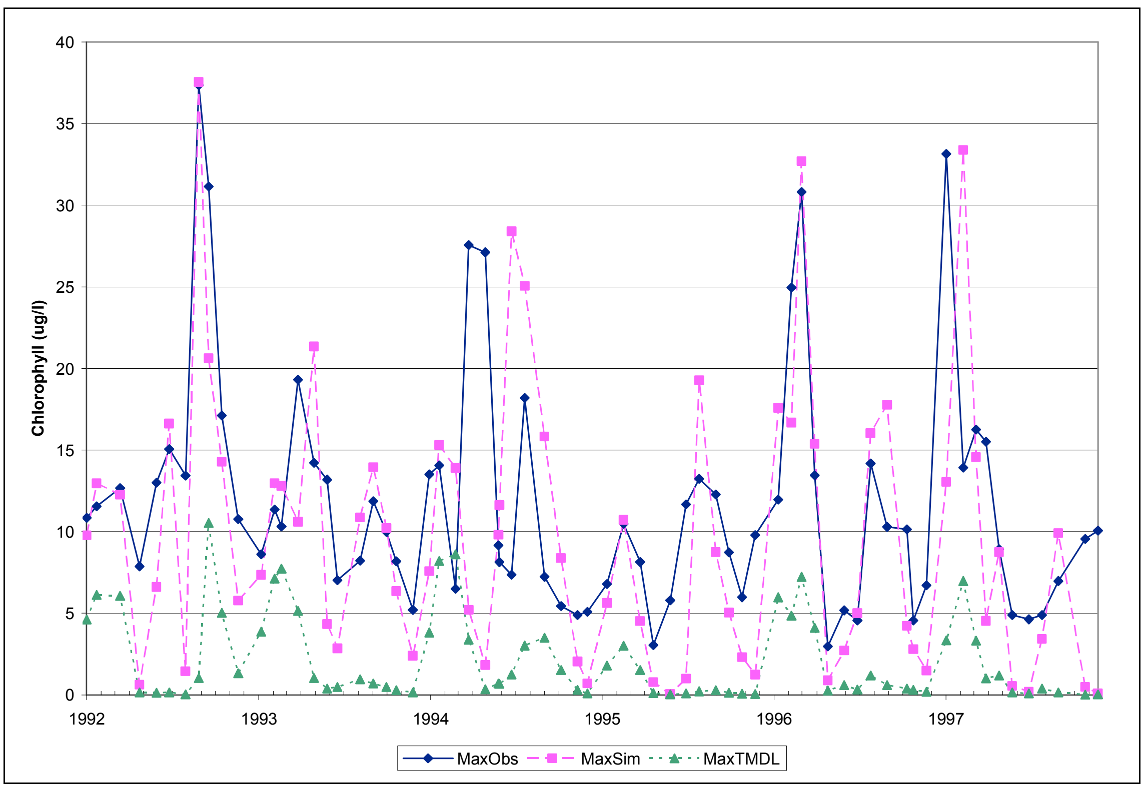

Figure E-14. Observed and Simulated Maximum Chlorophyll Concentrations by Date, TMDL Scenario, Loch Raven Reservoir

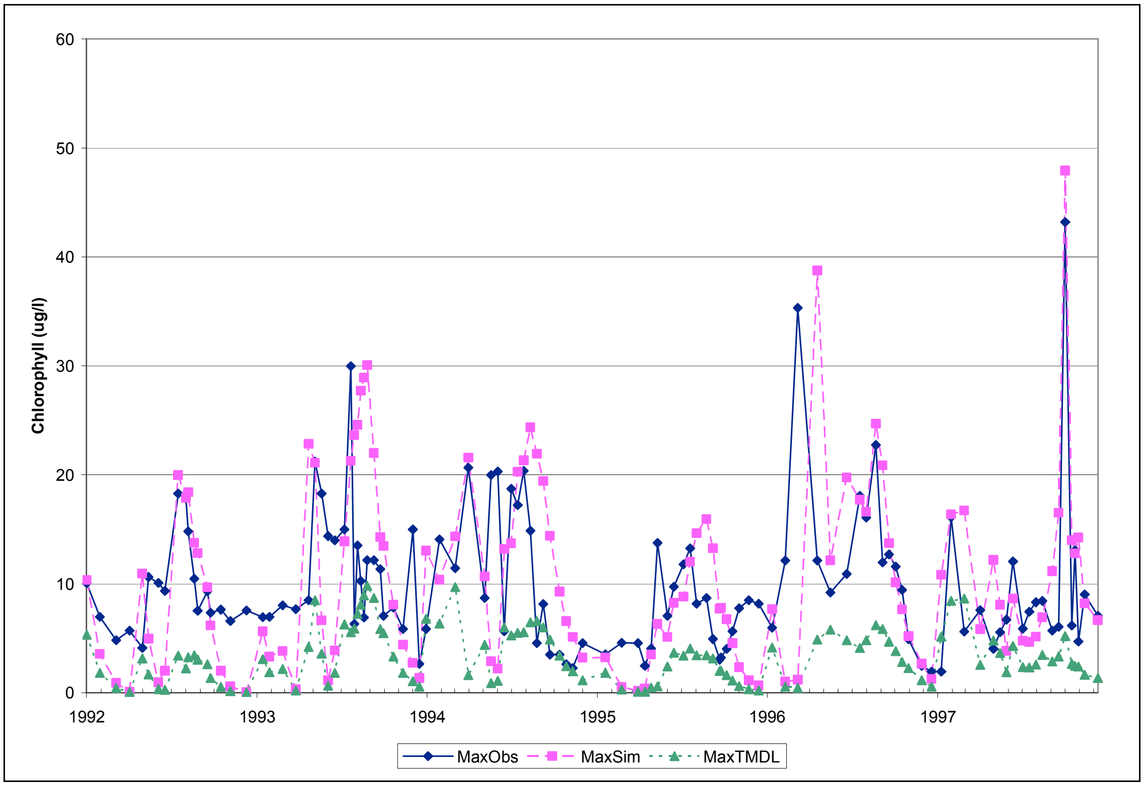

The models must also demonstrate that any proposed TMDL meets water quality standards for dissolved oxygen. This encompasses (1) A minimum dissolved oxygen concentration of 5.0 mg/l (and 6.0 mg/ daily average for Use III) to be maintained throughout the water column during periods of complete and stable mixing; and (2) a minimum dissolved oxygen concentration of 5.0 mg/l (and 6.0 mg/ daily average for Use III) to be maintained in the mixed surface layer at all times, including during stratified conditions, except during periods of overturn or other naturally-occurring disruptions of stratification. Maryland's policy is to address hypolimnetic hypoxia in lakes on a case-by-case basis. In the event of observed hypoxia in the deeper portions of lakes during stratification, Maryland will conduct an analysis to determine if current loading conditions result in a degree of hypoxia that significantly exceeds (in terms of frequency, magnitude and duration) that associated with natural conditions in the lake and its watershed. This analysis may vary from one lake to another in terms of type, approach and scope. Examples may include a review of setting, source assessment and land use, so as to assess current loads; a comparison of estimated current loads exported from the watershed with analogous load estimates under ‘natural’ land cover; and model scenario runs simulating natural conditions. This list is not inclusive, and Maryland expressly reserves the right to determine and conduct the most appropriate type of analysis on a case-by-case basis. In the current case, the models will be used to simulate an all-forest condition, which is interpreted as representative of natural conditions.

For the All-Forest Scenario, flows and temperature were taken from the Calibration Scenario, while constituent loads were taken from the HSPF model simulation in which all land in the watershed was forested. The All-Forest Scenario constitutes an estimate of hypolimnetic DO concentrations under natural conditions.

Figures E-15 and E-16 show the average bottom DO concentrations and minimum DO concentrations at the lower sampling locations in Prettyboy and Loch Raven Reservoirs under the All-Forest Scenario. The All-Forest Scenario demonstrates that hypolimnetic hypoxia would remain under the loading rates associated with all-forested conditions. It can therefore be concluded that hypolimnetic hypoxia is a natural condition in the reservoirs and that both reservoirs would meet water quality standards for dissolved oxygen under the TMDL loading rates.

Figure E-15. Observed and Simulated Average Bottom DO Concentrations, Lower Stations, All-Forest Scenario, Prettyboy Reservoir

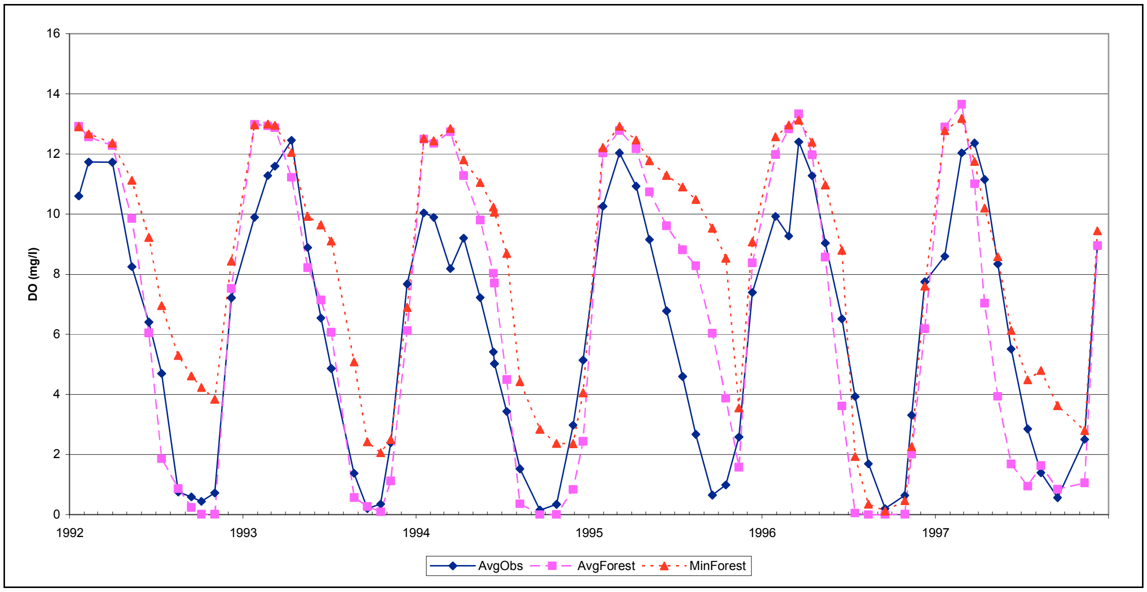

Figure E-16. Observed and Simulated Average Bottom DO Concentrations, Lower Station, All-Forest Scenario, Loch Raven Reservoir

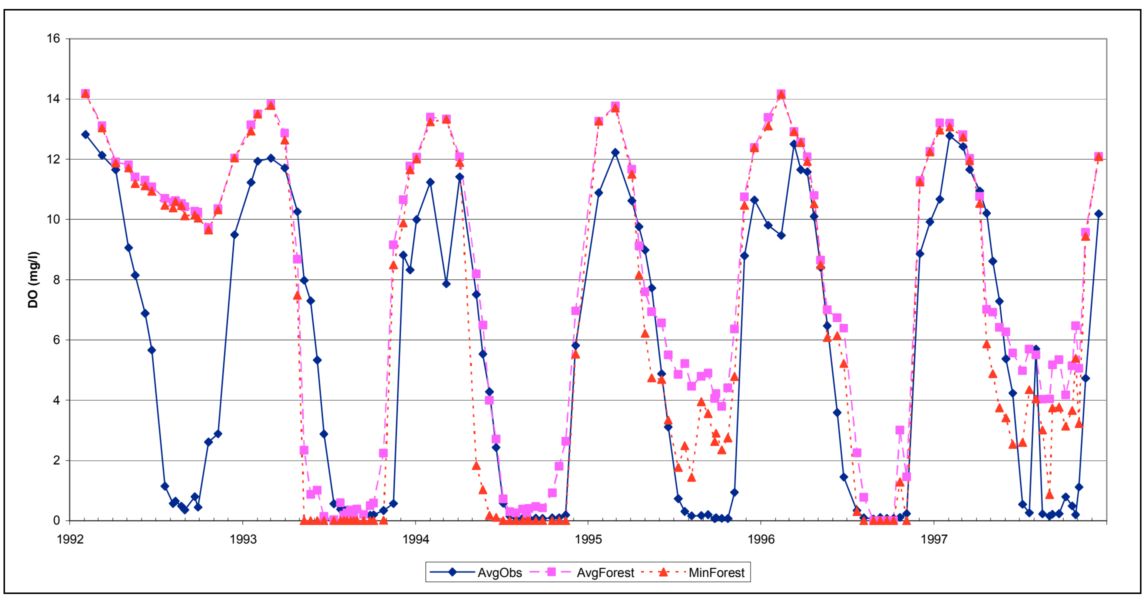

E.6. Summary

A modeling framework has been successfully developed to help establish TMDLs to address the nutrient impairments in Prettyboy and Loch Raven Reservoirs. The framework consists of an HSPF model of the Gunpowder Falls Watershed draining to the reservoirs and CE-QUAL-W2 models of each reservoir. The models have been successfully calibrated for the period 1992 to 1997. Load reduction scenarios have also been developed to determine the TMDLs and verify that the reservoirs meet water quality standards under the TMDLs. An All-Forest Scenario was also simulated to represent natural conditions. Hypolimnetic hypoxia persisted under the All-Forest Scenario, demonstrating that the hypoxia is the result of reservoir bathymetry and induced stratification, not external loads.

Section 1. INTRODUCTION

1.1. INTRODUCTION

Prettyboy Reservoir and Loch Raven Reservoir are two public water supply reservoirs operated by the City of Baltimore in the Gunpowder Falls Watershed. Together with Liberty Reservoir on the Patapsco River, they form the core of the City of Baltimore's water supply system, which provides water to over 1.6 million people, not only in Baltimore City but in Anne Arundel, Baltimore, Carroll, Harford, and Howard Counties. Figure 1.1-1 shows the location of the reservoirs.

The City of Baltimore first created a public water supply reservoir on the Gunpowder Falls in 1881 by building a dam just downstream of the present location of the Loch Raven Reservoir. The current Loch Raven Reservoir was impounded in 1923, when a new dam was built over an older dam previously built in 1914. (City of Baltimore, 1981) Loch Raven Dam is currently undergoing extensive renovations that will not, however, change the pool of the impoundment. Prettyboy Dam was completed in 1933. Both are concrete gravity dams. Table 1.1-1 gives the basic characteristics of the dams and their impoundments.

Water from Loch Raven Reservoir travels by gravity seven miles to the Montebello Filtration Plants, where it is treated before distribution. Prettyboy Reservoir is used as a secondary impoundment to resupply Loch Raven Reservoir.

COMAR regulations classify both Prettyboy and Loch Raven Reservoirs, as well as their tributaries, as Class III-P Use Cold Water and Water Supply. The Maryland Department of the Environment (MDE) placed both reservoirs on Maryland's 303 (d) List of impaired waters. Excess nutrients are one cause of the impairments in both reservoirs. Loch Raven Reservoir is also impaired by sediment. Table 1.1-2 summaries the reservoirs' impairments.

Waters placed on the 303(d) List are not meeting water quality standards and are not expected to do so by the implementation of technology-based controls on permitted point sources. Under these conditions, the Clean Water Act specifies that a Total Maximum Daily Load (TMDL) must be determined. A TMDL is the maximum amount of a pollutant a waterbody can receive and still meet water quality standards. This report documents the development of a modeling framework for determining TMDLs in Prettyboy and Loch Raven Reservoirs for nutrients, and, in the case of Loch Raven, sediment.

The modeling framework builds upon a set of computer simulation models previously developed: (1) MDE has developed an HSPF (Hydrological Simulation Program - Fortran) model of the Gunpowder Falls Watershed. The Watershed Model has been peer-reviewed and presented to the public at a meeting of the Reservoir Technical Group of the Baltimore Metropolitan Council. (2) On behalf of MDE, the University of Virginia's Civil Engineering Department developed a pair of simulation models for each reservoir, (i) a CE-QUAL-W2 model of reservoir hydrodynamics, and (ii) a WASP model of oxygen dynamics and eutrophication (Leung and Zou, 2000). The models cascade into each other. Flows and temperature from the HSPF Watershed Model drive the hydrodynamics of the QUAL-W2 models of each reservoir. THE WASP Eutrophication Model of each reservoir is built upon the simulation of the circulation of water in the QUAL-W2 Models as well as the nutrient and sediment loads from the watershed model. The goal of this project described in this report is to bring this set of models up to code, so to speak, for their use in TMDL development.

Figure 1.1-1. Location of Prettyboy and Loch Raven Reservoirs

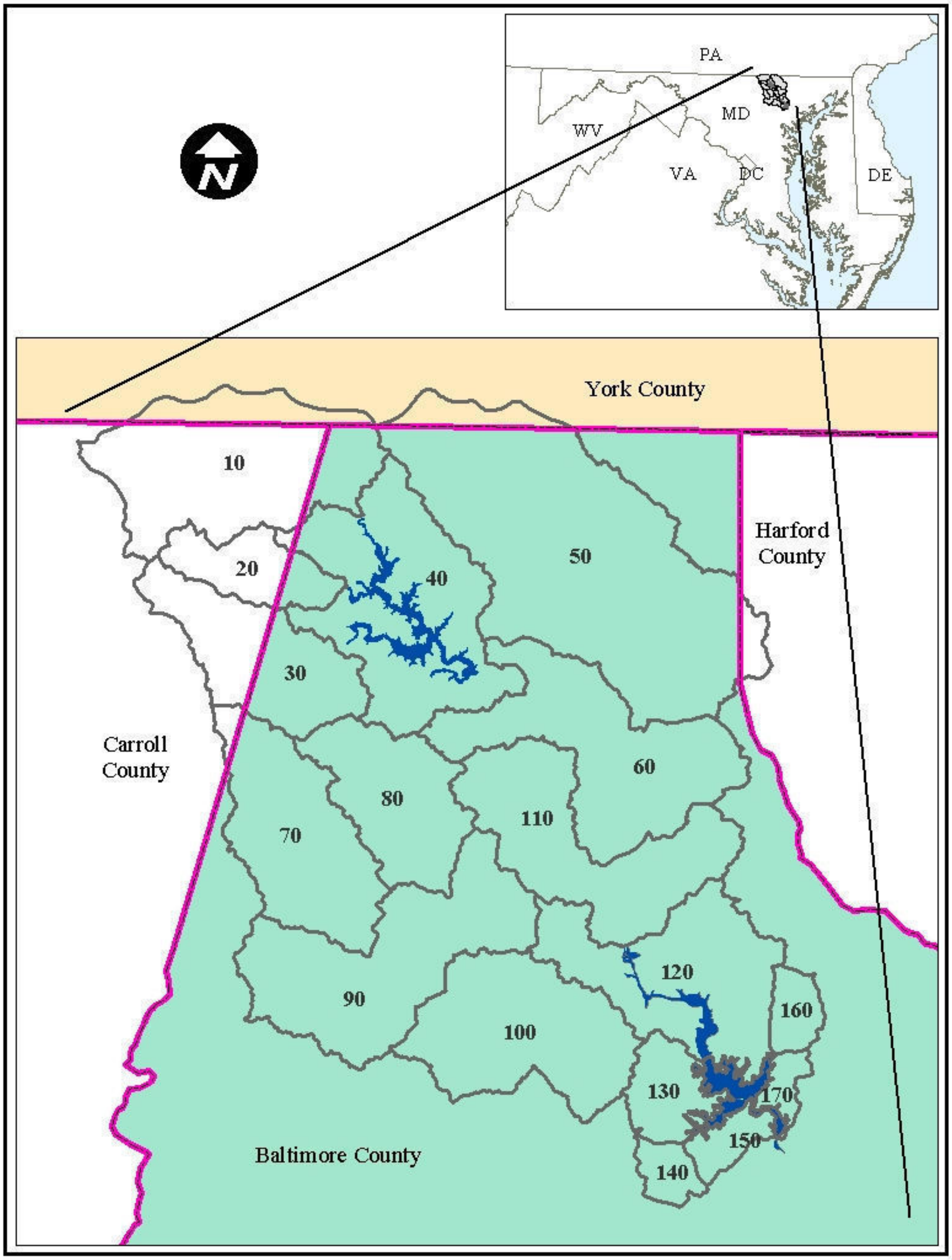

Table 1.1-1. Reservoir and Dam Characteristics (Weisberg et al. 1985)

	Prettyboy	Loch Raven
Drainage Area (mi2)	80	303
Surface Area (acres)	1500	2400
Normal Depth (ft)	98.5	76
Normal Capacity	60,100	72,700
Year Built	1936	1923
Dam Height (ft)	155	101
Crest Length (ft)	692	623
Spillway Width (ft)	274	288
Required Minimum Release	23 cfs, May-Nov.	None

Table 1.1-2. Water Quality Impairments in Prettyboy and Loch Raven Reservoirs

Name	Code	Impairment Category: Impairing Substance	Year Listed
Prettyboy Reservoir	02130806	Nutrients: Nutrients, Dissolved Oxygen	1996
Prettyboy Reservoir	02130806	Metals: Metals	1996
Prettyboy Reservoir	02130806	Metals: Methylmercury - fish tissue	2002
Loch Raven Reservoir	02130805	Nutrients: Nutrients, Dissolved Oxygen	1996
Loch Raven Reservoir	02130805	Sediments: Suspended Sediments	1996
Loch Raven Reservoir	02130805	Metals: Metals	1996
Loch Raven Reservoir	02130805	Metals: Methylmercury—fish tissue	2002
Loch Raven Reservoir	02130805	Toxics: PCBs—fish tissue	2002

Section 2. DESCRIPTION OF THE GUNPOWDER WATERSHED

2.1. BASIN CHARACTERISTICS

The Gunpowder Falls Watershed above the Loch Raven Dam is 304.0 square miles, including 79.8 square miles that lie above the dam for the Prettyboy Reservoir. Seven square miles of the watershed above Prettyboy Reservoir and 4.2 square miles below Prettyboy are in York County, PA. The remainder of the watershed lies in Baltimore, Carrol, and Harford Counties in Maryland, occupying 257.9, 33.7, and 1.3 square miles of those counties, respectively. Table 2.1-1 shows the breakdown of area of the watershed by county. Figure 2.1-1 shows the location of the watersheds with respect to the counties.

Table 2.1-1. Distribution of Watershed Area By County (in square miles) (From DEPRM, 2000)

Watershed	Baltimore	Carroll	Harford	York	Total
Prettyboy	39.9	32.8		7.0	79.8
Loch Raven	217.9	0.9	1.3	4.2	224.3
Total	257.9	33.7	1.3	11.2	304.0

South and east of Loch Raven Reservoir, in Baltimore County, suburban development dominates the watershed. The rest of the watershed in Baltimore County is largely rural. For the most part, a forest buffer protects the reservoirs, and much of the rest of the watershed is zoned to preserve its rural character. Crops and other agricultural activities account for approximately one third the land use in the watershed. The portion of the watershed in Carroll County is also predominately rural, but there is increasing development around Manchester and Hampstead as these areas become part of the Baltimore exurbs.

Figure 2.1-1. Gunpowder Watersheds and Counties

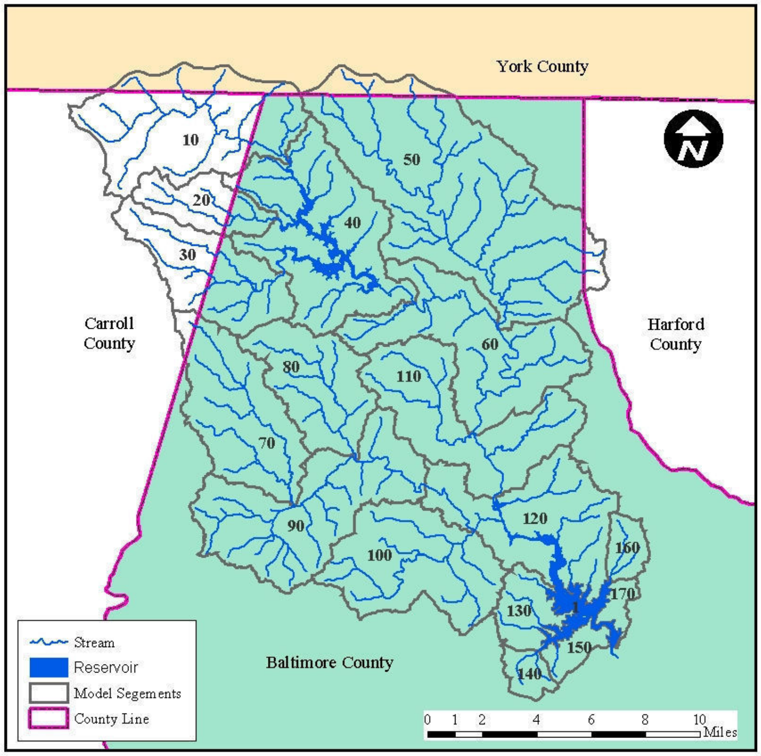

2.2. CLIMATE

The climate of the region is humid, continental with four distinct seasons modified by the close proximity of the Chesapeake Bay. Tables 2.2.-1 and 2.2-2 give the mean, minimum, and maximum monthly temperatures and average monthly precipitation at Baltimore Washington International Airport, southeast of the watershed, and Millers in Carroll County, in the northwest portion of the watershed. The prevailing direction of storm tracks is from the west-northwest from November through April with the prevailing direction shifting from the south in the month of May through September. The fall, winter and early spring storms tend to be of longer duration and lesser intensity than the summer storms. During the summer, convection storms often occur during the late afternoon and early evening producing scattered high-intensity storm cells that may produce significant amounts of rain in a short time span. Based on National Weather Service (NWS) data, thunderstorms occur approximately 30 days per year, with the majority occurring from May through August (Tetra Tech, 1997).

Table 2.2-1. Summary Statistics Meteorological Data Baltimore-Washington International Airport, 1971 – 2000

Month	Normal Maximum Temperature	Normal Minimum Temperature	Normal Temperature	Normal Monthly Precipitation
January	41.2	23.5	32.3	3.47
February	44.8	26.1	35.5	3.02
March	53.9	33.6	43.7	3.93
April	64.5	42	53.2	3.00
May	73.9	51.8	62.9	3.89
June	82.7	60.8	71.8	3.43
July	87.2	65.8	76.5	3.85
August	85.1	63.9	74.5	3.74
September	78.2	56.6	67.4	3.98
October	67	43.7	55.4	3.16
November	56.3	34.7	45.5	3.12
December	46	27.3	36.7	3.35
Annual	65.1	44.2	54.6	41.94

Table 2.2-2. Summary Statistics Meteorological Data Millers 4NE, 1971 – 2000

Month	Normal Maximum Temperature	Normal Minimum Temperature	Normal Temperature	Normal Monthly Precipitation
January	38	22.8	30.4	3.64
February	41.7	25	33.4	2.9
March	50.9	32.4	41.7	3.77
April	62.3	41.2	51.8	3.45
May	71.7	50.8	61.3	4.28
June	79.6	59.7	69.7	3.62
July	83.6	64.1	73.9	3.57
August	82.3	62.6	72.5	3.71
September	75.3	55.9	65.6	4.14
October	64.6	45.4	55	3.44
November	53.2	36.3	44.8	3.61
December	42.8	27.9	35.4	3.54
Annual	62.2	43.7	53	43.67

2.3. GEOLOGY, TOPOGRAPHY AND SOILS

The study area is in the Piedmont physiographic province. The Piedmont region is underlain by metamorphic rock of Precambrian and Cambrian age (Reybold and

Matthews 1976, Matthews 1969). Prettyboy schist is the underlying bedrock of the Prettyboy Reservoir watershed (MDE, 2004). The underlying metamorphic rock complex Loch Raven watershed below Prettyboy consists mainly of crystalline schists and gneiss with smaller areas of marble. The underlying marble formations, Cockeysville Marble and Patuxent Formation, are less resistant to weathering than the schists and gneiss and consequently occur mainly in valleys. These areas typically have higher infiltration rates and greater groundwater flow rates. This in turn makes groundwater in the Cockeysville Marble and the Patuxent Formation more susceptible to contamination. The majority of the soils overlying the bedrock in the Piedmont are seven to twenty feet deep (Tetra Tech, 1997).

The Piedmont area is strongly dissected with rolling to steep topography. The highest elevation in the study area is 1087 feet at the extreme northwestern boundary of the watershed in Pennsylvania. The lowest elevation is at the Loch Raven Dam.

Soil formation is the result of the interaction of a variety of factors, including climate, parent material, relief, time, and biota. The humid continental climate results in strong weathering and leaching of soils. These processes have depleted free carbonates, and therefore the soils are strongly acid to extremely acidic (Reybold and Matthews 1976).

The primary soil associations in the watershed are:

- Manor-Glenelg,
- Chester-Glenelg,
- Baltimore-Conestoga-Hagerstown,
- Beltsville-Chillum-Sassafras,
- Glenelg-Chester-Manor, and
- Mt. Airy-Linganore.

These soils are mainly deep and well drained to moderately well drained (Reybold and Matthews 1976, Matthews 1969). Within the stream floodplains, alluvial, Codorus and Hatboro soil series predominate.

Table 2.3-1 shows the distribution of soils in the Baltimore County portions of the watersheds by hydrologic group. Nearly 85% of the soils in the watershed below Pretttyboy Reservoir are classified as Hydrologic Group B, which means that they have low to moderate surface runoff potential, moderate infiltration rates, and moderately fine to moderately coarse soil texture (Tetra Tech, 1997).

Table 2.3-1. Distribution of Hydrologic Soil Groups in Baltimore County Portion of Prettyboy and Loch Raven Reservoir Watersheds (DEPRM, 2000)

	A	B	C	D
Prettyboy Reservoir	15.7%	73.3%	6.8%	4.2%
Loch Raven Reservoir	0.7%	86.3%	8.8%	4.2%
Total	2.9%	84.4%	8.5%	4.2%

Section 3. MODEL DESCRIPTION AND STRUCTURE OF THE GUNPOWDER WATERSHED

3.1. INTRODUCTION

The modeling framework of the Gunpowder Falls Watershed was developed primarily to provide loading estimates to the reservoir models for TMDL development, and secondarily to provide a tool to managers and planners to estimate the effects of various growth scenarios on nutrient loads. The framework consists of an HSPF (Hydrological Simulation Program—Fortran) watershed model to generate nutrient loads from the watershed subbasins, and a pair of two-dimensional CE-QUAL-W2 models to simulate hydrodynamics and water quality in Prettyboy and Loch Raven Reservoirs. The watershed model will be described in this and the following chapter. Subsequent chapters will describe the development and calibration of the reservoir models.

3.2. OVERVIEW OF THE HYDROLOGIC SIMULATION PROGRAM FORTRAN (HSPF)

The HSPF Model simulates the fate and transport of pollutants over the entire hydrological cycle. Two distinct sets of processes are represented in HSPF: (1) processes that determine the fate and transport of pollutants at the surface or in the subsurface of a watershed, and (2) in-stream processes. The former will be referred to as land or watershed processes, the latter as in-stream or river reach processes.

Constituents can be represented at various levels of detail and simulated both on land and for in-stream environments. These choices are made in part by specifying the modules that are used, and thus the choices establish the model structure used for any one problem. In addition to the choice of modules, other types of information must be supplied for the HSPF calculations, including model parameters and time-series of input data. Time-series of input data include meteorological data, point sources, reservoir information, and other type of continuous data as needed for model development.

A watershed is subdivided into model segments, which are defined as areas with similar hydrologic characteristics. Within a model segment, multiple land use types can be simulated, each using different modules and different model parameters. There are two general types of land uses represented in the model: pervious land, which uses the PERLND module, and impervious land, which uses the IMPLND module. More specific land uses, like forest, crop, or developed land, can be implemented using these two general types. In terms of simulation, all land processes are computed for a spatial unit of one acre. The number or acres of each land use in a given model segment is multiplied by the values (fluxes, concentrations, and other processes) computed for the corresponding acre. Although the model simulation is performed on a temporal basis, land use information does not change with time.

Within HSPF, the RCHRES module sections are used to simulate hydraulics of river reaches and the sediment transport, water temperature, and water quality processes that result in the delivery of flow and pollutant loading to a bay, reservoir, ocean or any other body of water. Flow through a reach is assumed to be unidirectional. In the solution technique of normal advection, it is assumed that simulated constituents are uniformly dispersed throughout the waters of the RCHRES; constituents move at the same horizontal velocity as the water, and the inflow and outflow of materials are based on a mass balance. HSPF primarily uses the "level pool" method of routing flow through a reach. Outflow from a free-flowing reach is a single-valued function of reach volume, specified by the user in an F-Table, although within a time step, the HSPF model uses a convex routing method to move mass flow and mass within the reach. Outflow may leave the reach through as many as five possible exits, which can represent water withdrawals or other diversions.

3.3. MODEL ASSUMPTIONS

The simulation of the Gunpowder Watershed used the following assumptions: (1) variability in patterns of precipitation were estimated from existing National Oceanic and

Atmospheric Administration (NOAA) meteorologic stations; (2) hydrologic response of land areas were estimated for a simplified set of land uses in the basin; and (3) agricultural information was estimated from the Maryland Office of Planning (MDP) land use data, the 1997 Agricultural Census Data, and the Farm Service Agency (FSA).

3.4. WATERSHED SEGMENTATION

The watershed model segmentation was based on several factors such as the location of flow gauges and water quality monitoring stations, the location of point sources, the location of the Prettyboy and Loch Raven reservoirs, and the scale at which land use and agricultural information was available. The basin was divided into 17 segments, with segment areas ranging from 2 to 60 mi^2 (Figure 3.4-1). Figure 3.4-1 shows the segmentation.

Figure 3.4-1. Gunpowder Watershed Model Segmentation

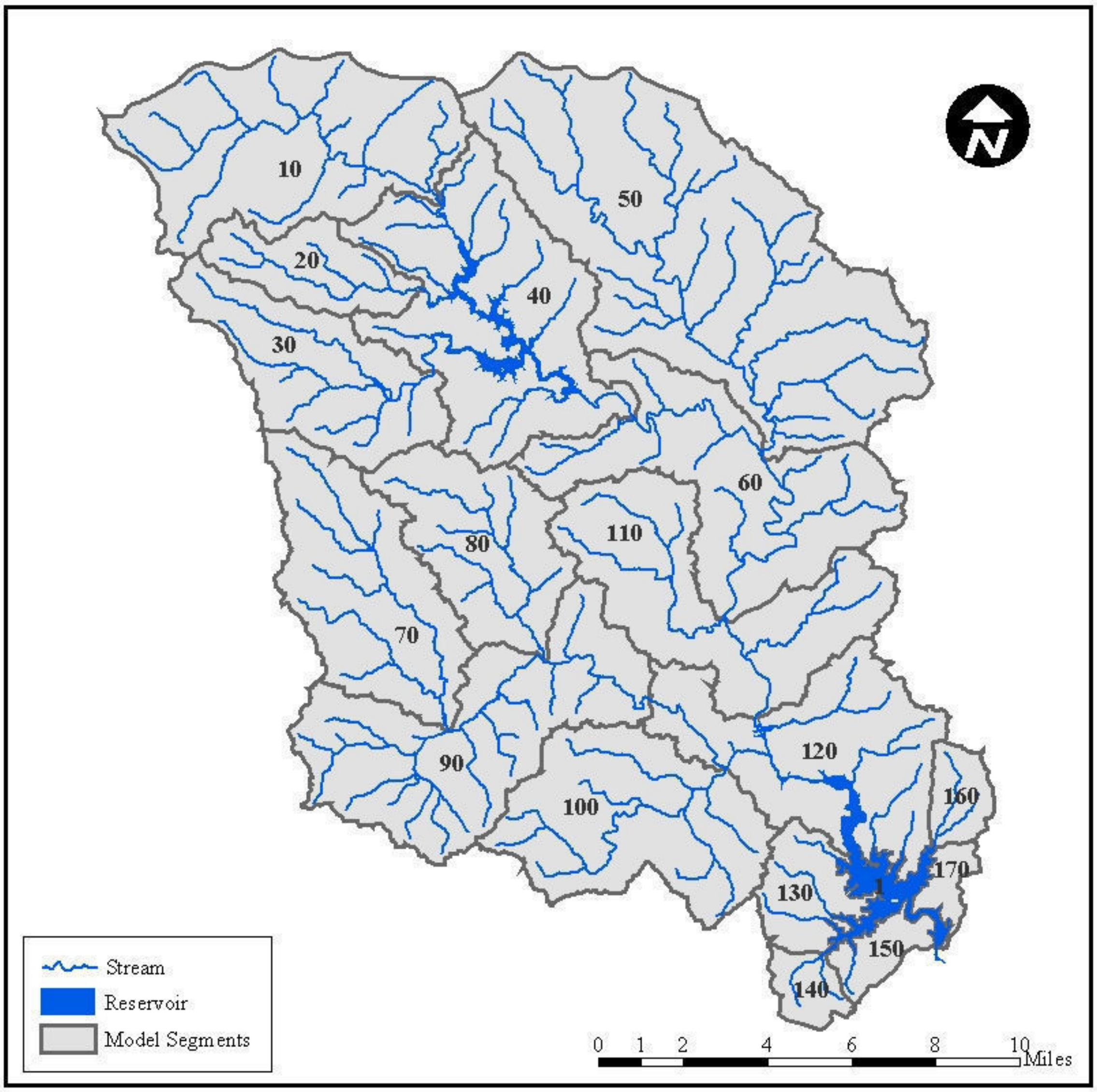

3.5. LAND USE

Land use information by model segment (Table 3.5-1) was derived from the 1994 Maryland Department of Planning (MDP) land cover database, data from the Farm Service Agency (FSA), the 1997 Agricultural Census, and information from the 1996 Conservation Technology Information Center (CTIC). Of the total area, 80.9 mi^2 drain to the Prettyboy Reservoir and 313.5 mi^2 drain to the Loch Raven Reservoir (including the drainage through the Prettyboy). A survey conducted by Maryland Department of

Agriculture (MDA) indicated that the FSA and the 1997 Agricultural Census were the most accurate agricultural information in the region. The FSA data collected at a finer resolution (of 4.32 mi^2 /cell) provided a better spatial scale to compute crop acres by model segment than the Agricultural Census, in which the information is at the county scale. The Agricultural Census was used to derive the crop types by model segment. Tillage in the crop categories was derived from information provided by the 1996 Conservation Technology Information Center (CTIC).

For modeling purposes, land categories were aggregated into five major groups: forest, agriculture, pasture, pervious urban and impervious urban.

3.5.1. Developed Land

Initial values by model segment for urban land use were obtained from the MDP database. However, these values were modified when the FSA crop acres were different from those reported by MDP. Following the practice of the Chesapeake Bay Program's Phase 4.3 Watershed Model, a positive difference between MDP and FSA values was assumed to be mixed open land. Mixed open land uses represent a mixture of several categories of anthropogenically modified open land, including low-density urban cover, horse pasture, fallow cropland or transitional agricultural land. Since it receives no identifiable sources of nutrients, it is modeled as pervious developed land.

MDP provided the percent imperviousness of the 12-digit watersheds making up the Gunpowder Falls Watershed. This percent imperviousness was applied to model segments by GIS analysis to determine the impervious land in each model segment. Table 3.5-2 gives the breakdown of pervious and impervious developed land by model segment.

3.5.2. Undeveloped Land

Undeveloped land includes forest and wetlands. These two land cover categories are simulated as forest because of HSPF limitations in simulating chemical processes in wetlands. The forest area was derived through the combination of model segmentation, MDP data, and the 1994 MRLC land cover databases.

Figure 3.5.1. Gunpowder Watershed Land Use

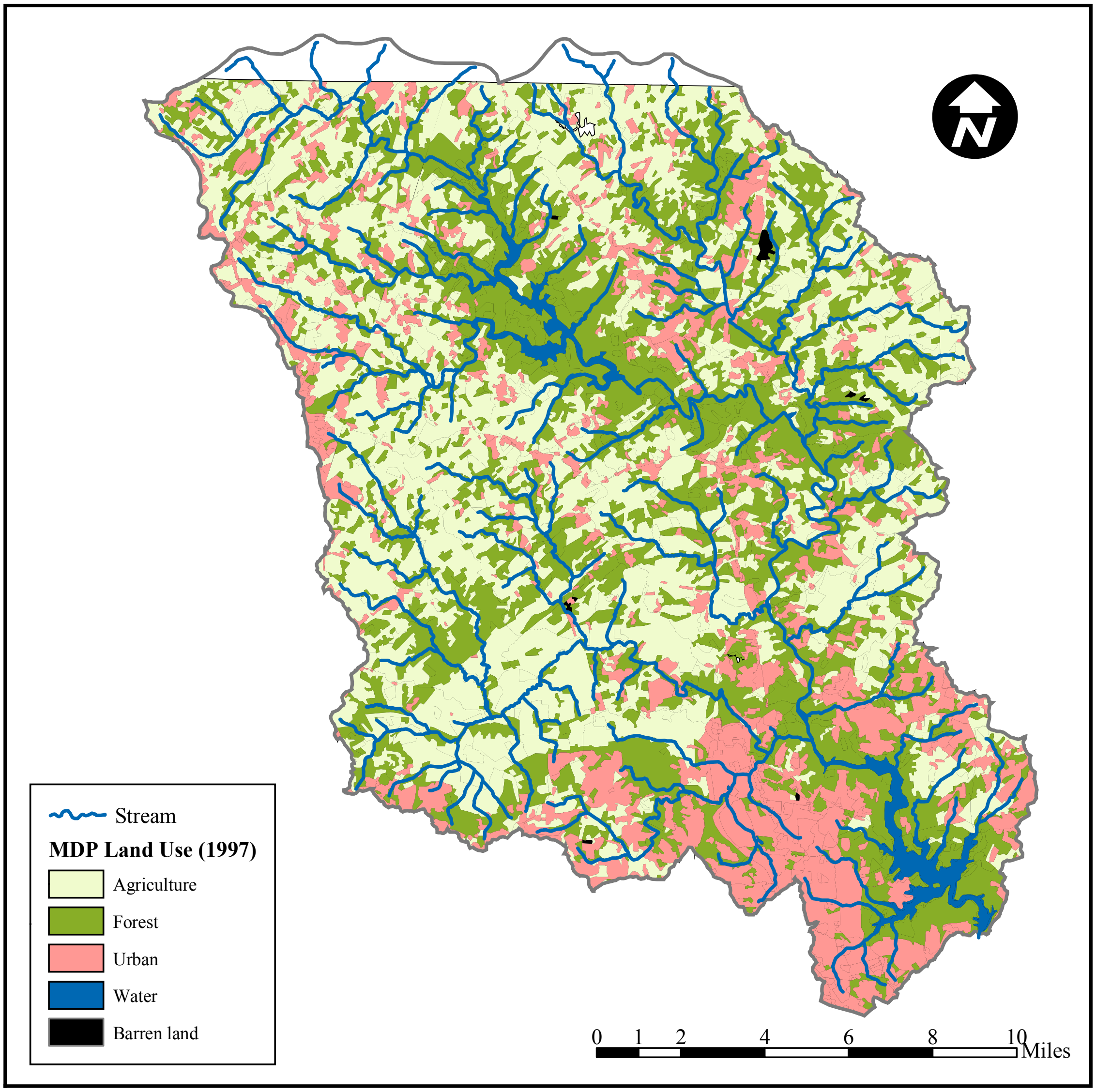

Table 3.5-1. Gunpowder Basin Land Use by Model Segment (in acres)

Segment	Developed	Forest	Crops and Hay	Mixed Open	Pasture	Vegetables
10	1,951	5,356	6,945	333	2,871	399
20	479	1,710	1,601	0	1,119	85
30	1,661	2,479	3,829	0	2,145	239
40	1,263	9,573	3,941	0	1,800	310
50	3,648	13,341	8,031	4,645	4,128	685
60	2,306	7,994	1,780	2,154	1,694	153
70	1,103	4,133	3,503	2,371	1,401	286
80	763	3,400	2,302	1,989	934	199
90	1,822	5,018	3,016	4,278	2,419	260
100	7,156	3,842	1,405	897	159	99
110	1,910	4,709	2,761	2,607	1,958	238
120	4,432	5,844	652	1,305	939	56
130	2,262	1,290	0	0	100	
140	1,459	304	0	0		
150	866	930	13	0		
160	865	534	192	225	183	
170	202	846	40	0	23	

3.5.3. Agricultural Land

In order to use the FSA information, it was necessary to develop a Geographic Information System (GIS) layer representing the FSA photographs (Figure 3.5-2). This layer was developed with information provided by the USDA office in Utah, and data provided by the Maryland counties. The county data contain the number of acres of farmland and cropland. The approximate area covered by one photograph is 4.32 mi^2/cell (2,700 acres/cell). The *total number of crop acres* by model segment was determined by overlaying the created FSA layer on top of the Watershed Model segmentation.

The term *farmland*, as used here, refers to an entire farm parcel, lot, or tract. It includes cropland, pasture, woodland, buildings (farm residence, barns, silos, covered feedlot areas), roads and ponds. The term *cropland* refers to the portion of farmland that is used to grow crops. The term *pasture* refers to open land used for grazing.

Table 3.5-2. Pervious and Impervious Developed Land by Model Segment (in acres)

Segment	Pervious	Impervious
10	1,874	78
20	440	39
30	1,525	136
40	1,209	54
50	3,358	290
60	2,136	171
70	1,068	35
80	713	50
90	1,538	284
100	5,540	1,616
110	1,717	193
120	3,915	517
130	1,958	303
140	1,263	196
150	750	116
160	719	146
170	175	27

Records of cropland were apportioned to model segments as follows:

(1) Through GIS methodologies, the photograph grid was overlaid on the model segmentation to obtain the percent of each photograph in each model segment as shown in Figure 3.5.2-2.

(2) This percent is multiplied by the total cropland in the associated aerial photograph and results in the crop-acres from that specific photograph within the segment.

(3) The total crop-acres by model segment is obtained by adding the information from step 2 in all the aerial photographs overlaying the segment.

An initial value for pasture acres was obtained directly from the MDP database. This initial value was modified by adding the acres reported in the Agricultural Census categories as *conservation reserve program* and *cover crop* acreage. The acreage for these two categories is subtracted from the FSA crop acres.

As was explained above, a positive difference between the cropacres reported by MDP and the FSA in each model segment is assumed to be mixed open land, which is modeled like pervious developed land.

Figure 3.5.2-2. Gunpowder Watershed Model Segments Overlaid by the FSA Grid

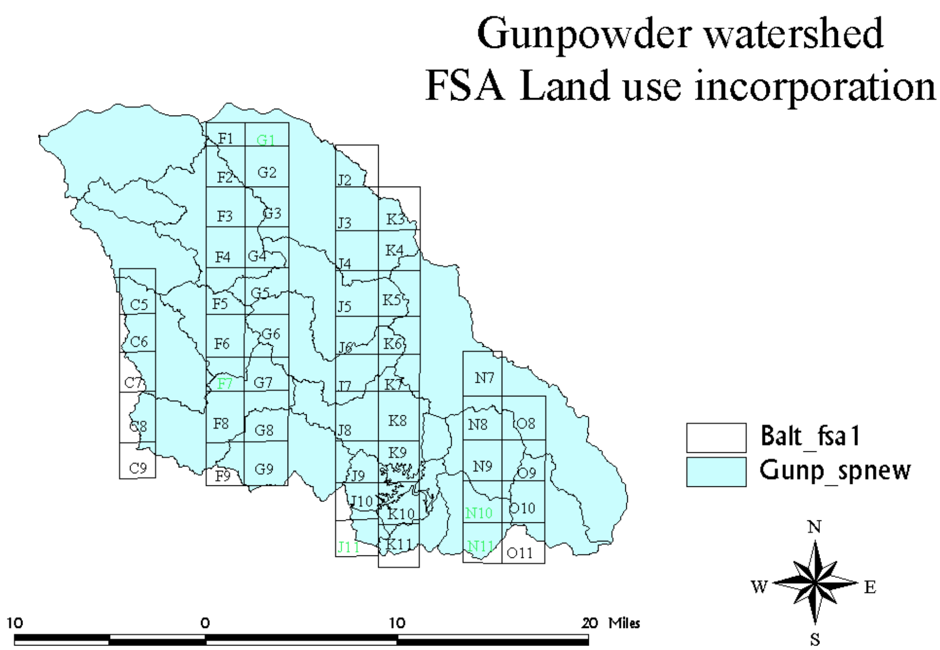

3.5.3.1. Crop and Tillage Distribution. Concerns about the simulation of agricultural land use are usually related to the development of parameters for simulated composite crops because of aggregated processes. The term *composite* denotes more than one major category within the simulated land use. For instance, a simulated composite corn category could be 50% corn and 50% wheat or winter crops. This aggregation would occur because wheat is planted during the Fall (after the corn has been harvested), and grown until Spring of the following year (before a crop of full season beans is planted). Because harvesting is not simulated in the current model framework, soil conditions are reset at the beginning of each simulation year.

The 1997 Agricultural Census information was used to determine crop type proportions, which were assumed to be uniform throughout a given county. These values were modified by the MDA intra-seasonal rotation factors, and the resulting values indicated crop types, full season (FS), and double crop (DC). Finally, values or ratio estimators were in turn used to modify corresponding CTIC crop categories to indicate tillage practices. The resulting values indicated crop type, intra-seasonal rotation, and tillage practices (no-till, mulch-till, ridge-till, and conventional-till). These ratios were applied to the total crop acres calculated from the FSA to determine the acreage of the simulated crops within the model segments. Six major categories were derived: high till corn, low till corn, full season beans, double crops, hay and vegetables. Double crops, hay and vegetables, the justification for combining was the similarity in nutrient uptakes, tillage practices, and planting time within each group.

MDA acreage data comprise managed cropland aggregated by county and differentiated into the following categories:

1. Field crops including full season (FS) and double-cropped (DC) corn, soybeans and sorghum, and spring seeded (SPSD) and fall seeded (FLSD) small grains.
2. Forage crops.
3. Other crops.
4. Newly established pasture cultivated under any of the above mentioned tillage categories.
5. Land cover including the following.
   - Fallowed land or cropland not planted during a given year as part of a crop rotation plan.
   - Annual conservation use or cropland not planted because of emergency events such as droughts or excessive precipitation.
   - Conservation Reserve Program (CRP) acreage.

The associated tillage practices include:

1. *No-till,* defined as planting seeds in a narrow slot while leaving over 90% of the soil undisturbed.
2. *Ridge-till,* defined as planting seeds in seedbeds on ridges while leaving vegetation between ridges intact.
3. *Mulch-till,* defined as limited tillage in which the soil is disturbed before planting.
4. 15-30% residue or a planting system that leaves 15-30% of the preceding vegetative cover after planting.
5. Less than 15% residue or a planting system that leaves less than 15% of the preceding vegetative cover after planting.

The apportionment of CTIC cropland was based on the assumption that the percent of acreage of the CTIC categories in each county occurred identically in each model segment. Appendix A shows the aggregation of the Agricultural Census Categories into CTIC categories, and into watershed model simulation classifications.

3.6. NON-POINT SOURCES INFORMATION

Mineral and animal waste fertilizer calculations were based on methodologies developed by the Chesapeake Bay Program Office and found in the Chesapeake Bay Program Office (CBPO) Watershed Model documentation. The University of Maryland (Wye Institute) and the MDA guided modifications to these methodologies. Nutrient application rates are based on a mass balance between the animal waste produced within each model segment and the expected average yield in the corresponding county, reported in the 1996 Maryland Statistics. The objective in developing these rates was to define information representative of field and farm practices. However, it is necessary to recognize the high degree of uncertainty in the development of nutrient balances for each cropland category.

3.6.1. Animal Counts

Animal count values used to calculate manure acres and manure available for application to cropland were derived from two primary sources. These sources were the U.S Census of Agriculture, (reported on a countywide scale) and the 1996 Animal Count Survey conducted by the Department of Agricultural Engineering (Mr. Herbert Brodie) from the University of Maryland (reported on a DNR 8-digit watershed scale). Ratio factors were derived from the survey and used to allocate county data to HSPF model segments.

3.6.2. Manure Acres

Manure acres is a derived land use which represents what is susceptible to runoff from confined animals within a model segment. The associated acres are subtracted from the pasture land use category. The animal categories used to calculate manure acres are beef and dairy cattle, swine, horses, and sheep. Because manure acres only represent what is susceptible to runoff from confined animals, animal units used in the manure acres calculation were adjusted by the percentages shown in Table 3.6.2-1, column 3 (% of time confined). Finally the adjusted animal units were divided by a “compromise animal density” of 145 animal units per acre to yield the final number of manure acres (CBP, 1994). Manure is stored and treated through the implementation of a control program; a portion of these acres will revert back to pasture acres for simulation purposes. Because control actions such as guttering, diversions, and manure containment are not totally effective, some proportion of each manure acre will remain in the manure land use to account for control efficiencies less than 100% (CBP, 1994). Following recommendation from MDA, poultry data was not used to calculate manure acres.

Table 3.6.2-1. Constants Used to Calculate Animal Units and Confinement by Animal Type

Animal Type	Animals/ Animal Unit	Percent of Time Confined	Percent of Time Unconfined
Beef	1	0.2	0.8
Dairy	0.71	0.8	0.2
Hogs	5	1.0	0.0
Chickens	250	1.0	0.0
Broilers	500	1.0	0.0
Turkeys	100	0.85	0.15
Layers	250	1.0	0.0
Sheep	5	0.5	0.5
Horses	0.855	0.5	0.5

3.6.3. Nutrient Applications

Manure applied to cropland is calculated on the assumption that manure is stored for Spring and Fall applications; manure to pasture is assumed to be uniformly applied throughout the year.

Animal count information is defined in terms of animal units using values from column 1, Table 3.6.2-1. The amount of animal waste available for application to pasture and cropland is based on the amount of time that the animals spend in confinement using columns 3 and 4 of Table 3.6.2-1. These amounts are then expressed in terms of total nitrogen (TN) and total phosphorous (TP) per animal unit, and calculated using data from Table 3.6.3-1. The constants represent the amount of nitrogen and phosphorous contained in a pound of manure by animal unit category. Once TN and TP are calculated, runoff and volatilization losses from Table 3.6.3-2 are applied to obtain the final amounts of TN and TP in lbs./yr. to be applied to pasture and cropland. The forms of nutrients simulated by the HSPF AGCHEM module include nitrate (NO3), ammonia (NH4) (adsorbed and dissolved), organic nitrogen (ORN), Orthophosphate (PO4) (adsorbed and dissolved), and organic phosphorus (ORP). Values of TN and TP are multiplied by the mass fraction values from table 3.6.3-3 to derive each of these constituents.

Mass fraction values for animal waste were obtained from the Chesapeake Bay Program office and information from MDA.

Table 3.6.3-1. Manure Constants

Animal Type	Animals/ Animal Unit	N (lb/yr)	P (lb/yr)
Beef	1	113.15	40.15
Dairy	0.71	164.25	25.55
Swine	5	153.30	58.40
Chicken	250	302.95	113.15
Layers <3	250	302.95	113.15
Broilers	500	401.5	124.50
Sheep	10	113.15	40.15
Horses	0.855	113.15	40.15
Turkeys	100	270.10	102.20

Table 3.6.3-2. Runoff Losses and Volatilization Factors

Animal Type	Storage Type	Percent Not Volatilized Or Lost To Runoff	
		N	P
Beef	Stored	0.30	0.85
Dairy	Stored	0.40	0.85
Swine	Stored	0.25	0.85
Layers >3	Stored	0.69	0.85
Layers <3	Stored	0.69	0.85
Broilers	Stored	0.60	0.85
Turkeys	Stored	0.53	0.85
Pasture – Beef	Pasture	0.30	0.85
Dairy	Pasture	0.70	0.85
Swine	Pasture	0.25	0.85
Layers < 3	Pasture	0.69	0.85
Layers < 3	Pasture	0.69	0.85
Broilers	Pasture	0.60	0.85
Turkeys	Pasture	0.53	0.85

Table 3.6.3-3. Mass Fractions Per Animal Type

Animal Type	NH4	ORN	PO4	ORP
Cattle	0.48	0.52	0.17	0.82
Poultry	0.22	0.78	0.38	0.62

The following are the assumptions made regarding pasture and cropland nutrient applications:

1. For the simulation of pasture, it is assumed that manure is the only source of fertilizer and 15% volatilization losses are applied during the model simulation.
2. Manure will only be applied up to 75% of the hi-till corn acres; the other 25% will receive mineral fertilizer. If there is not enough animal waste, mineral fertilizer will be supplemented as needed.
3. If manure is left after application to hi-till corn acres, it will be applied up to 20% of low-till corn acres.
4. If animal waste is still left, it will be applied to 10% of the double crop acres. Otherwise, 100 % of the double crop acres will receive mineral fertilizer.
5. If animal waste is still left after double crop acres have received manure, it will be allocated to full season beans for up to 50% of the expected plant uptake.
6. If additional manure is still left, it will be applied to pasture land.

The ratio of nitrogen to phosphorus in mineral fertilizer was assumed to be 5:1, except for applications to double-crops, which was assumed to be 2.5:1.

3.6.3.1. Schedule of Nutrient Applications

Manure. Manure applications were applied according to the following schedule as needed:

High till corn →	Applied to the soil surface (10%) and to the upper zone (90%).
Low till corn →	Applied to the soil surface (80%) and the upper zone (20%) layers.
Full season beans→	Applied to the surface (50%) and upper zone (50%) soil layers.
Double Crops →	Applied to the surface (10%) and the upper zone (90%) soil layers.

Table 3.6.3.1-1. Manure Applications to Crops

Crop Type	APPLICATIONS						
	March	April	May	September	October	November	December
Corn	25%	25%		10%	20%	10%	10%
Double Crops	5%	5%		20%	70%		
Full Season Beans	40%	30%	30%				
Hay	40%	30%	30%				
Vegetables	40%	30%	30%				
Pasture	X	X	X	X	X	X	X

Mineral Fertilizer

Corn→Applied daily between mid May to Mid June

20% N at planting.

100% P, 80% N: 30 to 40 days after planting.

Double crops→Applied daily throughout the month of October 10% N - 100% P

Applied daily throughout the month of February 20% N

Applied daily throughout the month of March 70% N

Full season beans→ Applied daily throughout the month of May 100%P

3.6.3.2. Recommended Applications

The recommended applications refer to the amount of fertilizer that a farmer applies and expects to be used by the crops during its growing cycle. The yield will increase or decrease from year to year based on meteorological conditions in the area. MDA, provided recommended application rates for corn; other crops application rates were based on the annual yields reported in the "*Maryland Agricultural Statistics Summary for 1996*". It was assumed that the entire basin was under nutrient management, therefore, the recommended rates were increased by only 15%.

3.6.4. Atmospheric Deposition

As part of the nutrient balance, atmospheric deposition was input in the forms of NO_3 (wet and dry), NH_4, ORN, ORP, and PO_4. This information was produced through the application of a regression model, and was obtained from the time series for the

Chesapeake Bay Watershed model, developed by the EPA-Chesapeake Bay Program office.

3.6.5. Septic Information

GIS was used to overlay the Gunpowder Watershed model segments with the DNR 12-digit watersheds. The two coverages were intersected to determine the percentage of each model segment in each 12-digit basin. The coverage resulting from this intersection was in turn intersected with the State of Maryland counties coverage to determine the percentage of the each county in each model segment. This information was used in conjunction with US Census block-group data to ascertain the number of septic units within that segment. The number of individuals using each septic unit was calculated at the county level using U.S. census data compiled by EPA (1997). The mean EPA Bay Program NO3-N loading coefficient (0.0256 lbs. per person per day) was used to generate estimated loads per model segment.

Table 3.6.5-1. Number of Septic Systems and Nitrogen Loads (Lbs/Day) by County and Model Segment

Segment	Baltimore County		Carroll County		Harford County		Total Loads
	Systems	Loads	Systems	Loads	Systems	Loads	
10	128	9.37	1209	94.64	0	0.00	104.01
20	75	5.49	326	25.52	0	0.00	31.01
30	311	22.76	1030	80.63	0	0.00	103.39
40	934	68.32	41	3.21	0	0.00	71.53
50	2,232	163.31		0.00	38	2.90	166.21
60	1,287	94.15		0.00	0	0.00	94.15
70	520	38.05	308	24.11	0	0.00	62.16
80	560	40.94	0	0.00	0	0.00	40.94
90	1,616	118.26	0	0.00	0	0.00	118.26
100	3,415	249.87	0	0.00	0	0.00	249.87
110	1,193	87.30	0	0.00	0	0.00	87.30
120	2,098	153.51	0	0.00	0	0.00	153.51
130	540	39.49	0	0.00	0	0.00	39.49
140	209	15.29	0	0.00	0	0.00	15.29
150	275	20.14	0	0.00	0	0.00	20.14
160	243	17.77	0	0.00	0	0.00	17.77
170	156	11.43	0	0.00	0	0.00	11.43
Total	23,145	1,693.49	2914	228.12	3587	273.52	2195.12

3.7. POINT SOURCES

Point Source information was obtained from Maryland's point source database, which includes elements from the Permit Compliance System (PCS). The PCS is a database management system that supports the National Pollutant Discharge Elimination System (NPDES) regulations. Quality Control is performed by MDE for municipal information, but not for industrial data. A list of the municipal facilities is shown in Table 3.7-1, while the industrial discharges are contained in Table 3.7-2. Figure 3.7-1 shows the location of point sources throughout the basin. Flow and concentrations are reported as monthly average values in units of million of gallons per day (MGD) for flow, and milligrams per liter (mg/lt.) for concentrations. This information was input into the model as a load in pounds per day (lbs./day) in a time series format for the following constituents: BOD5, TSS, DO, NH3, NO23, PO4, and FLOW. Annual loads of these constituents are contained in Table 3.7-3, and 3.7-4.

Table 3.7-1. Municipal Point Source Facilities

NPDES	NAME
MD0022446	Hampstead
MD0022578	Manchester

Table 3.7-2. Industrial Point Source Facilities

NPDES	FACILITY
MD0000174	Genstar Stone /Cockeysville
MD0000175	Genstar Stone /Cockeysville
MD0001694	Maryland Specialty Wire Inc
MD0002348	Noxell Corporation
MD0063568	Gray & Son Inc.
MD0064070	Crest Contracting Co., Inc.
MD0065901	Teledyne Energy Systems
MD0066672	McCormic & Company Inc.
MD0067113	Transcontinental Gas Pipeli
MD0067687	MD State Military Facility

Figure 3.7-1. Point Source Facilities in the Gunpowder Watershed

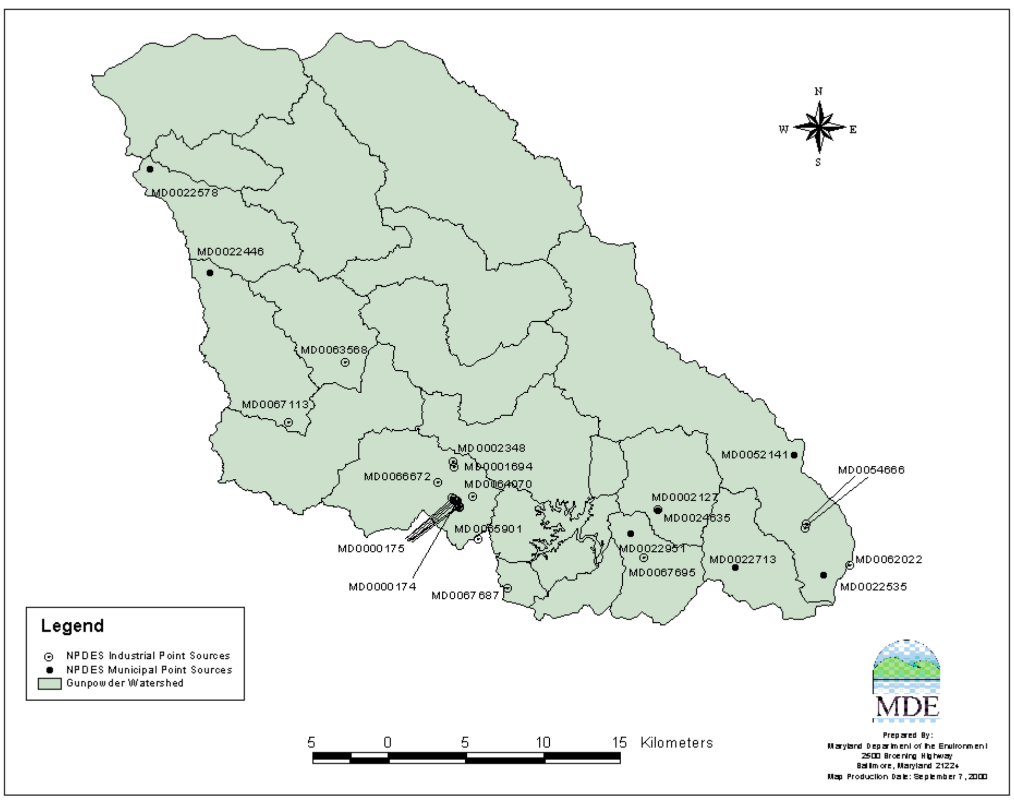

Table 3.7-3. Annual Sediment Point Source Loads by Model Segment

Units: tons/year

Segment		30	70
TSSX	1992	2.77	0.27
TSSX	1993	4.15	0.35
TSSX	1994	7.06	0.39
TSSX	1995	0.89	0.40
TSSX	1996	0.83	0.85
TSSX	1997	3.30	0.39

Table 3.7-4. Annual Point Source Loads by Model Segment and by Constituent

Units: lbs./year

Segment		30	70
BODX	1992	4,786	8,307
BODX	1993	6,721	13,854
BODX	1994	6,008	8,756
BODX	1995	1,324	9,023
BODX	1996	1,154	10,238
BODX	1997	4,826	5,296
NH3X	1992	9,704	
NH3X	1993	13,173	
NH3X	1994	12,788	
NH3X	1995	2,798	
NH3X	1996	1,909	
NH3X	1997	6,398	
NO3X	1992	1,452	25,518
NO3X	1993	1,971	24,663
NO3X	1994	2,174	21,555
NO3X	1995	317	21,898
NO3X	1996	934	27,877
NO3X	1997	3,144	26,940
ORGN	1992	3,445	2,785
ORGN	1993	4,676	2,481
ORGN	1994	4,127	2,246
ORGN	1995	613	1,927
ORGN	1996	166	2,218
ORGN	1997	556	2,518
PO4X	1992	192	276

Units: lbs./year

Segment		30	70
PO4X	1993	300	489
PO4X	1994	382	255
PO4X	1995	196	139
PO4X	1996	91	169
PO4X	1997	127	208
ORP	1992	178	173
ORP	1993	276	291
ORP	1994	370	195
ORP	1995	37	147
ORP	1996	81	107
ORP	1997	115	89
FLOW	1992	109	175
FLOW	1993	148	282
FLOW	1994	151	493
FLOW	1995	38	149
FLOW	1996	31	328
FLOW	1997	103	358

3.8. METEOROLOGIC INFORMATION AND CALIBRATION DATA

3.8.1. Meteorologic Data

After testing alternative precipitation time series in the hydrology simulation, the hourly precipitation time series for Baltimore County from Phase 5 of Chesapeake Bay Watershed Model was used in the Gunpowder Watershed Model. The results of the test are described in the following chapter. All other meteorological data except precipitation--evaporation, cloud cover, wind speed, radiation, air temperature and dew point–were obtained from BWI Airport.

3.8.2. Calibration Data

The hydrologic calibration was performed using the general guidelines described in the HSPF Application Guide (Donigian et al. 1984). The primary focus of the hydrologic calibration was on daily flow time series, monthly flow volumes, annual flow volumes, and cumulative distribution of flows for the simulation period. There are eight active United States Geological Survey stream gages in the watershed, but only four were active during the simulation period. Table 3.8-1 lists the currently active gages, their location, and their recent period of record. Figure 3.8-1 also shows the location of the active gages.

There are three primary sources of water quality data which could be used to help develop the Gunpowder Watershed Model (1) The Maryland Department of Natural Resources (DNR) maintains two CORE trend monitoring stations in the watershed and one station just below the Loch Raven Reservoir; (2) The City of Baltimore monitors stormwater and baseflow concentrations of key constituents in five reservoir tributaries; and (3) MDE, DNR, Baltimore City, and Baltimore, Harford, and Carroll Counties have jointly conducted a comprehensive study of the Gunpowder Watershed, including both stormwater and baseflow monitoring at reservoir tributaries in addition to an intensive study of the Piney Run watershed. Table 3.8.-2 shows the period of record at each monitoring station under each program. Table 3.8.-3 shows the constituents monitored by each program.

The Baltimore City monitoring program is the primary source of monitoring data during the simulation period. Table 3.8-3 gives the location of the monitoring stations and the modeling segments associated with them. Figure 3.8-1 shows the location of the monitoring stations. Table 3.8-4 shows the number of samples collected at each location during the simulation period 1992-1997. Except for Jenkins Run and Dulaney Valley Branch, two small watersheds that drain directly into Loch Raven Reservoir, monitoring stations are located at segment outlets. Four of the stations are associated with USGS gaging stations active during the simulation period.

The DNR CORE monitoring stations coincide with Baltimore City monitoring stations. Table 3.8-4 shows the number of samples collected at the DNR CORE stations during the simulation period 1992-1997. Samples are collected monthly, and there is no explicit storm flow monitoring. Table 3.8-4 also shows the number of samples collected during the simulation period for the Gunpowder Comprehensive Study (DEPRM, 2000) at the monitoring stations used by Baltimore City. The Gunpowder Study also collected monitoring data on five smaller tributaries that drain directly into Loch Raven Reservoir, at three locations in the Piney Run Reservoirs, and in Mingo Branch and Peggy Run, two small homogeneous watersheds which were used in the Piney Run Study to represent the impact of forest and agricultural land uses, respectively.

The data available in the Gunpowder Falls watershed during the simulation period is quite extensive; nevertheless, the following limitations of the available data should be recognized:

- Baltimore City did not collect storm events samples during the second half of the simulation period, 1995-1997;
- No storm sampling was performed on any Prettyboy Reservoir tributary during the simulation period, although Baltimore County began storm monitoring on Prettyboy tributaries in 2004; and

- Baltimore City did not analyze storm samples for TKN, BOD, TOC, or COD, making it difficult to estimate total loads, not just for these constituents, but for TN as well.

Summary statistics for the constituents over the simulation period can be found in Section 4.9.

Figure 3.8.2-1. Monitoring Stations in the Gunpowder Basin

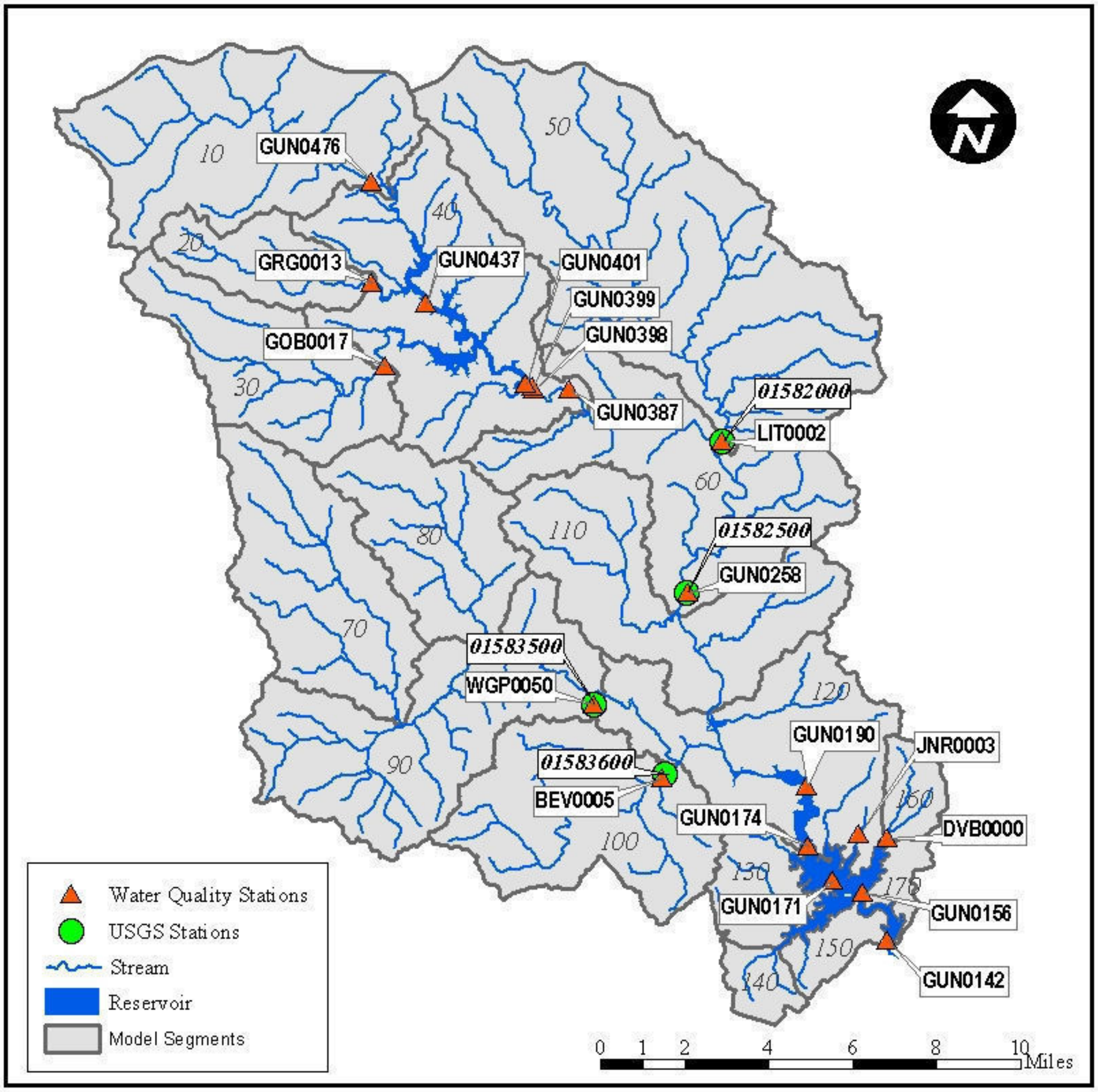

Table 3.8-1. Active USGS Gages in the Gunpowder Falls Watershed above Loch Raven Reservoir

Station Number	Name	Watershed Area (mi.^{2})	Average Flow (cfs)	Period of Record
01581810	Gunpowder Falls near Hoffmanville, MD	27.0	29.6	3/00-
01581830	Grave Run near Bekleysville, MD	7.68	8.85	3/00-
01581870	Georges Run near Beckleysville, MD	15.8	18.1	3/00-
01581920	Gunpowder Falls near Parkton, MD	81.5	88.9	7/00-
01581940	Mingo Branch near Hereford, MD	0.78	0.80	10/99-
01581960	Beetree Run at Bently Springs, MD	9.72	11.6	10/99-
01582000	Little Falls at Blue Mount, MD	52.9	68.1	6/44-
01582500	Gunpowder Falls at Glencoe, MD	160	200	12/77-6/80 12/82-
01583100	Piney Run at Dover, MD	12.3	14.1	5/82-2/88 10/96-
01583500	Western Run at Western Run, MD	59.8	68.9	9/44-
01583570	Pond Branch at Oregon Ridge, MD	0.12	0.12	1/83-9/86 4/98-
01583580	Baisman Run at Broadmoor, MD	1.47	1.18	8/64-9/69 11/99-
01583600	Beaverdam Run at Cockleysville, MD	20.9	29.8	10/82-

Table 3.8-2. Sample Collection Period for Monitoring Programs

Program	Period of Operation
DNR CORE	1985-
Baltimore City Dry Weather	1981-
Baltimore City Wet Weather	1981-1994; 1998-
Gunpowder Study	1997-1998

Table 3.8-3. Constituents Sampled by Monitoring Program

Parameter	Baltimore City Dry Weather	Baltimore City Wet Weather	DNR CORE	Gunpowder Study
Temperature	X	X	X	X
pH	X	X	X	X
Dissolved Oxygen	X	X	X	X
Suspended Sediment/TSS	X	X	X	X
Ammonia	X	X	X	X
Nitrite-Nitrate	X	X	X	X
Total Kjeldahl Nitrogen			X	X
Orthophosphate			X	X
Dissolved Phosphorus		X		
Total Phosphorus	X	X	X	X
Total Organic Carbon			X	X
BOD				X
COD				X
Chlorophyll a	X		X	X
Pheophytin			X	

Table 3.8-4. Number of Samples Collected 1992-1997 at Major Monitoring Stations In Gunpowder Falls Watershed

Station	Baltimore City Dry Weather	Baltimore City Wet Weather	DNR CORE	Gunpowder Study
BEV0005	87	106		6
DVB0000	67			
GOB0017	68			
GRG0013	68			
GUN0258	87	102	72	6
GUN0387	106			
GUN0398	60			
GUN0476	68		72	
JNR0003	30			
LIT0002	68			
WGP0050	88	114		6

Section 4. HSPF MODEL CALIBRATION/VERIFICATION IN THE GUNPOWDER WATERSHED

4.1. INTRODUCTION

To facilitate the development of the TMDLs, it was decided to preserve as much of the original HSPF model of the Gunpowder Reservoir as possible. Significant changes were made to hydrology calibration. Some of those changes were made to make the model more consistent with the parameterization of Phase 5 of the Chesapeake Bay Watershed Model, which will probably be used as the starting point for most HSPF model development in the Chesapeake Bay Watershed in the coming years. PEST, a parameter optimization software program, was also used to improve the fit between observed and simulated flows.

The primary change to the calibration of the original model was the adoption of new calibration targets for sediment and total phosphorus. The main use of the revised HSPF model of the Gunpowder Watershed is to calculate nutrient and sediment loads delivered to Prettyboy and Loch Raven Reservoirs. Given that the reservoirs have residence times on the order of months, monthly nutrient and sediment loads can serve as an appropriate calibration targets. Monthly nutrient and sediment loads for Western Run and Beaverdam Run, two key watersheds where storm monitoring data were available, were calculated using the USGS's ESTIMATOR software. The HSPF models of these watersheds were calibrated against the monthly loads from ESTIMATOR. Other portions of the Gunpowder Model were then parameterized based on the results of the calibration of Western Run and Beaverdam Run.

4.2. HYDROLOGY CALIBRATION

As described in Section 3.8, there are eight USGS gages currently operating the Gunpowder Falls Watershed. Only three of those, however, operated during the simulation period, and one of those, the Gunpowder Falls at Glencoe (01582500), is highly influenced by the management of outflows from Prettyboy Reservoir. In particular, there were no operating gages on the tributaries to Prettyboy Reservoir during the simulation period.

The simulation of any reservoir is dependent on properly simulating the inflows to the reservoir. To increase confidence in the simulation of flow to Prettyboy Reservoir, synthetic flow records were developed to represent daily flows for its main tributaries: Gunpowder Falls, Graves Run, and Georges Run. These synthetic flow records were simply an area-adjustment of the Little Falls daily flow record, which was found, after some experimentation, to have the best overall agreement with the gage record of the Prettyboy Reservoir tributaries. Table 4.2-1 shows the coefficient of determination between Little Falls flows and the Prettyboy tributaries for their periods of record. The synthetic flows were then used as calibration targets for the hydrology simulation of the Prettyboy Reservoir tributaries.

Table 4.2-1. Correlation Coefficient between Flow at Little Falls and Prettyboy Reservoir Tributaries, May 2000-Septmber 2003

Tributary	Gage	Segment	Correlation Coefficient		Area Correction
			Daily	Monthly	
Gunpowder Falls	01581810	10	0.81	0.98	0.52
Graves Run	01581830	20	0.79	0.97	0.15
Georges Run	01581870	30	0.82	0.95	0.30

In addition to the three Prettyboy tributaries, representing Segments 10, 20, and 30, the hydrology simulation was calibrated at the outlet of Segment 50, 90, and 100, representing Little Falls, Western Run, and Beaverdam Run, respectively. In contrast to the original model, there is no HSPF representation of Prettyboy Reservoir. Outflows and loads from the CE-QUAL-W2 model of Prettyboy Reservoir were input into Segment 60.

The hydrology calibrations were performed using version 5 of PEST, the model-independent parameter estimation software developed by J. Doherty (Doherty, 2001). PEST determines the values of parameters that optimize a user-specified objective function. In these simulations, the objective function was the sum of the squares of the differences between daily observed and simulated flows. This is equivalent to maximizing the coefficient of determination (R^2) between observed and simulated flows.

Table 4.2-2 gives the key parameters adjusted in hydrology calibration. Each land use represented in HSPF has its own set of hydrology parameters. Comparing observed flows to simulate flows can help determine the best values of infiltration rates and baseflow recession coefficient, but cannot, by itself, help distinguish the infiltration rates for different land uses, like forest, pasture, or cropland. In the development of the Phase 5 Watershed Model, a set of rules relating the values of calibration parameters on different land used was determined by best professional judgment. These rules were adopted for the calibration of the Gunpowder Watershed HSPF Model. The rules can be formulated in terms of the values of parameters for cropland. Table 4.2-3 gives the ratio of cropland parameters to other land uses. The seasonal distribution of monthly UZSN values, shown in Table 4.2-4, was also adopted from the Phase 5 Model. The calibration of the Gunpowder Watershed Model differed from the Phase 5 Model primarily in two respects. First, the ratio between UZSN and LZSN was allowed to vary; in the Phase 5 Model it had a fixed value for each land use. The rules specifying the variability of the ratio with land use, however, was adopted from the Phase 5 Model. These are given in Table 4.2-3. Second, the LZETP was also treated as a calibration parameter, varying monthly. Table 4.2-4 shows the monthly values of the LZETP as a function of the base rate for pasture and urban land.

The most important input to any hydrology simulation is precipitation. The hourly precipitation time series for the original Gunpowder Watershed Model used a weighted-average of observed precipitation from six stations. The weights for each modeling segments were derived from Thiessen polygons. In developing an HSPF model of the neighboring Patapsco Watershed, MDE had found that better simulation results could be found by using precipitation data from BWI Airport, despite the fact that the airport lay farther outside the watershed than other meteorological stations. Presumably, there is something to be said for the quality and consistency of meteorology data from an airport.

The USGS developed precipitation inputs for the Phase 5 Watershed Model using a set of regional regression equations that represented precipitation as a function of latitude, longitude, and elevation. The results from the regression equations were averaged over counties, which are the primary simulation unit of the Phase 5 Model. Thus hourly precipitation time series from the Phase 5 Model exist for both Baltimore County and Carroll County.

Table 4.2-2. Key Hydrology Calibration Parameters

Parameter	Description
LAND_EVAP	PET adjustment (similar to pan evaporation coefficient)
INFILT	Base infiltration rate
LZSN	Lower zone soil moisture storage index
UZSN	Upper zone soil moisture storage index
AGWR	Baseflow recession coefficient
INTFW	Ratio of interflow to surface runoff
IRC	Interflow recession coefficient
LZETP	Evapotranspiration from lower zone storage
RETSC	Impervious surface retention storage

Table 4.2-3. Ratio of Cropland Parameters to Those for Other Land Uses

Land Use	INFILT	LZSN	AGWR	INTFW	IRC	Max LZETP
Forest	1.6	1.0	1.0	1.25	1.0	1.1
Grasses	1.0	1.0	1.0	1.0	1.0	1.0
Pervious Urban	0.8	1.0	1.0	1.0	1.0	1.0

Table 4.2-4. Monthly Hydrology Parameters

Month	Fraction Max Crop UZSN	Fraction Max Crop LZEPT	Grassland Base and Winter LZEPT	Forest Base and Winter LZEPT
Jan	0.6	0.6	0.1	0.1
Feb	0.6	0.6	0.1	0.1
Mar	0.6	0.6	0.1	0.1
Apr	0.6	0.6	Base	0.1
May	0.6	0.6	Base	Base
Jun	0.7	0.7	Base	Base
Jul	0.95	0.95	Base	Base
Aug	1.0	1.0	Base	Base
Sep	1.0	1.0	Base	Base
Oct	0.8	0.8	Base	Base
Nov	0.7	0.7	Base	0.1
Dec	0.65	0.65	0.1	0.1

PEST was run using hourly precipitation from (1) the original Gunpowder model, (2) BWI Airport, and (3) Baltimore County for hydrology simulation of Little Falls, Western Run, and Beaverdam Run. The Phase 5 Carroll County precipitation data were substituted for the BWI data in similar simulation experiments for Gunpowder Falls, Graves Run, and Georges Creek. For the most part, the Phase 5 data for Baltimore County tended to give the best results and were therefore used to simulate all segments in the model. Table 4.2-5 shows the coefficient of determination for each of these simulation trials.

Table 4.2-6 gives the final hydrology simulation parameters used in the simulation. Table 4.2-7 shows the coefficient of determination for monthly flows, the overall bias, and storm flow and low flow volumes, as represented by the sum of flows greater than 90th percentile and less than the 50th percentile flows. Appendix B shows, for each calibration station, (1) time series of simulated and observed daily flows, (2) scatter plots of daily flows, (3) scatter plots of monthly flows, and (4) comparative empirical cumulative distribution of flows over the simulation period. The model tends to slightly over-simulate base flow and under-simulate some medium-sized storms, but generally, it compares well with observed flows. Table 4.2-8 compares the coefficient of determination for daily and monthly flows for current model and the original. The current model is an improvement on the original calibration.

Table 4.2-5. Coefficient of Determination for Hydrology Calibration with Alternative Precipitation Time Series

Segment	Original	Phase 5 Watershed Model Baltimore County	BWI Airport	Phase 5 Watershed Model Carroll County
10	0.69	0.73		0.72
20	0.69	0.72		0.71
30	0.62	0.67		0.76
50	0.74	0.73	0.69	
90	0.62	0.72	0.65	
100	0.66	0.73	0.65	

Table 4.2-6. Hydrology Calibration Parameter Values

Parameter	Segments					
	10	20	30	50	70-90	100
LAND_EVAP	0.9	0.9	0.9	1.0	1.0	1.0
CCFACT	0.454	0.482	0.421	0.395	0.485	0.372
INFILT	0.142	0.142	0.116	0.284	0.144	0.135
LZSN	5.08	5.02	5.10	5.11	9.0	5.00
UZSN	0.916	0.878	1.01	0.504	0.918	0.735
AGWR	0.992	0.992	0.992	0.991	0.992	0.992
INTFW	1.087	1.309	1.328	0.329	0.557	0.900
IRC	0.725	0.634	0.547	0.725	0.766	0.603
LZETP	0.437	0.445	0.794	0.360	0.463	0.377
RETSC	0.002	0.002	0.002	0.1	0.1	0.1

Table 4.2-7. Hydrology Calibration Results

Statistic	Segments					
	10	20	30	50	70-90	100
Water Balance	100%	100%	101%	99%	100%	95%
Flows < 50^{th} Percentile	116%	115%	116%	114%	119%	105%
Flows > 90^{th} Percentile	92%	93%	96%	86%	89%	94%
Daily R^2	0.73	0.72	0.67	0.72	0.72	0.71
Monthly R^2	0.89	0.89	0.93	0.91	0.90	0.84

Table 4.2-8. Comparison of Coefficients of Determination from Original and Current Calibrations

Watershed	Segment	Gage	Original		Current	
			Daily	Monthly	Daily	Monthly
Little Falls	50	01582000	0.60	0.71	0.72	0.91
Western Run	70-90	01583500	0.55	0.80	0.72	0.90
Beaverdam Run	100	01583600	0.63	0.76	0.71	0.84

4.3. TEMPERATURE CALIBRATION

Inflow temperatures are an important factor in determining temperature dynamics and the dynamics of stratification in reservoirs. PEST was again used to help calibrate the simulation of water temperatures in river reaches. Because temperature can vary considerably during the day, the objective function used in the calibration was the sum of the differences between observed and simulated hourly temperatures. Table 4.3-1 shows the parameters varied during the calibration. Table 4.3-2 shows the final calibration parameters for each reach with temperature monitoring data on it. Table 4.3-2 also shows the coefficient of determination between observed and simulated hourly temperature at the calibration points.

Table 4.3-1. Temperature Calibration Parameters

Parameter	Description
CFSAEX	Solar radiation correction factor; fraction of exposed reach surface.
KATRAD	Longwave radiation coefficient.
KCOND	Conduction convection heat transport coefficient.
KEVAP	Evaporation coefficient.

Table 4.3-2. Temperature Calibration Parameter Results

	Segment					
Parameter	10	20	30	50	90	100
CFSAEX	0.465	0.216	0.135	0.935	0.291	0.255
KATRAD	20.0	14.6	17.3	20.0	14.545	16.3
KCOND	20.0	7.56	18.5	20.0	8.11	6.54
KEVAP	5.561	1.0	1.38	10.0	1.0	1.27
R^2	0.92	0.95	0.92	0.92	0.95	0.92

4.4. CALIBRATION TARGETS FOR THE SEDIMENT AND NUTRIENT CALIBRATIONS

4.4.1. ESTIMATOR and Monthly Load Calibration Targets

The primary purpose of the Gunpowder Watershed HSPF Model is to calculate nutrient and sediment loads to Prettyboy and Loch Raven Reservoirs for use in TMDLs. As will be shown in later chapters, phosphorus is the limiting nutrient in both reservoirs, and their nutrient TMDLs will be expressed in total phosphorus. Storm-driven sediment loads will transport much of the phosphorus loads to the reservoirs; Loch Raven Reservoir also has a sediment impairment that will be addressed by a sediment TMDL. It is important, therefore, that the Gunpowder Watershed Model represent storm loads of phosphorus and sediment accurately.

It is difficult to determine, however, the nutrient and sediment loads in storms, unless continuous monitoring is performed, because storm concentrations of nutrients and sediments are highly variable. It is generally agreed that concentrations of sediment and total phosphorus increase with flow. Concentrations vary, however, both between storms and within storms. Statistical inference is therefore necessary to determine storm loads from monitoring data.

The USGS has developed the software program, ESTIMATOR, for that purpose. ESTIMATOR calculates daily, monthly, or annual constituent loads based on observed daily average flows and grab-sample monitoring data. ESTIMATOR has been used to calculate nutrient and sediment loads for the RIM (River Input Monitoring) program for the Chesapeake Bay Program, as well as estimate sediment and nutrient trends in the region. Cohn et al. (1989) and Cohn et al. (1992) give the theory behind ESTIMATOR. Langland et al. (2001, 2005) demonstrate the application of ESTIMATOR in the Chesapeake Bay Watershed.

ESTIMATOR contains three elements. The heart of ESTIMATOR is a multiple regression equation which relates the log of constituent concentrations to flow, time and season. The equation for C, the constituent concentration, takes the following form:

$$\ln[C] = \beta_0 + \beta_1 \ln[Q] + \beta_2 \ln[Q]^2 + \beta_3 T + \beta_4 T^2 + \beta_5 \sin[2\pi T] + \beta_6 \cos[2\pi T] + \varepsilon$$

Where

Q is the daily discharge
T is time, expressed in years

The flow and time variables are centered so that terms are orthogonal. Regression relation is essentially a multivariate rating curve, which takes into account temporal trends and seasonal trends as well as trends in flow.

The second element is the use of a minimum variance unbiased (MVUE) procedure to obtain estimates of concentrations and loads from the log of constituent concentrations determined from the regression. Cohn et al. (1989) describe the motivations for using the MVUE procedure, as opposed to simpler methods.

The transformed constituent concentrations are combined with daily flows to estimate daily, monthly, and annual loads. Standard errors, confidence intervals, and standard errors of prediction can also be calculated.

In order for ESTIMATOR to provide good estimates of nutrient and sediment loads, monitoring data must be available over the range of flows for which loads are to be calculated. In particular, there must be monitoring data taken during storm events. As noted in Section 3.8, both the City of Baltimore, and, more recently, Baltimore County have performed storm sample monitoring in the Gunpowder Falls Watershed. Three monitoring locations are on reaches represented in the model: Western Run, Beaverdam Run, and Gunpowder Falls at Glencoe. The Gunpowder Falls location is below Prettyboy Reservoir and is subject to the influence of the management for the reservoir. The same flow could occur (1) when only the minimum flow requirements are met, (2) when water is being deliberately released from Prettyboy to refill Loch Raven Reservoir, or (3) when flow is overtopping the spillway at Prettyboy. These different management scenarios make it difficult to treating the monitoring results from Gunpowder Falls as representative of a homogeneous watershed, so ESTIMATOR was not used to calculate loads at that location.

ESTIMATOR was used to calculate suspended sediment, total phosphorus, ammonia, and nitrate loads for Western Run and Beaverdam Run. Generally, the procedures outlined in, Langland et al.(2004), which describes how ESTIMATOR was used to determine annual loads for the RIM program, were used to estimate loads for the Gunpowder Falls watersheds. In particular, data from 1985 to 2003 were used in estimating the regression equations.

Table 4.4-1 and 4.4-2 show the regression parameter estimates and statistics for the ESTIMATOR regression equations for Western Run and Beaverdam Run, respectively. Generally, the statistics show the regression results are acceptable, though serial correlation remains a problem, as it often is in regressions which use multiple grab samples from storm events.

4.4.2. Edge-of-Field and Edge-of-Stream Calibration Targets

The monthly ESTIMATOR loads provide calibration targets for river reaches and therefore for the watersheds as a whole. Edge-of-field (EOF) and Edge-of-stream (EOS) concentration or load targets help determine the contribution of individual land uses to the watershed load. The EOS load is the load delivered to the represented river or stream from the land segments. EOF loads represent the load leaving a field. It is primarily used to characterize sediment loads, since sediment losses can be measured from a field and losses from a field can be estimated using accepted techniques like the Universal Soil Loss Equation (USLE) or its descendent, the revised Universal Soil Loss Equation (RUSLE). Not all of the EOF sediment load is delivered to the stream or river. Some of it stored on fields down slope, at the foot of hillsides, or in smaller rivers or streams that are not represented in the model. The ratio of the sediment load at a watershed outlet to the

EOF load generated in the watershed is the sediment delivery ratio. The EOS sediment load can therefore be represented as the product of the EOF load and the sediment delivery ratio.

Table 4.4-1. Coefficients of Regression Equation and Regression Statistics, Western Run

Coefficient or Statistic	Suspended Sediment	Total Phosphorus	Ammonia	Nitrate
Constant	3.54	-2.43	-3.09	1.05
Log Flow	1.43	0.96	0.67	-0.10
Log Flow^2	-0.07 *	-0.05 *	-0.05 *	-0.04
Time (years)	-0.043	-0.04	-0.05	0.01
Time^2	0.00	0.01	0.00 *	0.00
Sin (2π*Time)	-0.34	-0.35	0.04 *	0.04
Cos(2π*Time)	-0.75	-0.42	-0.21	0.09
Standard Error of Regression	1.26	0.87	0.96	0.21
Number of Observations	678	490	484	458
Coefficient of Determination	0.50	0.50	0.33	0.27
Serial Correlation Coefficient	0.58	0.52	0.44	0.46
Probability Plot Correlation Coefficient	0.99	1.00	1.00	0.97
Average Annual Load (tons)	11051	12	6	232

* Not significant at 0.05

Table 4.4-2. Coefficients of Regression Equation and Regression Statistics, Beaverdam Run

Coefficient or Statistic	Suspended Sediment	Total Phosphorus	Ammonia	Nitrate
Constant	3.39	-2.64	-2.70	0.49
Log Flow	1.54	0.96	0.41	-0.24
Log Flow^2	-0.36	-0.12	-0.05 *	0.03 *
Time (years)	-0.07	-0.03	-0.06	-0.00 *
Time^2	0.01	0.01	-0.01	-0.00
Sin (2π*Time)	-0.29	-0.25	0.12 *	0.08
Cos(2π*Time)	-0.53	-0.34	0.12 *	0.06
Standard Error of Regression	1.47	0.92	1.01	0.36
Number of Observations	728	530	523	488
Coefficient of Determination	0.52	0.51	0.29	0.26
Serial Correlation Coefficient	0.45	0.40	0.43	0.43
Probability Plot Correlation Coefficient	1.00	1.00	1.00	0.97
Average Annual Load (tons)	3696	5	4	62

* Not significant at 0.05

Agricultural EOF load targets were based on National Resource Inventory's (NRI) estimated average annual erosion rates for cropland and pasture for Baltimore County. These same erosion rates were used as the target erosion rates for the Phase 5 Watershed Model. Target erosion rates for forest and hay were taken from the Phase 4.3 Watershed Model. Table 4.4-3 shows the target erosion rates for these land uses.

Table 4.4-3. Average Annual EOF Erosion Rates by Land Use

Land Use	EOF Erosion Rate (tons/yr)
Conventional Till	12.5
Conservation Till	7.5
Hay	3.2
Pasture	1.3
Forest	0.34

EOS loads for these land uses were determined by applying a sediment delivery ratio based on watershed size, using the following formula:

Sediment Delivery Ratio = $0.417762 * (\text{Watershed Area})^{-0.134958} - 0.127097$
(SCS,1983)

Table 4.4-4 gives the sediment delivery ratio for each segment. The relevant area was taken to be either the calibration point for the segment or the reservoirs themselves.

Calibration targets for developed land were derived from average event mean concentrations reported for monitoring performed as part of the Phase I MS4 permits for Maryland counties. Table 4.4-5 gives the average EMCs for modeled constituents. Total Kjeldahl Nitrogen, and not ammonia, was monitored for stormwater NPDES permits; it was assumed that 10% of TKN was ammonia. The EMCs were used to derive calibration target annual average loads by multiplying the EMC by the average annual runoff, as simulated in the model. Pervious and impervious land had the same calibration targets, with one exception: a sediment delivery ratio was applied to loads from pervious developed land in rural areas. In more developed areas, a sediment delivery ratio was not applied, and a sediment delivery ratio was never applied to impervious developed land, whether in rural or suburban areas. Table 4.4-5 classifies subwatershed as rural or suburban.

Table 4.4-4. Sediment Delivery Ratios

Segment	Area (mi.^{2})	SDR	% Urban	Class
10	27.3	0.14	13%	Rural
20	7.7	0.19	10%	Rural
30	15.8	0.16	16%	Rural
40	25.9	0.14	8%	Rural
50	52.8	0.12	25%	Rural
60	24.9	0.14	28%	Rural
70	19.5	0.15	28%	Rural
80	14.7	0.16	29%	Rural
90	25.9	0.14	37%	Rural
100	21.0	0.15	60%	Developed
110	21.8	0.15	33%	Rural
120	20.6	0.15	44%	Rural
130	5.7	0.20	62%	Developed
140	2.8	0.24	85%	Developed
150	3.5	0.23	40%	Rural
160	3.1	0.23	55%	Developed
170	1.9	0.26	20%	Rural

Table 4.4-5. Average EMCs Derived From Maryland NPDES Stormwater Permits (Bahr, 1997)

Constituent	Average Event Mean Concentration (mg/l)
Total Suspended Solids	66.6
Total Phosphorus	0.33
Nitrate	0.85
TKN	1.94
BOD	14.44

As will be explained below, with the exception of baseflow TP loads from forest, there were no explicit EOF or EOS calibration targets on forest or agricultural land for constituents other than sediment. As will also be explained below, implicit targets were set for forest and pasture runoff loads based on soil phosphorus concentrations.

4.5. IMPLEMENTATION OF SEDIMENT AND NUTRIENT DYNAMICS IN THE GUNPOWDER WATERSHED HSPF MODEL

HSPF is a modular simulation program. The user can choose how to simulate constituents by turning modules on off. Table 4.5-1 lists the relevant modules available in HSPF.

In simulating nutrients, the primary choice is between using the PQUAL module or the AGCHEM modules, NITR and PHOS. The PQUAL module simulates user-specified constituents. The concentration of the constituent in eroded sediment, interflow, and baseflow is fixed by the user. The concentration of the constituent in runoff is determined by a simple build-up, wash-off model, which can also take into account the decay of the constituent on the land surface. In the AGCHEM modules, on the other hand, the nitrogen and phosphorus species are defined in the model. The AGCHEM modules keep a mass balance of nitrogen and phosphorus. Inputs, losses, and the transformation of one species to another are all explicitly simulated.

Table 4.5-1. Description of HSPF Subroutines

Subroutine	Description
MSTLAY	Solute transport (pervious land)
PQUAL	Build-up, wash-off, decay of constituent on surface; Fixed monthly concentrations in subsurface. For PERLND (pervious land)
IQUAL	Build-up, wash-off, decay of constituent on surface. For IMPLND (impervious land)
NITR	Full mass balance: nitrification, mineralization, vegetation uptake and cycling.
PHOS	Full mass balance: sorption, mineralization, vegetation uptake and cycling.
SEDMNT	Detachment, washoff, and storage of sediment. For PERLND (pervious land).
SOLIDS	Accumulation and washoff of solids. For IMPLND (impervious land).
NUTRX	Transformation of inorganic nitrogen and phosphorus by nitrification, denitrification, sorption, deposition, and scour.
OXRX	Oxygen dynamics: rearation, BOD decay.
PLANK	Phytoplankton dynamics and organic nutrient cycling.
SEDTRN	Deposition, scour and transport of sediment.

Following the CBP Phase 4.3 Watershed Model and previous MDE HSPF models, the AGCHEM module NITR was used to simulate nitrogen species on all pervious land uses. PHOS, on the other hand, was used to simulate phosphorus species on crops and hay;

PQUAL was used to simulate phosphorus on forest, pasture, and pervious developed land. IQUAL, the impervious equivalent to PQUAL, is the only choice for simulating nutrients on impervious surfaces. Full nutrient cycling of inorganic and organic nutrient species, including plankton dynamics, was simulated in river reaches. Table 4.5-2 summaries the constituents simulated and the modules used to simulate them.

Nutrient losses are a small fraction of nutrient inputs from fertilizer, manure, and atmospheric deposition, and crop uptake. Chapter 3 described how nutrient inputs were calculated. Crop uptake rates were based on established literature values and local crop yields. The rate of the loss of nutrients in sediment, runoff, interflow, and base flow is fairly insensitive to model parameters, once input loads and crop uptake targets are fixed. For that reason, it was decided not to set explicit calibration targets for AGCHEM modules or adjust model parameters unless loss rates were significantly at variance with the results of the original model.

Table 4.5-2 HSPF Subroutines Used in the HSPF Model by Land Use and Constituent

Land Use	Ammonia	Nitrate	Organic N	Total P	BOD	DO	Chla	Sediment
Cropland	NITR	NITR	NITR	PHOS	PQUAL			SEDMNT
Pasture	NITR	NITR	NITR	PQUAL	PQUAL			SEDMNT
Forest	NITR	NITR	NITR	PQUAL	PQUAL			SEDMNT
Pervious Urban	PQUAL IQUAL	PQUAL IQUAL	PQUAL IQUAL	PQUAL IQUAL	PQUAL IQUAL			SEDMNT SOLIDS
Impervious Urban	PQUAL IQUAL	PQUAL IQUAL	PQUAL IQUAL	PQUAL IQUAL	PQUAL IQUAL			SEDMNT SOLIDS
River Reach	NUTRX	NUTRX	PLANK	NUTRX PLANK	OXRX	OXRX	PLANK	SEDTRN

Model parameters can and do affect the speciation of nutrients lost from pervious land. Nutrient speciation, however, has added complications for the following three reasons:

1. The reservoir TMDLs will be expressed in terms of total phosphorus. It is therefore important to preserve a mass balance of total phosphorus throughout the simulation.

2. There is mismatch between the nutrient species simulated in NITR and PHOS modules for pervious land and the nitrogen and phosphorus species simulated in river reaches. NITR simulates labile organic nitrogen; PHOS simulates organic phosphorus in total and only as attached to sediment; NUTRX does not explicitly simulate labile organic nitrogen or phosphorus although they are implicitly simulated as part of the BOD state variable.

3. THE CE-QUAL-W2 does not simulate organic nitrogen or organic phosphorus as separate state variables; it simulates organic matter in various forms (labile, refractory, particulate, and dissolved) with fixed stoichiometry of nitrogen and phosphorus, and BOD, also with fixed stoichiometry of nitrogen and phosphorus.

Because of these constraints, and because lack of storm event monitoring samples precludes calibrating the model for organic nitrogen and BOD, the inputs of organic matter to the reservoir were set in the following way:

1. All organic matter inputs were calculated on the basis of organic phosphorus.

2. Organic phosphorus from the land simulation was divided between BOD and organic refractory phosphorus (ORP) in the river reaches. BOD was used to represent dissolved organic matter and ORP was used to represent particulate organic matter.

3. The oxygen content of BOD was determined by comparison with limited in-stream monitoring data; the oxygen content of ORP was determined by the reservoir DO calibration.

4. Organic nitrogen, although simulated, was not used to calculate input loads to the reservoir models.

5. The nitrogen content of the simulated organic matter entering the reservoir was determined by setting the stoichiometry of the reservoir organic matter.

The matching of HSPF nutrient species outputs to QUAL-W2 inputs is described in more detail in the following chapter.

4.6. SEDIMENT CALIBRATION

The sediment calibration focused on Western Run and Beaverdam Run, the two sub-watersheds where storm data in any quantity existed and for which monthly ESTIMATOR loads could be calculated. Since the EOF load targets and sediment delivery ratios fix the loads that are delivered to the reaches, only the calibration of in-stream processes remained.

It was also assumed that clays would erode from banks and bed at approximately the 99th percentile flow and silts would only erode at the 99.9th percentile flow or greater in Western Run, while in Beaverdam Run, a more developed watershed, clay erosion occurred at the 95th percentile flow and silt erosion occurred at the 99th percentile flow. The erosion rate was then adjusted so that the simulated average annual sediment loads in these two watersheds matched the average annual sediment load for the simulation period derived from ESTIMATOR.

Figures 4.6-1 and 4.6-2 show time series plots and scatter plots comparing ESTIMATOR and HSPF loads for Western Run on a monthly basis. Figures 4.6-3 and 4.6-4 show the same plots for Beaverdam Run. Generally, the plots show that the calibration captures a good deal of inter-annual and inter-monthly variation in sediment loads, as predicted by ESTIMATOR. A majority of modeled loads are with the corresponding 95th percent confidence intervals for ESTIMATOR's predictions, which admittedly are rather broad.

Table 4.6-1 summarizes the results of the sediment calibration. Average annual sediment loads, as simulated by the model, match loads from ESTIMATOR within 10%. The coefficient of determination for annual loads shows that the model captures a good deal of the inter-annual variability of sediment loads. The model also distributes loads within years similarly to ESTIMATOR, as shown by the coefficient of determination for monthly loads.

In Beaverdam Run, net in-stream scour accounts for about 35% of the total load, Western Run experiences net deposition of about 11%. The results from the Western Run and Beaverdam Run simulations were then used to develop calibration rules for watersheds without storm data. Western Run was used as the model for the rural watersheds (see Table 4.4-5). The following rules were applied:

- In-stream erosion of fine sediment is approximately 12% of the EOS load;
- Erosion of clays occurs above the 99% flow; and
- Erosion of silts occurs above the 99.9% flow.

For more urbanized watersheds, the calibration of Beaverdam Run was used as a model. These watersheds do not have reaches. The following rules were applied:

- In-stream erosion of fine sediment is approximately 35% of the total load;
- Erosion of clays occurs above the 95% flow; and
- Erosion of silts occurs above the 99% flow.

Table 4.6-1. Summary Statistics for Sediment Calibration

Statistic	Western Run	Beaverdam Run
Average Annual Load (tons/year) ESTIMATOR Model 1992-1997	11,051	2,696
Average Annual Load (tons/year) HSPF1992-1997	11,384	3,874
Net Scour (tons/year)	8,614	1,476
Coefficient of Determination for Monthly Loads	0.72	0.50

Figure 4.6-1. Time Series of ESTIMATOR and HSPF Monthly Sediment Loads (tons), Western Run

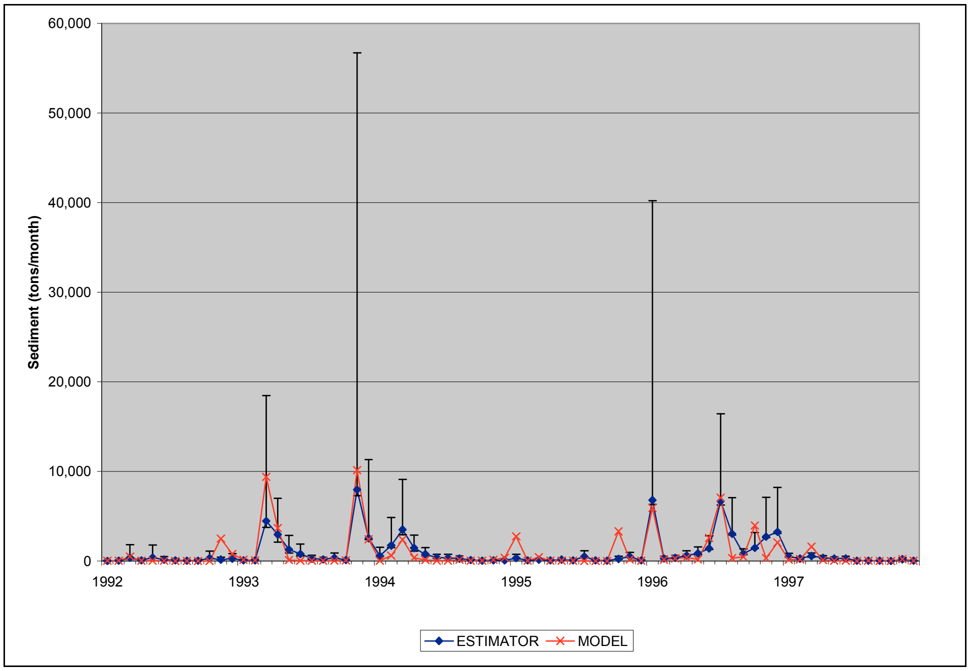

Figure 4.6-2. Scatter Plot of ESTIMATOR and HSPF Monthly Sediment Loads (tons), Western Run

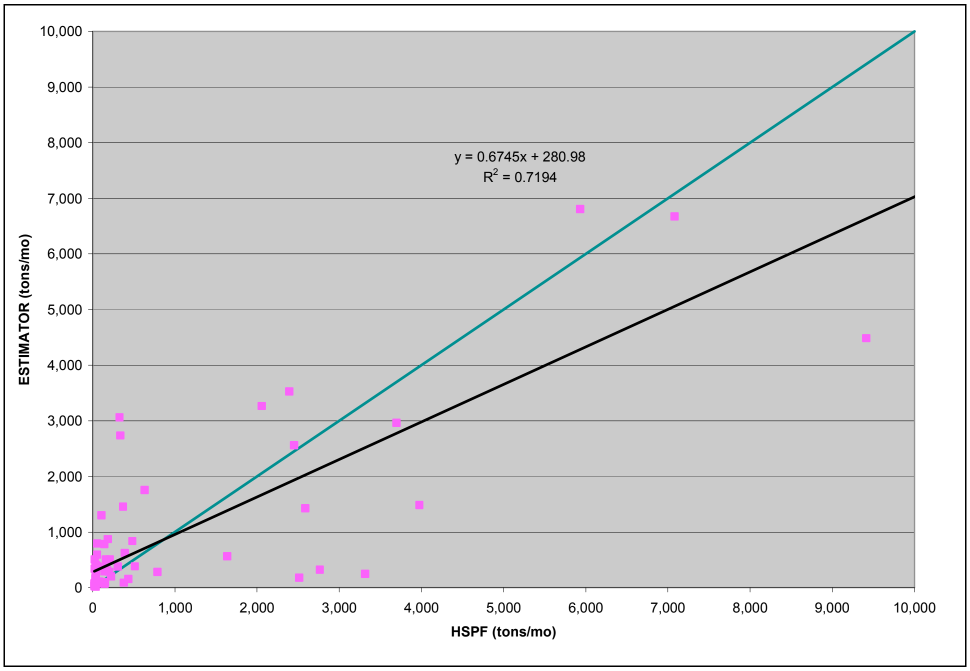

Figure 4.6-3. Time Series of ESTIMATOR and HSPF Monthly Sediment Loads (tons), Beaverdam Run

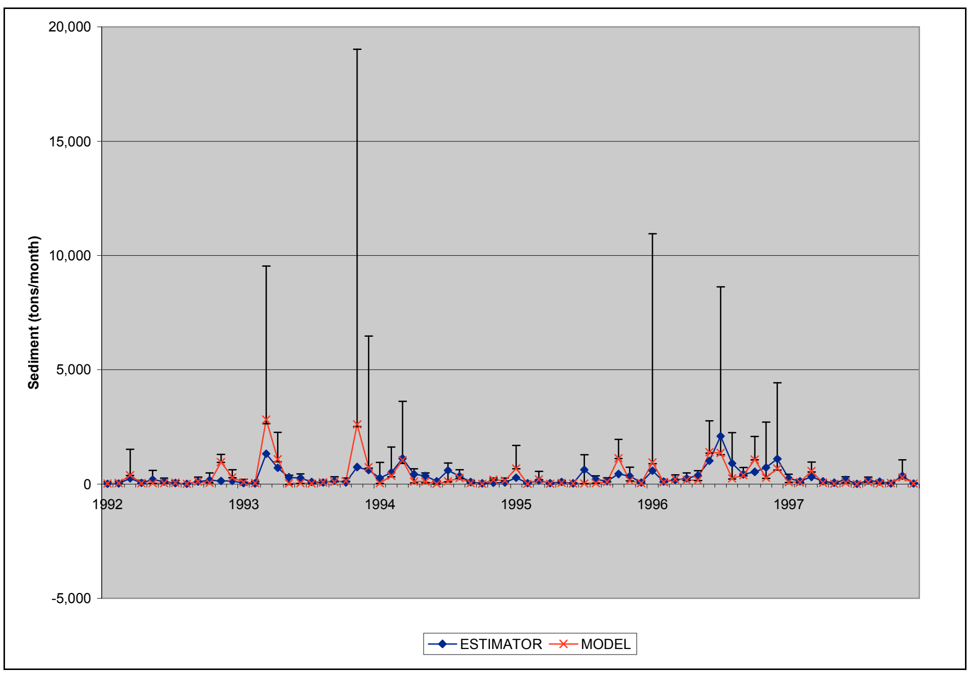

Figure 4.6-4. Scatter Plot of ESTIMATOR and HSPF Monthly Sediment Loads (tons), Beaverdam Run

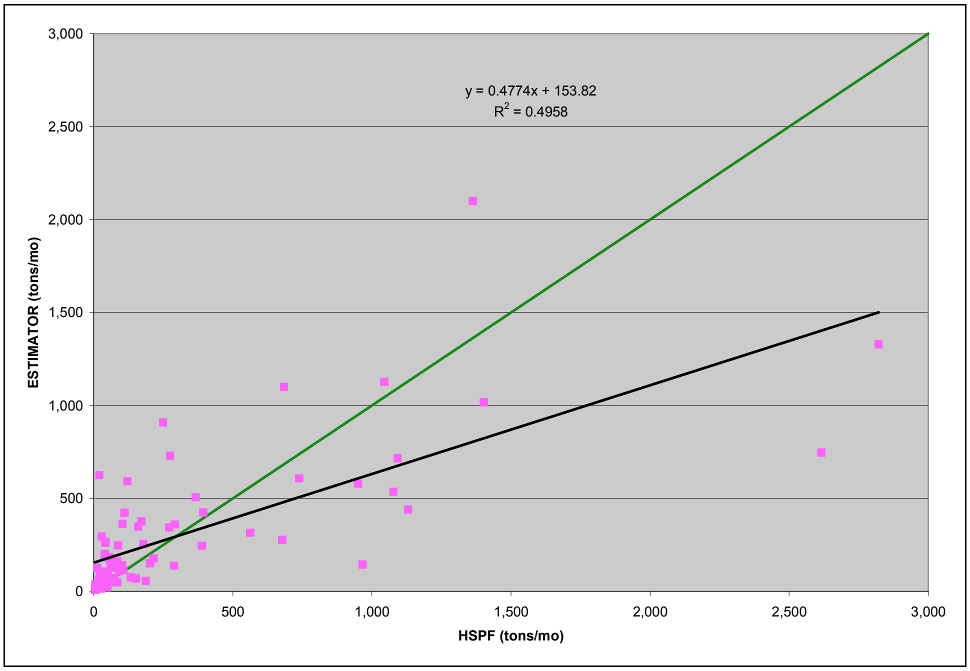

4.7. NUTRIENT CALIBRATION

4.7.1. Edge of Stream (EOS) Nutrient Loads

Although the AGCHEM module simulates a wide variety of processes that can affect the fate and transport of nutrients in the soil, nutrient losses are primarily determined by (1) inputs of nutrients in fertilizer, manure, and atmospheric deposition; (2) crop uptake targets; and (3) background soil nutrient concentrations. Altering the hydrology and sediment transport does not alter overall nutrient losses significantly, provided these three elements remain the same. For this reason, the EOS loads from land uses using AGCHEM modules were not explicitly recalibrated, and the EOS loads from these land uses remain approximately what they were in the original model.

4.7.1.1. EOS Loads from Urban Land Uses, Forest and Pasture

AGCHEM is used to simulate the fate and transport of nitrogen from developed pervious land. The simulation of phosphorus on pervious developed land and the simulation of all nutrients on all impervious land is implemented using the PQUAL or IQUAL modules.

There are two issues in implementing PQUAL to model phosphorus: (1) the phosphorus load transported in runoff, baseflow, and interflow; and (2) the division of the load among phosphorus species.

Since a scenario was planned in which loads from an all-forested watershed would be used in the reservoir water quality models, an explicit target, 0.06 lbs/ac, was adopted for forest base flow loads. The target was derived from monitoring of the forest-dominated Mingo Branch watershed as part of the Gunpowder Study (DEPRM, 2000). Unfortunately, only one storm sample was taken in the study. Storm loads from forested watersheds were determined essentially as a loading function based on eroded sediment. The phosphorus load for forest is a product of eroded sediment, an enrichment factor of 2.0, and a soil phosphorus concentration. The minimum value soil phosphorus concentrations for the Maryland Piedmont region, 430 mg P/kg, as reported in McElroy et al. (1976), was used in the model. A similar approach was used for stormwater loads from pasture, except that the median concentration, 650 mg P/kg, not the minimum value, was used for the soil phosphorus concentration from pasture. Calibration targets for stormflow loads for developed and impervious land uses were set according to the average site EMC from MS4 permits as described in Section 4.5.

For pasture and pervious developed land, the concentration of total phosphorus in baseflow and interflow was set on a monthly basis to match the average monthly total phosphorus concentration observed in base flow samples at the monitoring station associated with the segment over the simulation period. Table 4.7-1 gives the monthly concentrations for each segment. DPW (1996) observed that total phosphorus in baseflow tends to be higher in summer when flows are lower and there are less stormflow inputs. Model baseflow TP concentrations were adjusted to take into account the base flow and load associated with agricultural land and forest. The AGCHEM simulations tend to have negligible simulated TP concentrations in baseflow, but they contribute to baseflow concentrations through interflow loads which have a long residence time in reaches under low flow conditions.

Table 4.7-1. Average Monthly Baseflow TP Concentrations by Segment

Segment	10	20	30	50	60	90	100	160	170
JAN	0.025	0.02	0.019	0.027	0.024	0.035	0.046	0.12	0.019
FEB	0.02	0.018	0.012	0.019	0.018	0.025	0.017	0.084	0.016
MAR	0.035	0.031	0.015	0.03	0.024	0.024	0.016	0.077	0.021
APR	0.022	0.017	0.017	0.019	0.025	0.024	0.016	0.037	0.02
MAY	0.041	0.033	0.021	0.024	0.027	0.039	0.028	0.065	0.024
JUN	0.059	0.04	0.023	0.033	0.03	0.092	0.046	0.113	0.049
JUL	0.062	0.053	0.023	0.1	0.084	0.089	0.061	0.1	0.064
AUG	0.031	0.023	0.014	0.015	0.02	0.03	0.021	0.083	0.021
SEP	0.033	0.032	0.014	0.021	0.036	0.056	0.039	0.137	0.026
OCT	0.018	0.033	0.012	0.016	0.023	0.024	0.029	0.188	0.017
NOV	0.028	0.029	0.015	0.023	0.025	0.039	0.023	0.418	0.02
DEC	0.022	0.021	0.011	0.018	0.031	0.032	0.02	0.172	0.015

It is reasonable to assume that baseflow and interflow carry dissolved species of phosphorus while phosphorus in runoff is primarily in solid-phase. Based on limited data from the DNR CORE monitoring stations, approximately two-thirds of the phosphorus in baseflow is phosphate and one-third is organic phosphorus. The organic phosphorus was represented in reaches as BOD. Baseflow BOD concentrations monitored by DEPRM (2000) were rarely above the detection limit of 2 mg/l, so the ratio of BOD:P was set at 0.018 so that simulated concentrations also fell primarily below 2 mg/l. The phosphorus exported attached to sediment in runoff from forest, pasture, and developed land was represented as ORP. Phosphorus washed off from impervious surfaces was set at 10% dissolved phosphate and 90% inorganic phosphorus.

4.7.2. Calibration of In-stream Nutrient Processes

Both nitrogen and phosphorus undergo transformations while they are transported in river reaches. Phosphorus, for example, can sorb onto suspended sediments or be taken up by algae. Bed sediments can serve as a source or sink for ammonia and inorganic phosphorus. Ammonia can also volatilize.

The only phosphorus in-stream process that was recalibrated was the concentration of inorganic phosphorus associated with bed sediment, its consequent resuspension, and the sorption rate between inorganic phosphorus in its dissolved and solid phases. For

Western Run and Beaverdam Run, monthly simulated total phosphorus loads were compared to monthly ESTIMATOR loads, and the concentration of inorganic phosphorus was adjusted so that the average annual simulated total phosphorus load agreed with the ESTIMATOR values. Table 4.7.2 shows the average annual loads and the percent contribution from scoured sediment for Western Run and Beaverdam Run. In Western Run, scoured sediment made up 12% of the total load, whereas in Beaverdam Run, scoured sediment accounted for about 2% of the load. Table 4.7.-2 also shows the calibrated bed sediment inorganic phosphorus concentration. Following the principle that Western Run is representative of more rural subwatersheds, the Western Run bed sediment phosphorus concentration was used in other rural segments with reaches, Segments 10-60 and Segment 110.

4.7.3. Calibration Results

Tables 4.7-2, 4.7-3, and 4.7-4 give summary statistics for the calibration of total phosphorus, ammonia, and nitrate, respectively. Figures 4.7-1 and 4.7-2 show the time series and scatter plots of average monthly loads of total phosphorus from ESTIMATOR and the Gunpowder Falls HSPF model for Western Run. Figures 4.7-3 and 4.7-4 show the same figures for Beaverdam Run.

The model matches the total phosphorus average annual load from ESTIMATOR, which is the constituent of interest for the nutrient TMDLs. The coefficients of determination for monthly and annual loads show that the model captures a good deal of the variability determined by ESTIMATOR.

Figures 4.7-5 and 4.7-6 show the time series and scatter plots of average monthly loads of ammonia-nitrogen from ESTIMATOR and the Gunpowder Falls HSPF model for Western Run. Figures 4.7-7 and 4.7-8 show the same figures for Beaverdam Run. The model is within 10% of the average annual ammonia loads calculated by ESTIMATOR for the simulation period. The model’s estimate of nitrate loads is about 20% less than ESTIMATOR’s. Figures 4.7-9 and 4.7-10 show the time series and scatter plots of average monthly loads of nitrate-nitrogen from ESTIMATOR and the Gunpowder Falls

HSPF model for Western Run. Figures 4.7-11 and 4.7-12 show the same figures for Beaverdam Run. The model's nitrate load estimates, for both monthly and annual values, is within the 95% confidence interval for ESTIMATOR's loads. For both ammonia and nitrate, the coefficients of determination between annual and monthly ESTIMATOR loads and the model's calculations show that the model loads reflect the variability in loads determined by ESTIMATOR. As explained in Chapter 3, there was no storm monitoring of TKN or organic nitrogen, so it was not possible to evaluate total nitrogen loads using ESTIMATOR.

Table 4.7-2. Summary Statistics for Total

Statistic	Western Run	Beaverdam Run
Average Annual Load (tons/year) ESTIMATOR Model 1992-1997	12.9	4.9
Average Annual Load (tons/year) HSPF1992-1997	13.3	5.1
Bed Phosphorus Concentration (ppm)	200	50
Net Scour (tons/year) (+ scour, -deposition)	0.51	0.04
Coefficient of Determination for Monthly Loads	0.69	0.67

Table 4.7-3. Summary Statistics for Ammonia-N Calibration

Statistic	Western Run	Beaverdam Run
Average Annual Load (tons/year) ESTIMATOR Model 1992-1997	7.95	4.3
Average Annual Load (tons/year) HSPF1992-1997	7.88	4.0
Coefficient of Determination for Monthly Loads	0.55	0.64

Table 4.7-4. Summary Statistics for Nitrate Calibration

Statistic	Western Run	Beaverdam Run
Average Annual Load (tons/year) ESTIMATOR Model 1992-1997	233	67.4
Average Annual Load (tons/year) HSPF1992-1997	195	54.5
Coefficient of Determination for Monthly Loads	0.73	0.63

Figure 4.7-1. Time Series of ESTIMATOR and HSPF Monthly Phosphorus Loads (tons), Western Run

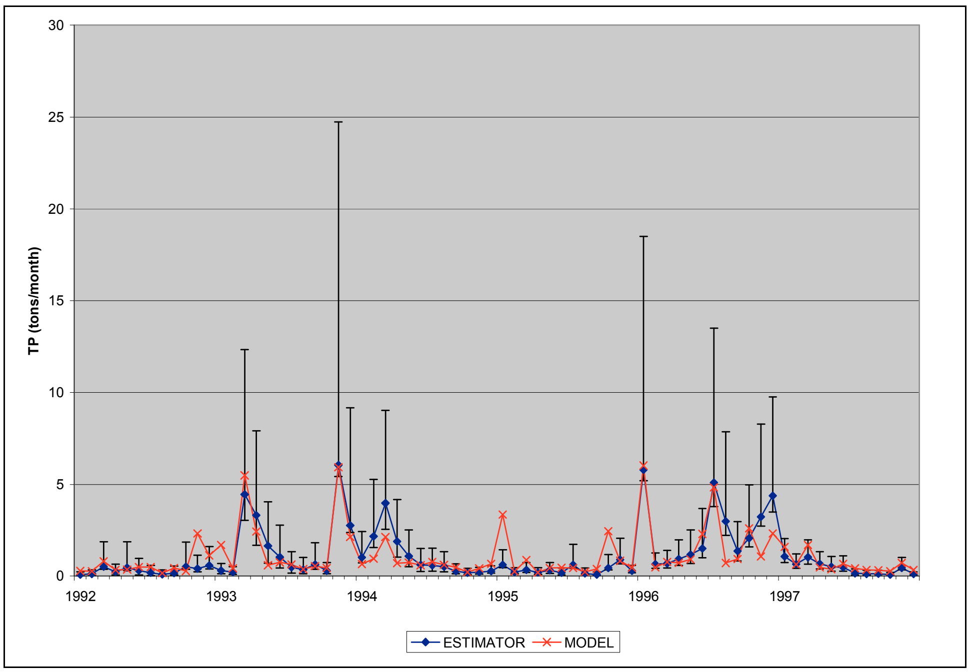

Figure 4.7-2. Scatter Plot of ESTIMATOR and HSPF Monthly Phosphorus Loads (tons), Western Run

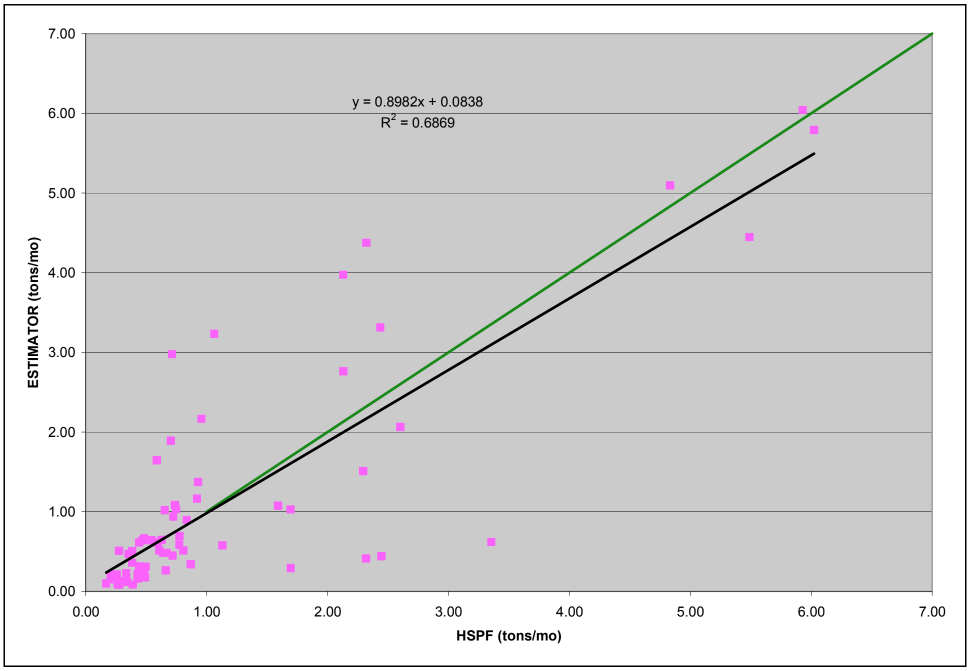

Figure 4.7-3. Time Series of ESTIMATOR and HSPF Monthly Phosphorus Loads (tons), Beaverdam Run

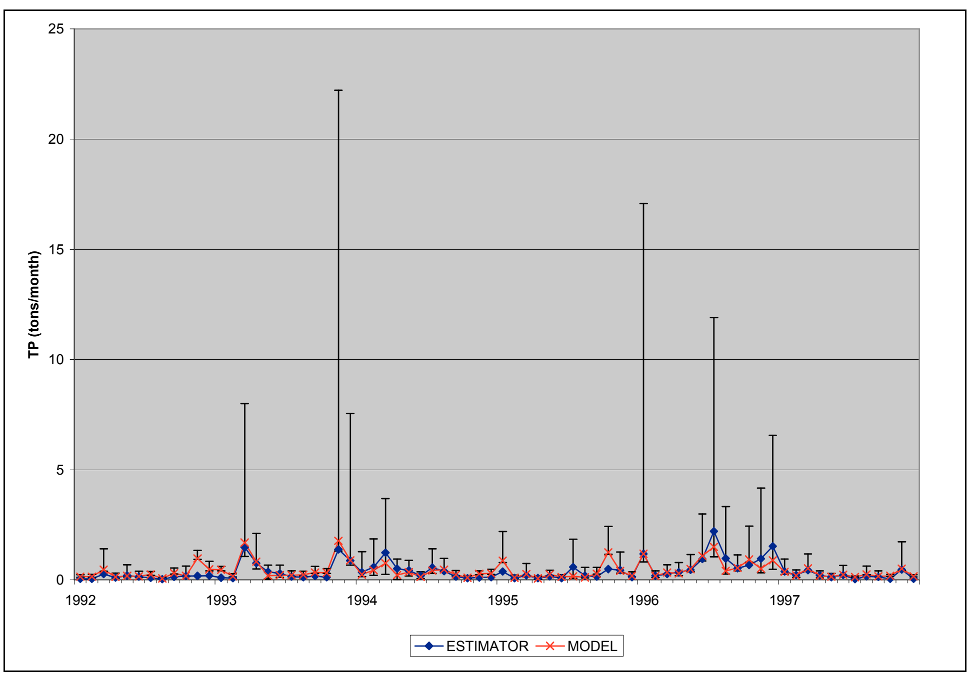

Figure 4.7-4. Scatter Plot of ESTIMATOR and HSPF Monthly Phosphorus Loads (tons), Beaverdam Run

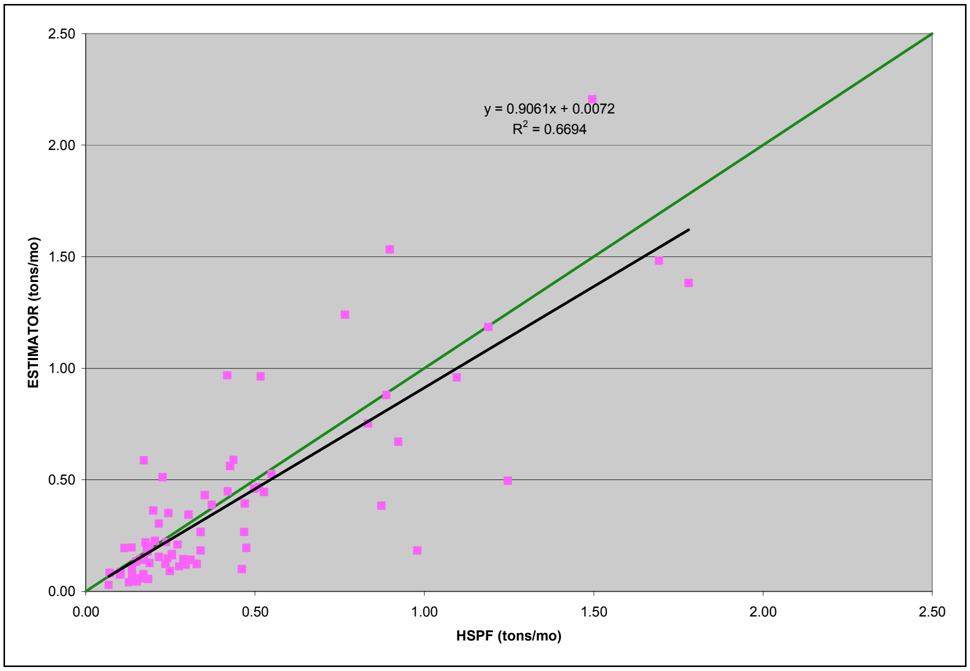

Figure 4.7-5. Time Series of ESTIMATOR and HSPF Monthly Ammonia Nitrogen Loads (tons), Western Run

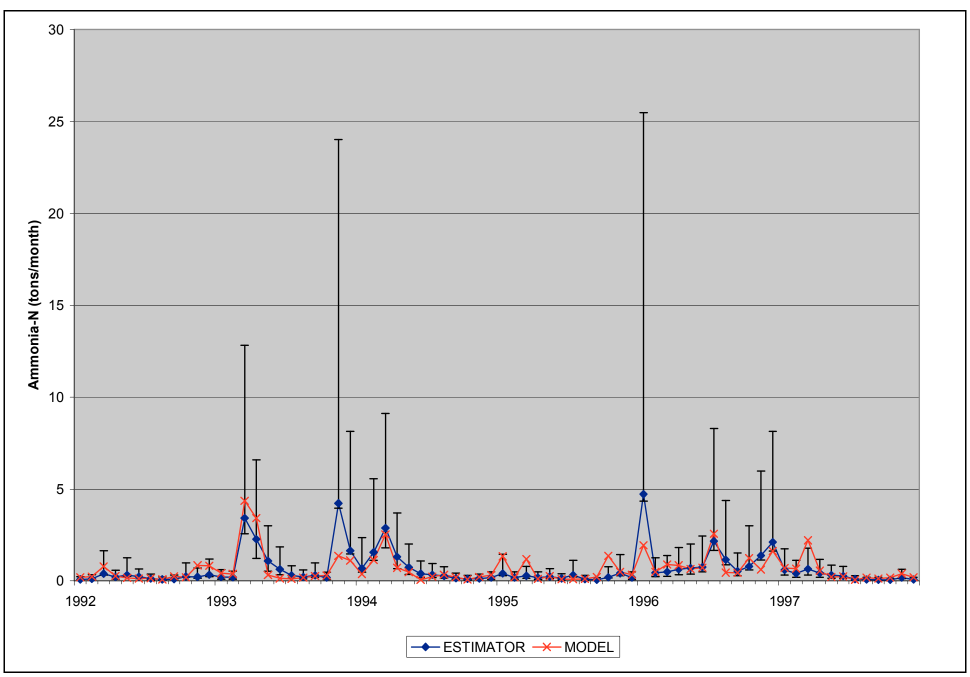

Figure 4.7-6. Scatter Plot of ESTIMATOR and HSPF Monthly Ammonia Nitrogen Loads (tons), Western Run

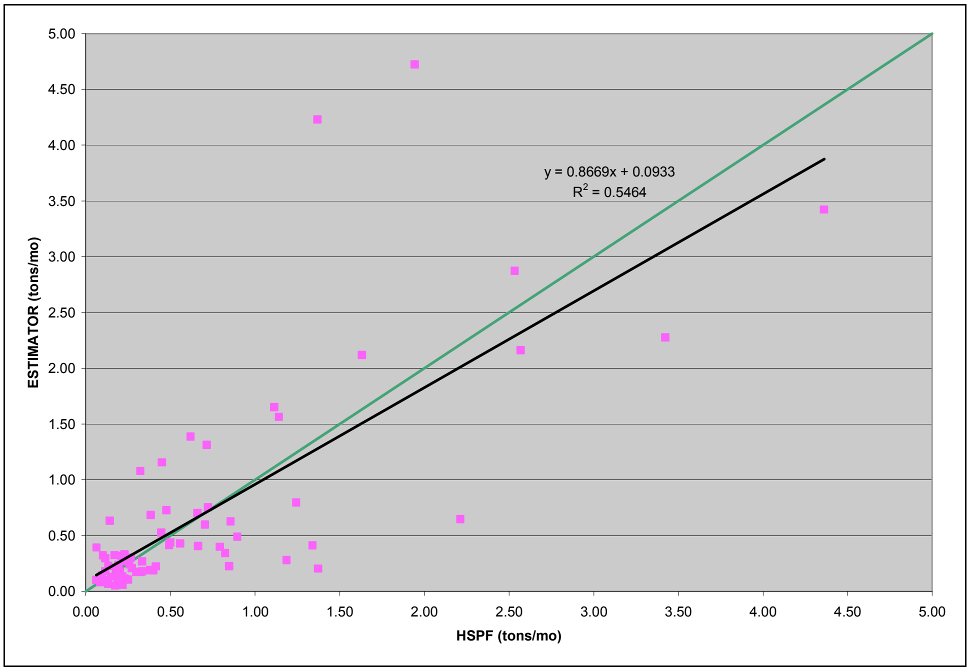

Figure 4.7-7. Time Series of ESTIMATOR and HSPF Monthly Ammonia Nitrogen Loads (tons), Beaverdam Run

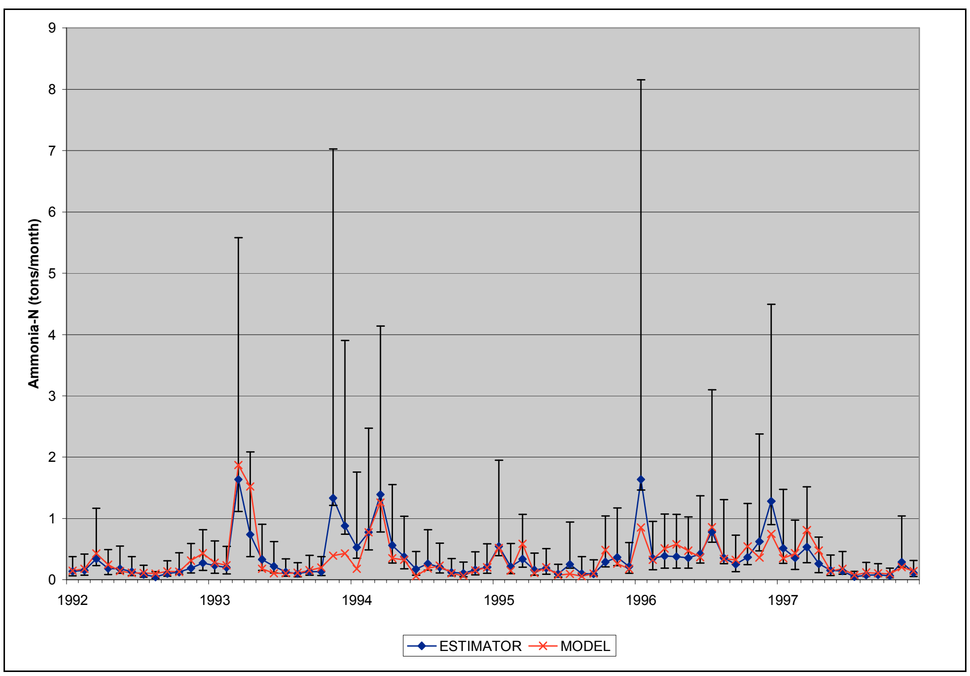

Figure 4.7-8. Scatter Plot of ESTIMATOR and HSPF Monthly Ammonia Nitrogen Loads (tons), Beaverdam Run

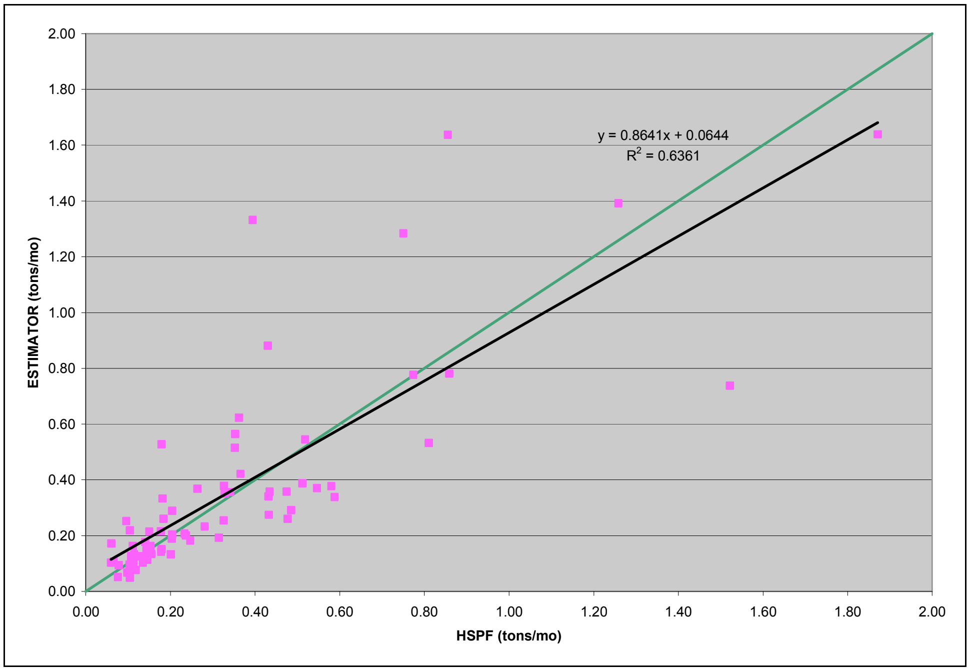

Figure 4.7-9. Time Series of ESTIMATOR and HSPF Monthly Nitrate Loads (tons), Western Run

Figure 4.7-10. Scatter Plot of ESTIMATOR and HSPF Monthly Nitrate Loads (tons), Western Run

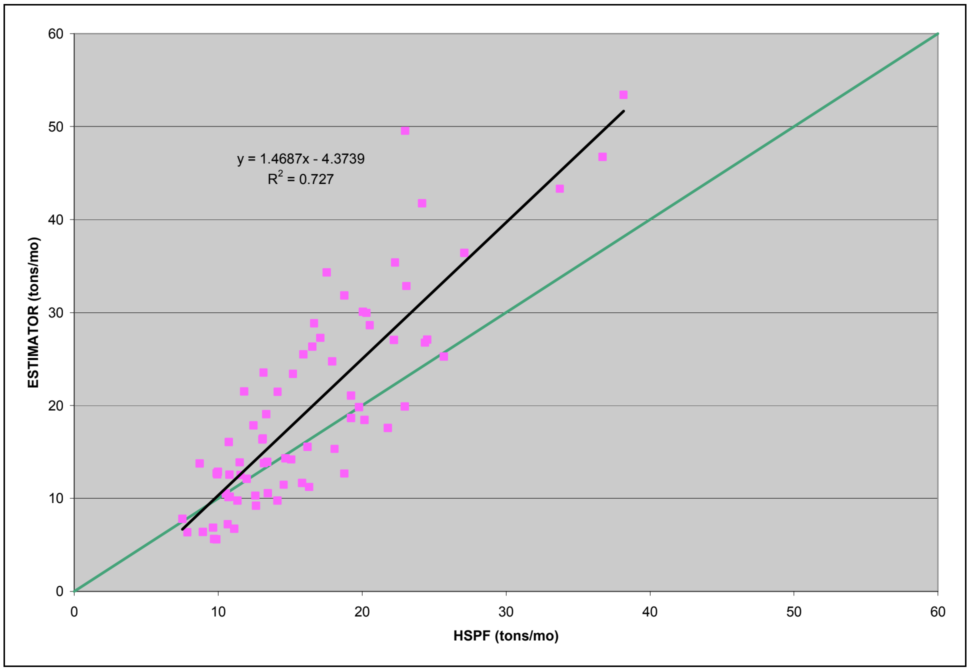

Figure 4.7-11. Time Series of ESTIMATOR and HSPF Monthly Nitrate Loads (tons), Beaverdam Run

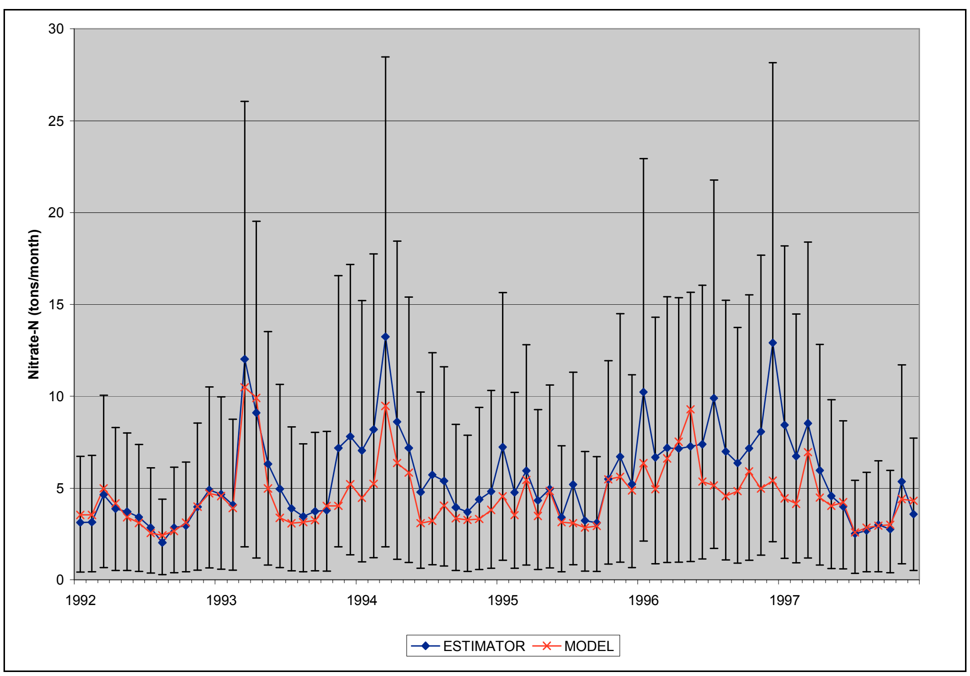

Figure 4.7-12. Scatter Plot of ESTIMATOR and HSPF Monthly Nitrate Loads (tons), Beaverdam Run

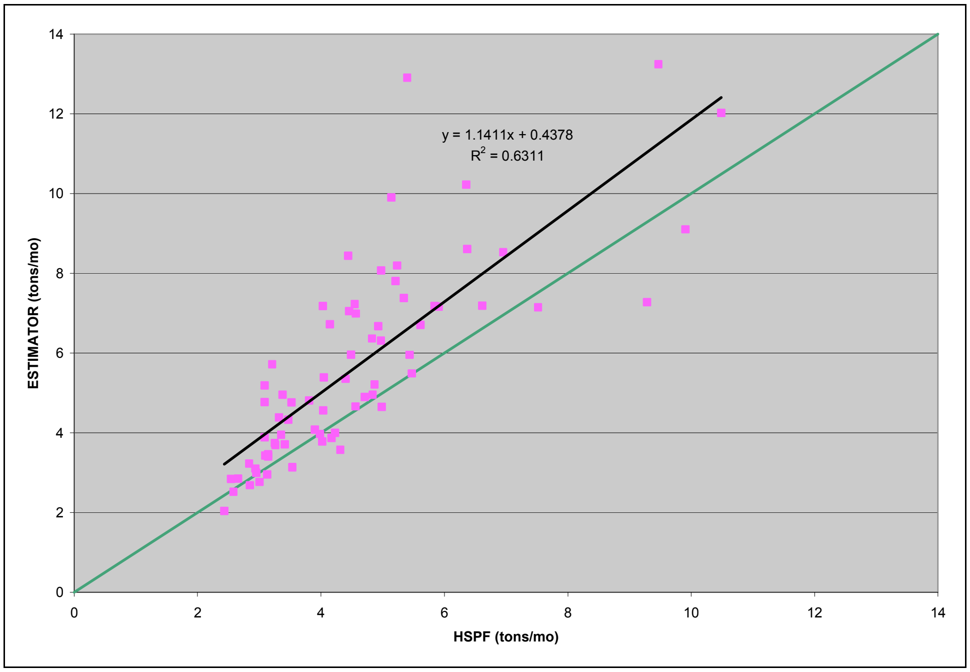

4.8. DIRECT COMPARISON OF OBSERVED AND SIMULATED CONCENTRATIONS

It has been emphasized that the HSPF model of the Gunpowder Falls watershed used monthly loads as calibration targets. As was said earlier, monthly loads are the appropriate calibration target, because the primary purpose of the HSPF model is to simulate loads for the CE-QUAL-W2 models of the reservoirs, and the residence time in the reservoirs is on the order of months. For completeness sake, Table 4.8-1 gives summary statistics of the observed and simulated daily average concentrations for segments correlated with monitoring stations. It also gives the coefficient of determination between observed and simulated concentrations. As might be expected from a review of other HSPF models, the agreement between observed and simulated nutrient concentrations, as measured by R^2 is fair to poor, and the summary statistics, which in the case of the simulated output represent daily average values over the whole simulation period, is fair at best.

In the case of temperature and oxygen, there is good agreement between observed and simulated values. The parameters governing the simulation of oxygen in river reaches were not recalibrated, and the agreement between observed and simulated concentrations justifies keeping the original parameterization of the oxygen simulation. In the case of temperature, it should be kept in mind that the model was calibrated by comparing hourly simulated and observed values, whereas the summary statistics and figures are based on daily average simulated values. Nevertheless, they still show excellent agreement between simulated and observed temperature.

Table 4.8-1. Summary Statistics Comparing Observed and Simulated Concentrations

SEG	STAT	Temperature		Oxygen		Ammonia		NO3		Total Phosphorus		Suspended Solids	
		OBS	MODEL	OBS	MODEL	OBS	MODEL	OBS	MODEL	OBS	MODEL	OBS	MODEL
10	MEAN	52.113	55.327	11.198	10.475	0.026	0.023	2.974	3.112	0.042	0.130	9.109	28.535
	STDEV	12.433	13.574	1.909	1.836	0.026	0.044	0.566	0.697	0.052	0.413	12.410	163.385
	MIN	31.874	32.072	7.900	7.120	0.005	0.000	1.765	1.506	0.001	0.011	0.050	1.413
	1STQ	40.357	42.989	9.493	8.778	0.010	0.001	2.545	2.578	0.021	0.026	2.825	2.754
	MED	51.629	54.926	10.900	10.273	0.020	0.006	2.978	2.995	0.030	0.047	5.000	3.520
	3RDQ	62.960	68.009	12.575	12.036	0.030	0.025	3.319	3.577	0.043	0.104	10.700	4.868
	MAX	76.460	83.790	16.280	14.310	0.188	0.545	4.600	7.286	0.407	7.123	84.000	3285.789
	COUNT	131	2192	131	2192	126	2192	96	2192	125	2192	131	2192
	R^2		0.94		0.84		0.06		0.00		0.41		0.18
20	MEAN	49.897	57.294	11.300	10.289	0.024	0.017	3.341	3.101	0.016	0.137	3.918	34.063
	STDEV	11.544	14.753	1.887	1.943	0.021	0.034	0.458	0.661	0.009	0.517	4.440	231.393
	MIN	31.928	32.072	7.570	6.871	0.005	0.000	2.660	1.482	0.001	0.007	0.050	0.002
	1STQ	39.560	43.690	9.480	8.485	0.005	0.001	2.900	2.595	0.011	0.017	1.200	1.240
	MED	48.866	57.085	11.380	10.011	0.020	0.004	3.330	3.088	0.015	0.041	3.200	1.737
	3RDQ	61.718	71.193	12.633	11.975	0.040	0.017	3.608	3.540	0.020	0.111	4.650	2.886
	MAX	68.360	86.806	15.300	14.310	0.100	0.340	4.350	6.832	0.045	11.361	27.200	3868.322
	COUNT	68	2192	68	2192	63	2192	30	2192	66	2192	68	2192
	R^2		0.96		0.91		0.00		0.05		0.03		0.27
30	MEAN	50.859	56.152	11.319	10.256	0.041	0.064	5.038	3.740	0.030	0.130	4.483	21.814
	STDEV	12.371	13.799	1.966	1.872	0.056	0.055	0.769	0.791	0.019	0.363	4.493	126.786
	MIN	31.964	32.072	8.070	7.177	0.005	0.000	3.620	1.400	0.001	0.012	0.050	0.002
	1STQ	39.569	43.446	9.230	8.562	0.010	0.024	4.490	3.224	0.017	0.035	1.600	0.768
	MED	49.307	56.288	11.560	9.989	0.020	0.053	4.955	3.760	0.025	0.054	2.400	0.974
	3RDQ	63.262	68.834	12.790	11.836	0.050	0.093	5.460	4.199	0.036	0.105	5.600	1.957
	MAX	70.646	84.669	15.130	14.278	0.290	0.629	6.910	9.139	0.110	6.808	23.200	1931.005
	COUNT	68	2192	68	2192	63	2192	30	2192	66	2192	67	2192
	R^2		0.95		0.86		0.04		0.01		0.04		0.00
50	MEAN	51.590	54.988	11.580	10.750	0.032	0.010	3.369	2.858	0.029	0.079	7.850	22.455
	STDEV	12.714	13.504	2.046	1.865	0.033	0.021	0.504	1.005	0.052	0.250	22.847	115.462
	MIN	31.838	32.072	8.590	7.619	0.005	0.000	2.530	0.730	0.001	0.015	0.050	1.016

SEG	STAT	Temperature		Oxygen		Ammonia		NO3		Total Phosphorus		Suspended Solids	
		OBS	MODEL	OBS	MODEL	OBS	MODEL	OBS	MODEL	OBS	MODEL	OBS	MODEL
	1STQ	39.461	42.789	9.670	9.008	0.005	0.000	2.960	2.114	0.016	0.022	1.600	2.311
	MED	50.225	54.338	11.710	10.592	0.020	0.001	3.275	2.675	0.021	0.032	3.200	3.167
	3RDQ	63.725	67.478	12.735	12.357	0.040	0.008	3.630	3.436	0.030	0.064	7.900	4.339
	MAX	71.654	83.327	18.150	14.582	0.130	0.317	4.530	5.728	0.440	6.910	188.400	2291.732
	COUNT	68	2192	68	2192	64	2192	30	2192	66	2192	67	2192
	R^2		0.95		0.86		0.01		0.03		0.09		0.01
	MEAN	52.024	54.825	11.199	10.437	0.046	0.004	2.477	2.235	0.054	0.071	19.675	18.270
	STDEV	11.145	13.104	1.748	1.820	0.069	0.009	0.704	0.479	0.091	0.141	45.010	89.153
	MIN	32.180	32.072	8.000	6.946	0.005	0.000	1.570	0.496	0.001	0.011	0.050	0.002
	1STQ	42.067	43.207	9.715	8.736	0.012	0.001	2.146	1.971	0.017	0.035	3.000	2.537
60	MED	53.600	54.551	10.700	10.178	0.020	0.001	2.387	2.181	0.025	0.046	7.000	3.609
	3RDQ	61.610	66.805	12.440	11.956	0.050	0.004	2.667	2.411	0.045	0.062	12.000	6.283
	MAX	71.240	81.594	16.500	14.403	0.637	0.127	9.500	4.260	0.594	3.057	317.500	1847.611
	COUNT	131	2192	131	2192	170	2192	155	2192	169	2192	178	2192
	R^2		0.96		0.89		0.07		0.12		0.29		0.29
	MEAN	53.288	59.361	11.401	10.172	0.063	0.050	3.023	2.751	0.085	0.085	36.659	25.630
	STDEV	12.759	13.255	1.941	1.677	0.082	0.082	0.609	0.678	0.129	0.163	73.906	98.439
	MIN	32.054	32.072	8.130	7.292	0.005	0.004	1.260	0.721	0.001	0.021	0.050	7.010
	1STQ	40.964	47.929	9.325	8.623	0.020	0.010	2.665	2.229	0.026	0.033	4.900	7.018
90	MED	51.836	58.738	11.695	10.012	0.040	0.017	3.050	2.720	0.039	0.046	9.800	8.554
	3RDQ	65.170	71.523	12.918	11.523	0.070	0.050	3.440	3.308	0.069	0.077	24.700	12.153
	MAX	73.238	87.450	15.200	14.548	0.470	0.985	4.320	4.388	0.884	3.251	518.000	1699.671
	COUNT	68	2192	68	2192	114	2192	99	2192	115	2192	120	2192
	R^2		0.96		0.89		0.07		0.06		0.56		0.42
	MEAN	54.664	58.448	11.098	10.109	0.121	0.070	2.238	1.966	0.072	0.069	42.088	13.678
	STDEV	11.504	12.400	1.959	1.555	0.182	0.084	0.965	0.513	0.153	0.071	133.951	39.062
	MIN	34.826	32.072	8.190	7.315	0.005	0.002	0.830	0.480	0.004	0.017	0.050	0.002
	1STQ	42.994	47.868	9.130	8.694	0.020	0.009	1.910	1.629	0.016	0.029	2.800	0.759
100	MED	54.428	57.901	11.390	9.972	0.060	0.028	2.190	1.926	0.024	0.044	5.900	0.806
	3RDQ	65.003	69.583	12.555	11.359	0.148	0.111	2.465	2.265	0.061	0.073	30.500	4.736
	MAX	72.500	85.616	15.330	14.310	1.350	0.732	10.030	5.255	1.472	0.722	1352.000	505.461
	COUNT	67	2192	67	2192	114	2192	99	2192	113	2192	116	2192
	R^2		0.92		0.81		0.05		0.06		0.28		0.24
	MEAN	60.199		10.413		0.053	0.051	0.843	1.702	0.106	0.035	9.900	2.370
	STDEV	15.299		2.189		0.065	0.068	0.797	0.516	0.076	0.031	5.657	12.640
	MIN	36.626		6.790		0.005	0.001	0.010	0.711	0.020	0.012	1.200	0.000
	1STQ	44.600		8.560		0.020	0.005	0.315	1.349	0.055	0.018	5.200	0.000
160*	MED	61.565		9.960		0.030	0.018	0.680	1.612	0.086	0.028	9.800	0.000
	3RDQ	75.421		12.138		0.058	0.073	0.930	1.958	0.135	0.042	13.900	0.464
	MAX	82.598		14.210		0.270	0.425	2.690	4.854	0.418	0.618	27.400	300.445
	COUNT	30		30		26	2192	17	2192	28	2192	30	2192
	R^2		NA		NA		0.00		0.02		0.20		0.02
170*	MEAN	55.787		10.779		0.029	0.032	3.958	0.801	0.026	0.020	4.555	2.710
	STDEV	10.222		1.579		0.028	0.040	0.402	0.312	0.033	0.024	10.624	18.570
	MIN	37.364		8.070		0.005	0.002	3.350	0.314	0.001	0.006	0.050	0.000
	1STQ	45.572		9.370		0.005	0.009	3.620	0.571	0.016	0.009	1.200	0.000
	MED	56.138		10.725		0.020	0.015	3.910	0.770	0.021	0.014	2.400	0.000

SEG	STAT	Temperature		Oxygen		Ammonia		NO3		Total Phosphorus		Suspended Solids	
		OBS	MODEL	OBS	MODEL	OBS	MODEL	OBS	MODEL	OBS	MODEL	OBS	MODEL
	3RDQ	65.129		11.835		0.040	0.040	4.150	0.947	0.026	0.023	3.800	0.169
	MAX	71.114		14.320		0.140	0.342	4.790	2.210	0.250	0.420	71.500	367.762
	COUNT	66		66		63	2192	30	2192	65	2192	67	2192
	R^2		NA		NA		0.06		0.13		0.01		0.02

* Temperature and DO not simulated because there is no reach associated with segment.

4.9. LOADINGS TO THE PRETTYBOY AND LOCH RAVEN RESERVOIRS

Table 4.9-1 gives the simulated average annual sediment, total phosphorus, ammonia, and nitrate loads by segment. It also shows the average annual loads to Prettyboy and Loch Raven and Reservoirs.

Tables 4.9-2 through 4.9-5 give the sediment, total phosphorus, ammonia, and nitrate loading rates by segment and land use. Land use loads are given on a per acre basis.

4.9.1. Comparison of Gunpowder Falls HSPF Model Loads To Other Load Estimates

Two types of load comparisons can be made between the simulation loads from the Gunpowder Falls HSPF Model and load estimates from other sources. The loads from different land uses can be compared on a per acre basis. Estimates of the land use loads were available from (1) the CBP Phase 4.3 Watershed Model, and (2) Tetra Tech's SWMM Model for the Loch Raven Watershed's Water Quality Management Plan. Tables 4.9.1-1 and 4.9.1-2 give the loads per acre for these studies by land use.

Estimates of the average annual load entering Loch Raven Reservoir and selected subwatersheds were available from (1) the Tetra-Tech SWMM model, and (2) the City of Baltimore's 1996 Reservoir Watershed Management Report. The estimates from the latter are based on a statistical analysis of monitoring data the City of Baltimore collected. Table 4.9.1-3 gives the SWMM model load estimates for the portion of Loch Raven Reservoir below Prettyboy Reservoir. Table 4.9.1-4 gives the City of Baltimore's estimates of average annual sediment and TP loads from Western Run and Beaverdam Run.

The Phase 4.3 Model loads are taken from neighboring Segment 480, Gwynn Falls, rather than from Segment 470 which represents Gunpowder Falls, because Segment 470 EOS loads include a reduction in loads due to trapping in the reservoirs. Total phosphorus loads from the current Gunpowder Falls Watershed Model tend to be higher on cropland than the loading rates in the Phase 4.3 Model by more than a factor of two. Loading rates on pasture and hay are lower than the Phase 4.3 Model. Forest loads are higher by an order of magnitude, but still small on a per acre basis. It is somewhat difficult to compare loads on developed land, because, in contrast to Phase 5, loads from developed land in Phase 4.3 primarily come from pervious land. Sediment loading rates also tend to be higher in the Gunpowder Falls HSPF model, except on the conventional-tilled cropland. Nitrate and ammonia loads are also higher in the current Gunpowder Falls model.

Compared to the SWMM Model, TP loads from crops and developed land are higher in the Gunpowder Falls Model. TP loads on forest and pasture are comparable. Suspended sediment loads in the SWMM model are uniformly lower than the Gunpowder HSPF Model. Total nitrogen loads in the SWMM model are lower than the corresponding nitrate loads in the Gunpowder HSPF model.

On the whole, the Gunpowder Falls HSPF Model predicts higher total phosphorus and suspended sediment loads than either the Phase 4.3 Model or the SWMM Model. Land use loading rates are still within the range of values reported in the literature (Beaulac and Reckhow, 1982).

It is a somewhat different story when the loads from the Gunpowder HSPF Model are compared to the available load estimates for subwatersheds. With the exception of the TP load for Beaverdam Run, the Gunpowder HSPF Model estimates for TP and suspended sediment loads are about half of Baltimore City's estimates for corresponding subwatersheds. TP loads from the HSPF model are also significantly smaller than the loads from the SWMM model, although sediment and nitrogen loads are comparable.

It seems paradoxical that the TP loads from the SWMM model on the watershed scale are larger than the loads from the HSPF model, given that the loads from the land uses are generally smaller. It turns out that in the SWMM model the loads from feedlots and farm buildings contribute significantly to the overall TP watershed load and make up for the lower loading rates for other land uses. It is not clear how the TP loads for feedlots and farm buildings in the SWMM model were arrived at, but, in contrast, in the HSPF model, (1) the nutrient content of waste is quantified, based on animal populations, and (2) the fate of waste nutrients is accounted for, as described in Chapter 3.

There are no estimates of land use loading rates associated with the Baltimore City load estimates. They are derived from a statistical analysis of monitoring data using the FLUX model (Walker, 1999). FLUX and ESTIMATOR use similar methodologies Both estimate loads by first building a regression model of concentrations and calculating loads by multiplying flows by the modeled concentrations. In this case the following differences can be highlighted: (1) ESTIMATOR uses a single seven-parameter model of concentrations whereas FLUX can estimate distinct simple linear regression equations over different ranges of flow; (2) FLUX uses instantaneous flows as the independent variable where ESTIMATOR uses daily average flow, both in the regression equation and the load estimate; (3) ESTIMATOR uses an MVUE procedure to transform log of concentrations whereas the transformation used in FLUX can be biased upwards; (4) ESTIMATOR loads are calculated for individual months and years while the average annual load estimate for Baltimore City is based on flow duration curves; and (5) Baltimore City's estimate is based on monitoring data collected between 1981 and 1989 whereas the ESTIMATOR calculations were performed using data from 1985 to 2003 (Stack and Belt, 1989).

The last difference is probably the most important. When ESTIMATOR was run with monitoring data from the 1981-1989, the average annual load was 22 tons/yr, approximately the same estimate load calculated by Baltimore City using FLUX. The other differences in methodology are probably less important than the monitoring data used to make the estimates.

Nevertheless, it is important to note that Baltimore City's independent analysis indicates that the land use loading rates should be at least as high as the Gunpowder HSPF model calculates, for it would not be possible to obtain the watershed loads predicted by the in-stream monitoring data unless land use loads were higher than those predicted, for example, by the Phase 4.3 CBP Watershed Model. The Gunpowder Watershed HSPF Model has attempted to take into account all available sources of data relevant to the calculation of loads: monitoring data, animal population, septic system populations, point source discharges, and atmospheric deposition. It represents the most comprehensive attempt to integrate all available information in order to calculate nutrient and sediment loads to Prettyboy and Loch Raven Reservoirs.

Table 4.9-1. Average Annual Loads by Segment (ton/yr)

Segment	Ammonia	Nitrate	Total Phosphorus	Suspended Solids
10	1.69	120.99	9.76	9,415
20	0.32	32.81	2.99	2,971
30	2.04	84.13	6.52	6,341
40	4.73	70.07	5.95	5,442
50	7.57	122.61	14.37	9,658
60	2.40	22.68	4.66	3,188
70	2.42	74.31	4.57	4,175
80	1.64	42.60	3.01	2,697
90	2.59	73.27	5.66	4,513
100	4.13	54.41	5.33	3,874
110	1.28	78.99	5.45	6,040
120	5.80	21.85	2.77	2,392
130	2.53	4.77	0.77	376
140	1.61	2.86	0.44	142
150	1.04	1.25	0.35	244
160	1.36	6.89	0.80	444
170	0.34	2.04	0.26	236
Prettyboy	8.78	308.00	25.21	24,167
Prettyboy Outflow	2.47	245.10	6.50	587
Loch Raven	37.18	753.63	54.94	38,567

Table 4.9-2. Edge-of-Stream Total Phosphorus Loading Rates (lbs/ac/yr)

SEG	DEVELOPED	FOREST	HAY	DOUBLE CROP	HTCORN	IMPERVIOUS	BEANS	LTCORN	PASTURE	VEG	MANURE
10	0.34	0.18	0.78	2.96	2.92	3.11	1.19	2.06	0.81	1.91	235
20	0.19	0.18	0.86	3.41	3.31	3.14	1.38	2.45	0.82	1.94	240
30	0.32	0.19	0.88	3.25	3.05	3.09	1.34	2.43	0.91	2.03	232
40	0.49	0.17	0.52	2.63	2.47	3.11	0.99	2.06	1.02	1.49	235
50	0.33	0.16	0.87	3.13	2.78	3.23	1.60	2.15	0.73	2.58	247
60	0.34	0.18	0.77	2.53	2.10	3.28	1.29	2.14	0.86	1.79	255
70	0.34	0.15	0.43	2.11	1.65	2.67	0.88	1.56	0.76	1.09	184
80	0.34	0.15	0.44	2.11	1.64	2.67	0.89	1.55	0.76	1.11	184
90	0.35	0.15	0.44	2.14	1.66	2.67	0.89	1.76	0.76	1.14	184
100	0.32	0.16	0.93	3.13	2.65	2.69	0.77	2.28	0.80	2.19	187
110	0.34	0.19	0.79	2.63	2.09	3.28	1.32	1.87	0.86	1.65	255
120	0.22	0.16	0.71	2.83	2.39	2.66	1.11	2.05	0.70	1.96	184
130	0.18	0.20				2.66			0.89		184
140	0.22	0.22				2.66					0
150	0.22	0.21				2.66		2.12			0
160	0.22	0.21	1.00			2.66	1.62	2.52	0.98		184
170	0.22	0.24				2.66		2.46	1.07		184
Min	0.18	0.15	0.43	2.11	1.64	2.66	0.77	1.55	0.70	1.09	0.00
1st Q	0.22	0.16	0.46	2.14	1.66	2.66	0.89	1.84	0.76	1.14	183.90
Median	0.32	0.18	0.78	2.73	2.43	2.67	1.19	2.12	0.82	1.85	184.25
3rd Q	0.34	0.20	0.87	3.13	2.82	3.11	1.34	2.36	0.90	1.98	235.30
Max	0.49	0.24	1.00	3.41	3.31	3.28	1.62	2.52	1.07	2.58	254.72
Mean	0.29	0.18	0.72	2.74	2.39	2.88	1.17	2.10	0.85	1.74	186.66

Table 4.9-3. Edge-of-Stream Sediment Loading Rates (ton/ac/yr)

SEG	DEVELOPED	FOREST	HAY	DOUBLE CROP	HTCORN	IMPERVIOUS	BEANS	LTCORN	PASTURE	VEG
10	0.002	0.07	0.45	1.72	1.77	0.29	1.04	1.12	0.18	1.88
20	0.002	0.08	0.60	2.31	2.32	0.30	1.33	1.46	0.25	1.85
30	0.002	0.07	0.52	1.93	2.02	0.29	1.23	1.23	0.23	2.09
40	0.002	0.06	0.42	1.93	1.58	0.29	0.98	1.31	0.20	1.76
50	0.000	0.06	0.37	1.47	1.49	0.30	0.83	0.89	0.15	1.54
60	0.001	0.06	0.47	1.78	1.79	0.30	1.06	1.09	0.19	2.04
70	0.000	0.05	0.37	1.42	1.46	0.25	0.84	0.88	0.15	1.35
80	0.000	0.05	0.37	1.40	1.42	0.25	0.84	0.88	0.15	1.30
90	0.000	0.05	0.37	1.42	1.42	0.25	0.84	0.88	0.15	1.34
100	0.005	0.07	0.48	1.84	1.87	0.25	1.15	1.22	0.19	1.76
110	0.001	0.07	0.47	1.89	1.86	0.30	1.10	1.12	0.19	1.74
120	0.004	0.07	0.48	1.88	1.88	0.25	1.12	1.13	0.20	1.90
130	0.004	0.09				0.25			0.27	
140	0.004	0.11				0.25				
150	0.004	0.10				0.25		1.65		
160	0.004	0.10	0.75			0.25	1.65	1.69	0.30	
170	0.004	0.12				0.25		1.82	0.34	
Min	0.00	0.05	0.37	1.40	1.42	0.25	0.83	0.88	0.15	1.30
1st Q	0.00	0.06	0.37	1.42	1.46	0.25	0.84	0.89	0.15	1.35
Median	0.00	0.07	0.47	1.81	1.78	0.25	1.06	1.13	0.19	1.76
3 rd Q	0.00	0.09	0.48	1.90	1.88	0.29	1.15	1.39	0.24	1.88
Max	0.01	0.12	0.75	2.31	2.32	0.30	1.65	1.82	0.34	2.09
Mean	0.00	0.08	0.47	1.75	1.74	0.27	1.08	1.22	0.21	1.71

Table 4.9-4. Edge-of-Stream Ammonia-N Loading Rates (lbs/ac/yr)

SEG	DEVELOPED	FOREST	HAY	DOUBLE CROP	HTCORN	IMPERVIOUS	BEANS	LTCORN	PASTURE	VEG	MANURE
10	0.35	0.04	0.43	1.38	1.96	1.60	0.90	1.22	0.59	0.58	94
20	0.26	0.03	0.29	1.30	1.38	1.61	0.92	1.47	0.58	0.53	96
30	0.32	0.04	0.36	1.48	1.41	1.59	0.96	1.45	0.53	0.56	93
40	0.32	0.30	0.38	1.93	2.33	1.61	0.84	1.63	1.04	0.69	94
50	0.25	0.02	0.25	1.14	0.77	1.83	0.32	1.00	0.54	0.32	99
60	0.35	0.03	0.37	1.28	1.03	1.83	0.42	1.58	0.40	0.59	102
70	0.24	0.14	0.20	1.03	0.90	1.39	0.40	1.17	0.56	0.44	74
80	0.24	0.14	0.20	1.04	0.89	1.39	0.39	1.14	0.64	0.57	74
90	0.19	0.14	0.20	1.03	0.90	1.39	0.40	1.29	0.35	0.54	74
100	0.44	0.10	0.56	1.84	2.46	1.40	1.25	2.26	1.69	1.22	75
110	0.36	0.02	0.38	1.31	0.89	1.83	0.43	1.35	2.50	0.62	102
120	0.43	0.13	0.45	1.71	2.11	1.39	0.74	2.11	0.89	0.91	74
130	0.41	0.06				1.39			0.38		74
140	0.41	0.06				1.39					0
150	0.45	0.06				1.39		1.66			0
160	0.44	0.08	0.36			1.39	0.74	1.44	0.57		74
170	0.44	0.08				1.39		1.36	0.83		74
Min	0.19	0.02	0.20	1.03	0.77	1.39	0.32	1.00	0.35	0.32	0.00
1st Q	0.25	0.03	0.21	1.04	0.89	1.39	0.40	1.21	0.49	0.53	73.56
Median	0.35	0.06	0.36	1.31	1.21	1.39	0.74	1.44	0.58	0.58	73.70
3rd Q	0.43	0.13	0.38	1.54	2.00	1.61	0.90	1.60	0.86	0.63	94.12
Max	0.45	0.30	0.56	1.93	2.46	1.83	1.25	2.26	2.50	1.22	101.89
Mean	0.35	0.09	0.34	1.37	1.42	1.52	0.67	1.48	0.80	0.63	74.66

Table 4.9-5. Edge-of-Stream Nitrate-N Loading Rates (lbs/ac/yr)

SEG	DEVELOPED	FOREST	HAY	DOUBLE CROP	HTCORN	IMPERVIOUS	BEANS	LTCORN	PASTURE	VEG	MANURE
10	9.48	0.19	14.34	31.83	34.50	6.80	13.45	20.08	20.35	31.12	376
20	9.99	0.20	12.27	32.27	27.83	6.83	13.67	21.48	20.73	31.40	384
30	9.90	0.21	12.63	32.52	30.48	6.77	13.58	27.52	19.49	29.52	372
40	4.53	1.20	13.70	27.92	36.83	6.84	30.10	21.36	18.26	30.23	375
50	2.25	2.19	14.03	21.37	33.07	8.42	49.65	19.87	26.04	38.15	395
60	1.72	0.19	14.86	25.12	23.83	8.42	29.16	23.31	7.41	22.99	408
70	2.39	5.64	12.13	24.21	16.20	6.24	27.50	14.24	14.81	28.08	295
80	2.39	5.63	7.54	24.24	16.21	6.24	27.52	14.16	15.22	28.30	295
90	2.44	5.64	6.43	24.36	16.30	6.25	27.52	16.01	13.92	22.83	295
100	3.85	1.30	15.49	27.42	25.41	6.26	18.69	21.52	16.70	30.57	298
110	1.73	1.67	14.84	25.07	18.63	8.41	29.10	21.86	13.60	30.63	407
120	2.75	1.19	13.07	22.71	22.37	6.24	4.86	19.74	10.15	24.23	294
130	3.57	0.22				6.24			4.93		294
140	3.57	0.22				6.23					0
150	1.70	0.22				6.23		12.49			0
160	9.79	0.48	11.28			6.24	6.36	12.01	8.02		294
170	9.79	0.48				6.23		12.22	38.60		294
Min	1.70	0.19	6.43	21.37	16.20	6.23	4.86	12.01	4.93	22.83	0.00
1st Q	2.28	0.21	11.49	24.21	16.30	6.24	13.48	13.74	9.62	24.23	294.24
Median	3.57	0.48	13.07	25.10	24.62	6.25	27.50	19.87	15.22	29.88	294.79
3rd Q	9.48	1.67	14.34	28.90	31.13	6.83	29.10	21.50	19.92	30.75	376.47
Max	9.99	5.64	15.49	32.52	36.83	8.42	49.65	27.52	38.60	38.15	407.55
Mean	4.81	1.58	12.51	26.59	25.14	6.76	22.40	18.52	16.55	29.00	298.65

Table 4.9.1-1. Constituent Loads By Land Use, CBP Phase 4.3 Watershed Model, Segment 480 (Gwynn Falls)

Land Use	Ammonia (lbs/ac/yr)	Nitrate (lbs/ac/yr)	Total Nitrogen (lbs/ac/yr)	Total Phosphorus (lbs/ac/yr)	Sediment (tons/ac/yr)
Forest	0.02	0.46	1.48	0.02	0.08
High Till	1.26	11.69	23.09	0.99	2.68
Low Till	0.86	15.76	20.00	0.88	0.70
Pasture	0.56	3.82	7.65	1.12	0.40
Pervious Urban	0.45	12.46	17.98	3.01	0.31
Hay	0.14	4.21	6.37	0.70	0.45
Mixed Open	0.22	6.23	8.99	1.51	0.15
Imp Urban	2.02	5.56	9.67	0.70	0.00
Manure	210.56	52.64	2026.41	246.59	0.00

Table 4.9.1-2. Constituent Loads From Loch Raven SWMM Model (Tetra Tech,1997)
(lbs/acre/year)

Land Use	BOD	Total Nitrogen	Total Phosphorus	Total Suspended Solids
Developed	16.86-78.92	4.87-11.36	0.5-0.88	125 -279
Crop	13.19	13.13	1.25	446.3
Pasture	15.83	4.95	0.66	243.8
Forest	6.25	0.86	0.12	48.17
Feed Lots	127.9	111.9	31.97	152.2

Table 4.9.1-3. Average Annual Constituent Loads (lbs/ac/yr) from Loch Raven Reservoir Watershed Below Prettyboy Reservoir SWMM Model (Tetra Tech, 1997)
(Gunpowder HSPF Loads in parentheses)

Constituent	TN	TP	TSS
Load	5.53 (12.15*)	0.79 (0.79)	380 (546)

* Nitrate only.

Table 4.9.1-4. Baltimore City Estimates of Average Annual Constituent Loads for Selected Watersheds.
(Gunpowder HSPF Model loads in parentheses)

Watershed	Total Phosphorus (lbs/ac/yr)	Suspended Solids (tons/ac/yr)
Beaverdam Run	0.76 (0.79)	0.42 (0.29)
Gunpowder Falls at Glencoe	0.48 (0.39)	0.18 (0.13)
Western Run	1.09 (0.79)	0.31 (0.30)

Section 5. WATER QUALITY SIMULATION OF PRETTYBOY AND LOCH RAVEN RESERVOIRS

This section presents what in many respects is the heart of the modeling framework. It contains (1) a review of the water quality monitoring data in Prettyboy and Loch Raven Reservoirs, (2) a brief overview of the CE-QUAL-W2 model and how it was modified to represent the reservoirs, and (3) an extended discussion of the water balance, temperature and water quality calibration of both reservoir models.

5.1. WATER QUALITY MONITORING DATA AND ANALYSIS

The Maryland Water Quality Standards Stream Segment Designations for Prettyboy and Loch Raven Reservoirs are Use III-P: Nontidal Cold Water and Public Water Supply (COMAR 26.08.02.08J(4)). Designated Uses present in the Prettyboy and Loch Raven Reservoirs are: 1) growth and propagation of trout and 2) public water supply.

Prettyboy and Loch Raven Reservoirs are subject to periodic algae blooms that are the mark of excessive eutrophication. Both reservoirs also suffer from low dissolved oxygen concentrations in bottom waters during stratified conditions. Although only Loch Raven is listed as impaired by sediment, both reservoirs are affected by extensive sedimentation in their upper reaches. Prettyboy and Loch Raven Reservoirs have other water quality problems. Both are listed as impaired by metals and mercury; excess chlorides and dissolved solids have recently become a cause for concern for those jurisdictions using the reservoirs for water supply (RTG, 2004). Only eutrophication, dissolved oxygen concentrations, and sedimentation, however, will be addressed in this effort. The monitoring data collected in the reservoirs relevant to these problems are described and analyzed below.

5.1.1. The Application of Water Quality Standards to Stratified Reservoirs

Seasonal thermal stratification is an important phenomenon often observed in reservoirs as water quality systems. The differential heating of the water column, combined with wind-driven mixing of the surface layers, leads to the establishment of regions of temperature and density differences in the spring and summer. Typically, a reservoir with temperature stratification can be divided into three distinct layers: the epilimnion, or well-mixed surface layer with relatively homogeneous temperature; the hypolimnion, or bottom-layers, which are also relatively homogeneous in temperature; and the metalimnion or thermocline connecting these two regions, which is characterized by a steep gradient in temperature and density. As the reservoir cools in fall, the well-mixed layer deepens, which can lead to a fall overturn in which water from the hypolimnion is mixed throughout the water column. Stratification can also occur in the winter, especially if temperatures in the surface layer drop enough for ice to form.

5.1.1.1. Dissolved Oxygen. Use III waters are subject to DO criteria of not less than 6.0 mg/l daily average and 5.0 mg/l at any time (COMAR 26.08.02.03-3E(2)) unless natural conditions result in lower levels of DO (COMAR 26.08.02.03A(2)). New standards for tidal waters of the Chesapeake Bay and its tributaries take into account stratification and its impact on deeper waters. MDE recognizes that stratified reservoirs and impoundments (there are no natural lakes in Maryland) present circumstances similar to stratified tidal waters, and is applying an interim interpretation of the existing standard to allow for the impact of stratification on DO concentrations. This interpretation recognizes that, given the morphology of the reservoir or impoundment, the resulting degree of stratification, and the naturally occurring sources of organic material in the watershed, hypoxia in the hypolimnion is a natural consequence. The interim interpretation of the non-tidal DO standard, as applied to reservoirs, is as follows:

- A minimum DO concentration of 5.0 mg/l (and 6.0 mg/ daily average for Use III) will be maintained throughout the water column during periods of complete and stable mixing;
- A minimum DO concentration of 5.0 mg/l (and 6.0 mg/ daily average for Use III) will be maintained in the mixed surface layer at all times, including during stratified conditions, except during periods of overturn or other naturally-occurring disruptions of stratification; and

- Hypolimnetic hypoxia will be addressed on a case-by-case basis, taking into account morphology, degree of stratification, sources of diagenic organic material in reservoir sediments, and other such factors.

5.1.1.2. Chlorophyll *a*. Maryland's General Water Quality Criteria prohibit pollution of waters of the State by any material in amounts sufficient to create a nuisance or interfere directly or indirectly with designated uses (COMAR 26.08.02.03B(2)). Excessive eutrophication, indicated by elevated levels of Chla, can produce nuisance levels of algae and interfere with designated uses such as fishing and swimming. The excess algal blooms eventually die off and decompose, consuming oxygen. Excessive eutrophication in Prettyboy and Loch Raven Reservoirs is ultimately caused by nutrient overenrichment.

The chlorophyll TMDL endpoints selected for the reservoirs are (1) a maximum permissible instantaneous chlorophyll concentration of 30 μg/l in the surface layers and (2) a 30-day moving average concentration not to exceed 10 μg/l in the surface layers. A concentration of 10 μg/l corresponds to a score of approximately 53 on the Carlson Trophic State Index (TSI). This is at the boundary of mesotrophy and eutrophy, which is an appropriate trophic state at which to manage these reservoirs and should avoid nuisance algal blooms. Reduction of the phosphorus loads is predicted to reduce excessive algal growth and therefore prevent violations of narrative criteria associated with nuisances such as taste, and odor problems or the physical impedance of direct contact use.

5.1.1.3. Sediment. In conjunction with excessive nutrients, Loch Raven Reservoir has experienced excessive sediment loads, resulting in a shortened projected lifespan of the reservoir. The bulk of phosphorus entering a reservoir is usually bound to sediment. Any control strategy directed toward reducing total phosphorus entering a reservoir will concurrently reduce sediment. In reservoirs and impoundments where both a nutrient and sediment impairment exits, MDE believes that the implementation of the total phosphorus TMDL will also remove the sediment impairment.

5.1.2. Baltimore City DPW Monitoring Program

DPW is the only agency that monitors water quality in the reservoirs. DPW samples at three locations in Prettyboy Reservoir and five locations in Loch Raven Reservoir. Figure 5.1.2-1 and 5.1.2.-2 show the location of the sampling locations. Not all locations are sampled at the same time. Sampling is performed by boat at locations GUN0401, GUN0171, and GUN0190, weather permitting; otherwise, in the winter months, samples are taken at fixed locations GUN0399, GUN0156, and GUN0174. Sampling at GUN0142 and GUN0437 can occur either by boat or from a fixed platform.

Samples are analyzed for water temperature, dissolved oxygen, total phosphorus, ammonia, nitrate, turbidity, and Secchi depth, among others. Samples are not analyzed for phosphorus species, organic or total nitrogen, or suspended sediment. Starting at the surface, samples are taken every five feet up to sixty feet; samples are taken at ten-foot intervals thereafter.

Not every sample is analyzed for the entire suite of constituents. Generally, only field measurements like temperature and dissolved oxygen are measured at every depth sampled. Lab analysis is performed for chlorophyll a for each sample collected at the surface and at ten-foot depths up to a depth of 50 feet. In Loch Raven, chemical analysis is performed on samples collected at the surface and every ten feet until a depth of sixty feet. In Prettyboy, chemical analysis is performed on samples taken at the surface and at 10, 20, and 40 feet below the surface, with an additional sample taken at either 60 feet below the surface, in the case of GUN01437, or 80 feet below at the other two stations.

For the purpose of analysis, the locations in Loch Raven sampled by boat and the locations with fixed sampling positions have been paired to yield an annual representation of the lower, middle, and upper portion of the reservoir. Stations GUN0399 and GUN401 in Prettyboy have been paired to represent the lower portion of the reservoir. GUN0437 by itself represents the middle portion of Prettyboy. There are no sampling locations in the upper portion of the reservoir. Table 5.1.2-1 summarizes how the sampling locations are grouped together in this report.

Table 5.1.2-1. Characterization of Reservoir Monitoring Locations

Station	Reservoir	Location	Classification
GUN0142	Loch Raven	Gatehouse	Lower
GUN0156	Loch Raven	Loch Raven Drive bridge	Middle
GUN0171	Loch Raven	Between picnic area and golf course	Middle
GUN0174	Loch Raven	Dulaney Valley Road bridge	Upper
GUN0190	Loch Raven	At the powerlines	Upper
GUN0399	Prettyboy	Gatehouse	Lower
GUN0401	Prettyboy	1000 upstream of dam	Lower
GUN0437	Prettyboy	Beckleysville Road Bridge	Middle

Figure 5.2.1-1. Sampling Locations in Prettyboy Reservoir (from DPW)

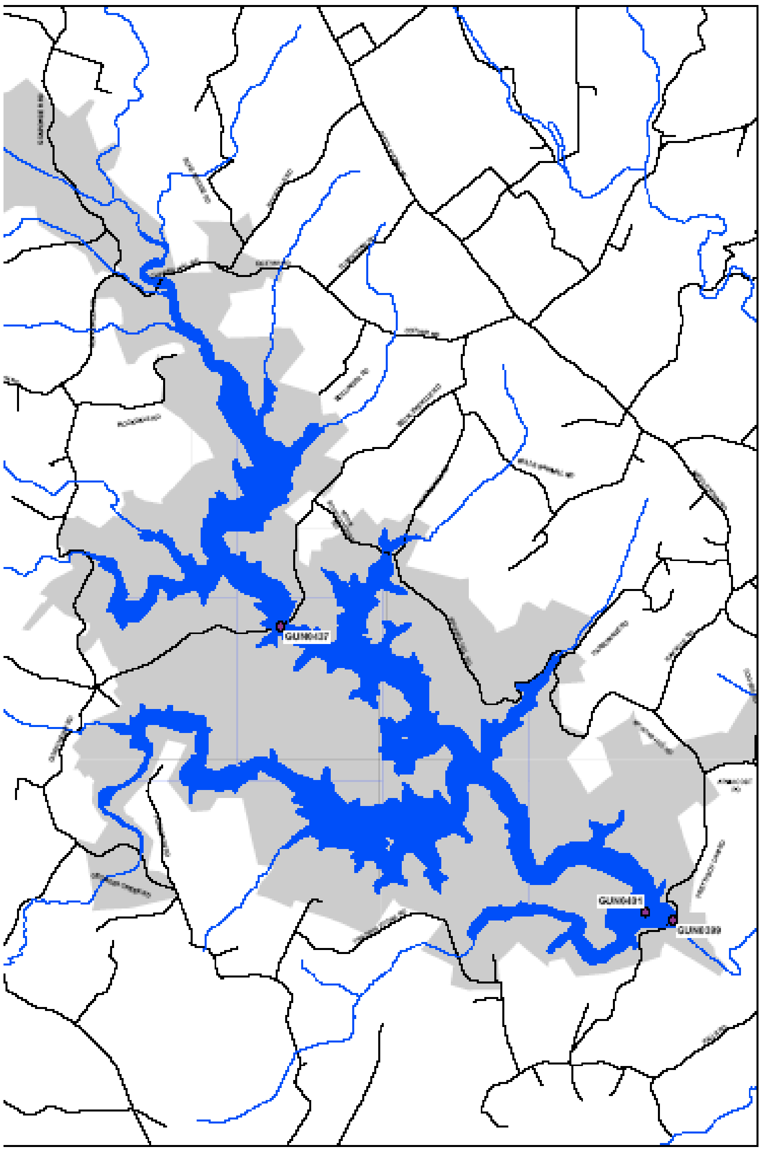

Figure 5.2.1.-2. Sampling Locations, Loch Raven Reservoir (from DPW)

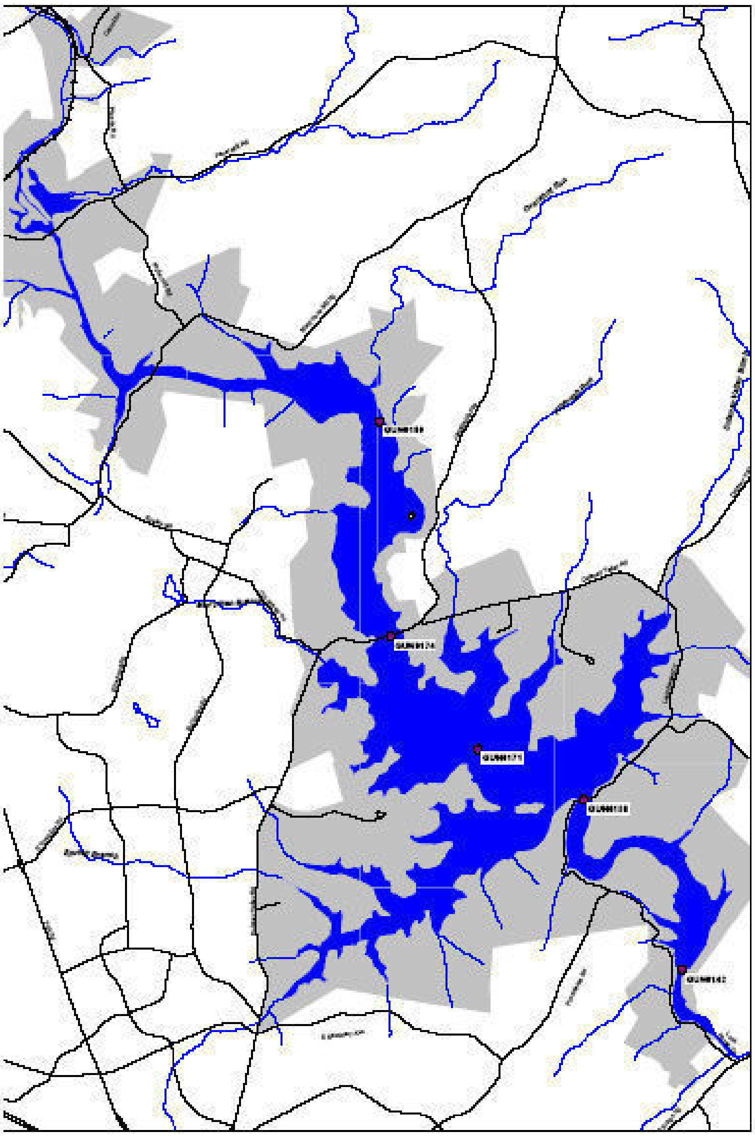

5.1.3. Temperature Stratification

Prettyboy and Loch Raven Reservoir both regularly exhibit temperature stratification starting in April or May and lasting until November. Stratification sometimes occurs in winter but without significant consequences for water quality. During the summer and fall under stratified conditions, bottom waters in both reservoirs become hypoxic, because stable density differences inhibit the turbulent mixing which transports oxygen from the surface.

In order to apply the interim DO criteria to Prettyboy or Loch Raven Reservoir, the well-mixed surface layer must be demarcated. It is difficult, however, to find a fixed criterion that captures the intuitive boundary between the epilimnion and metalimnion that is apparent in temperature profiles, especially since the boundary changes over time. Contour plots of isotherms are a good way of showing seasonal position of the epilimnion. Figure 5.1.3-1 shows a contour plot of isothermals for GUN0142 in Loch Raven Reservoir for the year 1993. Contours are shown only for the first 30 feet from the surface. In the winter, isothermal lines are vertical, showing that the reservoir has fairly uniform temperature over the first 30 feet of depth. In spring, isothermal lines begin to tilt away from the vertical, until by May at depths greater than 15 to 20 feet they are parallel to each other horizontally. At the surface, isothermal lines run perpendicular to a depth of 10 to 15 feet: this defines the epilimnion.

FiguresC.1 through C.8 in Appendix C show isothermal contour plots for Prettyboy Reservoir at the middle and lower sampling locations over the period 1992-2004. Figures C.9 though C.20 in Appendix C gives contour plots the lower, middle and upper sampling locations in Loch Raven Reservoir over the period 1992-2004. Generally, in both Prettyboy and Loch Raven Reservoirs, the epilimnion is limited to a depth of 10 to 15 feet in the summer. For the purposes of this analysis, the surface layer will be considered to be 20 feet deep, with the understanding that in spring and fall, the epilimnion can extend deeper than 20 feet, and that in the summer, it is likely to be shallower.

Figure 5.1.3-1 Isothermal Temperature Contours, Loch Raven Reservoir, Middle Stations, 1993

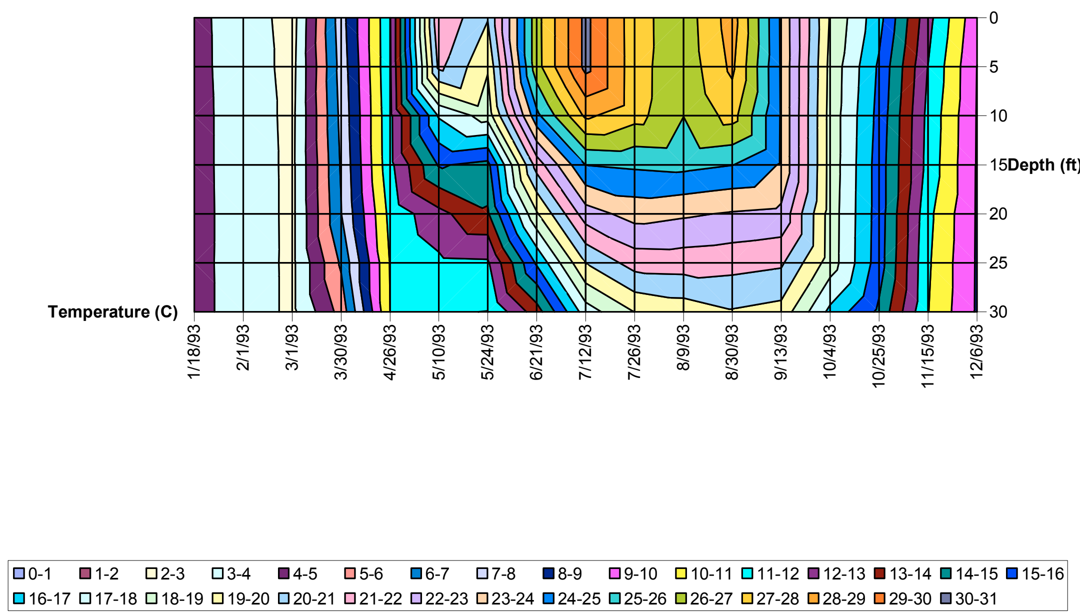

5.1.4. Dissolved Oxygen

Figures C.21 through C.25 in Appendix C show time series of bottom DO concentrations at all monitoring locations in Prettyboy and Loch Raven Reservoirs. Quite clearly, hypoxia occurs in the hypolimnion of both Prettyboy and Loch Raven Reservoirs with regularity.

Figures C.26 through C.30 show time series of DO at the surface and at five-foot intervals up to 20 feet, the screening-level definition of the epilimnion. For the most part, DO concentrations are above the 5 mg/l criterion, but there are periodic excursions below 5 mg/l at the 15 and 20-foot depths.

There are two causes of these low DO concentrations. Tables 5.1.4-1 and 5.1.4-2 list all dates on which the DO concentrations were below 5 mg/l at either 15 or 20-foot sampling depth in Loch Raven and Prettyboy Reservoirs, respectively. They also give the temperature measurements at the 5, 10, 15, and 20 foot sampling depths. In the majority of cases in which apparent hypoxia is observed in the epilimnion, the 20-foot screening depth has over-estimated the depth of the well-mixed layer, as shown by the temperature observations. As was noted the previous section, the depth of the epilimnion is somewhere between 10 and 15 feet in the summer months.

The second cause for low DO concentrations is the entrainment of low DO waters into the epilimnion. Entrainment refers to the process in which turbulent layer spread into a non-turbulent region by transferring turbulence to the non-turbulent fluid (Ford and Johnson, 1986). The non-turbulent fluid is drawn into the turbulent layer as the latter expands. This happens as lakes and reservoirs cool. Ultimately, it leads to the fall overturn typical of many lakes and reservoirs, including Prettyboy and Loch Raven, but it can also happen at any time under stratified conditions when the surface mixed-layer deepens.

All of the nineteen dates on which low DO occurred in Loch Raven without an approximately 2ºC difference in temperature between the 5 and 20 foot depths occurred in September, October or November, and all but five occurred in September alone. The onset of cool weather causes the epilimnion to increase in depth by entraining water from the metalimnion. This water can be low in oxygen and thereby lower the dissolved oxygen concentration in the well-mixed layer. This type of mixing can occur well before the lake or reservoir is fully-mixed during overturn.

This is illustrated by the low DO reading recorded on September 13, 1993, in GUN0171, the middle of Loch Raven Reservoir. Figure 5.1.4-1 shows the DO contour at this location. Figure 10, from the previous section, shows the temperature contour. A comparison of the figures shows that at the end of August, the reservoir at this location was highly stratified, with the well-mixed layer extending to about 15 feet. Throughout September, the surface waters cooled and the epilimnion deepened. The layers with low oxygen concentrations in the summer were drawn into the epilimnion. By October, the epilimnion once again had fairly uniform DO concentrations, although the reservoir had not completely overturned.

Entrainment and overturning account for the other low DO oxygen observations in Loch Raven and Prettyboy as well. In Prettyboy, a third factor also can influence entrainment--drawdown. Withdrawals from reservoir Withdrawals from a reservoir can induce currents which enhance mixing. Figure 5.1.4-2 shows the surface elevation of Prettyboy Reservoir from 1994 through 2004. In 1999 and 2002 (drought years), releases from Prettyboy to fill Loch Raven dropped the surface elevation by 30 feet or more. These drawdowns are probably a contributing factor in mixing low DO concentrations into the surface levels of the reservoir.

Table 5.1.4-1. Observed Low Dissolved Oxygen in the Surface Layer, Loch Raven Reservoir

Date	Location	DO (mg/l)			Temperature (ºC)			Cause
		15 ft	20 ft	5 ft	10 ft	15 ft	20 ft	
6/22/92	Upper	5.83	4.7	21.46	20.95	19.37	17.35	Stratification
8/31/92	Lower	9.21	3.72	24.53	24.18	24.12	22.19	Stratification
8/9/93	Middle	8.43	4.61	26.3	26.01	25.29	23.14	Stratification
9/13/93	Lower	6.61	3.52	24.38	24.39	24	21.97	Stratification
9/13/93	Middle	8.23	4.75	23.88	23.91	23.9	22.76	Entrainment
9/27/93	Lower	1.61	0.26	21.12	20.93	20.48	19.34	Entrainment
7/19/94	Middle	8.57	4.83	28.5	28.33	27.42	23.61	Stratification
8/1/94	Lower	6.36	3.91	27.63	27.36	25.26	23.14	Stratification
8/1/94	Middle	4.85	2.15	27.8	27.55	25.75	23.43	Stratification
8/15/94	Lower	3.31	0.18	26.71	26.67	25.54	22.81	Stratification
8/15/94	Middle	8.68	1.37	26.17	26.11	25.9	23.47	Stratification
8/24/94	Lower	7.43	0.2	24.42	24.31	24.29	22.46	Entrainment
8/24/94	Middle	8.01	0.44	24.38	24.21	24.1	22.08	Stratification
8/29/94	Lower	4.56	0.34	25.97	25.88	24.27	21.43	Stratification
9/12/94	Middle	8.37	3.2	22.82	22.75	22.67	21.94	Entrainment
9/26/94	Lower	5	1.3	21.45	21.22	20.87	20.13	Entrainment
8/28/95	Lower	3.55	1.1	27.15	27.15	24.91	23.11	Stratification
8/28/95	Middle	8.51	2.34	27.11	27.11	27.01	23.8	Stratification
9/11/95	Lower	7.8	1.12	24.73	24.76	24.76	22.61	Stratification
9/11/95	Middle	8.62	3.01	24.67	24.62	24.55	21.39	Stratification
9/25/95	Lower	7.13	1.54	20.83	20.84	20.82	19.55	Entrainment
9/28/95	Lower	6.44	3.22	20.45	20.37	20.34	19.87	Entrainment
7/22/96	Lower	5.29	2.66	25.49	24.83	20.64	19.7	Stratification
7/22/96	Middle	5.81	4.4	25.3	25.15	10.96	19.89	Stratification
8/5/96	Lower	4.13	1.71	25.67	22.53	20.8	19.92	Stratification
8/26/96	Lower	3.42	1.81	26.09	22.4	20.17	19.44	Stratification
9/9/96	Lower	7.12	3.4	24.08	22.91	21.61	19.86	Stratification
9/9/96	Middle	6.98	4.51	24.91	23.42	21.58	20.08	Stratification
9/23/96	Lower	8.44	3.5	21.01	20.98	20.96	20.12	Entrainment
9/23/96	Middle	7.84	1.88	20.6	20.59	20.59	20	Entrainment
9/8/97	Lower	8.84	4.18	23.93	23.92	23.91	22.03	Entrainment
9/22/97	Lower	9.43	2.9	22.59	22.55	22.5	21.29	Entrainment
10/27/97	Lower	2.56	3.4	15.27	15.26	15.1	14.97	Entrainment
8/31/98	Lower	8.4	4.26	27.6	27.49	25.54	23.57	Stratification
9/15/98	Lower	5.37	2.45	24.42	23.91	23.19	22.54	Entrainment
9/28/98	Lower	9	2.85	24.15	23.64	23.08	22.05	Stratification
10/6/98	Lower	6.55	0.26	20.4	20.39	20.35	19.6	Entrainment
11/10/98	Lower	5.62	2.24	12.67	12.67	12.67	12.22	Entrainment
6/21/99	Lower	8.54	4.04	22.82	22.82	22.83	19.61	Stratification

Date	Location	DO (mg/l)			Temperature (ºC)			Cause
		15 ft	20 ft	5 ft	10 ft	15 ft	20 ft	
6/21/99	Middle	9.17	4.15	22.72	22.7	22.66	19.19	Stratification
8/6/02	Upper	4.73	3.57	28.44	27.47	25.96	23.98	Stratification
9/10/02	Lower	8.37	4.89	24.34	24.27	24.22	23.74	Entrainment
9/23/02	Upper	7.92	4.54	23.94	23.67	23.46	22.34	Entrainment
10/29/02	Lower	4.97	4.95	15.32	15.32	15.33	15.33	Entrainment
11/12/02	Lower	4.59	6.56	12.43	12.38	12.21	11.67	Entrainment
8/5/03	Middle	7.46	4.97	26.42	23.51	20.12	19.06	Stratification
8/19/03	Middle	5.84	4.53	26.98	22.6	20.65	19.68	Stratification
8/19/03	Upper	6	4.05	25.7	22.14	20.53	19.45	Stratification
9/9/03	Lower	2.76	0.66	23.85	23.75	20.34	19.71	Stratification
9/9/03	Middle	4.76	3.24	23.82	23.38	20.98	19.67	Stratification
9/23/03	Lower	4.23	2.07	20.55	20.46	19.85	18.9	Entrainment
7/13/04	Middle	4.48	4.61	26.55	24.77	22.08	21.05	Stratification

Table 5.1.4-2. Observed Low Dissolved Oxygen in the Surface Layer, Prettyboy Reservoir

Date	Location	DO (mg/l)		Temperature (º C)				Cause
		15 ft	20 ft	5 ft	10 ft	15 ft	20 ft	
9/14/92	Lower	9.74	3.75	23.04	22.95	22.9	22.57	Entrainment
8/12/96	Lower	5.08	2.7	25.52	25.53	23.97	22.53	Stratification
9/21/99	Lower	5.48	4.27	21.95	21.96	21.78	21.44	Entrainment
10/19/99	Lower	4.96	4.98	17.05	17.05	17.05	17.05	Entrainment
7/22/02	Middle	6.59	2.63	27.35	27.24	25.93	24.34	Stratification
8/26/02	Lower	6.55	4.11	27.66	27.64	27.08	26.21	Entrainment
8/26/02	Middle	6.12	2.24	27.04	27.04	26.93	26.13	Entrainment
9/17/02	Lower	4.34	1.68	23.78	23.57	23.18	22.98	Entrainment
9/17/02	Middle	5.86	3.92	23.34	23.26	23.04	22.8	Entrainment
10/21/02	Lower	4.09	2.81	16.68	16.68	16.68	16.59	Entrainment
6/17/03	Lower	7.4	4.15	17.3	15.85	14.32	12.88	Stratification
6/17/03	Middle	6.14	4.54	21.12	17.59	13.98	11.48	Stratification
7/29/03	Middle	10.46	4.03	26.87	26.65	23.56	20.14	Stratification
8/12/03	Lower	3.42	5.95	26.45	26.37	23.82	21.52	Stratification
8/12/03	Middle	5.58	2.14	26.72	26.53	23.96	21.57	Stratification
6/21/04	Middle	6	4.03	24.27	22.89	20.34	16.63	Stratification

Figure 5.1.4-1. DO Contour, Loch Raven Reservoir, Middle Locations, 1993

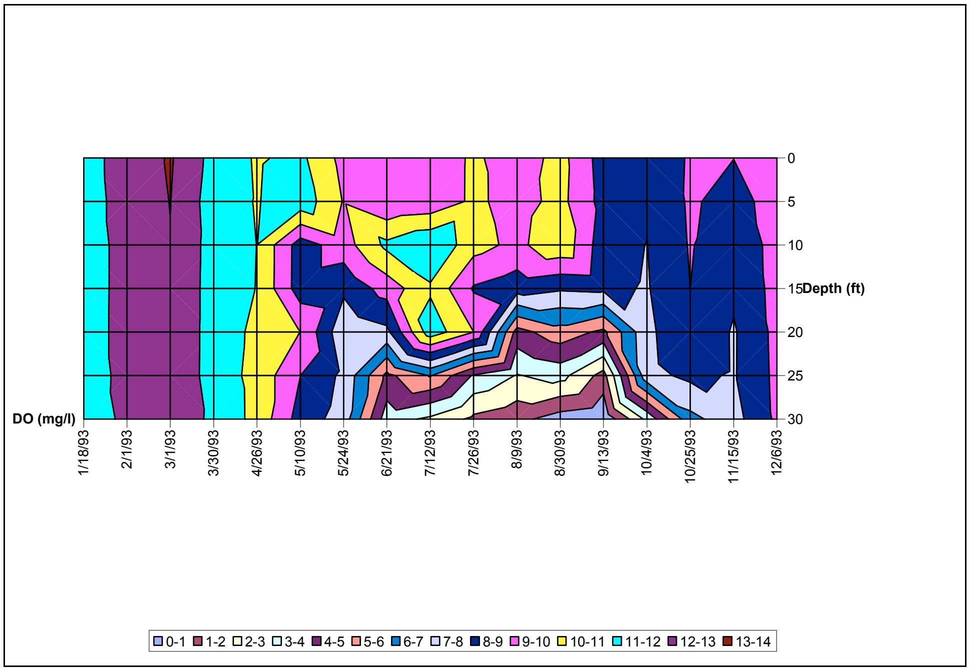

Figure 5.1.4-2. Surface Water Elevation in Prettyboy Reservoir, 1994-2004

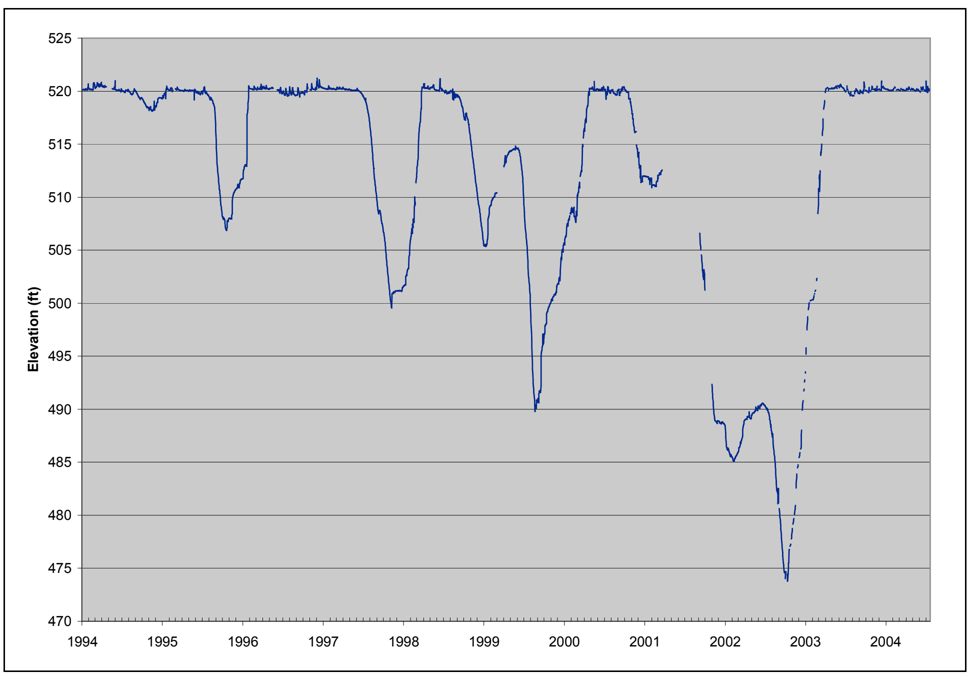

5.1.5. Total Phosphorus

Figures C.31 through C.35 in Appendix C show average total phosphorus concentrations in the top and bottom sampling depths at each monitoring location in Prettyboy and Loch Raven Reservoirs. Surface layer concentrations are an average of the 10 and 20 foot depth samples. Bottom concentrations are averages of samples taken at 40 foot depth or greater. Tables 5.1.5-1 and 5.1.5-2 give summary statistics for TP concentrations in Prettyboy and Loch Raven Reservoirs, respectively. As the tables show, there is a longitudinal gradient to TP concentrations, with concentrations generally decreasing downstream. Walker (1988) believes that this reflects the fact that much of the phosphorus entering the reservoir is bound to sediment, and thus settles out before reaching the dams.

Table 5.1.5-1. Summary Statistics for TP Concentrations in Prettyboy Reservoir, 1992-2004

Statistic	Surface		Bottom	
	Middle	Lower	Middle	Lower
Mean	0.079	0.058	0.075	0.067
Standard deviation	0.112	0.082	0.106	0.110
Minimum	0.002	0.003	0.002	0.002
1st Quartile	0.021	0.019	0.025	0.018
Median	0.045	0.035	0.041	0.040
3rd Quartile	0.078	0.065	0.073	0.066
Maximum	0.675	0.552	0.825	0.970
Count	127	127	127	127

Table 5.1.5-1. Summary Statistics for TP Concentrations in Loch Raven Reservoir, 1992-2004

Statistic	Surface			Bottom		
	Upper	Middle	Lower	Upper	Middle	Lower
Mean	0.078	0.066	0.054	0.084	0.082	0.062
Standard Deviation	0.108	0.102	0.092	0.092	0.148	0.109
Minimum	0.005	0.003	0.002	0.005	0.003	0.003
1st Quartile	0.027	0.023	0.019	0.033	0.026	0.022
Median	0.053	0.042	0.036	0.058	0.045	0.033
3rd Quartile	0.085	0.071	0.060	0.100	0.081	0.078
Maximum	1.010	0.835	1.040	0.580	1.313	1.260
Count	136	139	205	90	138	205

The surface sample itself was excluded from the analysis because samples periodically have concentrations as high as 1 mg/l. These high concentrations are confined to the surface layer and are suspected to be surface films. For this reason DPW also excludes surface layer concentrations (DPW, 1996).

Other problems are suspected in the TP measurements taken in Prettyboy and Loch Raven Reservoirs. Walker (1988) noted that the intra-annual variance of observed TP concentrations in Loch Raven's epilimnion was greater than observed in comparable reservoirs. He noted that Loch Raven's relatively short residence time (3 months) and high sedimentation rate may be in part responsible for the high variance, but he also listed five other factors that might be responsible:

1. Variations in concentration due to flow or other natural factors;
2. Spatial variability in the epilimnion due to hydrodynamic factors;
3. Sampling error;
4. Analytical error; and
5. Data manipulation and reporting error.

Walker recommended, among other things, establishing a routine quality control program with replicate sampling and analytical error variance component analysis to investigate the source of variability.

In a report prepared on behalf of DPW, Jacobson questioned whether Walker had inadvertently inflated the relative size of the intra-annual variability by conflating $\log_{10}$ and natural log transformed data. He seconded Walker's recommendation, however, for more extensive quality control procedures. By comparing regressions of concentration vs. time before and after 1995, Jacobson detected a step increase in concentration in 1995, whose cause is unclear, but which may be related to laboratory procedures (KCI, 2004).

The difficulties in interpreting the reported TP concentrations is illustrated by Figure 5.1.5-1, which shows a time series of reported TP concentrations at the upper monitoring stations in Loch Raven Reservoir, as well as the daily average TP loading rate as calculated by ESTIMATOR, on a monthly basis. There does not appear to be any simple systematic relation between loading rates and observed TP concentrations, although, according to ESTIMATOR results, higher flows result in higher concentrations and higher loads in inflows.

This all goes to say that perhaps the reported reservoir TP concentrations should be treated with caution.

Figure 5.1.5-1. Observed TP Concentrations, Loch Raven Reservoir, Upper Stations, with Western Run monthly TP loading rates from ESTIMATOR.

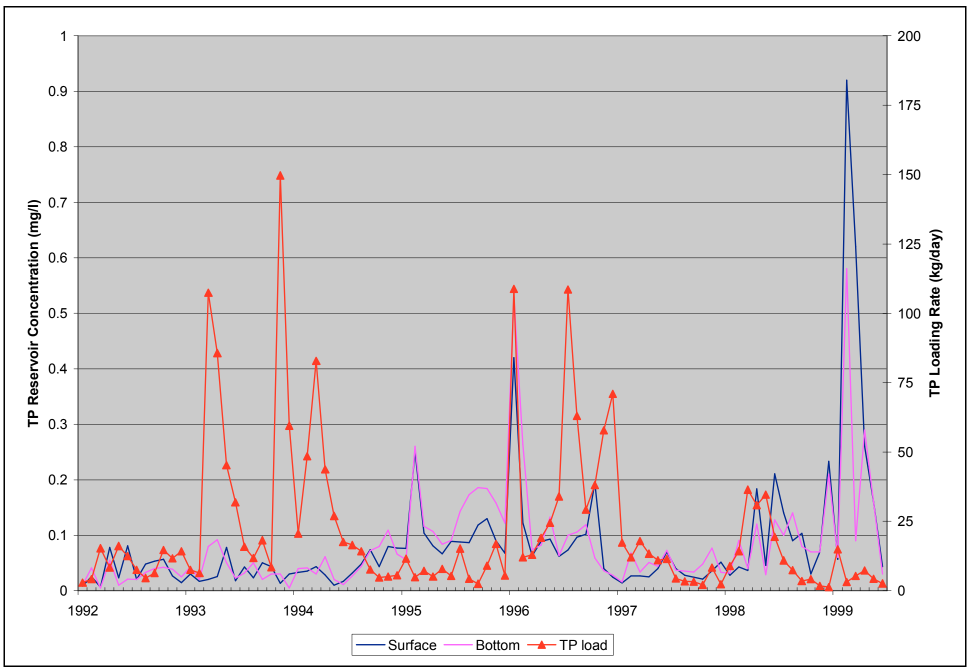

5.1.6. Ammonia and Nitrate

It is a general assumption that the Gunpowder Reservoirs are phosphorus limited, which may explain why DPW does not monitor organic nitrogen (DPW 1996, 2001) In general, a N:P ratio in the range of 5:1 to 10:1 by mass is associated with plant growth being limited by neither phosphorus nor nitrogen. If the N:P ratio is greater than 10:1, phosphorus tends to be limiting, and if the N:P ratio is less than 5:1, nitrogen tends to be limiting (Chianudani *et al*., 1974). In both Prettyboy and Loch Raven Reservoirs, about 7% of the samples taken at the 10 and 20 foot depths have Nitrate:TP ratios less than 10, which can be taken as a cutoff for distinguishing nitrogen limitation from phosphorus limitation. Since there are no data on organic nitrogen in the reservoir, the TN:TP ratio is underestimated by this assessment. The median nitrate:TP ratio in Loch Raven is 38 and the median in Prettyboy is 47. About half the samples from Loch Raven with nitrate:TP ratios less than 10 occur on five dates, all of which appear to be associated with storm events which possibly inflate the TP concentration and exacerbate the underestimation of TN. Thus the monitoring data overwhelmingly shows that phosphorus is the limiting nutrient in both Prettyboy and Loch Raven Reservoirs.

Figures C.36 through C.45 in Appendix C show the average surface and bottom concentrations of ammonia and nitrate in Prettyboy and Loch Raven Reservoirs. Since the surface layers of the reservoirs are not nitrogen limited, bottom concentrations of ammonia and nitrate are more important from the water quality standpoint in two respects. First, the time series graphs of ammonia show, particularly for Loch Raven, that there are significant releases of ammonia from the sediments. This contributes to oxygen demand. Second, nitrate concentrations for the most part remain above 0.5 mg/l. Nitrate is preferred to ferric iron (III) as an electron acceptor in diagenesis. Phosphate in the sediments is bound through ferric iron. It is less likely that phosphate will be released from sediments until ferric iron is reduced in diagenesis. Thus it can be anticipated that the phosphorus release rate from the sediments will remain low.

5.1.7. Secchi Depth

Figures C.46 through C.50 in Appendix C show the time series of observed Secchi depths in Prettyboy and Loch Raven Reservoirs. Secchi depths show a fairly consistent seasonal trend, which is illustrated by Figures 5.1.7-1 and 5.1.7-2, which show the average monthly Secchi depth at the lower stations in Prettyboy and Loch Raven Reservoirs, respectively. Secchi depths are highest in summer and lowest in winter or early spring, and vary almost by a factor of three over the year. The maximum observed Secchi depth in Loch Raven Reservoir over the period 1992-2004 is 24.4 feet; the maximum in Prettyboy Reservoir over the same period is 28.8 feet.

Figure 5.1.7-1. Average Monthly Secchi Depth, 1992-2004, Lower Stations in Prettyboy Reservoir

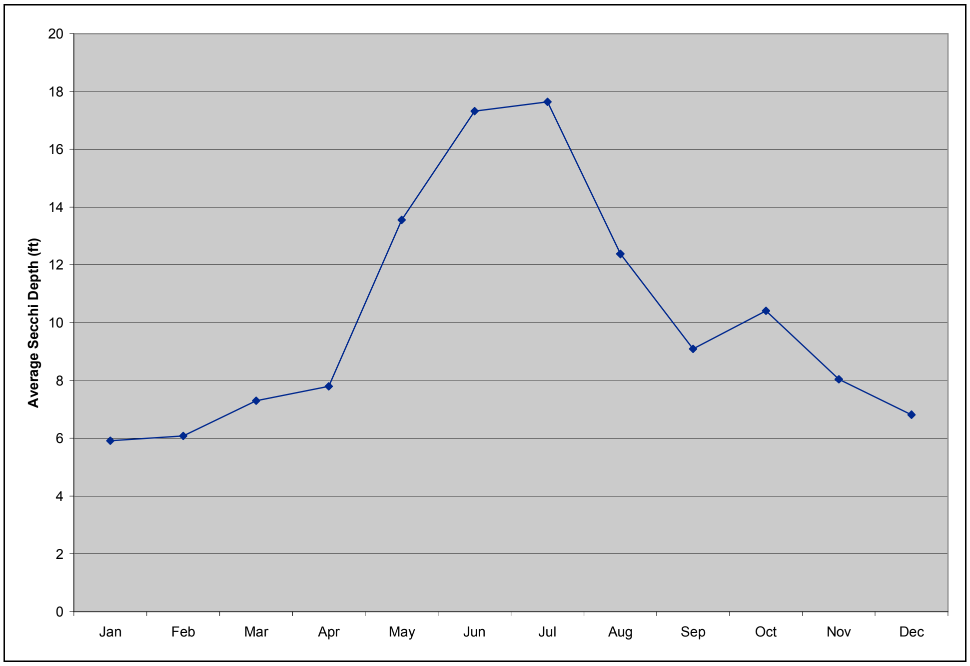

DPW routinely monitors turbidity and apparent color in Prettyboy and Loch Raven Reservoirs. To determine the contribution of non-algal solids to Secchi depth, the correlations between Secchi depth, turbidity, chlorophyll a, and apparent color were calculated. Turbidity, chlorophyll a, and apparent color were averaged over sampling depths less than or equal to 20 feet. The results are shown in Table 5.1.7-1 for Prettyboy and 5.1.7-2 for Loch Raven Reservoirs. Generally, the correlations among Secchi depth, turbidity and color are stronger than the correlation between chlorophyll a and either Secchi depth, turbidity, and color, especially in Loch Raven Reservoir. Non-algal sources of turbidity and light extinction are dominant in Loch Raven. The algal contribution to light extinction is stronger in Prettyboy.

A multiple regression equation was fitted for each reservoir with Secchi depth as the dependent variable and turbidity, chlorophyll a, and apparent color as the independent variables. The results are shown in Table 5.7.-3 Because of the high correlation between color and turbidity, color is not significant in the Prettyboy regression model and turbidity is not significant in the Loch Raven regression model. In Prettyboy turbidity is the dominant factor in reducing Secchi depth but in Loch Raven, the magnitude of the chlorophyll a coefficient is large enough that over the range of observed values it can decrease Secchi depth as much as color.

Figure 5.1.5-2 Average Monthly Secchi Depth, 1992-2004, Lower Station in Loch Raven Reservoir

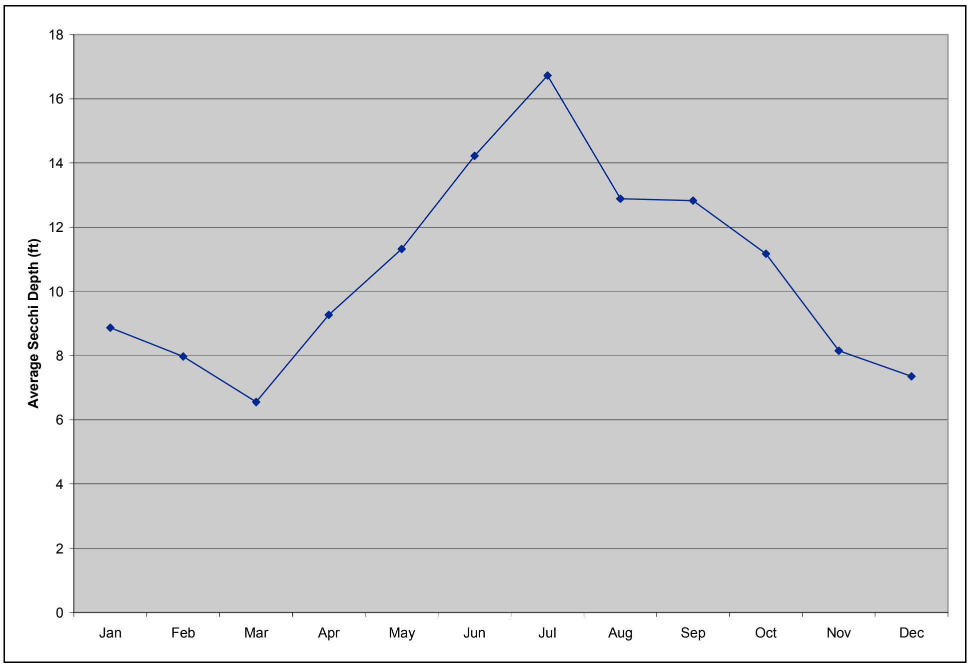

Table 5.1.7-1. Prettyboy Reservoir Water Clarity Correlations

	Secchi	Chlorophyll	Color	Turbidity
Secchi Depth	1			
Chlorophyll a	-0.52224	1		
Color	-0.51869	0.319404	1	
Turbidity	-0.66981	0.393389	0.614317	1

Table 5.1.7-2. Loch Raven Reservoir Water Clarity Correlations

	Secchi	Chloropyll	Color	Turbidity
Secchi	1			
Chloropyll	-0.21575	1		
Color	-0.66541	0.172617	1	
Turbidity	-0.51967	0.067589	0.761641	1

Table 5.1.7-3. Secchi Depth vs. Cholorophyll a, Color and Turbidity Regression Equation Results

Coefficient Estimate	Prettyboy	Loch Raven
Intercept	15.97	15.80
Chlorophyll a	-0.29	-0.13
Color	-0.11	-0.48
Turbidity	-1.40	-0.07
R Square	0.54	0.45

5.1.8. Algae and Chlorophyll a

Figures C.51 through C.55 Appendix C contains figures showing the time series of maximum chlorophyll a concentrations in the surface layer at the sampling locations in Prettyboy and Loch Raven Reservoirs. The same information is presented in perhaps a clearer format in Tables 5.1.8-1 and 5.1.8-2, which show the maximum chlorophyll a concentrations by month and year, 1992-2004. As the tables show, chlorophyll concentrations above 10 µg/l occur frequently but not regularly. Concentrations above 30 µg/l are infrequent but not unusual.

In Loch Raven Reservoir, the largest concentrations tend to occur in early spring or in October. Concentrations are most consistently above10 µg/l in the summer months. Concentrations are most consistently below 10 µg/l in the winter months. In Prettyboy Reservoir, in contrast, surface chlorophyll a concentrations are most consistently above 10 µg/l in late winter and early spring. Concentrations above 30 µg/l are most frequently found in March or secondarily in September and October. Surface chlorophyll concentrations tend to be below 10 µg/l from May through July, as well as in November and December.

Counts of algal taxa are available April through September from Loch Raven and May through September from Prettyboy Reservoir. Colonies are counted as individuals, so it is impossible to calculate algal biomass from the available data. The relative abundance of taxa, however, indicates a typical seasonal pattern to algal succession. Figures 5.1.8-1 and 5.1.8.2 show the average relative abundance of the algal taxa by month for Loch Raven and Prettyboy Reservoirs, respectively, 1992-1996. In Loch Raven diatoms are usually dominant until July. Greens dominate briefly in midsummer. Then, if conditions are right for a bloom, blue-green algae dominate in late summer and early fall; otherwise diatoms resume dominance. A similar pattern holds in Prettyboy Reservoir. Occasionally, other algal groups can dominate. Chrosophytes were abundant in Loch Raven Reservoir in spring, 1996. Dinoflagellates can account for 15-25% of the algae counted.

Table 5.1.8-1. Maximum Chlorophyll A Concentration (Mg/L) in Surface Layer by Month, Loch Raven Reservoir

Location	Year	Jan	Feb	Mar	Apr	May	Jun	Jul	Aug	Sep	Oct	Nov	Dec
Lower	1992	8.1	6.4	4.4	4.8	10.6	7.7	15.7	17.8	7.3	5.1	4.8	5.9
Lower	1993	5.7	6.4	8.0	8.5	21.2	14.4	12.9	11.2	11.3	5.6	2.8	13.5
Lower	1994	5.9	11.2	11.4	20.6	18.4	20.3	8.5	9.8	3.8	3.0	2.3	1.4
Lower	1995	2.6	4.6		4.4	7.3	5.8	11.4	7.4	3.0	3.7	3.9	7.1
Lower	1996	6.0	12.1	35.3	9.8	7.4	4.6	18.1	22.7	11.7	6.6	4.9	2.2
Lower	1997	1.9	12.0	4.8	3.0	4.8	6.8	5.6	8.4	3.6	8.9	4.7	5.3
Lower	1998	4.4	3.5	14.3	1.2	11.1	10.2	10.8	5.8	8.2	42.8	3.5	4.7
Lower	1999	6.5	5.8	8.9	14.8	8.9	8.9	4.9	6.4	10.5	5.6	4.4	4.6
Lower	2000		6.5	6.9	7.1	7.2	5.6	15.5	10.9	6.7	7.9	6.9	4.7
Lower	2001	5.9	6.7	8.0	8.7	4.7	11.6	4.5	9.4	7.2	4.2	6.2	6.8
Lower	2002	5.8	4.0	4.5	1.7	7.9	3.8	2.8	2.4	6.5	8.1	2.4	4.9
Lower	2003	9.8	7.2	8.1	10.0	9.4	26.0	9.4	19.2	9.6	7.2	9.0	2.1
Lower	2004	2.6	5.3	20.3	12.5								
Middle	1992	9.9	7.0	4.6	5.7	2.6	10.1	18.3	14.1	8.8	4.8	5.9	7.5
Middle	1993	6.9	7.0	5.7	8.3	15.6	14.0	30.0	13.5	6.9	7.8	5.1	6.9
Middle	1994	2.8	14.1	5.1	15.2	19.6	10.1	18.7	20.4	3.8	2.6	2.1	1.0
Middle	1995	2.6	4.2		4.0	13.0	8.2	13.3	8.2	3.5	5.6	5.6	7.4
Middle	1996		8.9	21.2	10.4	2.4	10.9	8.3	9.6	9.8	6.4	3.7	2.5
Middle	1997	1.6	16.1	5.6	3.5	4.0	12.0	7.1	8.3	5.7	13.3	6.8	7.0
Middle	1998	3.7	4.2	8.1	3.8	10.1	13.6	10.5	10.1	4.5	17.3	2.6	5.4
Middle	1999	6.5	5.6	27.0	10.7	19.6	9.3	8.5	7.9	6.9	5.6	5.1	3.9
Middle	2000		6.5	6.9	7.9	6.6	4.5	9.3	10.3	7.1	8.6	8.5	5.6
Middle	2001	2.8	4.5	9.2	9.6	4.7	8.2	6.9	11.6	6.0	4.5	7.4	8.1
Middle	2002	7.6	4.2	5.1	3.1	7.4	6.1	5.4	5.3	8.5	4.9	7.4	6.4
Middle	2003	7.0	6.5	7.6	7.4	15.1	11.4	17.2	19.1	10.3	52.6	6.5	2.6
Middle	2004	2.3	5.1	15.5	12.1								
Upper	1992	10.0	4.5	4.8	3.0	4.1	7.7	10.0	12.1	9.3	7.6	6.6	6.4
Upper	1993	4.8	6.1	6.4	6.7	10.3	5.2	10.2	12.9	12.2	6.7	5.8	15.0
Upper	1994	3.7	4.9	2.6	9.4	20.0	9.9	10.7	14.9	8.1	3.5	1.6	4.5
Upper	1995	3.5	3.2		4.5	13.8	9.7	8.5	8.7	4.9	5.3	8.5	8.2
Upper	1996		2.1	27.7	12.1	9.2	3.9	8.5	13.4	12.7	11.6	3.7	2.5
Upper	1997	1.5	8.3	5.3	7.6	5.5	5.2	7.4	5.6	6.1	43.2	9.0	5.1
Upper	1998	4.7	5.3	6.9	4.2	8.1	6.4	14.2	6.4	5.8	9.4	9.4	4.4
Upper	1999	1.4	6.6	6.1	16.4	22.4	9.2	7.4	9.6	9.3	6.9	2.3	3.9
Upper	2000		7.4	6.5	6.7	6.1	6.3	17.0	10.5	10.8	11.2	7.8	4.7
Upper	2001	1.9	3.5	9.1	4.7	4.7	8.8	3.7	13.2	7.6	6.0	10.1	12.5
Upper	2002	6.9	4.7	4.7	4.0	7.9	3.1	14.2	4.5	7.4	5.4	9.4	6.0
Upper	2003	4.2	2.1	2.3	4.0	47.1	19.3	12.3	16.1	10.7	8.1	1.9	1.4
Upper	2004	2.1	1.7	14.0	11.0								
Lower	Average	5.4	7.1	11.2	8.2	9.9	10.5	10.0	11.0	7.4	9.1	4.6	5.3
Middle	Average	4.9	7.2	10.1	7.8	10.1	9.9	12.8	11.5	6.8	11.2	5.5	5.4
Upper	Average	4.1	4.6	8.0	7.3	13.3	7.9	10.3	10.7	8.7	10.4	6.3	6.2

Table 5.1.8-2. Maximum Chlorophyll A Concentration (Mg/L) in Surface Layer by Month, Prettyboy Reservoir

Location	Year	Jan	Feb	Mar	Apr	May	Jun	Jul	Aug	Sep	Oct	Nov	Dec
Lower	1992	4.2	11.3	5.3		7.9	6.1	3.9	10.7	20.1	11.0	6.4	7.9
Lower	1993	3.9	9.4	9.6	19.3	12.9	7.7	6.9	8.2	11.9	10.0	5.4	4.2
Lower	1994	10.9	9.6	4.0	27.6	27.1	4.9	7.4	10.2	5.1	5.1	4.0	3.0
Lower	1995	5.4		10.5	8.1	3.0	4.6	11.7	13.2	12.3	5.8	3.8	6.0
Lower	1996	9.0	25.0	30.8	13.5	2.6	3.1	4.6	14.2	10.3	6.9	4.0	4.2
Lower	1997	11.8	13.9	16.3	15.5	7.1	3.1	4.6	4.9	7.0		9.6	4.4
Lower	1998	5.9	7.4	4.2	3.1	7.5	16.0	6.8	4.3	4.7	4.4	4.3	10.3
Lower	1999	5.3	22.3	4.0	8.0	1.3	2.6	3.7	11.6	17.0	12.0	4.1	3.1
Lower	2000	3.0	6.5	7.6	11.9	2.8	2.6	0.3	5.4	9.7	3.6	4.4	5.5
Lower	2001			7.8	3.7	5.4	2.3	2.1	6.1	10.8	6.0	4.2	4.5
Lower	2002	8.8	9.8	8.1	14.6	2.8	4.5	12.0	16.7	29.1	6.2	6.8	13.8
Lower	2003	12.5		34.3	22.9	6.5	22.8	32.8	11.2	13.6	8.1	2.6	2.4
Lower	2004	7.6	6.0	12.9	14.2								
Middle	1992	10.9	11.6	12.7		6.2	13.0	15.1	13.4	37.4	31.1	17.1	10.8
Middle	1993	8.6	11.4	10.3	8.1	14.2	13.2	7.0	7.5	6.5	9.4	8.2	5.2
Middle	1994	13.5	14.1	6.5	21.5	12.5	9.2	4.6	18.2	7.2	5.4	4.9	5.1
Middle	1995	6.8		9.5	7.1	2.7	5.8	7.7	12.0	9.7	8.7	6.0	9.8
Middle	1996	12.0	3.3	30.1	9.5	3.0	5.2		12.7	6.3	10.1	4.6	6.7
Middle	1997	33.1	10.7	10.9	13.4	8.9	4.9	2.1	4.7	4.0		6.6	10.1
Middle	1998	6.5	14.3	5.4	3.1	9.9	11.2	13.5	3.1	4.4	3.3	8.9	5.4
Middle	1999	5.3	20.6	6.6	8.5	2.1	1.9	5.2	19.3	25.6	21.5	7.9	9.1
Middle	2000	6.1	6.7	5.6	10.9	8.5	6.3	5.0	4.9	9.0	5.8	7.2	8.9
Middle	2001	12.9	7.4	9.3	8.8	5.1	3.0	3.1	6.5	11.6	10.8	13.4	14.6
Middle	2002	10.3	16.4	18.6	11.2	10.7	7.9	12.6	19.7	32.7	48.1	13.4	10.1
Middle	2003	8.7		16.8	8.3	5.8	19.1	23.0	4.7	7.2	6.9	4.9	7.1
Middle	2004	7.4	4.4	12.5	11.8								
Lower	Average	7.4	12.1	11.9	13.5	7.3	6.7	8.0	9.7	12.6	7.2	5.0	5.8
Middle	Average	10.9	11.0	11.9	10.2	7.5	8.4	9.0	10.6	13.5	14.7	8.6	8.6

Figure 5.1.8-1. Relative Abundance of Algal Taxa by Month, Loch Raven Reservoir GUN0142

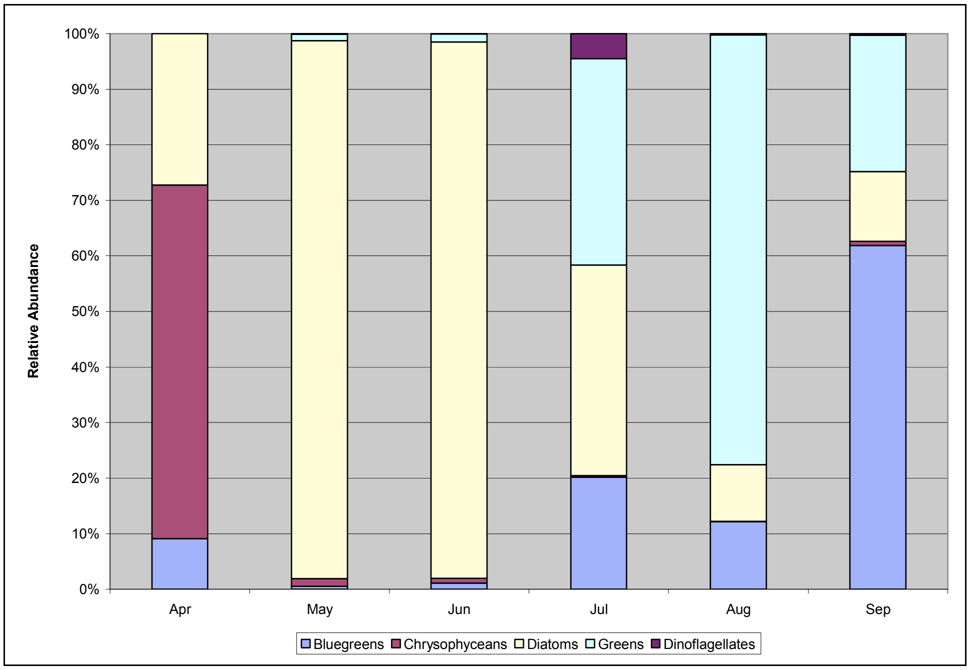

Figure 5.1.8-2. Relative Abundance of Algal Taxa by Month, Prettyboy Reservoir GUN0401

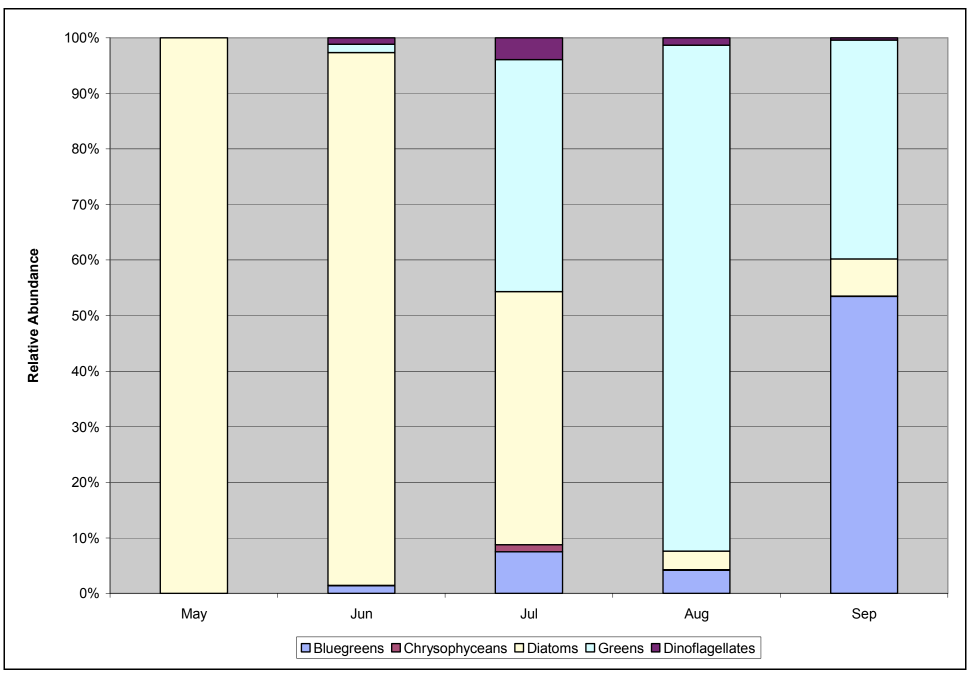

5.1.9. Trophic Indices

Prettyboy and Loch Raven Reservoirs have been "found to be in various states of eutrophication" (Reservoir Watershed Protection Committee, 1996) since the 1970s. In a recent review of its monitoring data, DPW (2000) used the Carlson Trophic State Index to classify chlorophyll *a*, Secchi depths, and total phosphorus samples in the reservoirs. Using a critical value of 10 µg/l TP to separate mesotrophic from eutrophic conditions, DPW found that chlorophyll *a* samples form the epilimnion in Prettyboy Reservoir met or exceeded the mesotrophic level 26.2 % of the time, while samples from Loch Raven Reservoir met or exceeded the level 19.8% of the time. DPW defined the depth of the epilimnion to be 30 feet, and samples were analyzed only from the months of April through September. For total phosphorus, DPW used 26 µg/l as the critierion separating mesotrophic from eutrophic conditions. By this criterion, 55.5% of Prettyboy's epilimnetic total phosphorus samples were eutrophic, as were 57.2% of the samples in Loch Raven. For Secchi depth, DPW used 1.86 m as the demarcation between mesotrophic and eutrophic states. Only 7.3% of the Secchi depth measurements in Prettyboy were below the criterion; similarly, only 7.9% of Loch Raven samples were below the criterion. Neither Prettyboy nor Loch Raven Reservoir are as eutrophic when measured by water clarity as when measured by the other trophic state indicators.

5.1.10. Sedimentation

The Maryland Geological Survey (MGS) performed new bathymetry surveys of Prettyboy and Loch Raven Reservoirs in 1998 (Ortt et al., 2000). The bathymetry of the reservoirs is described in more detail in Section 5.2. This section will discuss MGS's estimate of sedimentation rates. Average annual sediment rates can be described in many ways: percent loss of capacity, inches of sediment accumulation per year, or tons/mi^2/yr. The latter measure was estimated by RTG (2004), based on the MGS survey. Table 5.1.10-1 summarizes the average sediment accumulation rate for Prettyboy and Loch Raven Reservoirs.

The annual percent capacity loss rates in Prettyboy (0.12%) and Loch Raven (0.13%) Reservoirs compare favorably with the national averages, as reported by MGS (2000).

The mean average capacity loss rate for comparably sized reservoirs is 0.43%; the median is 0.27% (Ortt et al., 2000). Sediment accumulation varies spatially, however, within the reservoirs. MGS estimated that the Dulaney Branch of Loch Raven has lost 8% of its capacity, the Long Quarter Branch has lost 13% of its capacity, and the upper reservoir has lost 19% of its capacity. Sediment deposits in the former stream channel were greater than 10 feet thick and ran as high as 59 feet thick. The survey was not able to proceed above Warren and Merryman's Mill Road bridge because the reservoir became unnavigable.

Table 5.1.10-1. Sedimentation Rates in Prettyboy and Loch Raven Reservoirs

Sedimentation Rates	**Prettyboy**	**Loch Raven**
Total Capacity Lost Since Construction	7.5%	10.8%
Annual Average Capacity Lost	0.12%	0.13%
Sediment Accumulation Rate (in/yr)	0.6	0.6
Sediment Deposition Rate (tons/mi^2/year)	1.15	0.49

5.2. OVERVIEW OF THE CE-QUAL-W2 MODEL

CE-QUAL-W2 is a laterally-averaged two-dimensional computer simulation model capable, in its most recent formulations, of representing the hydrodynamics and water quality of rivers, lakes, and estuaries. It is particularly suited for representing temperature stratification that occurs in reservoirs like Prettyboy and Loch Raven.

The original version of CE-QUAL-W2 was the LARM (Laterally Averaged Reservoir Model) by Edinger and Buchak (1975). US Army Engineer Waterways Experiment Station (WES) added a water quality component to make CE-QUAL-W2 version 1. Version 2 (Cole and Buchak, 1995) added many computational improvements and permitted the simulation of reservoirs with multiple branches. Version 3 (Cole and Wells, 2003) expanded the hydrodynamic simulation capacities of the model so that rivers and estuaries could also be simulated.

Waterbodies represented in CE-QUAL-W2 are divided longitudinally into segments and vertically into layers. A model cell is defined by the intersection of layers and segments. The bottom cell in a segment is fixed by the waterbody's bathymetry. The number of cells in a segment varies with the position of the free surface of the waterbody. Every time step CE-QUAL-W2 simulates the location of the free surface in each segment.

Cole and Buchak (1995) provide a clear exposition of the CE-QUAL-W2 model structure as it is implemented for simulating reservoirs. Figure 5.2-1 gives six basic equations which constitute the W2 model. There are six unknowns associated with these six equations: (1) the free surface ,η; (2) the pressure, P; (3) the horizontal velocity ,U; (4) the vertical velocity, W; (5) the constituent concentration, φ; and (6) the density, ρ. Substituting the horizontal momentum equation (A-1), the pressure equation (A-4), and the equation of state (A-6) into the free surface equation and integrating in the vertical direction, an equation for the free surface can be determined which is a function of waterbody geometry and the hydrodynamic variables from the previous time step:

Figure 5.2-1.
THE BASIC EQUATIONS OF CE-QUAL-W2
(Cole and Buchak, 1995)

Horizontal Momentum

$$\frac{\partial UB}{\partial t} + \frac{\partial UUB}{\partial x} + \frac{\partial WUB}{\partial z} = -\frac{1}{\rho}\frac{\partial BP}{\partial x} + \frac{\partial \left(BA_x \frac{\partial U}{\partial x} \right)}{\partial x} + \frac{\partial B\tau_x}{\partial z} \qquad \text{(A-1)}$$

where

U = longitudinal, laterally averaged velocity, *m sec*$^{-1}$
B = waterbody width, m
t = time, *sec*
x = longitudinal Cartesian coordinate: x is along the lake centerline at the water surface, positive to the right
z = vertical Cartesian coordinate: z is positive downward
W = vertical, laterally averaged velocity, *m sec*$^{-1}$
ρ = density, *kg m*$^{-3}$
P = pressure, N *m*$^{-2}$
A_x = longitudinal momentum dispersion coefficient, *m2 sec*$^{-1}$
τ_x = shear stress per unit mass resulting from the vertical gradient of the horizontal velocity, U, *m*^{2} *sec*$^{-2}$

Constituent Transport

$$\frac{\partial B\Phi}{\partial t} + \frac{\partial UB\Phi}{\partial x} + \frac{\partial WB\Phi}{\partial z} - \frac{\partial \left(BD_x \frac{\partial \Phi}{\partial x} \right)}{\partial x} - \frac{\partial \left(BD_z \frac{\partial \Phi}{\partial z} \right)}{\partial z} = q_\Phi B + S_\Phi B \qquad \text{(A-2)}$$

where

Φ = laterally averaged constituent concentration, g m^{-3}
D_x = longitudinal temperature and constituent dispersion coefficient, m2 sec^{-1}
D_z = vertical temperature and constituent dispersion coefficient, m2 sec^{-1}
q_Φ = lateral inflow or outflow mass flow rate of constituent per unit volume, g m^{-3} sec^{-1}
S_Φ = kinetics source/sink term for constituent concentrations, g m^{-3} sec^{-1}

Free Water Surface Elevation

$$\frac{\partial\ B_\eta \eta}{\partial\ t} = \frac{\partial}{\partial\ x} \int_\eta^h UB\ dz - \int_\eta^h qB\ dz \qquad \text{(A-3)}$$

where

B_η = time and spatially varying surface width, m
η = free water surface location, m
h = total depth, m
q = lateral boundary inflow or outflow, m3 sec^{-1}

Hydrostatic Pressure

$$\frac{\partial\ P}{\partial\ z} = \rho g \qquad \text{(A-4)}$$

where

g = acceleration due to gravity, m sec^{-2}

Continuity

$$\frac{\partial\ UB}{\partial\ x} + \frac{\partial WB}{\partial\ z} = qB \qquad \text{(A-5)}$$

Equation of State

$$\rho = f\,(T_w\,, \Phi_{TDS}\,, \Phi_{ss}) \qquad \text{(A-6)}$$

where

$f(T,\Phi_{TDS},\Phi_{ss})$ = density function dependent upon temperature, total dissolved solids or salinity, and suspended solids

---

$$\frac{\partial \bar{B}\eta}{\partial t} - g\,\Delta t\,\frac{\partial}{\partial x}\left(\frac{\partial \eta}{\partial x}\int_{\eta}^{h} B\,dz\right) = \frac{\partial}{\partial x}\int_{\eta}^{h} UB\,dz - \frac{g\Delta t}{\rho_{\eta}}\frac{\partial}{\partial x}\int_{\eta}^{h}\left[B\int_{\eta}^{z}\frac{\partial \rho}{\partial x}\,dz\right]dz \tag{A-7}$$

$$+\frac{\partial}{\partial x}\left[B_h\tau_h - B_{\eta}\tau_{\eta} - \int_{\eta}^{h}\tau_x\frac{\partial B}{\partial z}\,dz\right]\Delta t$$

$$+\frac{\partial}{\partial x}\left[\int_{\eta}^{h} F_x\,dz\right]\Delta t - \int_{\eta}^{h} qB\,dz$$

(Cole and Burchak, 1995)

Each time step, the following computations are performed:

1. Equation A-7 is solved implicitly for the free surface elevation, η;
2. Horizontal velocities are calculated from wind shear, bottom shear, and the baroclinic and bartropic pressure gradients;
3. Vertical velocities are determined from the free surface elevations, horizontal velocities, and the continuity equation; and
4. Constituent concentrations are calculated using equation A-2.

More details of the CE-QUAL-W2 model structure can be found in Cole and Buchak (1995) and Cole and Wells (2003).

Model parameters specify, among other things, the kinetic rates which control how constituents are transformed among themselves. These transformations are counted among the sources and sinks of constituents in Equation A-2. In addition to model parameters, W2 requires (1) the specification of a time series of inflow volumes, temperatures, and constituent concentrations; (2) meteorological inputs such as wind speed, air temperature, dew point, and cloud cover; and (3) boundary conditions such as outflows or water surface elevations.

5.3. IMPLEMENTATION OF THE CE-QUAL-W2 MODEL FOR PRETTYBOY AND LOCH RAVEN RESERVOIRS

The original W2 models of Prettyboy and Loch Raven Reservoirs used Version 2 of the CE-QUAL-W2 model. Only hydrodynamics and temperature were simulated. Simulated flows from the W2 models were then used to drive WASP models that simulated dissolved oxygen and eutrophication in the reservoirs. Only the year 1992 was simulated.

The current reservoir models use version 3.2 of CE-QUAL-W2. The simulation period was expanded to 1992-1997 to coincide with the Gunpowder HSPF Model. Each year was simulated separately, and observed data, where available, was used to set the initial conditions for the simulation. The current W2 reservoir models were used to simulate not only hydrodynamics and temperature but dissolved oxygen and eutrophication dynamics as well.

5.3.1. Segmentation and Model Cell Properties

The longitudinal segmentation of the representation of Prettyboy and Loch Raven Reservoirs was adopted from the original models. Figures 5.3.1-1 and 5.3.1-2 show the longitudinal segmentation of Prettyboy and Loch Raven Reservoirs, respectively. As the figures show, Loch Raven Reservoir is represented as a single main branch, while Prettyboy Reservoir has, in addition to the main branch, a tributary branch representing Georges Run. The linkages between reservoir segments and tributary inflows were also adopted from the original model. Tables 5.3.1-1 and 5.3.1-2 show the percent of flows and loads from HSPF model segments which enter Prettyboy and Loch Raven segments, respectively.

Like the original model, layers were defined to be one meter thick. The number of cells in each segment, however, and the width of these cells, were recalculated, based on new reservoir bathymetry surveys conducted by the MGS (2000). Starting from a grid representing bottom elevations determined by the survey, the number of cells in each segment and their widths were calculated as follows:

1. The grid elevations were rounded to the nearest tenth of a meter;
2. The area at each tenth meter interval of bottom elevation was calculated by segment through a GIS overlay;
3. Starting from one-half meter below the normal surface elevation (the elevation of the spillway crest), the sum of the area in each segment less than or equal to that elevation was calculated. This represents the area of the cross-sectional area (in plane view) of the segment, taken at the midpoint of each cell;
4. The width of the cell was calculated by dividing the area slice in (3) by segment length; and
5. Following the recommendation of the CE-QUAL-W2 manual, the minimum width of a cell was set at five meters. This in effects set the number of cells in a segment and thus the depth of the segment.

Tables 5.3.1-3 and 5.3.1-4 show the number of cells and layer depths of the segments of Prettyboy and Loch Raven Reservoirs, respectively.

Figures 5.3.1-3 and 5.3.1-4 compare the volume-elevation curves calculated directly from bathymetric data with curves based on the representation of the reservoirs in the models. The representation of Prettyboy Reservoir matches the observed curve well at the highest water surface elevations but diverges somewhat at lower elevations. The model of Loch Raven appears to overpredict reservoir volumes, but the difference between observed and modeled volumes is due in part to the fact that the bathymetric survey did not cover completely the upper two segments of Loch Raven.

Figure 5.3.1-1. Model Segmentation of Prettyboy Reservoir

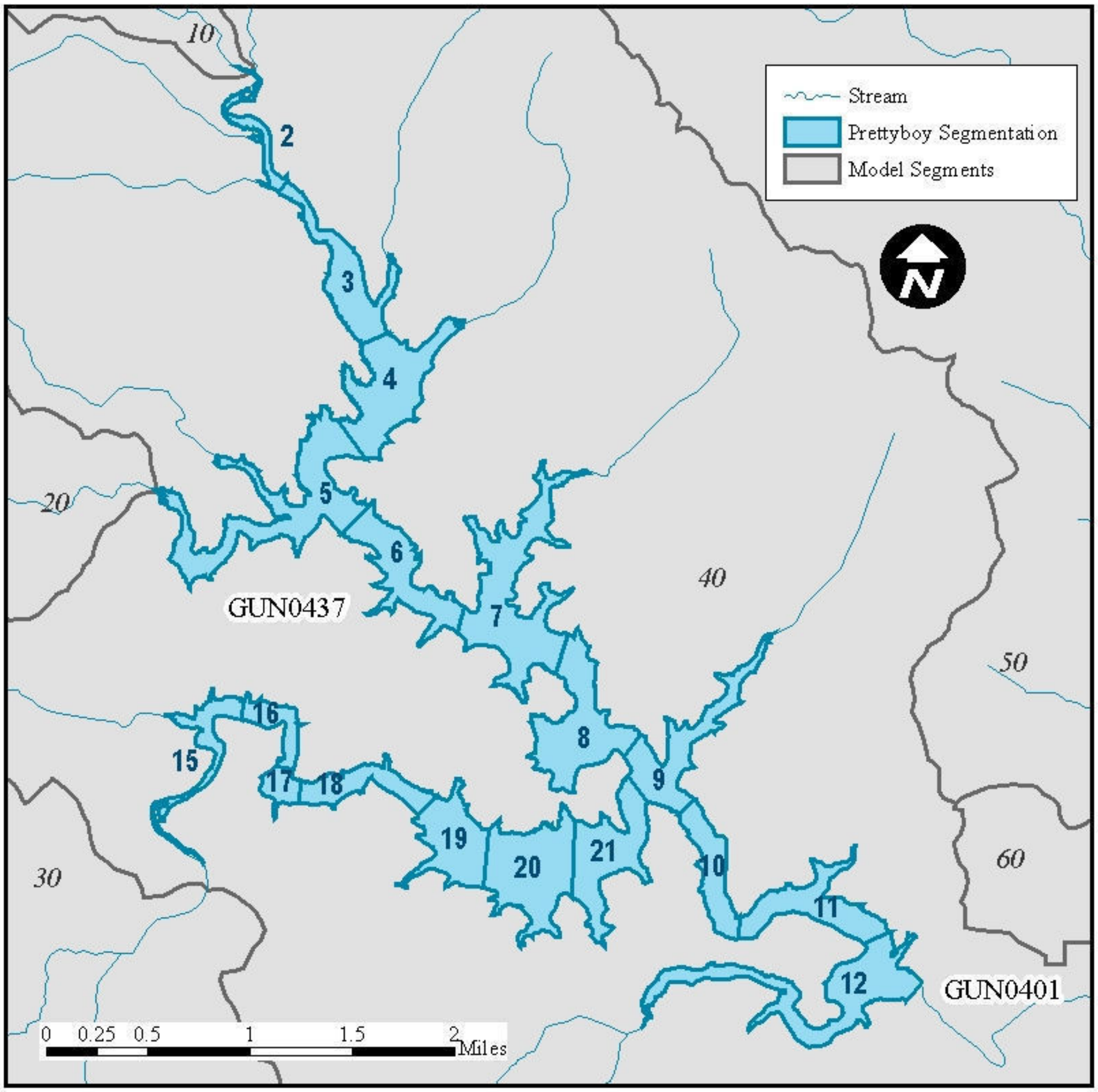

Figure 5.3.1-2. Model Segmentation of Loch Raven Reservoir

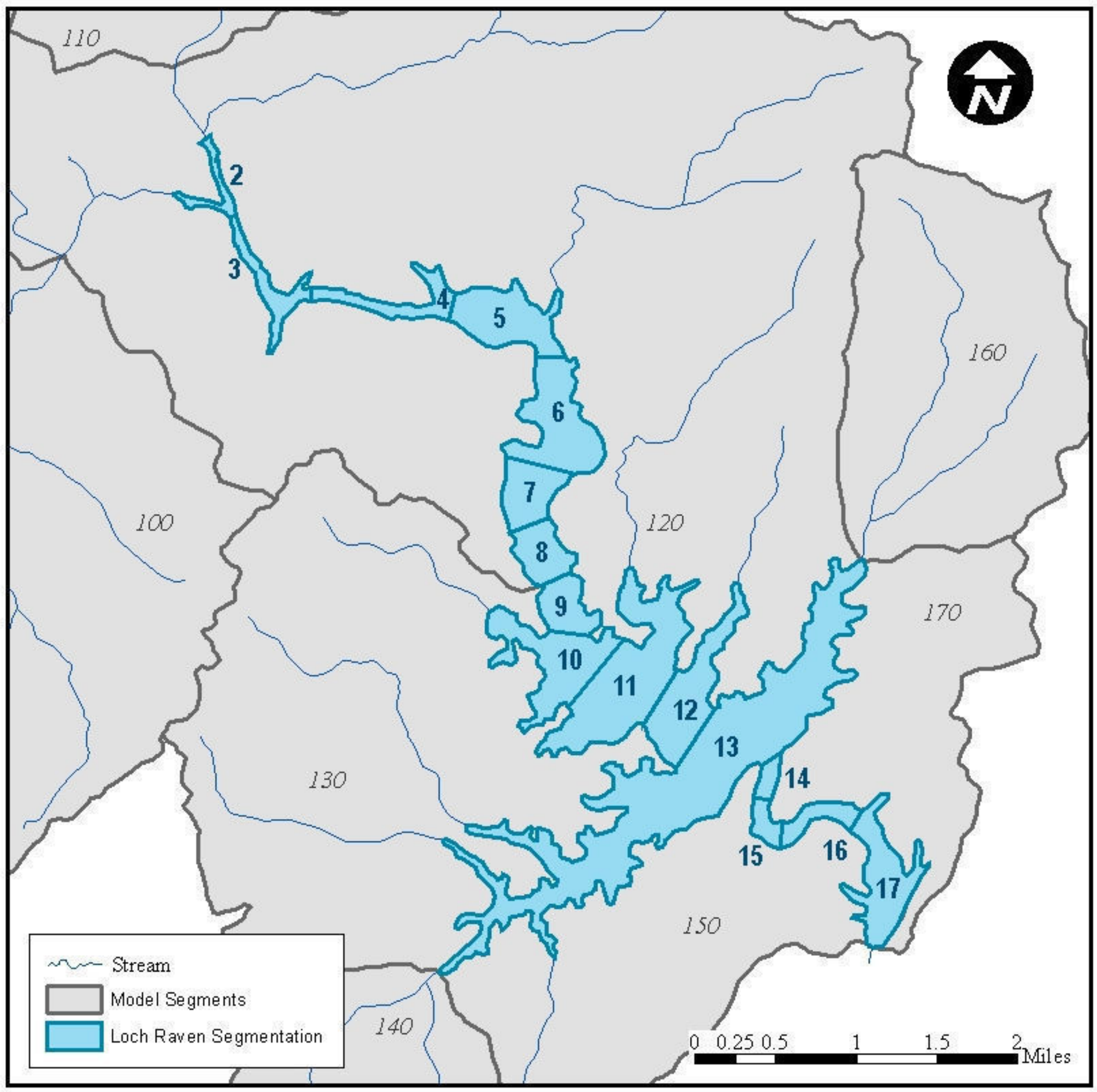

Table 5.3.1-1. Percent of Flows and Loads from HSPF Model Segments Entering CE-QUAL-W2 Model Segments, Prettyboy Reservoir

W2 Segments	HSPF Segments			
	10	20	30	40
2	100%			15%
3				5%
4		100%		5%
5				15%
6				
7				10%
8				
9				15%
10				
11				
12				20%
15			100%	5%
16				
17				
18				
19				5%
20				
21				5%

Table 5.3.1-2. Percent of Flows and Loads from HSPF Model Segments Entering CE-QUAL-W2 Model Segments, Loch Raven Reservoir

W2 Segments	HSPF Segments								
	90	100	110	120	130	140	150	160	170
2	100%	100%	100%	40%					
3									
4				30%					
5									
6									
7									
8									
9									
10					30%				
11				15%					
12				15%					
13					70%	100%	50%	100%	50%
14									
15									
16									50%
17							50%		

Table 5.3.1-3. Prettyboy Reservoir Model Bathymetry

	W2 Model Segments																	
	2	3	4	5	6	7	8	9	10	11	12	15	16	17	18	19	20	21
Segment Length (m)	11355	9875	8652	7630	6472	5419	4469	3611	2726	1560	629	4792	4109	3577	2866	1975	1289	464
W2 Model Layers	**Segment Width (m)**																	
2	51	206	447	572	256	753	417	485	190	240	820	233	144	246	168	456	626	396
3	37	198	434	554	253	725	405	474	190	238	784	172	140	232	165	450	615	390
4	21	186	416	526	245	683	384	458	188	235	744	109	131	213	159	435	596	379
5	10	168	392	490	233	638	360	437	183	229	700	56	119	194	150	418	570	366
6		145	366	446	222	594	335	414	178	221	658	20	99	176	141	400	544	350
7		118	345	399	212	550	311	388	172	213	620	5	59	157	132	384	516	332
8		92	324	356	202	508	290	363	167	204	588		23	136	122	368	485	312
9		67	305	325	193	469	270	343	162	196	560		11	114	112	354	453	296
10		45	286	298	184	432	253	325	157	188	537		5	90	102	339	424	281
11		29	264	272	174	399	237	308	152	181	514			56	91	324	396	267
12		14	234	245	165	369	222	290	147	174	493			18	78	308	371	254
13		12	171	221	156	340	209	271	142	167	472				58	290	347	241
14			87	198	147	314	197	253	137	160	451				37	270	325	228
15			39	176	138	289	185	236	132	153	432				21	249	303	215
16				144	130	268	174	221	127	146	412				10	224	282	201
17				94	121	247	164	206	122	139	393				5	185	260	188
18				49	112	227	154	193	118	133	373					125	236	175
19				26	101	208	144	181	113	127	354					59	208	162
20					81	190	135	169	108	121	336					14	171	150
21					52	168	125	156	103	115	318						120	139
22					33	140	116	144	98	109	301						71	127
23					23	108	105	130	93	103	284						40	114
24					12	69	93	117	88	97	268						16	96
25						36	76	106	82	91	251							70
26							49	94	75	86	234							40
27							26	81	67	80	218							20
28								66	59	74	203							11

29								41	49	67	187							5
30								17	38	60	169							
31									25	52	149							
32									17	43	124							
33										32	98							
34										17	73							
35										5	48							
36											21							
37											5							

Table 5.1.3-4. Loch Raven Reservoir Model Bathymetry

	W2 Model Segments															
	2	3	4	5	6	7	8	9	10	11	12	13	14	15	16	17
Segment Length (m)	13250	12160	10772	9451	8247	7308	6662	6066	5500	4856	4218	3545	2932	2485	1818	694
W2 Model Layers	**Segment Width (m)**															
2	99	137	221	452	544	470	435	437	1163	1539	1028	3571	228	240	170	359
3	94	130	208	435	528	462	417	421	1070	1462	973	3179	225	238	168	350
4	63	121	188	410	503	446	392	395	957	1343	905	2780	220	233	164	337
5	35	110	163	390	483	426	371	372	882	1230	851	2526	215	228	159	325
6		96	132	371	465	405	351	350	819	1126	802	2295	210	223	155	315
7		62	101	352	446	384	333	332	761	1034	758	2078	204	217	150	305
8			73	331	425	363	316	316	707	952	716	1870	199	210	145	295
9			51	308	403	342	298	299	657	873	674	1672	193	203	140	285
10			32	281	379	321	280	283	609	798	630	1490	187	196	135	275
11			13	238	352	301	261	268	562	733	589	1325	182	188	130	266
12				171	322	281	241	253	517	673	549	1178	176	180	124	256
13				94	286	261	220	238	474	621	510	1044	170	173	120	246
14				36	239	242	197	222	434	575	474	911	163	166	114	237
15				8	162	218	173	204	394	532	441	769	156	158	109	227
16					69	158	134	180	352	491	409	632	149	151	104	217
17					13	64	69	115	300	450	378	501	141	143	98	206
18						9	15	32	149	384	338	381	132	134	91	194
19									14	220	284	283	115	122	84	180
20										54	178	188	89	104	75	161
21										4	50	90	62	87	62	140
22												21	29	64	44	120
23													5	25	23	96
24															6	47

Figure 5.3.1-3. Volume vs. Elevation Curves, Prettyboy Reservoir

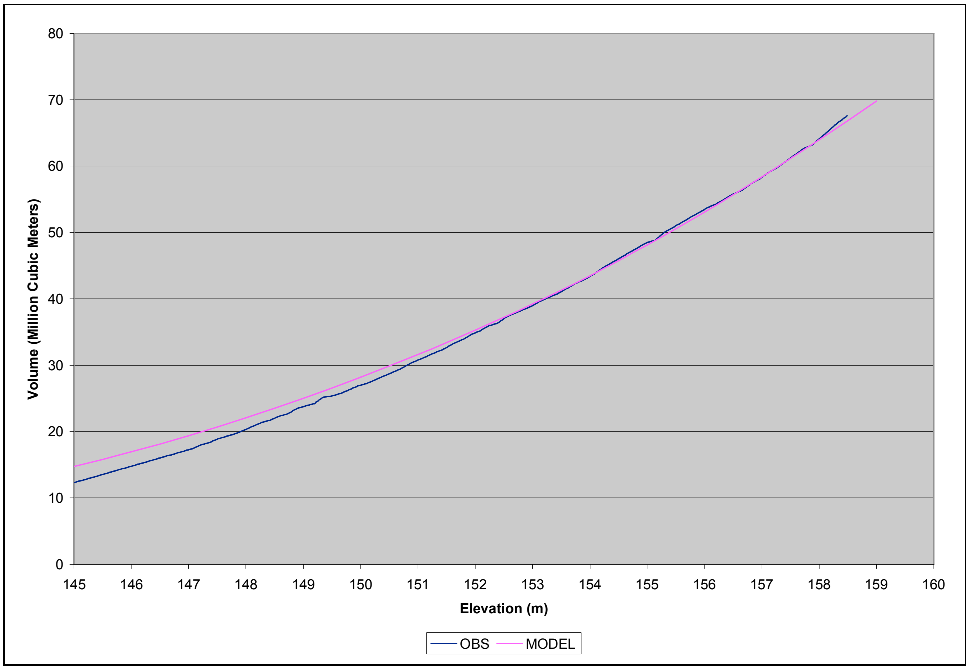

Figure 5.3.1-4. Volume vs. Elevation Curves, Loch Raven Reservoir

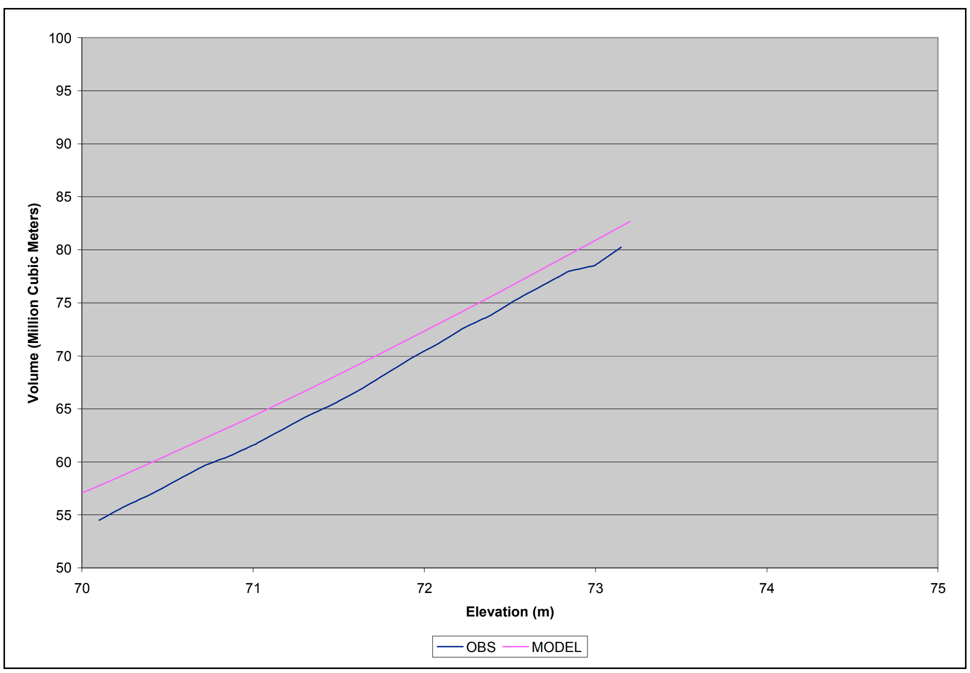

5.3.2. Inflows, Meteorological Data and Boundary Conditions

The CE-QUAL-W2 Model requires time series of inflows, inflow temperature, and inflow constituent concentrations. These were all taken from the output of the Gunpowder HSPF Model, according to the linkage between HSPF and W2 model segments described in Table 5.3.1-1 and 5.3.1-2. Hourly time series were used to represent inflows and temperature and constituent concentrations. For those HSPF model segments which do not have a reach –40, 120, 130, 140, 150, 160, and 170—inflow temperature was taken from the main tributary to the reservoir, Segment 10 in the case of Prettyboy and Segment 110 in the case of Loch Raven.

The W2 model requires time series of air temperature, dewpoint temperature, cloud cover, wind speed and wind direction. All meteorological data was taken from BWI Airport. Hourly time series were used to input meteorological data. As in the original model, direct precipitation to the reservoir was not simulated.

Boundary conditions for the CE-QUAL-W2 can be specified as either the elevation or flows across the model boundaries in the most upstream and downstream segments. The upstream boundary conditions were specified by the inflows from the HSPF model. Downstream boundary conditions were specified by reservoir outflows. The time series of reservoir outflows was determined in the water balance calibration described in Section 5.4. The elevation of the outflow was determined in the temperature calibration described in Section 5.5. Reservoir spillways and other outlet structures were not explicitly modeled.

5.3.3. Configuration of Water Quality Constituents

Table 5.3.3-1 shows the state variables that represent water quality constituents in Version 3.2 of the CE-QUAl-W2 model. The model can represent any number of user-specified inorganic solids, CBOD species, or algal species.

Total phosphorus is the regulated constituent for the nutrient TMDLs in Prettyboy and Loch Raven Reservoirs. It is critical, therefore, that the modeling framework maintain a mass balance of total phosphorus throughout the simulation. Dissolved inorganic phosphorus (DIP) is the only phosphorus species directly represented as a state variable in the W2 model. Phosphorus attached to sediment can be modeled by specifying the concentration of phosphorus on attached sediment. Organic phosphorus is modeled by specifying the stoichiometric ratio between phosphorus and organic matter or oxygen demand (in the case of CBOD species).

It is not possible to maintain a mass balance on total phosphorus by fixing a ratio to a state variable unless the quantity of the state variable is determined by its phosphorus content. This is exactly how the mass balance of phosphorus was implemented in the reservoir models. Specifically, the state variables in the W2 models were configured as follows:

1. The inorganic phosphorus attached to silt and clay was modeled as distinct inorganic solids. Sorption between sediment and the water column was not simulated in the model.
2. Three CBOD variables were used to represent allochthanous organic matter inputs to the reservoirs: (1) labile dissolved CBOD, (2) labile particulate CBOD, and (3) refractory particulate CBOD. The concentration of these CBOD inputs were calculated based on the concentration of organic phosphorus determined by the HSPF model, using the stoichiometric ratio between phosphorus and oxygen demand in the reservoir models. The fraction of total CBOD in each species was calibrated based on reservoir response. The calibration is described in section 5.6.
3. The organic matter state variables were reserved to represent the recycling of nutrients within the reservoir between algal biomass and reservoir nutrient pools. No organic matter, as represented by these variables, was input into the reservoirs. They were used only to track nutrients released from algal decomposition.

To use the W2 model in this configuration, several minor changes had to be made to the W2 code. Inorganic solids contribute to light extinction. The inorganic solids representing solid-phase phosphorus do not contribute to light extinction over and above the sediment to which they are attached. The W2 code was changed so that they don't contribute to light extinction.

The original CBOD variables in W2 do not contribute to light extinction, do not settle, and do not contribute to the organic matter in the sediment available for diagenesis. The W2 code was altered to represent BOD species which settled and which could contribute to both light extinction and sediment organic matter.

Table 5.3.3-1 summarizes the water quality state variables used in the CE-QUAL-W2 models of Prettyboy and Loch Raven Reservoirs. More of the details of the implementation of water quality simulation will be provided in sections on the calibration of constituents.

Table 5.3.3-1. Water Quality State Variables in CE-QUAL-W2 and their Realization in the Gunpowder Reservoir Models

W2 State Variable	Gunpowder State Variable	Description
DO	DO	Dissolved Oxygen
NH4	NH4	Ammonia Nitrogen
NO3	NO3	Nitrate Nitrogen
PO4	PO4	Dissolved Inorganic Phosphorus
LPOM	LPOM	Autochthonous Labile Particulate Organic Matter
RPOM	RPOM	Autochthonous Refractory Particulate Organic Matter
LDOM	LDOM	Autochthonous Labile Dissolved Organic Matter
RDOM	RDOM	Autochthonous Refractory Dissolved Organic Matter
CBOD	CBOD1	Allochthonous Labile Dissolved Organic Matter
	CBOD2	Allochthonous Labile Particulate Organic Matter
	CBOD3	Allochthonous Refractory Particulate Organic Matter
ISS (inorganic solids)	ISS1	Sand
	ISS2	Silt
	ISS3	Clay
	ISS4	Particulate Inorganic Phosphorus on Silt
	ISS5	Particulate Inorganic Phosphorus on Clay
AGL (algal biomass)	ALG1	Winter: diatoms
	ALG2	Spring: summer diatoms; green algae
	ALG3	Summer or fall: blue-green algae, diatoms

5.4. WATER BALANCE CALIBRATION

The objective of the water balance calibration is to calibrate the time series of inflows and outflows so that simulated water surface elevations match observed levels. DPW provided daily water elevation levels at the dams for both Prettyboy and Loch Raven Reservoirs. Some days had no observations. These were filled in by linear interpolation from days which had observations to make a complete time series of elevations for each reservoir.

Measured outflows were not available for the simulation period 1992-1997. Information was available, however, on (1) water withdrawals from Loch Raven Reservoir and (2) the position of gates in Prettyboy Reservoir. Water surface elevation could also be used to estimate the outflow over the spillways when observed elevations exceeded spillway crests. This information was used to set the initial estimate of daily outflows. These outflows were used as the starting point for the calibration, but were not used to constrain the final calibrated time series of daily outflows.

CE-QUAL-W2 comes with a calibration utility, waterbalance.exe, which, when given the time series of observed water surface elevations, determines how much the inflows or outflows need to be adjusted in order to minimize the error in the simulated water surface elevations. The inflows to the W2 model can be adjusted by using distributed tributary files. The distributed tributary inflow file applies a time series of inflows across all segments, in proportion to their surface area. It is intended to be used in conjunction with the waterbalance.exe to adjust inflows to match observed surface elevations (Cole and Wells, 2003).

The water balance was calibrated as follows. First, only the outflow time series were adjusted until the net adjustment in outflows, as determined by the water balance utility, were insignificant. At this point, if any adjustment needed to be made to the inflows, they usually occurred at particular points in time. Some of these were clearly storms that HSPF failed to simulate, because they were not present in the precipitation record. At this point flows from the distributed tributary model were added to the simulation. The distributed tributary requires a time series of temperature inputs, which were taken from the main inflow to each reservoir. No constituent concentrations were associated with the distributed tributary inflows.

Figures D.1 through D.6 in Appendix D compare the simulated and observed water surface elevations at the Prettyboy Reservoir dam for each simulation year. Figures D.7 through D.12 compare water surface elevations at the Loch Raven Reservoir dam for each simulation year. As the figures indicate, the error in simulated surface elevations is almost insignificant.

5.5. TEMPERATURE CALIBRATION

The simulation of temperature is among the most important aspects of reservoir modeling. Water temperature is the cause of the density differences that constitute stratification in the reservoirs and inhibit turbulent mixing between layers. The inhibition of mixing of course leads to low dissolved oxygen concentration in the hypolimnion during stratified conditions. In addition, most of the kinetic processes, including algal growth rates, are temperature dependent, and thus an accurate representation of temperature facilitates simulating eutrophication dynamics.

Calibrating the temperature simulation of the W2 model primarily involves balancing the magnitude and timing of mixing forces—primarily wind but also inflow and outflows—with heat exchange and transport. The sensitivity of the temperature simulation to about a dozen variables was tested, but, in the end, four variables were identified as significantly impacting the calibration: BETA, the surface heat exchange coefficient; WSC, the wind sheltering coefficient; SHD, the shading coefficient; and ESTR, the elevation of the outflows from the reservoirs. These are summarized in Table 5.5-1.

Table 5.5-1. Parameters Used in W2 Temperature Calibration

Parameter	Description
BETA	Fraction of radiation absorbed at the water surface
ESTR	Elevation of outflow from reservoir
WSC	Fraction of input wind speed applied to water surface
SHD	Faction of reservoir not in shade

The values of these parameters were calibrated as follows: Multiple parameter combinations were tested using the PEST utility, SENSAN, which automates the process of substituting parameter sets into model input files, performing multiple model runs, and recording the outcomes from the simulations. The outcomes measured were the root mean square error between observed and simulated temperatures and the mean absolute error of the same quantities. SENSAN also saved the output files so the simulations could be examined graphically. The first sets of parameters spanned the entire range of parameter values. Subsequent sets refined the results of previous sets. Hundreds, if not thousands of parameter combinations were simulated for each simulation year.

Cole and Wells (2003) suggest that it should be possible to achieve a temperature simulation in which the absolute mean error is less than 1° C. This was the calibration target, subject to the following constraints. The surface heat absorption coefficient, BETA, is a model parameter and should not vary through the simulation. Therefore, BETA must be the same for each simulation year, but not necessarily the same for each reservoir. Similarly, the shading coefficient can vary spatially by segment but not over time. The same shading coefficient was therefore used for each simulation year. As a matter of fact, but not necessity, the same shading coefficient was used for each segment. The outflow elevation and the wind sheltering coefficient, which can vary in time, were allowed to vary by simulation year. The final calibration parameter values were selected by first choosing values of the surface heat exchange coefficient and shading coefficient that had simulation runs with AME of less than 1º C, then by choosing the wind sheltering coefficient and outflow elevation in each simulation year that minimized the AME in that year. Parameter values determined in the reservoir simulations are given in Table 5.5-2.

Table 5.5-2. Temperature Calibration Parameter Values, Prettyboy Reservoir

Year	SHD	WSC	BETA	ESTR	RMS	AME
1992	0.9	0.5	0.6	145	1.17	0.86
1993	0.9	0.5	0.6	154	1.17	0.86
1994	0.9	0.5	0.6	154	1.33	0.93
1995	0.9	0.6	0.6	147	1.12	0.91
1996	0.9	0.6	0.6	151	0.75	0.56
1997	0.9	0.6	0.6	147	1.06	0.88

Table 5.5-3. Temperature Calibration Parameter Values, Loch Raven Reservoir

Year	SHD	WSC	BETA	ESTR	RMS	AME
1992	1	0.5	0.4	65.1	1.09	0.77
1993	1	0.5	0.4	67.6	1.19	0.96
1994	1	0.4	0.4	67.6	1.38	0.99
1995	1	0.5	0.4	65.1	1.14	0.87
1996	1	0.6	0.4	67.6	1.20	0.94
1997	1	0.5	0.4	65.1	1.39	1.09

The optimum outflow elevation tends to vary with the average surface water elevation in the simulation year: generally, high flow years have higher calibrated outflow elevations than low-flow years. This is as it should be, but it also raises the question whether more accurate and more detailed representation of outflows would have had the same effect. The answer is that it probably would not, given the information that was available for the simulation period. To reiterate what was said in the last section, while the position of the gates and the water surface elevation were to a certain extent known, the actual outflow rates above the spillway and through the gates were not. There was significant uncertainty, then, in how to prototype the outflows. Moreover, the selective withdrawal algorithm, which the W2 model uses to determine how much outflow to withdraw from each layer of the reservoir, only approximates outflow dynamics. Given that the primary objective of simulating the reservoirs is determining water quality within the reservoirs, and not the water quality in the outflows, as is sometimes the case, it is prudent to simplify the representation of outflow dynamics for the sake of improving the simulation of temperature within the reservoirs. In the case of the outflows from Prettyboy Reservoir, which are fed into the Gunpowder HSPF Model, the river reach temperature simulation in Segment 60 tends to erase any memory of outflow temperatures from the simulation of Prettyboy Reservoir.

It should be noted during the subsequent water quality calibration in Loch Raven Reservoir, AME values increased slightly in a few years primarily because high solids concentrations inhibited light penetration and decreased heat transfer to lower layers.

5.6. Water Quality Calibration

The primary focus of the water quality simulation is to calibrate the link between surface chlorophyll a concentrations and watershed total phosphorus loads. The response of hypolimnetic dissolved oxygen concentrations to allochthonous (external) and autochthonous (internal) organic matter is also a focus of interest.

The calibration of the simulation of water quality constituents in Prettyboy and Loch Raven Reservoirs can be divided into the following four steps:

1. calibration of surface total phosphorus concentrations;
2. calibration of surface chlorophyll a concentrations;
3. calibration of dissolved oxygen concentrations; and
4. calibration of ammonia and nitrate nitrogen concentrations.

Each year was simulated individually and initialized with observed concentrations, where available. One set of model parameters for each reservoir was used for all of the years simulated, except in the case of the simulation of algae, where some parameters were varied by year, as will be explained in Section 5.6.2. The simulation was compared with observed data using the classification of monitoring stations and definition of surface and bottom layers used in Section 5.1.

5.6.1. Calibration of Total Phosphorus Concentrations

The simulation of total phosphorus concentrations in the reservoirs is primarily determined by the simulation of watershed total phosphorus loads, whose calibration was described in Chapter 4. Settling rates were adjusted to improve the agreement between observed and simulated total phosphorus concentrations in the surface layers. Table 5.6.1-1 gives the settling rates used in the models.

Table 5.6.1-1. Simulated Settling Rates

Constituent	Settling Rate (m/d)
Sand	5.0
Silt	2.0
Organic Matter	0.5
Clay	0.5

Figures 5.6.1-1 and 5.6.1-2 compare time series of simulated average surface total phosphorus concentrations at the lower and middle stations in Prettyboy Reservoir, respectively, and Figures 5.6.1-3 through 5.6.1-5 compare simulated average surface total phosphorus concentrations at the lower, middle, and upper stations of Loch Raven Reservoir. Figures 5.6.1-6 and 5.6.1-7 show scatter plots of simulated and observed average total phosphorus concentrations in the surface layers of Prettyboy and Loch Raven Reservoirs, respectively, while Figures 5.6.1-8 and 5.6.1-9 compare the cumulative distribution of simulated and observed total phosphorus concentrations in the surface layers of Prettyboy and Loch Raven Reservoirs, respectively.

The reservoir models generally capture the trend in concentration in 1992, 1995, 1996, and 1997 but oversimulate observed surface TP concentrations in 1993 and 1994. As the scatter plots show, the simulations do not match the variability in the monitoring data. The models oversimulate late fall storm events in 1993, but fail to simulate some large concentrations in the monitoring data in the second half of the simulation period.

Similar trends are apparent in comparing simulated and observed total phosphorus concentrations in the bottom layers of the reservoirs. Figures 5.6.1-10 and 5.6.1-11 compare time series of simulated average surface total phosphorus concentrations at the lower and middle stations in Prettyboy Reservoir, respectively, and Figures 5.6.1-12 through 5.6.1-14 compare simulated average surface total phosphorus concentrations at the lower, middle, and upper stations of Loch Raven Reservoir. Figures 5.6.1-15 and 5.6.1-16 show scatter plots of simulated and observed average total phosphorus concentrations in the surface layers of Prettyboy and Loch Raven Reservoirs, respectively, while Figures 5.6.1-17 and 5.6.1-18 compare the cumulative distribution of simulated and observed total phosphorus concentrations in the surface layers of Prettyboy and Loch Raven Reservoirs, respectively. The bottom TP concentrations following the storms of late 1993 appear to be grossly oversimulated in the models.

The observed TP concentrations in the reservoirs for 1993 and 1994 seem out of line, however, with trends in flow and observed TP concentrations in the tributaries. Table 5.6.1-2 shows the observed average annual baseflow TP concentration and average annual flow for Western Run, Beaverdam Run, and Gunpowder Falls at Glencoe, compared to the average annual and median TP concentrations for Loch Raven Reservoir. 1994 has the highest, or second highest average baseflow TP concentrations, while 1993 has average baseflow TP concentrations. TP loads tend to be positively correlated with flows, and both 1993 and 1994 are relatively wet years. On the other hand, as measured either by median or average value, concentrations of TP in Loch Raven Reservoir in 1993 and 1994 are the lowest of the simulation period.

Table 5.6.1-2. Average Annual and Median TP Concentration in Loch Raven Reservoir, Compared to Average Annual Flow and Baseflow TP Concentrations in its Tributaries

Year	Western Run		Beaverdam Run		Gunpowder Falls at Glencoe		Loch Raven Reservoir	
	Average Flow (cfs)	Average Baseflow TP (mg/l)	Average Flow (cfs)	Average Baseflow TP (mg/l)	Average Flow (cfs)	Average Baseflow TP (mg/l)	Average TP (mg/l)	Median TP (mg/l)
1992	44	0.034	20	0.019	110	0.020	0.039	0.032
1993	100	0.039	38	0.030	253	0.031	0.026	0.022
1994	94	0.051	39	0.049	274	0.049	0.026	0.022
1995	55	0.040	28	0.022	180	0.027	0.067	0.056
1996	129	0.055	54	0.033	331	0.030	0.113	0.077
1997	67	0.027	29	0.022	208	0.018	0.075	0.070

In addition, while comparison with the ESTIMATOR model suggests that the late November 1993 storm may be oversimulated by about 40%, it is difficult to imagine the circumstances under which that storm and a subsequent storm the first week in December would not lead to a noticeable increase in observed total phosphorus in the reservoirs. The November 28th storm led to the largest daily flow observed during the simulation period at Gunpowder Falls at Glencoe and the second largest flows observed on Western Run and Beaverdam Run (The largest flows observed during the simulation period at those gages were due to the snowmelt event of January 1996.) The December 5 storm led to the third largest flow during the simulation period at Glencoe (the 1996 snowmelt event second) and Western Run, and the fourth largest on Beaverdam Run. The total volume from the two storms at those three gages amounts to about a third of Loch Raven's capacity. Given that the three gages do not cover the whole watershed, it is not unreasonable to assume that at least half of the volume of Loch Raven was displaced in a week's time by storm flow, but the monitoring data shows little impact from the two events. Many of the observations recorded two weeks later on December 20 were even below the detection limit for total phosphorus.

Conversely, large changes in the observed TP concentration are not necessarily the consequence of large inflows, though they can be associated with significant storms. For example, the large TP concentrations observed on December 2, 1996 can be associated with a significant event on November 8-9. Flows on that date are only about one-fifth the inflows from those in late fall 1993, which would imply that inflow concentrations would have to be about five times the 1993 model concentrations, already suspected to be oversimulated, to have comparable impact on reservoir concentrations.

Given the possibility of problems with the TP monitoring data that have already been discussed in Section 5.2, it is not unreasonable to permit the differences between the observed and simulated concentrations in the reservoirs exhibited in Figures 5.6.1-1 through 5.6.1-5. As was stated earlier, the simulated concentrations are for the most part determined by the input loads, which have been calibrated against observed data through ESTIMATOR.

Figure 5.6.1-1. Observed and Simulated Average Surface Total Phosphorus Concentrations, Middle Station, Calibration Scenario, Prettyboy Reservoir

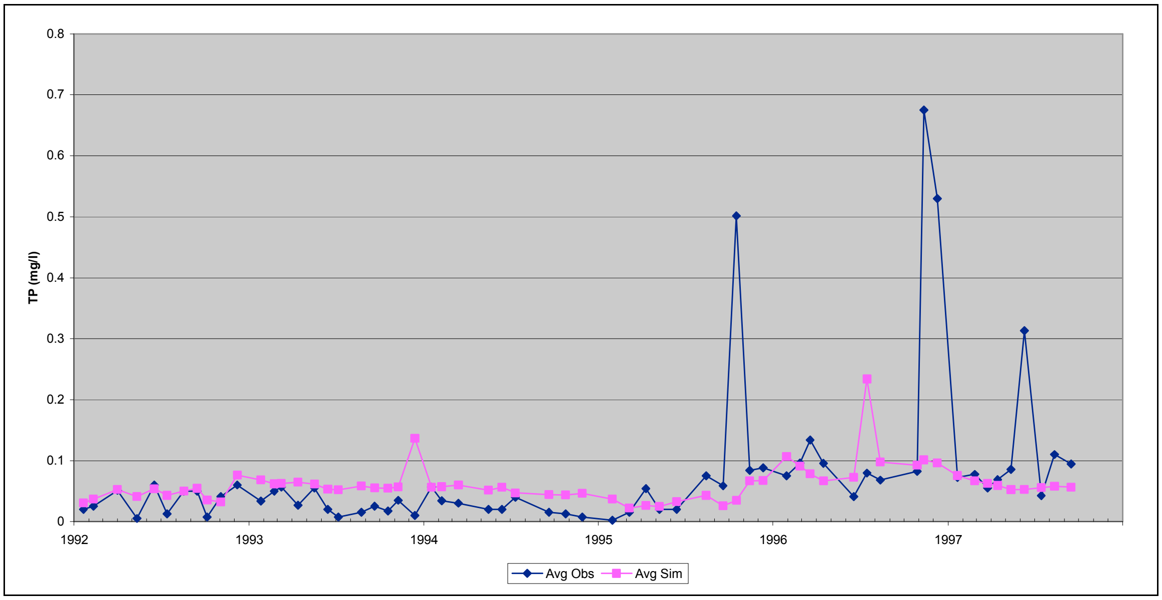

Figure 5.6.1-2. Observed and Simulated Average Surface Total Phosphorus Concentrations, Lower Station, Calibration Scenario, Prettyboy Reservoir

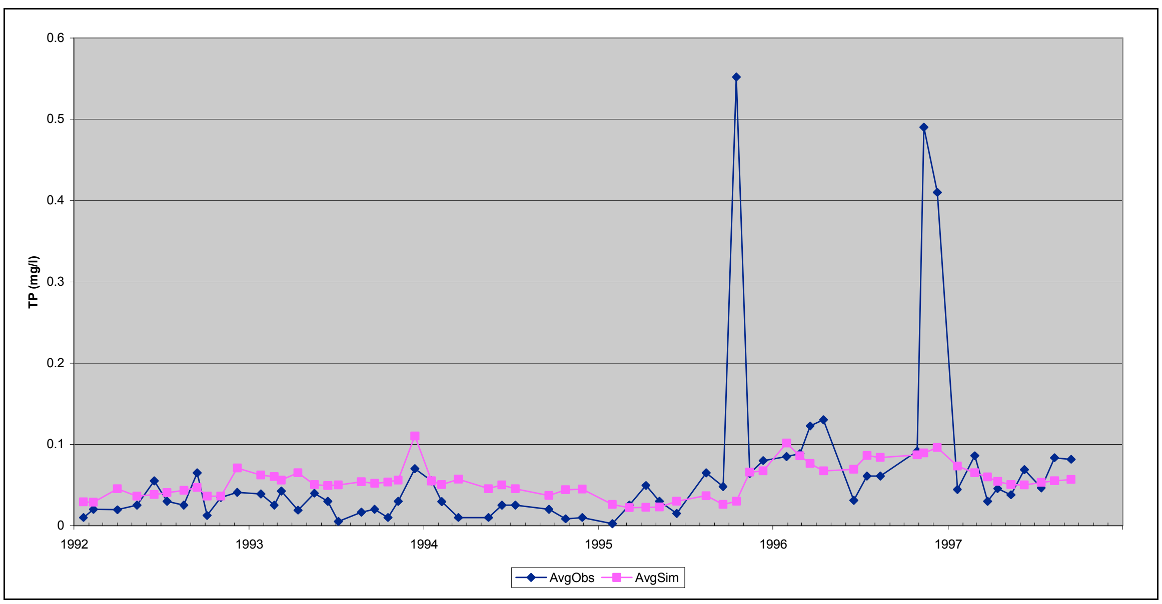

Figure 5.6.1-3. Observed and Simulated Total Average Surface Phosphorus Concentrations, Upper Station, Calibration Scenario, Loch Raven Reservoir

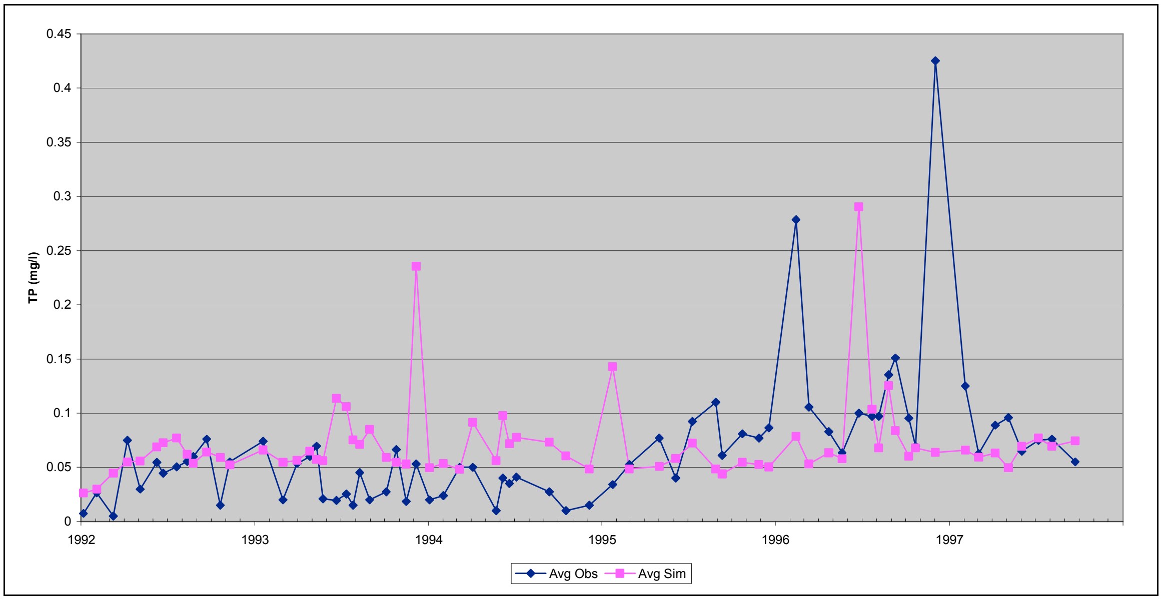

Figure 5.6.1-4. Observed and Simulated Total Average Surface Phosphorus Concentrations, Middle Station, Calibration Scenario, Loch Raven Reservoir

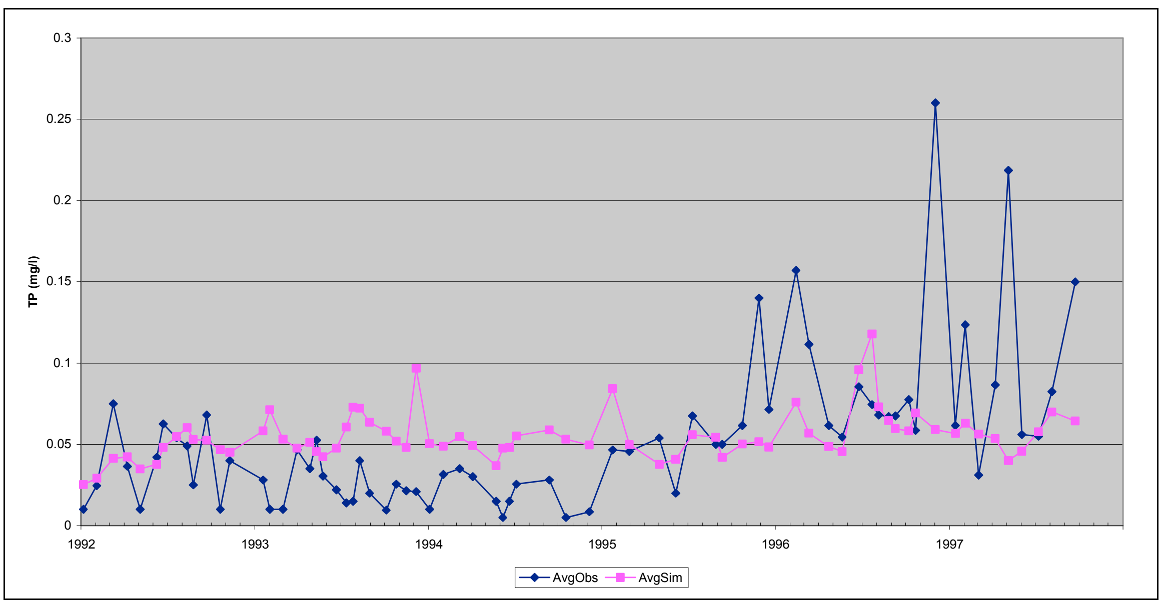

Figure 5.6.1-5. Observed and Simulated Total Average Surface Phosphorus Concentrations, Lower Station, Calibration Scenario, Loch Raven Reservoir

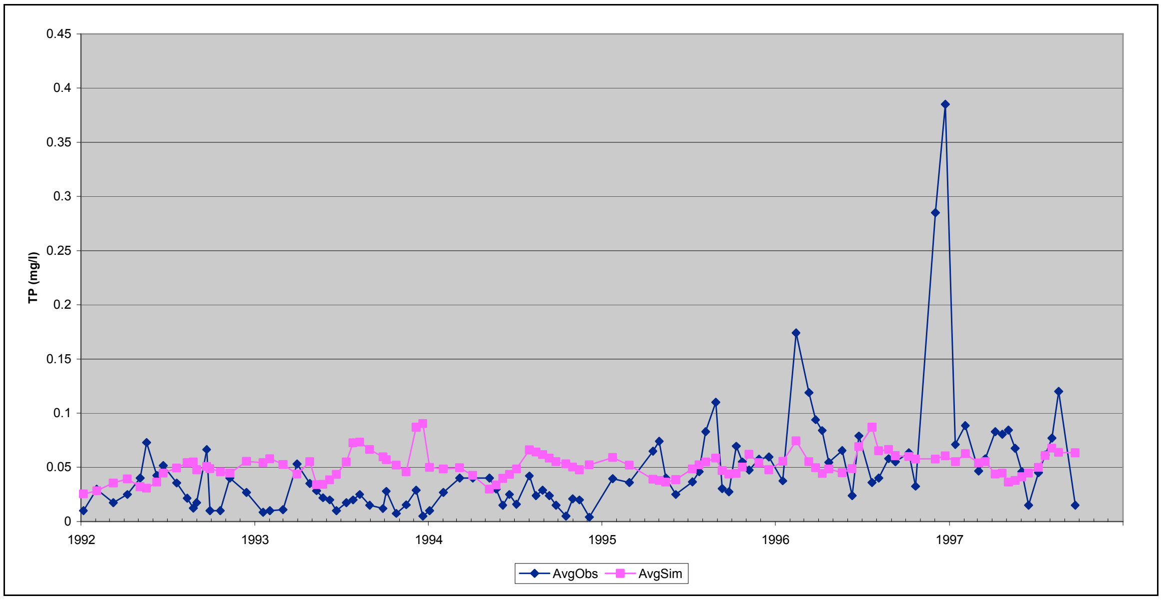

Figure 5.6.1-6. Observed and Simulated Average Surface Total Phosphorus Concentrations, Calibration Scenario, Prettyboy Reservoir

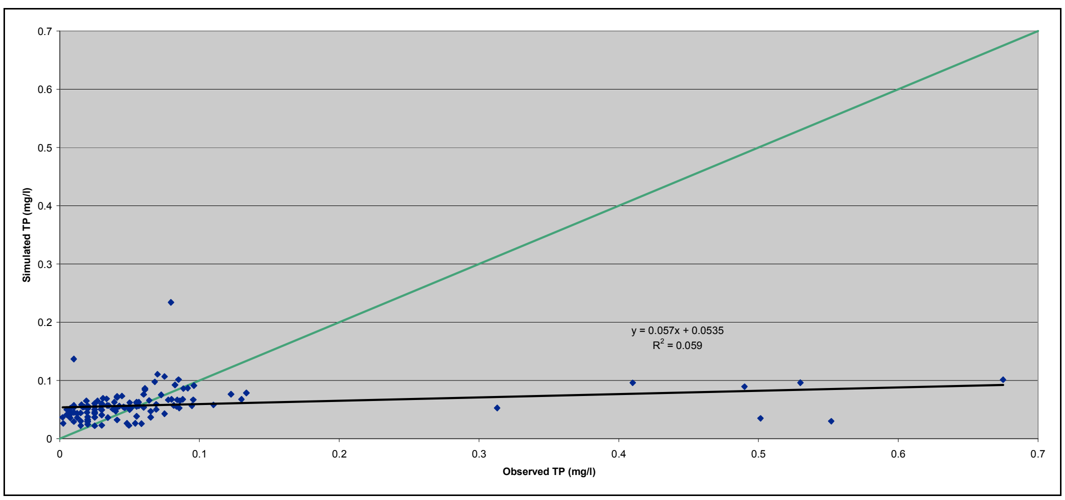

Figure 5.6.1-7. Observed and Simulated Total Average Surface Phosphorus Concentrations, Calibration Scenario, Loch Raven Reservoir

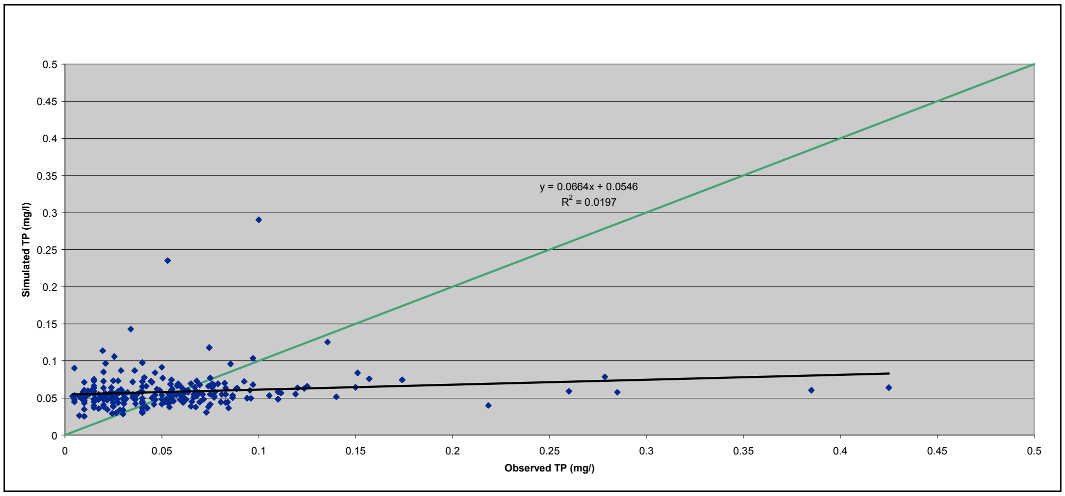

Figure 5.6.1-8. Cumulative Distribution of Observed and Simulated Average Surface Total Phosphorus Concentrations, Calibration Scenario, Prettyboy Reservoir

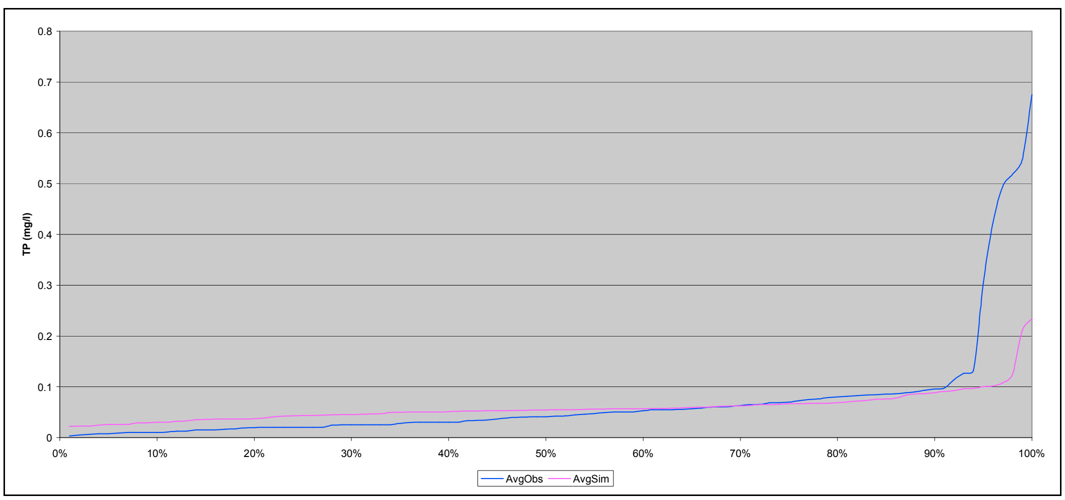

Figure 5.6.1-9. Cumulative Distribution of Observed and Simulated Average Surface Total Phosphorus Concentrations, Calibration Scenario, Loch Raven Reservoir

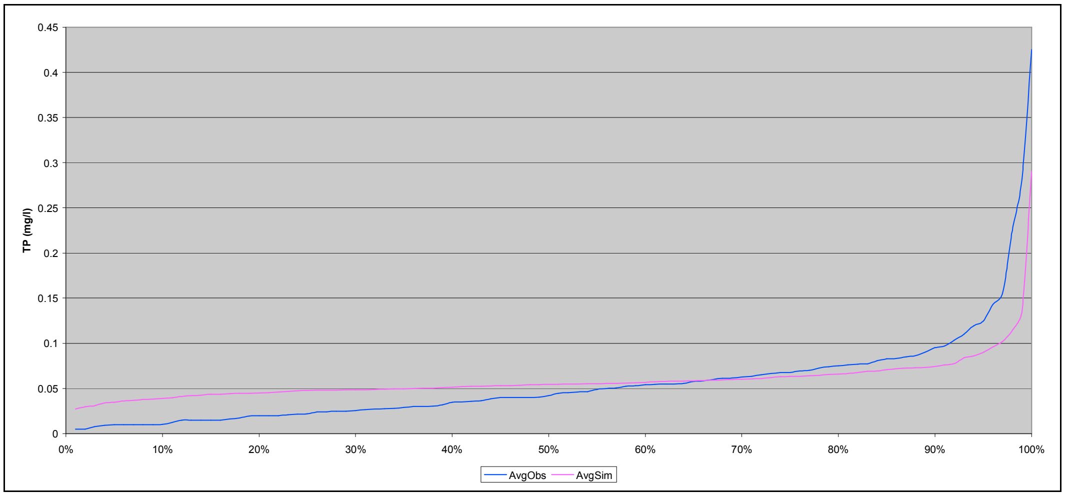

Figure 5.6.1-10. Observed and Simulated Average Bottom Total Phosphorus Concentrations, Middle Station, Calibration Scenario, Prettyboy Reservoir

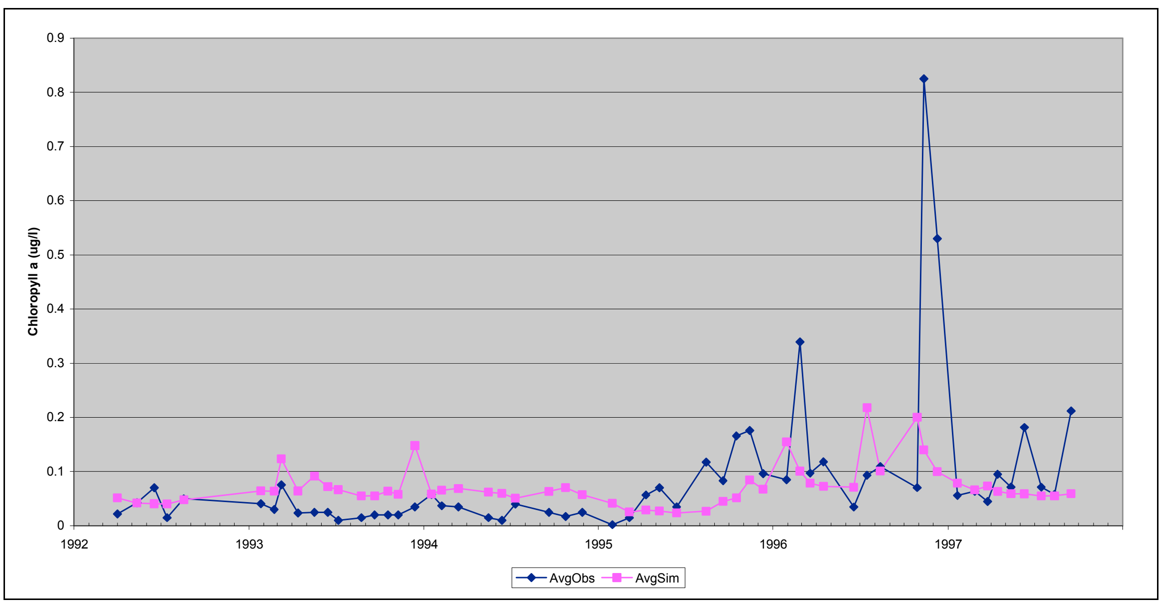

Figure 5.6.1-11. Observed and Simulated Average Bottom Total Phosphorus Concentrations, Lower Station, Calibration Scenario, Prettyboy Reservoir

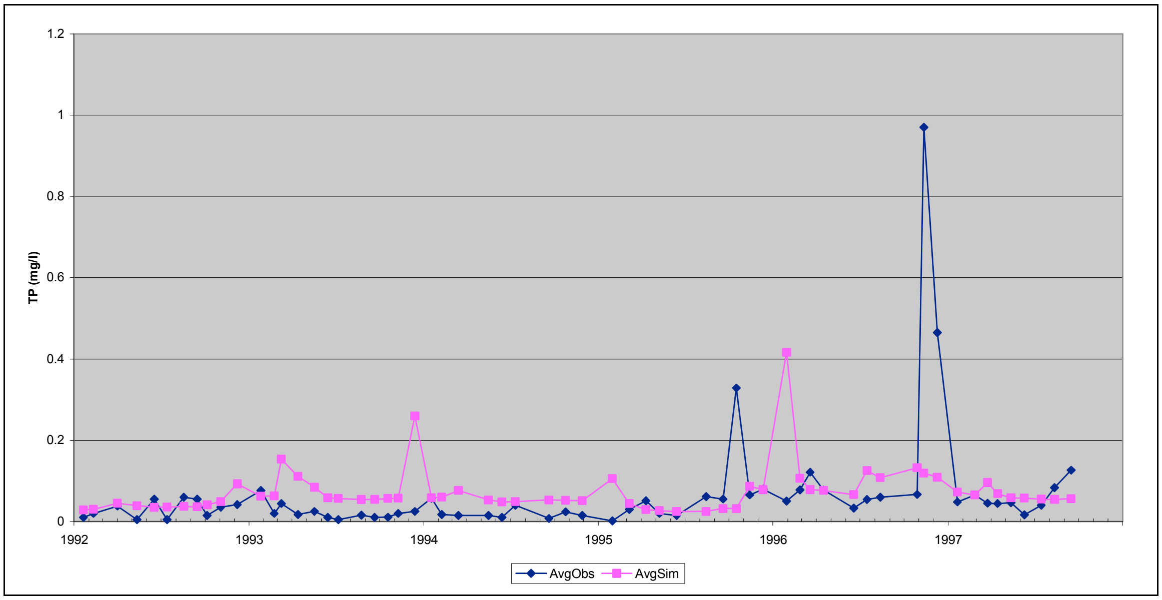

Figure 5.6.1-12. Observed and Simulated Total Average Bottom Phosphorus Concentrations, Upper Station, Calibration Scenario, Loch Raven Reservoir

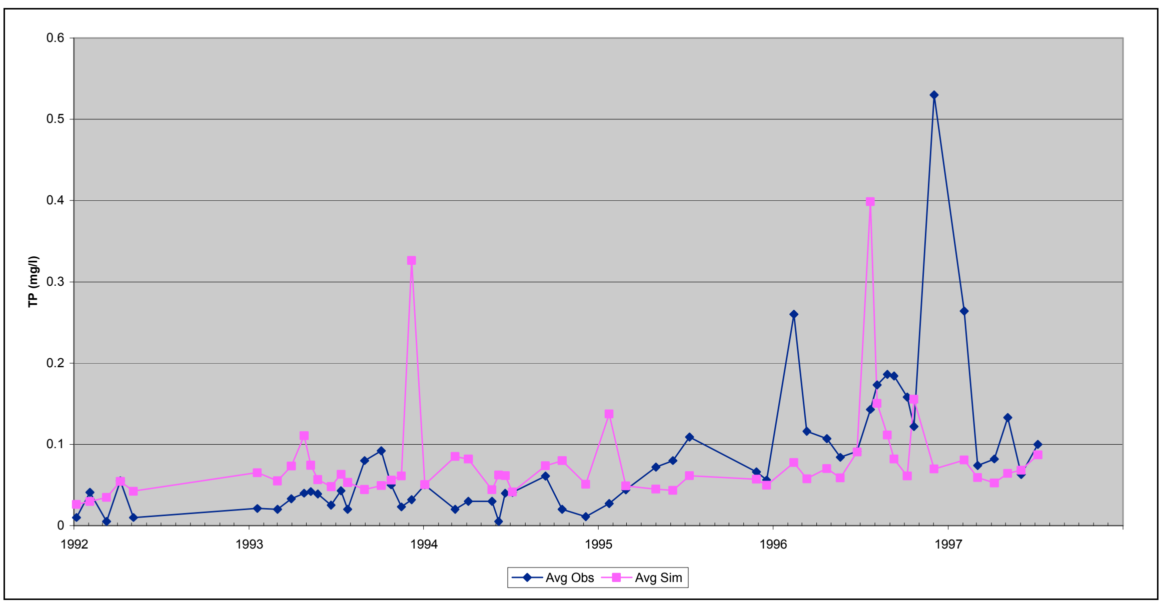

Figure 5.6.1-13. Observed and Simulated Total Average Bottom Phosphorus Concentrations, Middle Station, Calibration Scenario, Loch Raven Reservoir

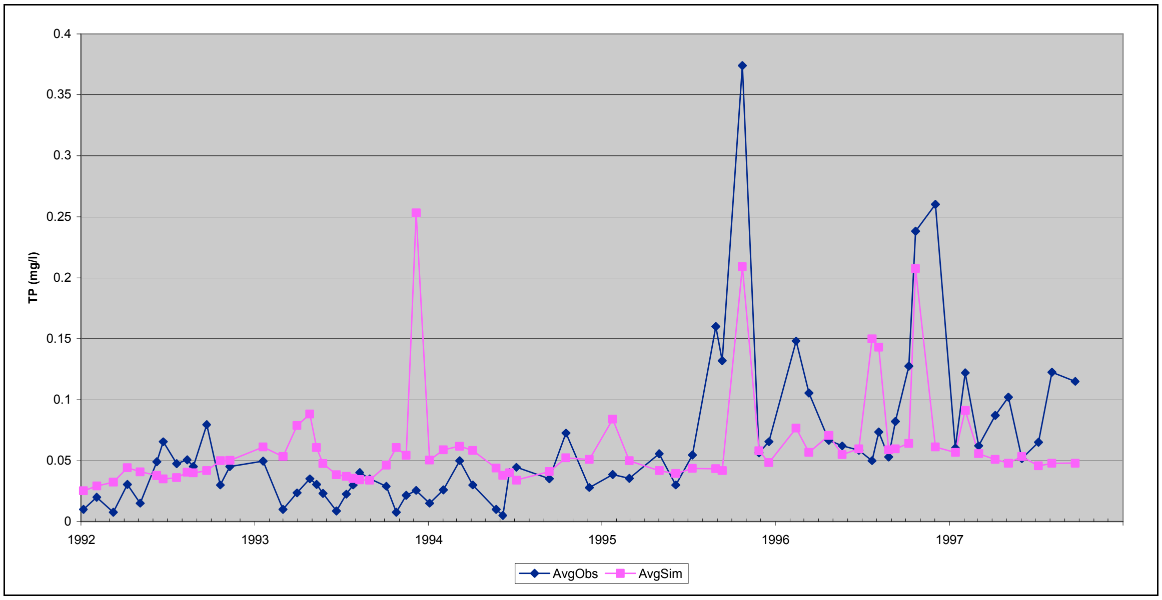

Figure 5.6.1-14. Observed and Simulated Total Average Bottom Phosphorus Concentrations, Lower Station, Calibration Scenario, Loch Raven Reservoir

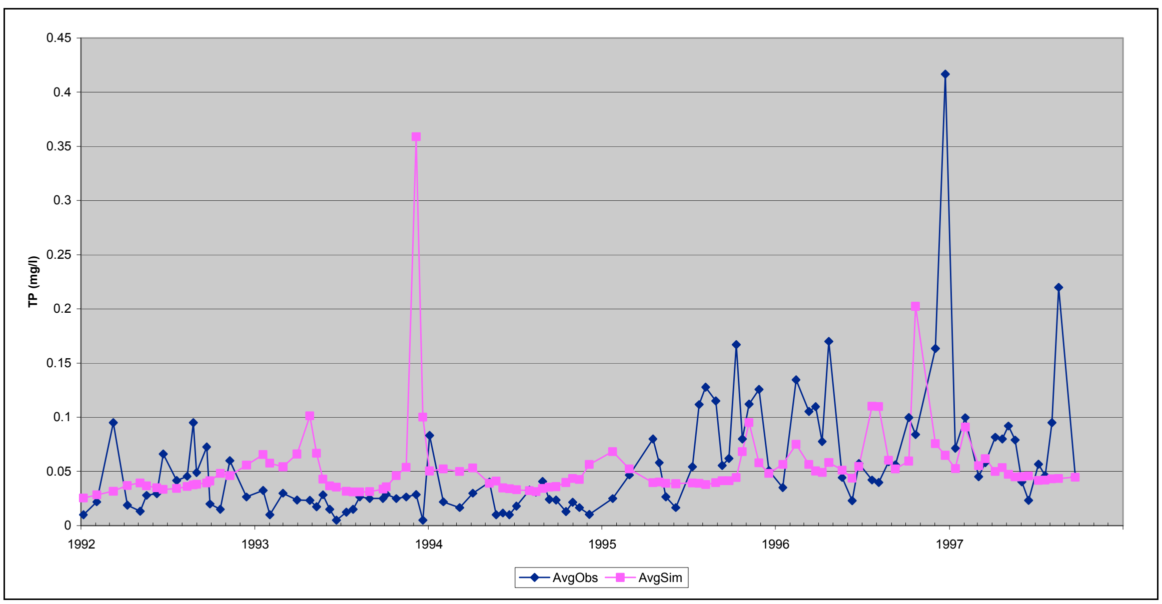

Figure 5.6.1-15. Observed and Simulated Total Average Bottom Phosphorus Concentrations, Calibration Scenario, Prettyboy Reservoir

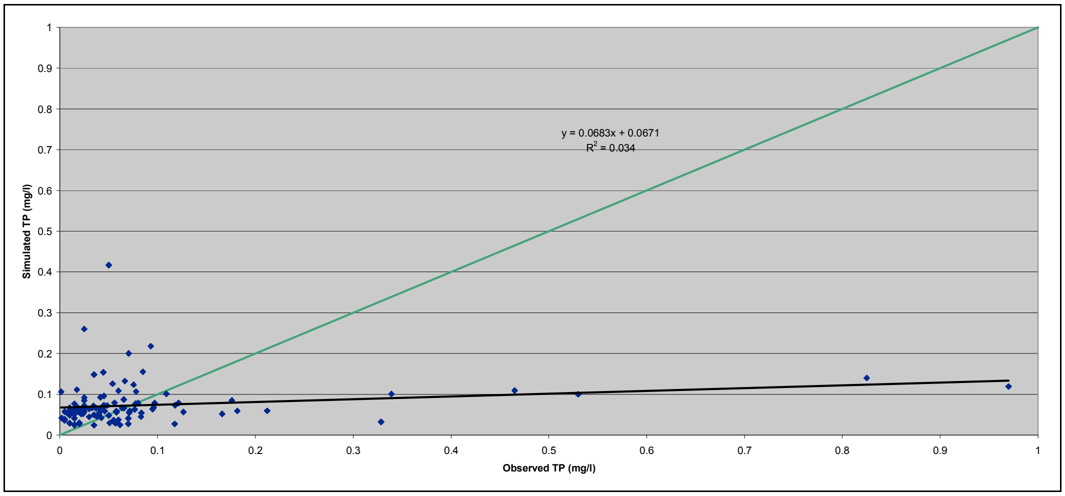

Figure 5.6.1-16. Observed and Simulated Total Average Bottom Phosphorus Concentrations, Calibration Scenario, Loch Raven Reservoir

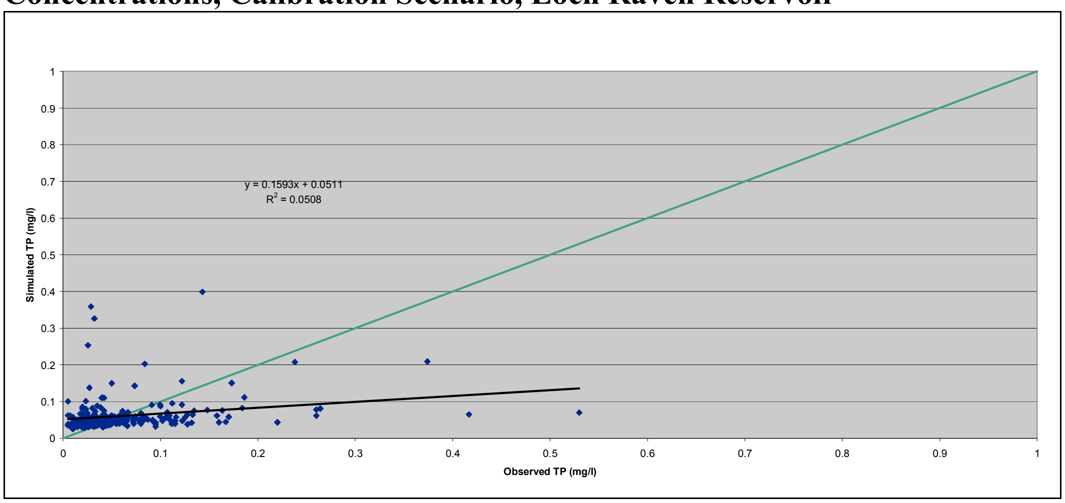

Figure 5.6.1-17. Cumulative Distribution of Observed and Simulated Total Average Bottom Phosphorus Concentrations, Calibration Scenario, Prettyboy Reservoir

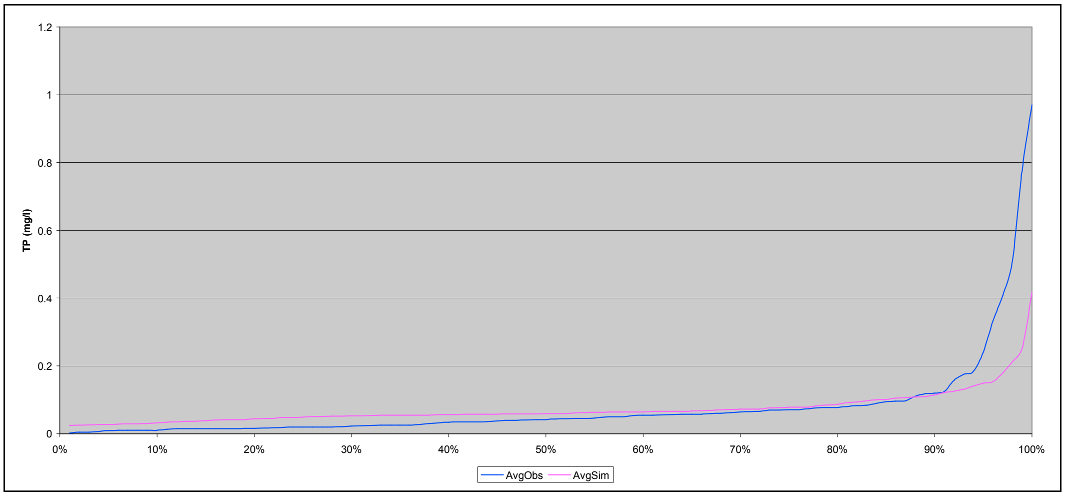

Figure 5.6.1-18. Cumulative Distribution of Observed and Simulated Total Average Bottom Phosphorus Concentrations, Calibration Scenario, Loch Raven Reservoir

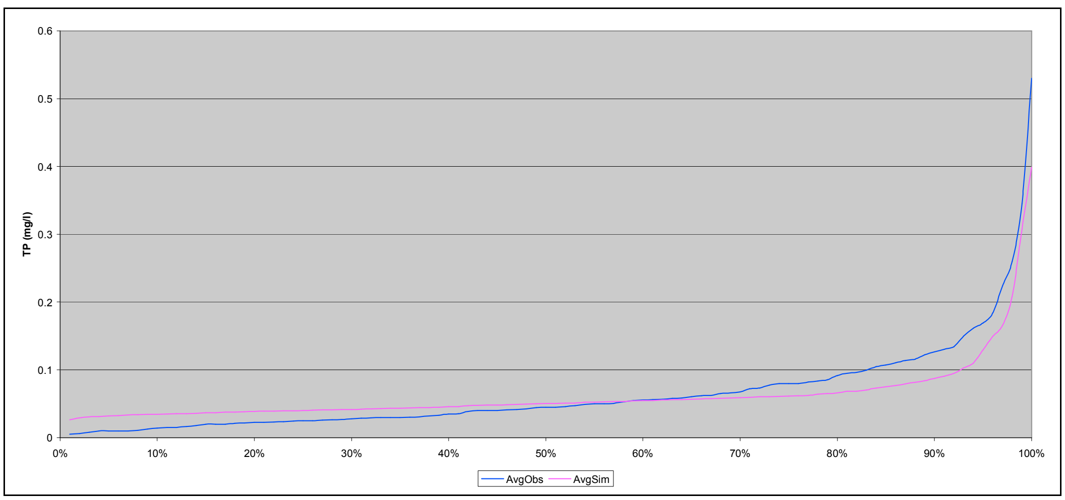

5.6.2. Simulation of Algae and Chlorophyll a

Three seasons of algae were simulated each year: (1) a mixed-species winter population, (2) dominant spring algal taxa, and (3) dominant summer/fall algal taxa. As described in Section 5.2, the dominant spring algal group was usually a species of diatom and the dominant summer algal group was either green algae or blue-green algae. There was no information on winter algal taxa, and less information on algal species in Prettyboy Reservoir than Loch Raven Reservoir. Tables 5.6.2-1 and 5.6.2-2 show how the seasons were defined for each year of the simulation and their dominant species in Prettyboy and Loch Raven Reservoirs. As Table 5.6.2-2 in particular shows, a wide variety of algal species was dominant in Loch Raven Reservoir; almost every spring and summer season is dominated by a different species, reflecting the wide variety of conditions under which high algal concentrations could occur.

The goal of the calibration was for the simulated chlorophyll a concentration in each season to be at least as large as observed chlorophyll a concentration in that season. In other words, the simulation would match the observed peaks in chlorophyll a concentration, though not necessarily on the same date or at the same location. To accomplish this goal, growth rates and temperature coefficients were varied in the simulation by year and season, reflecting the variety of dominant species and the variety of factors which determined species succession. Tables 5.6.2-1 and 5.6.2-2 show how the algal growth rates by season and Tables 5.6.2-3 and 5.6.2-4 show algal temperature parameters by season in Prettyboy and Loch Raven Reservoirs The resulting calibration is conservative: Ensuring that the simulated chlorophyll a peaks are at least as large as observed peaks helps guarantee that the models can be used to calculate what total phosphorus loads are compatible with the reservoirs meeting water quality standards.

The goals of the simulation were met. Table 5.6.2-5 shows the maximum simulated and observed peak phosphorus concentrations by season for Prettyboy and Loch Raven Reservoirs. Simulated peaks match observed peaks by season.

Figure 5.6.2-1 shows a time series of maximum chlorophyll a concentrations by date for Prettyboy Reservoir. There is good agreement between observed and simulated peaks by date, as can also be seen in the scatter plot in Figure 5.6.2-2. Figure 5.6.2-3 shows the cumulative distribution of simulated and observed chlorophyll a concentrations in Prettyboy Reservoir. Simulated maximum chlorophyll a concentrations dominate observed maximum concentrations for concentrations above 10 µg/l. Figures 5.6.2-4 and 5.6.2-5 show time series of simulated and observed maximum chlorophyll a concentrations for the lower and middle monitoring locations in Prettyboy Reservoir. The model sometimes simulates peaks at the lower location when the observed peak is at the middle location and vice versa.

Figure 5.6.2-6 shows a time series of maximum chlorophyll a concentrations by date for Loch Raven Reservoir. There is reasonable agreement between observed and simulated peaks by date, but peaks are more often displaced in time, as can also be seen in the scatter plot in Figure 5.6.2-7. Figure 5.6.2-8 shows the cumulative distribution of simulated and observed chlorophyll a concentrations in Loch Raven Reservoir. Simulated maximum chlorophyll a concentrations dominate observed maximum concentrations for concentrations above 10 µg/l.

Figures 5.6.2-9, 5.6.2-10, and 5.6.2-11 show time series of the observed and simulated chlorophyll a concentrations by date and location for the lower, middle, and upper sampling locations in Loch Raven Reservoir. There is less agreement between observed and simulated maximum chlorophyll by date and location in Loch Raven Reservoir than in Prettyboy Reservoir. Nevertheless, the simulated chlorophyll concentrations follow the seasonal pattern of the observed concentrations and dominate in magnitude by season.

Table 5.6.2-1. Algal Season Characteristics in Prettyboy Reservoir

Year	Season	Start Date	Growth Rate	Dominant Species
1992	1	11/18	0.925	
	2	4/1	0.79	Cyclotella
	3	8/29	4.062	Anabaena
1993	1	12/8	1	
	2	2/20	1.6	Cyclotella
	3	5/21	2	Chlorella, Oscillatoria
1994	1	11/18	1.03	
	2	2/10	0.8	
	3	4/1	2	Cyclotella
1995	1	11/28	1.29	
	2	2/20	1.5	
	3	6/20	2.25	
1996	1	11/18	1.55	
	2	4/21	1.25	
	3	5/11	1.4	Oocystis
1997	1	12/8	2.2	
	2	4/1	1.75	
	3	7/20	1.6	

Table 5.6.2-2. Algal Season Characteristics in Loch Raven Reservoir

Year	Season	Start Date	Growth Rate	Dominant Species
1992	1	11/18	0.7	
	2	4/1	2.3	Asterionella
	3	5/11	1.9	Chlorella
1993	1	12/8	0.85	
	2	4/1	3.65	Cyclotella
	3	6/10	2.31	Oscillatoria
1994	1	11/18	1.52	
	2	3/12	5	Cyclotella
	3	6/10	2.1	Anacystis
1995	1	11/18	1.1	
	2	4/1	1.55	Fragilaria
	3	5/11	1.95	Chlorella
1996	1	11/18	1.2	
	2	1/26	2.5	Synura
	3	5/11	2.1	Anabaena
1997	1	10/18	1.175	
	2	4/1	3.35	Fragilaria
	3	8/29	1.85	Anacystis, Anabaena

Table 5.6.2-3. Algal Temperature Parameters in Prettyboy Reservoir

Year	Season	Temp1	Temp2	Temp3	Temp4	Fraction1	Fraction2	Fraction3	Fraction4
1992	1	0	2	4	6	0.49	0.99	0.99	0.7
	2	5	15	20	25	0.59	0.99	0.99	0.3
	3	13	28	35	40	0.5	0.99	0.99	0.75
1993	1	0	3	5	6	0.79	0.99	0.99	0.9
	2	3	5	9	14	0.59	0.99	0.99	0.1
	3	13	28	35	40	0.1	0.29	0.99	0.1
1994	1	0	2	4	6	0.89	0.99	0.99	0.9
	2	3	5	15	17	0.59	0.99	0.99	0.01
	3	13	28	35	40	0.3	0.49	0.99	0.1
1995	1	0	2	4	6	0.49	0.99	0.99	0.7
	2	3	5	9	14	0.59	0.99	0.99	0.1
	3	13	30	35	40	0.1	0.79	0.99	0.1
1996	1	-5	0	2	6	0.59	0.99	0.99	0.7
	2	3	5	9	14	0.59	0.99	0.99	0.1
	3	13	28	35	40	0.1	0.69	0.99	0.1
1997	1	0	2	4	6	0.49	0.99	0.99	0.5
	2	3	5	9	14	0.59	0.99	0.99	0.1
	3	13	28	35	40	0.7	0.99	0.99	0.1

Table 5.6.2-4. Algal Temperature Parameters in Loch Raven Reservoir

Year	Season	Temp1	Temp2	Temp3	Temp4	Fraction1	Fraction2	Fraction3	Fraction4
1992	1	-2	2	3	4	0.49	0.99	0.99	0.3
	2	3	5	9	14	0.69	0.99	0.99	0.2
	3	5	28	35	40	0.6	0.79	0.99	0.1
1993	1	0	2	4	6	0.49	0.99	0.99	0.7
	2	3	5	9	14	0.59	0.99	0.99	0.45
	3	13	28	35	40	0.1	0.29	0.99	0.1
1994	1	0	2	4	6	0.49	0.99	0.99	0.7
	2	3	5	9	14	0.59	0.99	0.99	0.45
	3	13	28	35	40	0.1	0.29	0.99	0.1
1995	1	0	2	4	6	0.49	0.99	0.99	0.6
	2	3	5	10	15	0.59	0.99	0.99	0.5
	3	13	28	35	40	0.1	0.29	0.99	0.1
1996	1	0	2	4	6	0.49	0.99	0.99	0.7
	2	3	5	9	14	0.59	0.99	0.99	0.1
	3	13	25	35	40	0.1	0.29	0.99	0.1
1997	1	0	2	5	8	0.99	0.99	0.99	0.7
	2	3	5	9	14	0.79	0.99	0.99	0.1
	3	15	28	35	40	0.1	0.99	0.99	0.1

Table 5.6.2-5. Maximum Chlorophyll Concentration (µg/l) by Season

Year	Season	Prettyboy		Loch Raven	
		Observed	Simulated	Observed	Simulated
1992	1	11.56	12.96	10.04	10.33
	2	15.05	16.62	10.62	10.92
	3	37.35	37.54	18.27	19.96
1993	1	8.61	7.36	8.01	5.63
	2	19.31	21.34	21.21	22.83
	3	13.19	13.94	29.95	30.07
1994	1	14.06	15.31	14.06	14.33
	2	6.49	13.89	20.64	21.57
	3	27.55	28.4	20.35	24.34
1995	1	9.79	5.63	8.47	3.24
	2	10.48	10.73	4.54	3.48
	3	13.24	19.27	13.75	15.92
1996	1	30.82	32.69	5.96	7.68
	2	13.46	15.38	35.3	38.74
	3	14.19	17.77	22.73	24.67
1997	1	33.14	33.37	16.11	16.71
	2	8.93	8.74	12.04	12.18
	3	9.55	9.91	43.19	47.9

Figure 5.6.2-1. Observed and Simulated Maximum Chlorophyll Concentrations By Date, Calibration Scenario, Prettyboy Reservoir

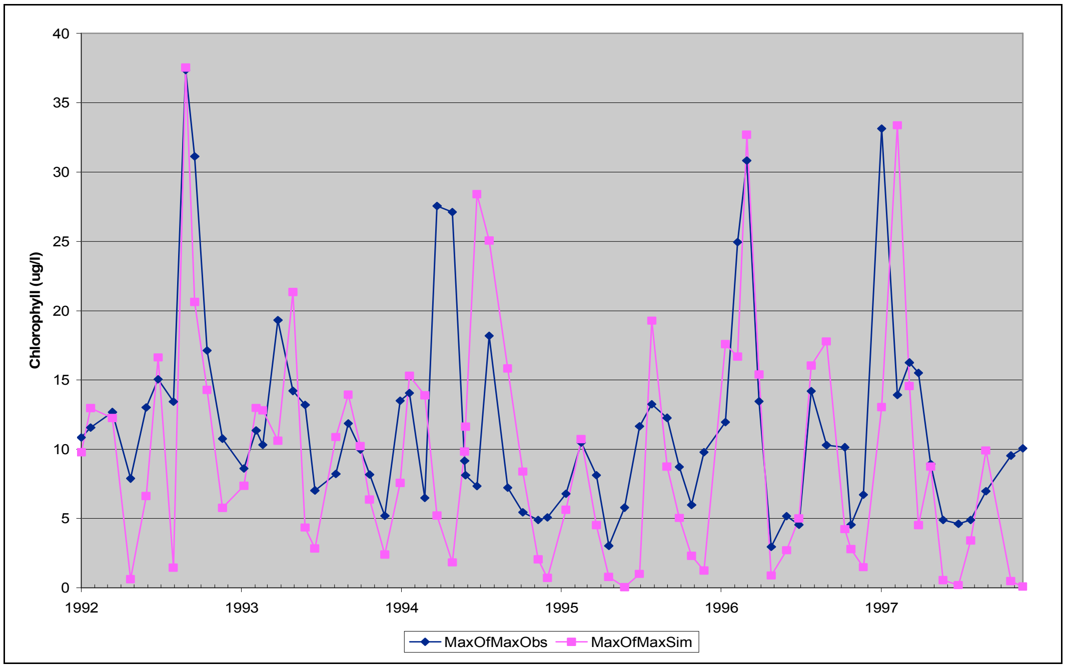

Figure 5.6.2-2. Observed and Simulated Maximum Chlorophyll Concentrations, Calibration Scenario, Prettyboy Reservoir

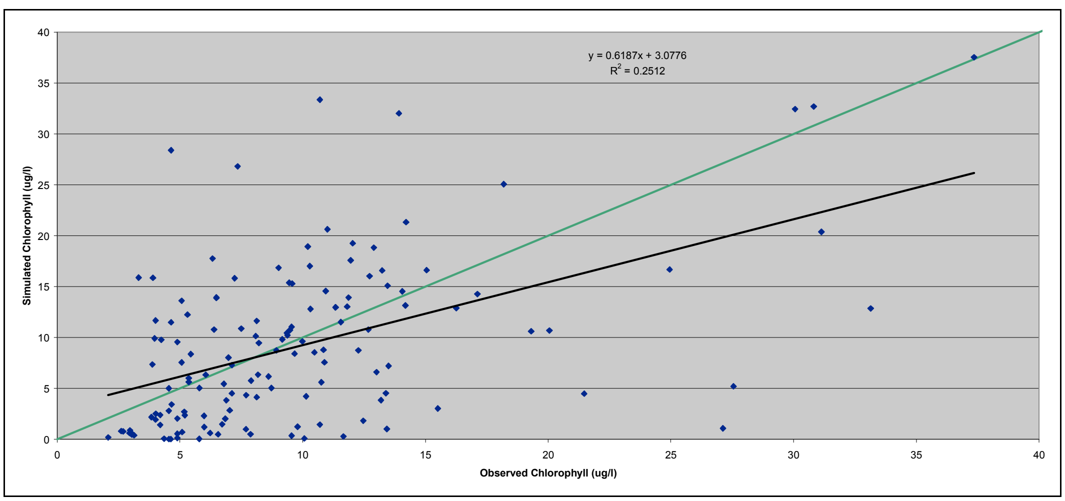

Figure 5.6.2-3. Cumulative Distribution of Observed and Simulated Maximum Chlorophyll Concentrations, Calibration Scenario, Prettyboy Reservoir

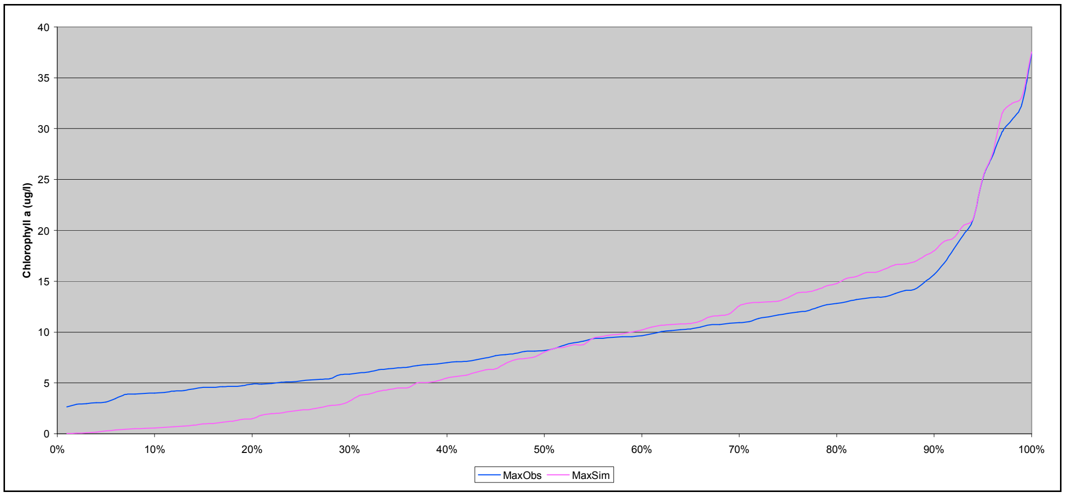

Figure 5.6.2-4. Observed and Simulated Maximum Chlorophyll Concentrations, Middle Station, Calibration Scenario, Prettyboy Reservoir

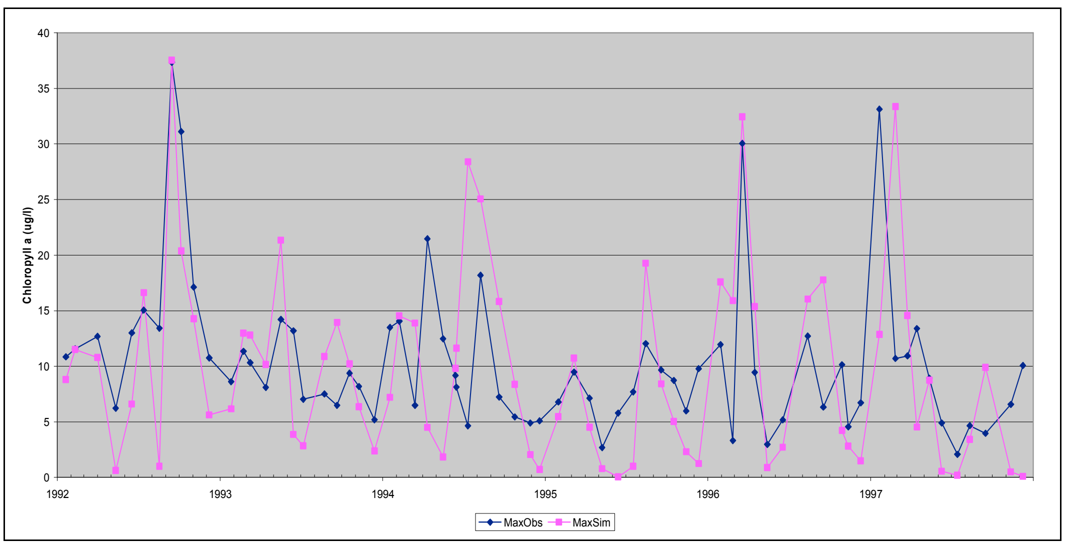

Figure 5.6.2-5. Observed and Simulated Maximum Chlorophyll Concentrations, Lower Stations, Calibration Scenario, Prettyboy Reservoir

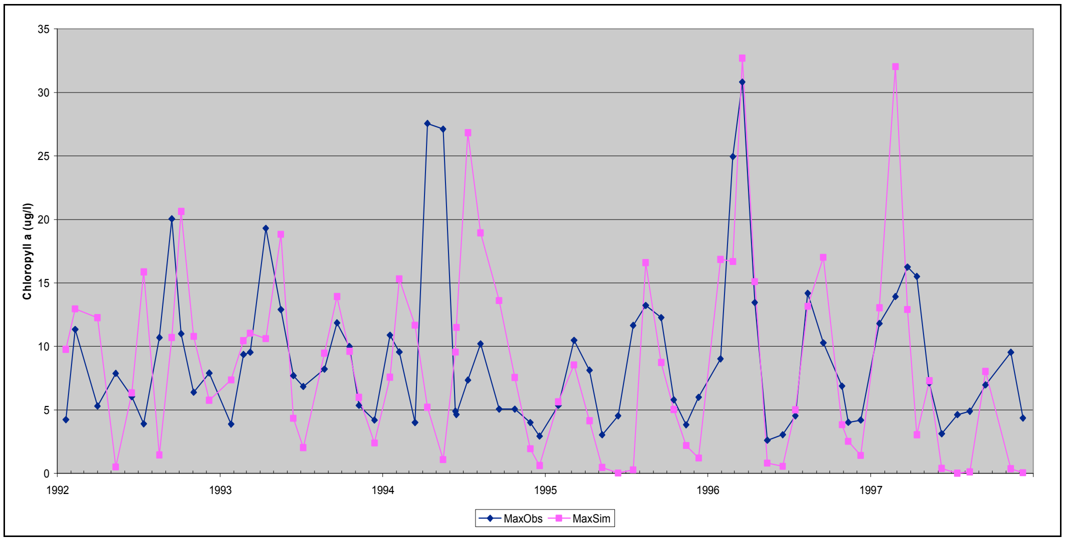

Figure 5.6.2-6. Observed and Simulated Maximum Chlorophyll Concentrations By Date, Calibration Scenario, Loch Raven Reservoir

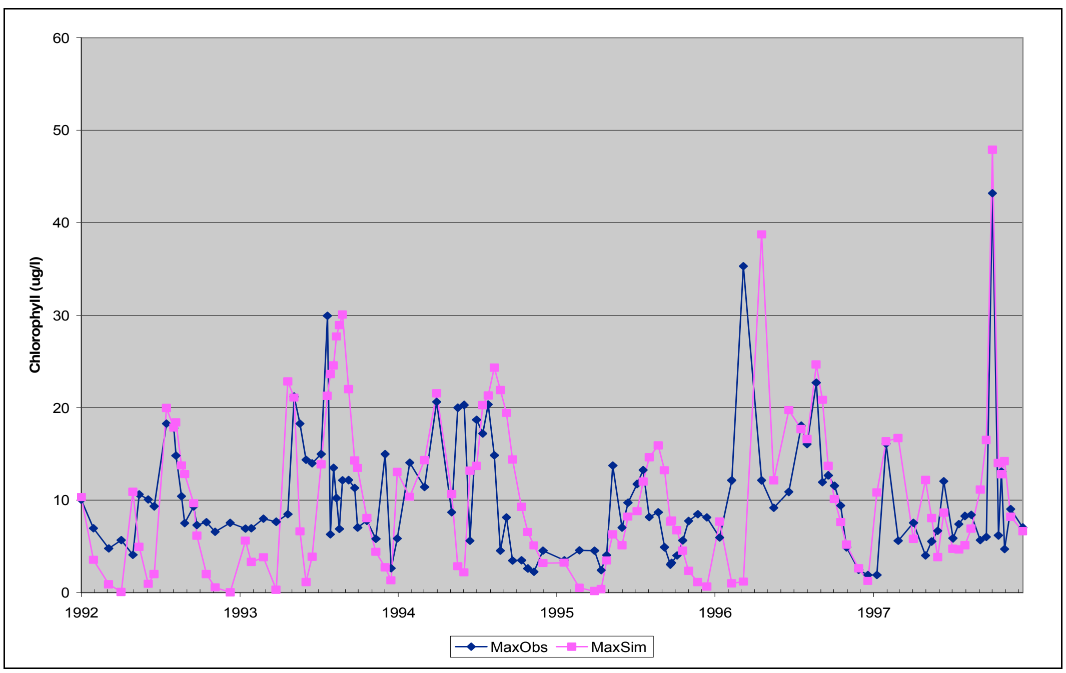

Figure 5.6.2-7. Observed and Simulated Maximum Chlorophyll Concentrations, Calibration Scenario, Loch Raven Reservoir

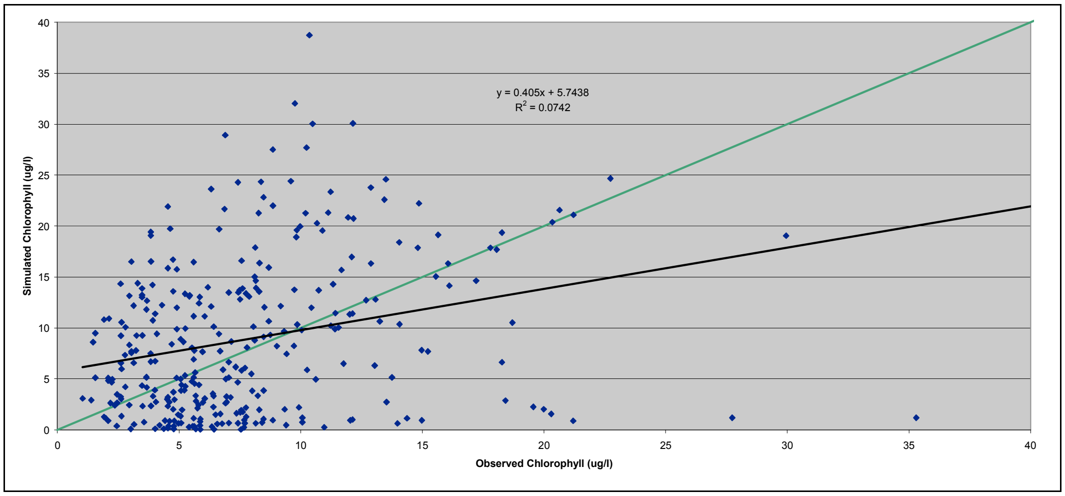

Figure 5.6.2-8. Cumulative Distribution of Observed and Simulated Maximum Chlorophyll Concentrations, Calibration Scenario, Loch Raven Reservoir

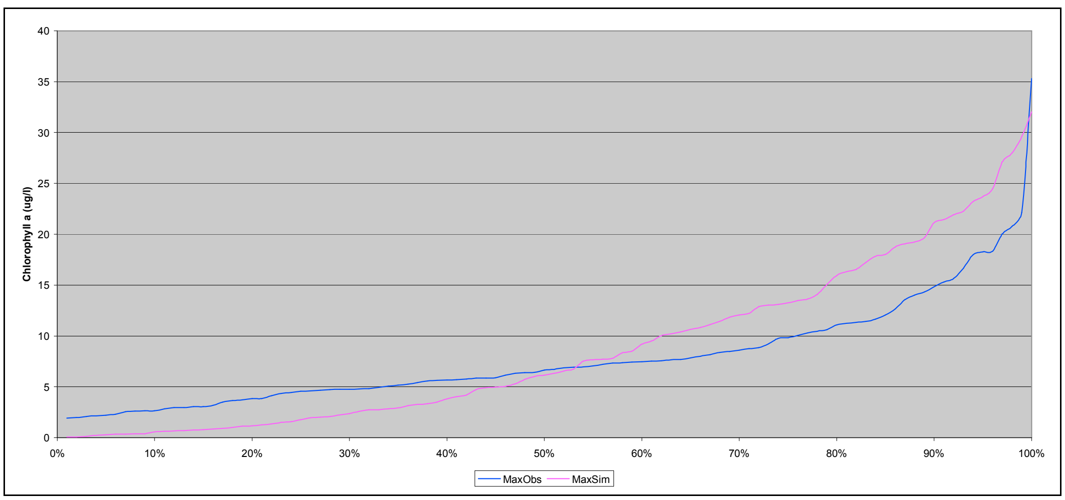

Figure 5.6.2-9. Observed and Simulated Maximum Chlorophyll Concentrations, Upper Stations, Calibration Scenario, Loch Raven Reservoir

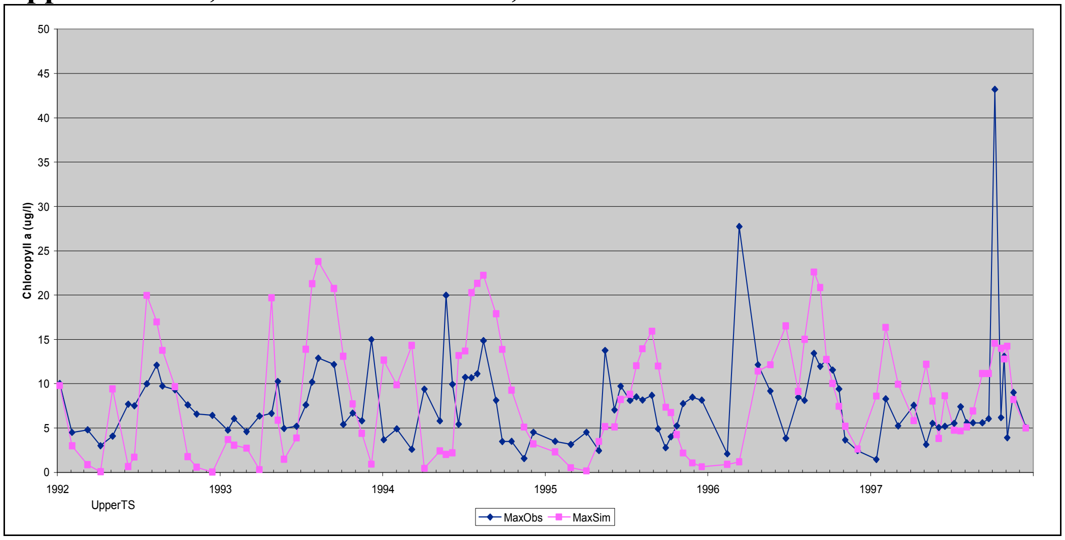

Figure 5.6.2-10. Observed and Simulated Maximum Chlorophyll Concentrations, Middle Stations, Calibration Scenario, Loch Raven Reservoir.

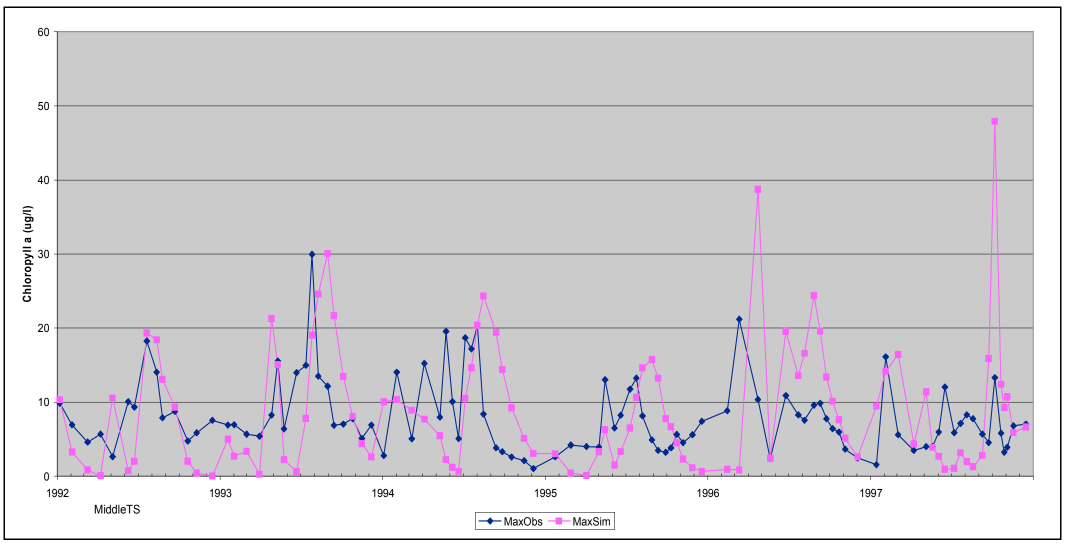

Figure 5.6.2-11 Observed and Simulated Maximum Chlorophyll Concentrations, Lower Station, Calibration Scenario, Loch Raven Reservoir

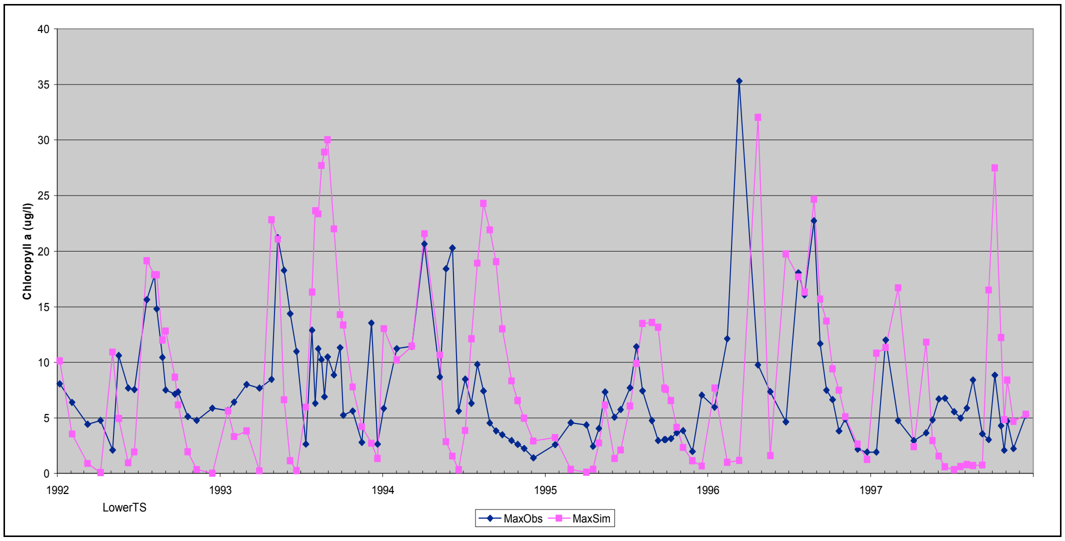

5.6.3. Simulation of Dissolved Oxygen

The simulation of dissolved oxygen is heavily dependent on the simulation of temperature and temperature-determined density differences which inhibit the transport of dissolved oxygen through turbulent diffusion. Under stratified conditions, the decay of organic material in the water column and the sediments exerts an oxygen demand that can lead to hypoxia below the well-mixed surface layer. As was shown in Section 5.1., both Prettyboy and Loch Raven Reservoirs suffer from seasonal hypoxia.

Oxygen demand in the water column is exerted by labile dissolved and particulate organic matter, which represents algal detritus, and dissolved and particulate CBOD, which represents external sources of organic matter. The nitrification of ammonia also consumes oxygen. Oxygen demand in the sediments is represented as a temperature-dependent first order decay of a single species of sediment organic matter. As was reported in Section 5.3.2., the W2 code was altered so that particulate CBOD contributed to sediment organic matter.

Sediment oxygen demand under stratified conditions primarily determines bottom dissolved oxygen. Because there was no monitoring information that could be used to initialize organic material in the sediments, the initial concentration of sediment organic matter in one simulation year was taken from the final conditions of the previous year, and the overall SOD simulation was consistently parameterized across simulation years. In addition to the first-order decay rate and temperature parameters, the fraction of particulate CBOD that is labile, as opposed to refractory, was treated as a calibration parameter. Table 5.6.3-1 shows the parameters used in the simulation. The labile particulate CBOD decay rate in the water column was set so that it did not contribute significantly to water column oxygen demand.

Figures 5.6.3-1 and 5.6.3-2 show the simulated and observed average bottom DO concentrations throughout the simulation in the middle and lower stations Prettyboy Reservoir. Figures 5.6.3-3 through 5.6.3-5 show the simulated and observed average bottom DO concentrations throughout the simulation in the upper, middle and lower stations in Loch Raven Reservoir. As the figures show, there is very good agreement between observed and simulated values. Figures 5.6.3-6 and 5.6.3-7, scatter plots of average bottom DO concentrations in Prettyboy and Loch Raven Reservoirs, and Figures 5.6.3-8 and 5.6.3-9, which compare the cumulative distribution of average bottom DO concentrations, also demonstrate that the simulation matches the observed data very well. The model does tend to lead the observed hypoxia in wet years and lag in drier years, but overall the model consistently captures the seasonal dynamics of bottom DO.

The model also captures the seasonal trends in average surface DO, as demonstrated in Figures 5.6.3-10 and 5.6.3-11, which show the average observed and simulated surface DO concentrations in Prettyboy Reservoir, and Figures 5.6.3-12, 5.6.3-13, and 5,6.3-14, which show the average observed and simulated surface DO concentrations in Loch Raven Reservoir. The model tends to overpredict the maximum winter DO concentration. The model also tends to lead the seasonal variation in DO concentrations. As will be demonstrated in Section 6.4.2, as loads are decreased, average surface DO concentrations become relatively independent of CBOD loading rates and primary production. The general pattern of simulated surface DO concentrations seems to be primarily a function of temperature-induced stratification. Figures 5.6.3-15 and 5.6.3-16 show the scatter plots and cumulative distribution functions comparing observed and simulated average surface DO concentrations for Prettyboy Reservoir. Figures 5.6.3-17 and 5.6.3-18 show the same plots for Loch Raven Reservoir. In the model calibration, reaeration rates were raised to improve agreement between observed and simulated concentrations. The agreement is fairly good, though on the whole surface DO concentrations are somewhat underpredicted in Loch Raven Reservoir

Table 5.6.3-1. DO Calibration Parameter Values

Parameter	Prettyboy	Loch Raven
Dissolved CBOD Decay Rate (day-1)	0.125	0.125
Particulate CBOD Decay Rate (day-1)	0.01	0.01
Temperature Coefficient	1.016	1.016
Reaeration Coefficient-1	2.0	2.0
Reaeration Coefficient-2	0.15	0.15
Reaeration Coefficient-3	2.0	2.0
Labile Fraction of Particulate CBOD	0.65	0.65
Organic Sediment Decay Rate (day-1)	0.08	0.08
Sediment Decay Temperature Start °C (% decay rate)	6 (10%)	8.5 (30%)
Sediment Decay Temperature Max °C (%decay rate)	7 (99%)	10 (99%)

.

Figure 5.6.3-1. Observed and Simulated Average Bottom DO Concentrations, Middle Station, Calibration Scenario, Prettyboy Reservoir

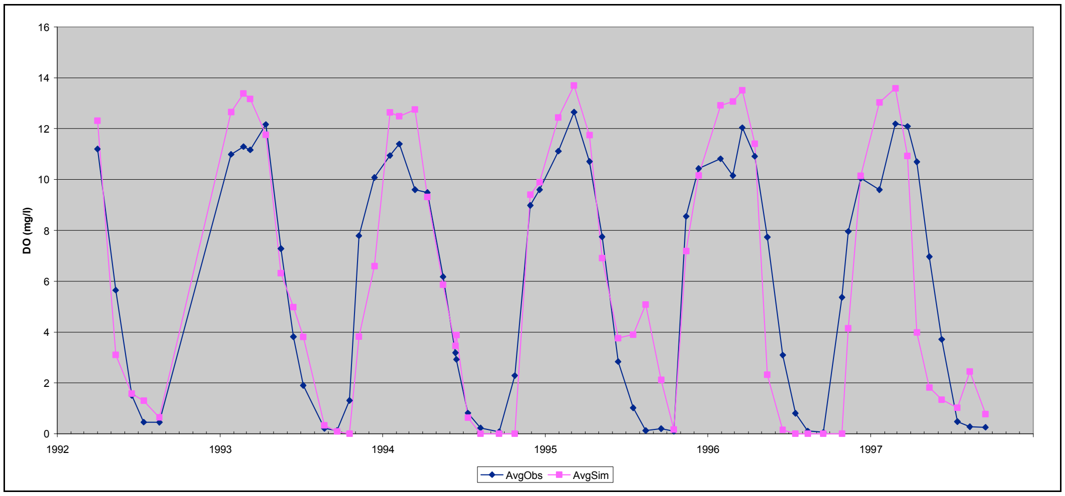

Figure 5.6.3-2. Observed and Simulated Average Bottom DO Concentrations, Lower Stations, Calibration Scenario, Prettyboy Reservoir

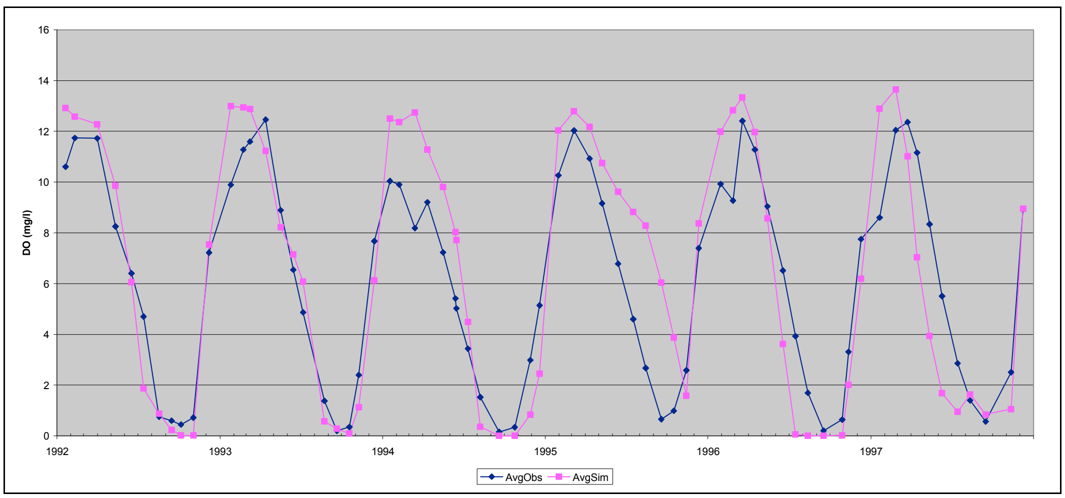

Figure 5.6.3-3. Observed and Simulated Average Bottom DO Concentrations, Upper Stations, Calibration Scenario, Loch Raven Reservoir

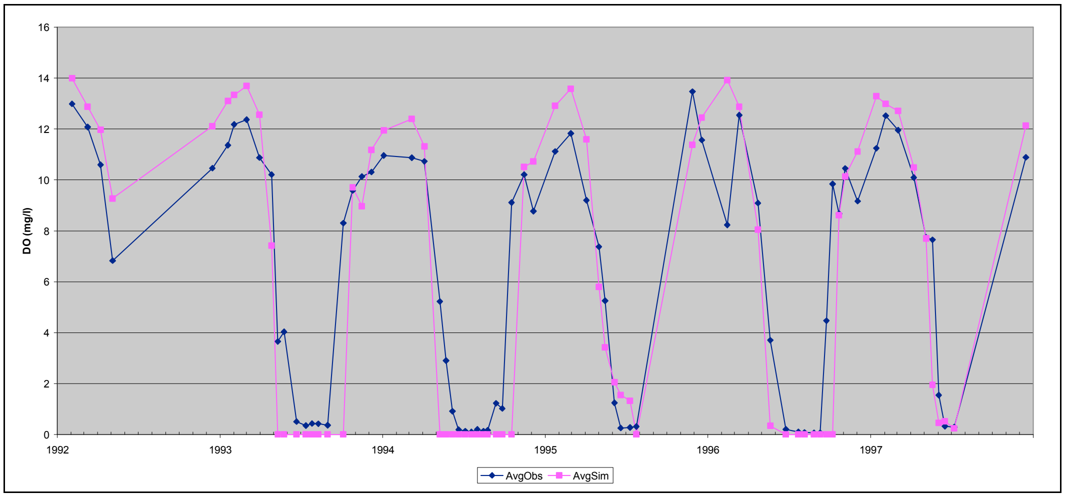

Figure 5.6.3-4. Observed and Simulated Average Bottom DO Concentrations, Middle Stations, Calibration Scenario, Loch Raven Reservoir

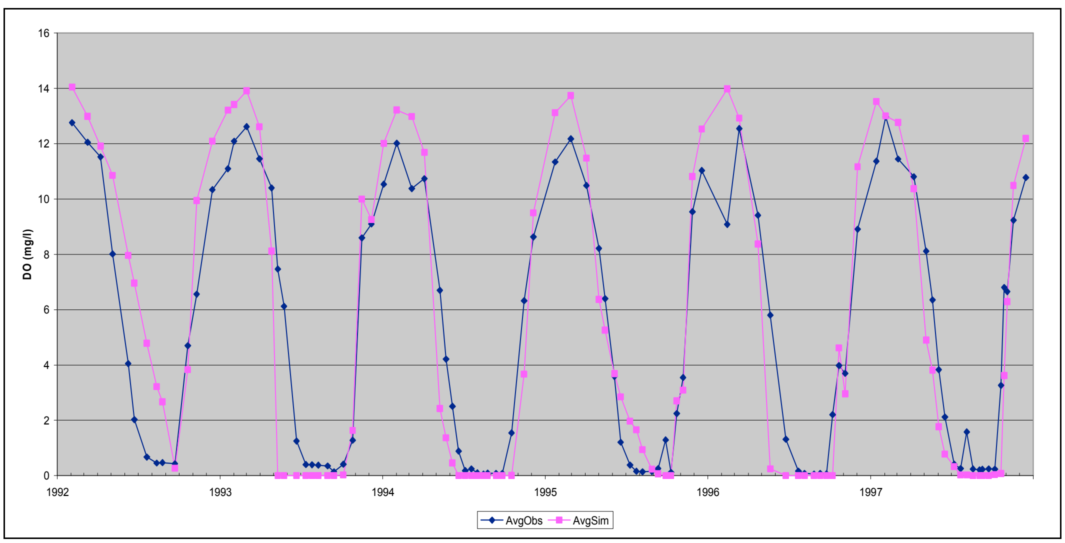

Figure 5.6.3-5. Observed and Simulated Average Bottom DO Concentrations, Lower Station, Calibration Scenario, Loch Raven Reservoir

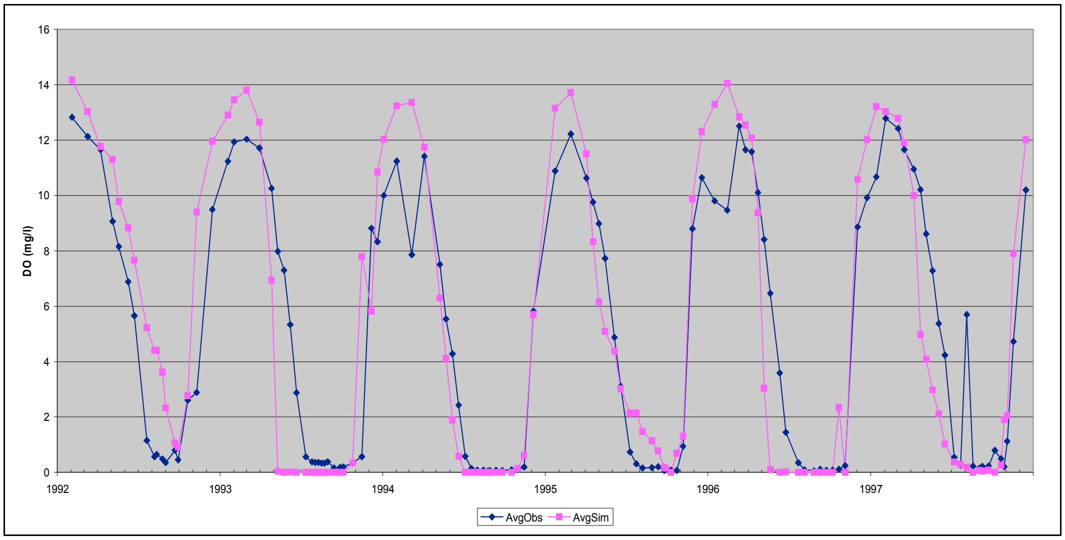

Figure 5.6.3-6. Observed and Simulated Average Bottom DO Concentrations, Calibration Scenario, Prettyboy Reservoir

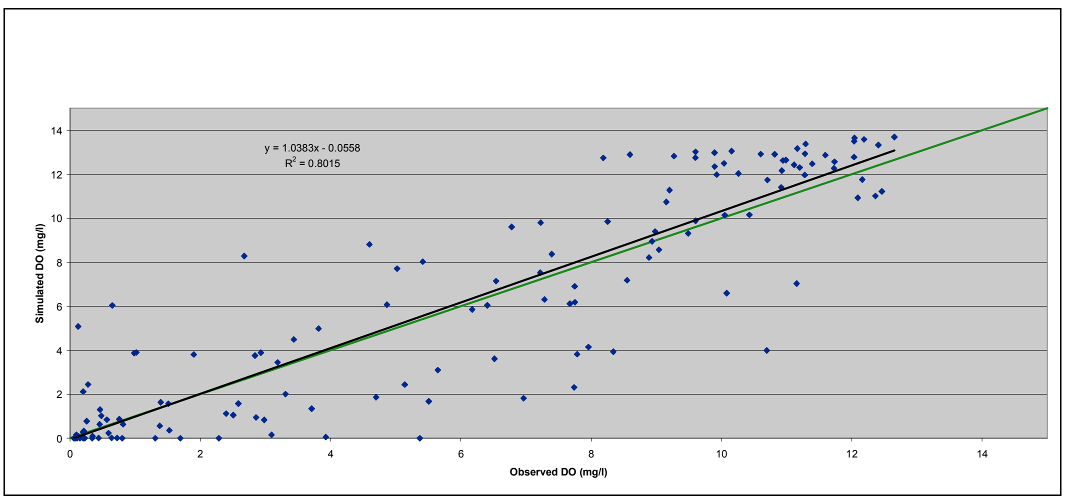

Figure 5.6.3-7. Observed and Simulated Average Bottom DO Concentrations, Calibration Scenario, Loch Raven Reservoir

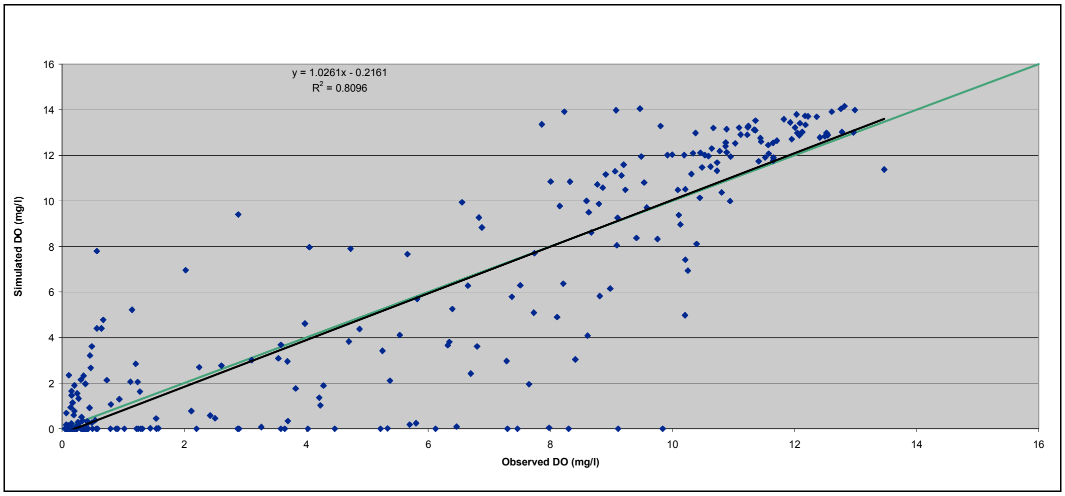

Figure 5.6.3-8. Cumulative Distribution of Observed and Simulated Average Bottom DO Concentrations, Calibration Scenario, Prettyboy Reservoir

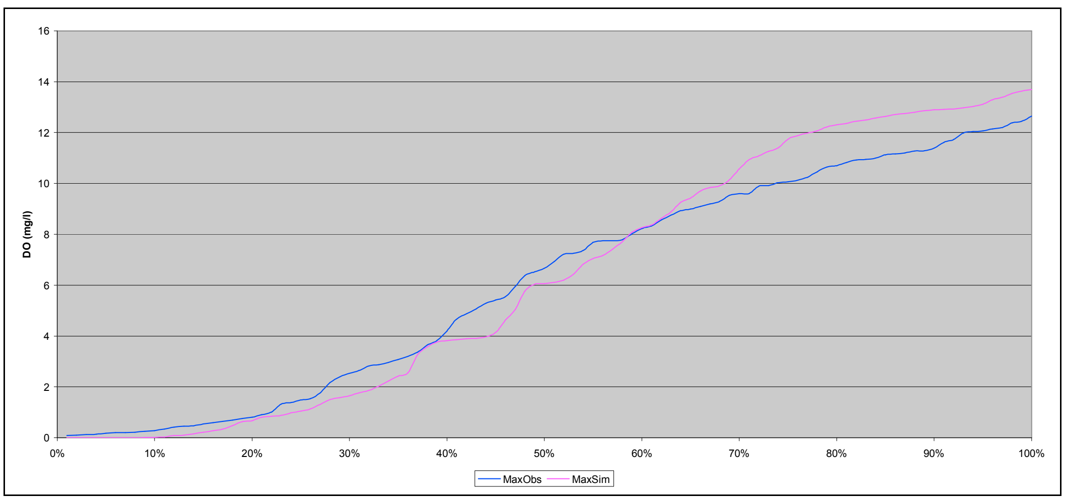

Figure 5.6.3-9. Cumulative Distribution of Observed and Simulated Average Bottom DO Concentrations, Calibration Scenario, Loch Raven Reservoir

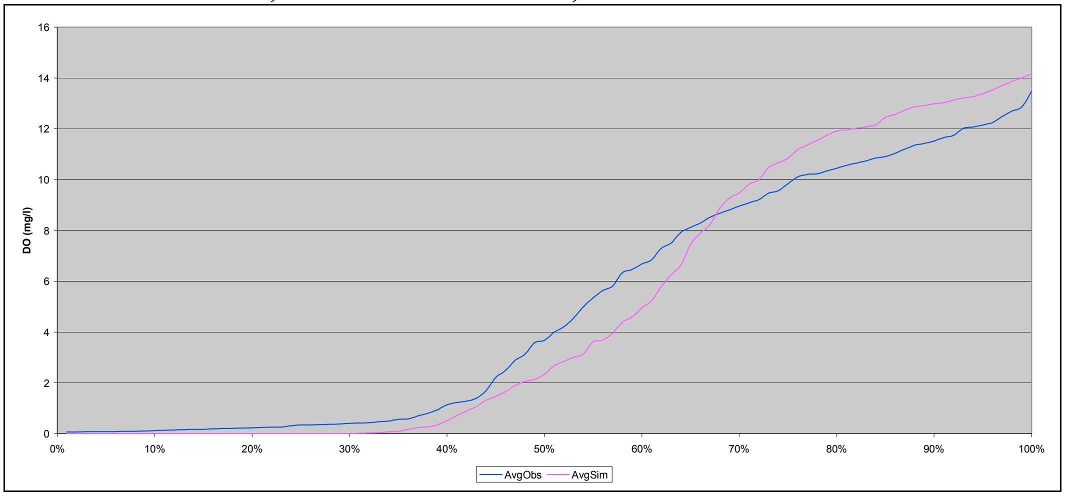

Figure 5.6.3-10. Observed and Simulated Average Surface DO Concentrations, Middle Station, Calibration Scenario, Prettyboy Reservoir

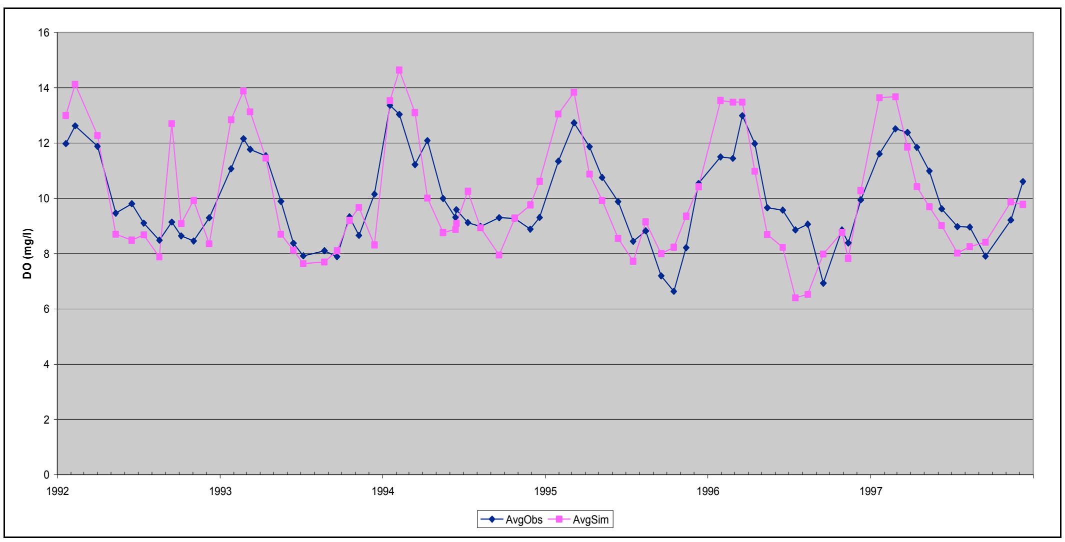

Figure 5.6.3-11. Observed and Simulated Average Surface DO Concentrations, Lower Stations, Calibration Scenario, Prettyboy Reservoir

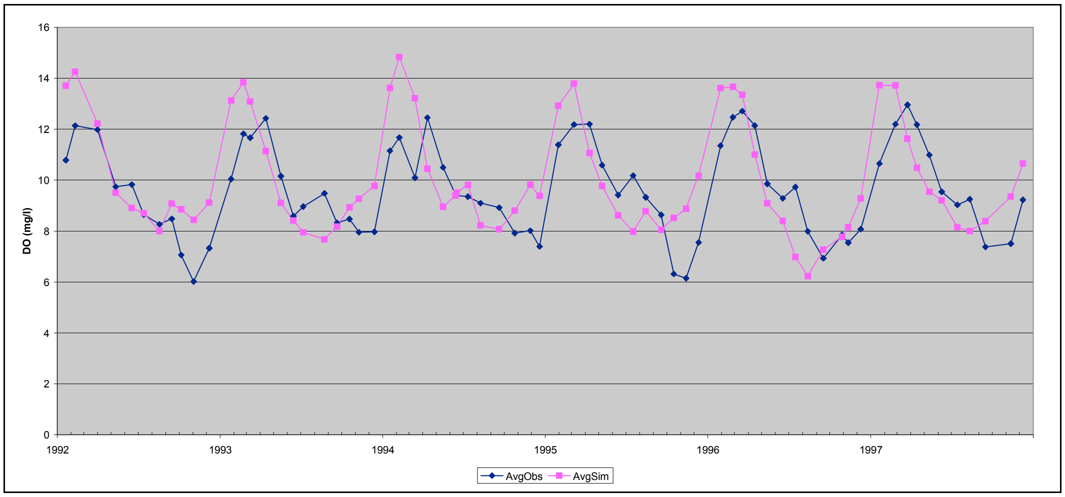

Figure 5.6.3-12. Observed and Simulated Average Surface DO Concentrations, Upper Stations, Calibration Scenario, Loch Raven Reservoir

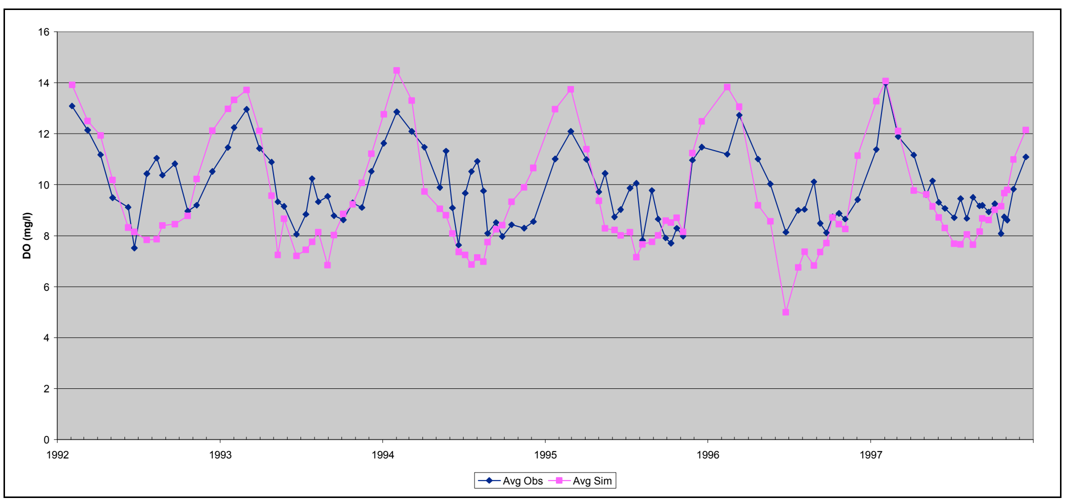

Figure 5.6.3-13. Observed and Simulated Average Surface DO Concentrations, Middle Stations, Calibration Scenario, Loch Reservoir

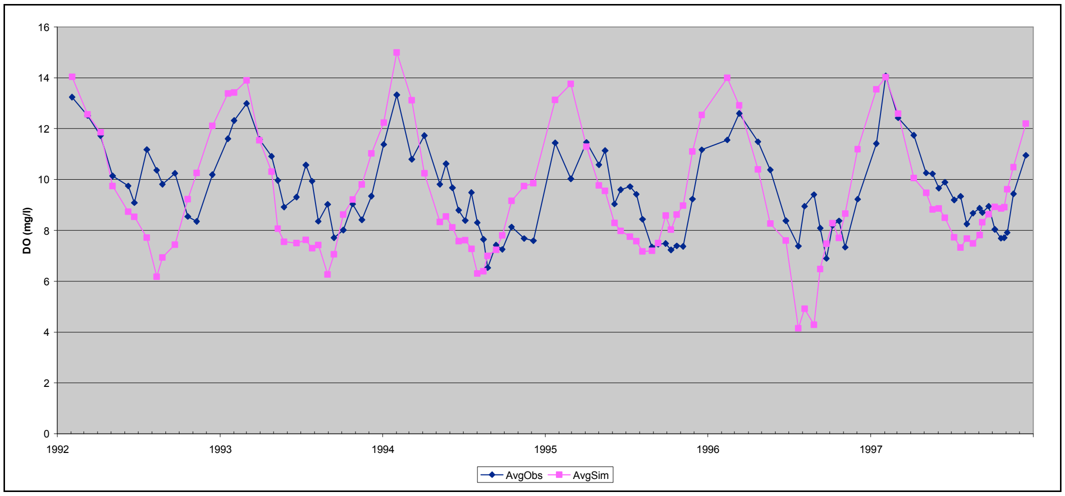

Figure 5.6.3-14. Observed and Simulated Average Surface DO Concentrations, Lower Station, Calibration Scenario, Loch Reservoir

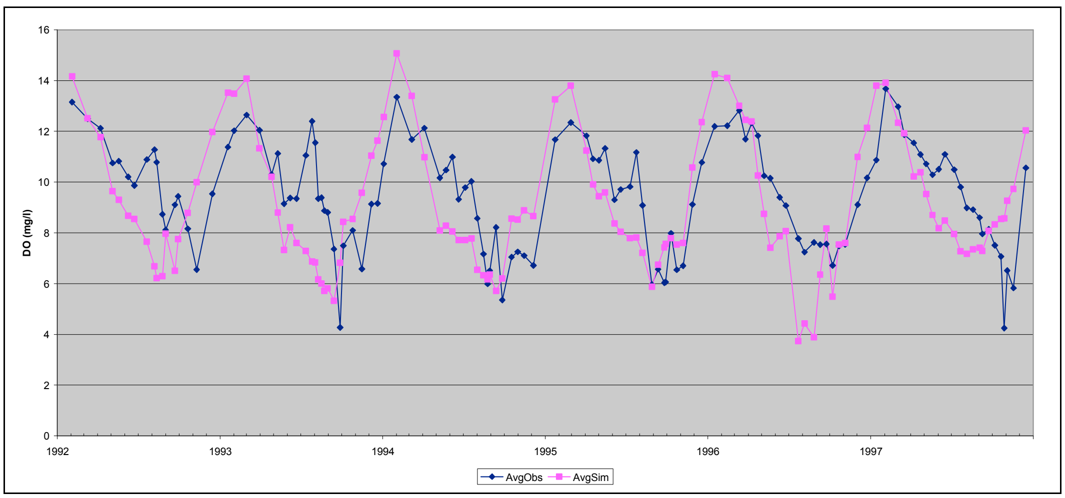

Figure 5.6.3-15. Observed and Simulated Average Surface DO Concentrations, Calibration Scenario, Prettyboy Reservoir

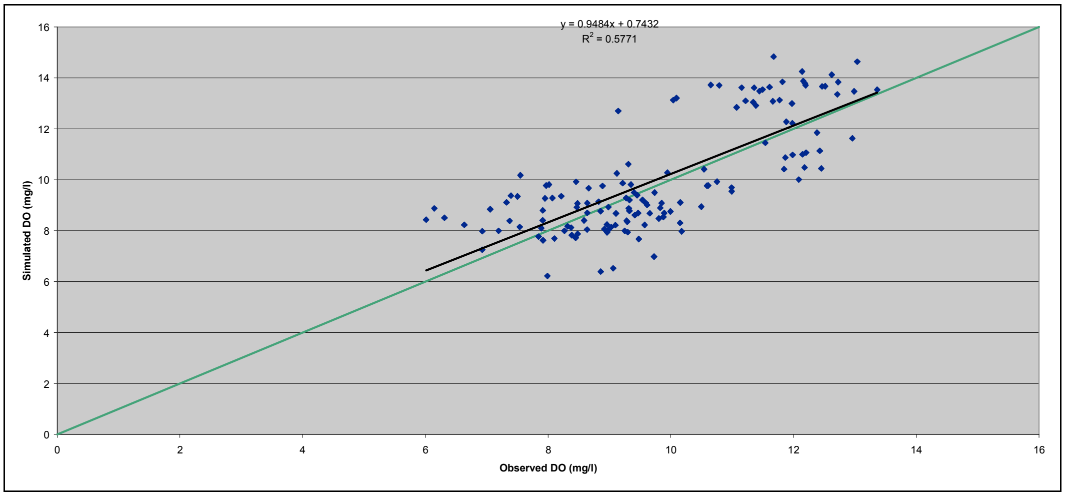

Figure 5.6.3-16. Observed and Simulated Average Surface DO Concentrations, Calibration Scenario, Loch Raven Reservoir

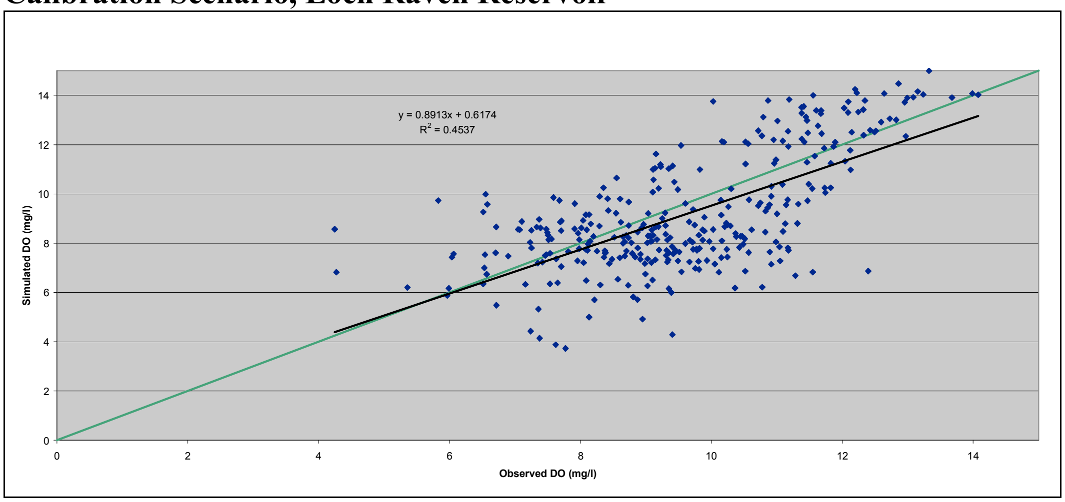

Figure 5.6.3-17. Cumulative Distribution of Observed and Simulated Average Surface DO Concentrations, Calibration Scenario, Prettyboy Reservoir

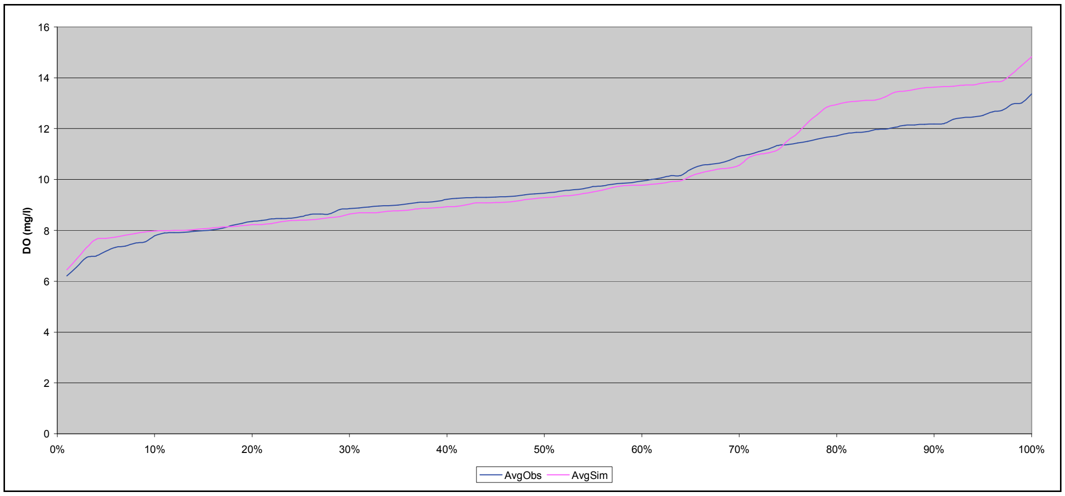

Figure 5.6.3-18. Cumulative Distribution of Observed and Simulated Average Surface DO Concentrations, Calibration Scenario, Loch Raven Reservoir

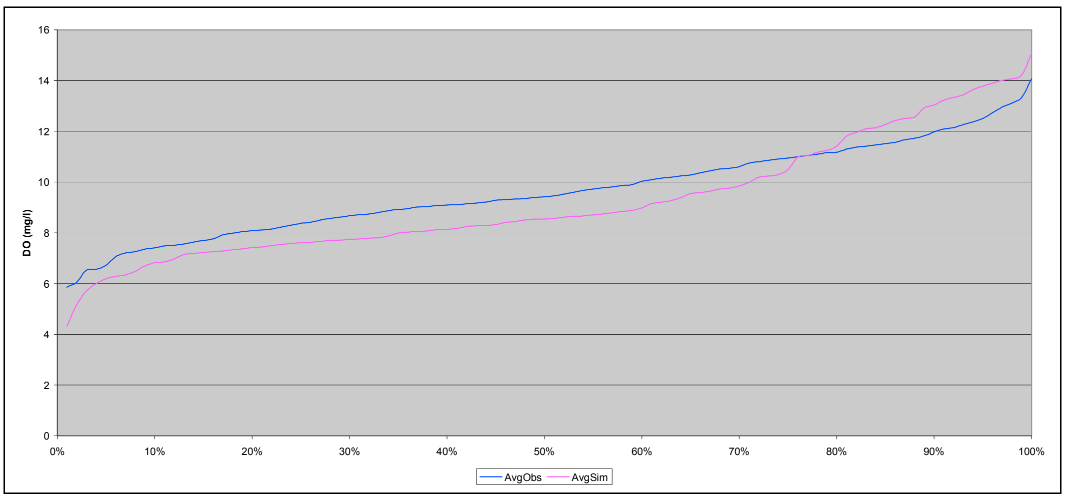

5.6.4. Simulation of Ammonia and Nitrate

The simulation of nitrogen species was calibrated against the observed data with some limited success. The simulation of ammonia and nitrate concentrations is secondary to the primary purposes of the reservoir models, which is to represent the relation between total phosphorus loads and chlorophyll concentrations and to simulate DO concentrations to evaluate whether the reservoirs are meeting water quality standards. Both monitoring data and the models agree that the reservoirs are phosphorus limited; there is more than enough nitrogen for algal growth.

As Section 5.1.6 showed, there is a lot of variability in observed ammonia-N concentrations. Generally ammonia in the surface layer is a function of external loading rates and algal consumption; ammonia concentrations in the bottom layer are determined by the release of ammonia from the sediments in diagenesis. Ammonia release from the sediments tend to peak in fall. Ammonia concentrations throughout the water column are also a function transformation of ammonia to nitrate in nitrification. Since nitrate-N concentrations are an order of magnitude larger than ammonia-N concentrations, nitrate concentrations are not as sensitive to nitrification rates. Nitrate concentrations in the bottom are a function of denitrification in the sediments that occurs under hypoxic conditions. Minimum nitrate concentrations also occur in the fall.

The reservoir models capture most of the seasonality of ammonia and nitrate concentrations but not their intra-seasonal variability. Figures 5.6.4-1 through 5.6.4-4 show the ammonia-N concentrations in the surface and bottom layers at the middle and lower sampling locations in Prettyboy Reservoir. Figures 5.6.4-5 through 5.6.4-8 show the nitrate-N concentrations in the surface and bottom layers at the middle and lower sampling locations in Prettyboy Reservoir. As the graphs show (1) ammonia-N is underpredicted in the surface layer, (2) the simulation underpredicts peak ammonia concentrations in bottom layer, and (3) simulated nitrate concentrations underpredict bottom layer concentrations in wet years like 1994 and 1996 and overpredict a dryer year like 1995. Table 6.4-1 shows summary statistics comparing observed and simulated concentrations. On average bottom nitrate concentrations match the observed concentrations and surface concentrations only slightly oversimulate observed ones. Simulated surface ammonia concentrations proved surprisingly insensitive to nitrification rates or algal nitrogen preferences. Ammonia concentrations in Prettyboy Reservoir are generally undersimulated, although some of the larger observed concentrations suggest improbable changes in loading rates or sediment releases.

Figures 5.6.4-9 through 5.6.4-14 show the ammonia-N concentrations in the surface and bottom layers at the upper, middle and lower sampling locations in Loch Raven Reservoir. Figures 5.6.4-15 through 5.6.4-20 show the nitrate-N concentrations in the surface and bottom layers at the upper, middle and lower sampling locations in Loch Raven Reservoir. The undersimulation of average bottom nitrate concentrations in wet years is again apparent. Simulated average surface nitrate concentrations exhibit the seasonal pattern of observed values but to a much lesser degree. As in Prettyboy Reservoir, there are several large peak ammonia concentrations in the observed data not captured by the simulation. Table 5.6.4-2 shows the summary statistics for average nitrogen species concentrations in Loch Raven Reservoir. Generally, the distribution of concentrations in the 1st to 3rd quartile range shows reasonable agreement with the observed data, and deviates from the observed distribution at the extremes.

Table 5.6.4-1 Average Nitrogen Species Concentration Statistics, Prettyboy Reservoir

Statistic	Ammonia-N				Nitrate-N			
	Surface		Bottom		Surface		Bottom	
	Observed	Model	Observed	Model	Observed	Model	Observed	Model
Min	.011	<.001	.008	.004	0.8	1.2	0.5	0.2
1st Q	.028	.003	.032	.019	1.5	1.9	1.5	1.8
Median	.040	.007	.061	.045	1.7	2.2	1.8	2.0
3rd Q	.067	.014	.139	.079	2.1	2.4	2.1	2.2
Max	.248	.194	.800	.216	2.7	3.0	2.6	2.7
Average	.058	.014	.110	.059	1.8	2.2	1.7	1.9
R^2	< .01		.01		.17		.14	

Table 5.6.4-2 Average Nitrogen Species Concentration Statistics, Loch Raven Reservoir

Statistic	Ammonia-N				Nitrate-N			
	Surface		Bottom		Surface		Bottom	
	Observed	Model	Observed	Model	Observed	Model	Observed	Model
Min	.009	.001	.005	.008	0.6	1.2	0.2	<0.1
1st Q	.027	.015	.048	.050	1.2	1.7	1.2	0.6
Median	.042	.033	.106	.126	1.6	1.8	1.6	1.6
3rd Q	.068	.059	.264	.281	1.9	1.9	1.9	1.9
Max	.387	.165	3.5	.532	2.6	2.4	3.2	2.7
Average	.059	.043	.238	.174	1.6	1.8	1.5	1.3
R^2	.08		.02		.02		.13	

Figure 5.6.4-1. Observed and Simulated Average Surface Ammonia Concentrations, Middle Station, Calibration Scenario, Prettyboy Reservoir

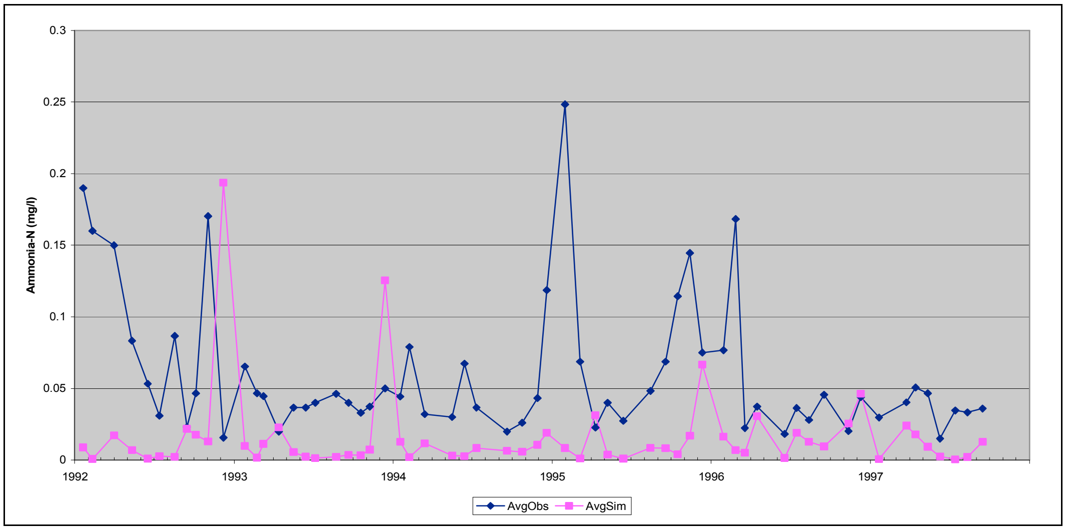

Figure 5.6.4-2. Observed and Simulated Average Bottom Ammonia Concentrations, Middle Station, Calibration Scenario, Prettyboy Reservoir

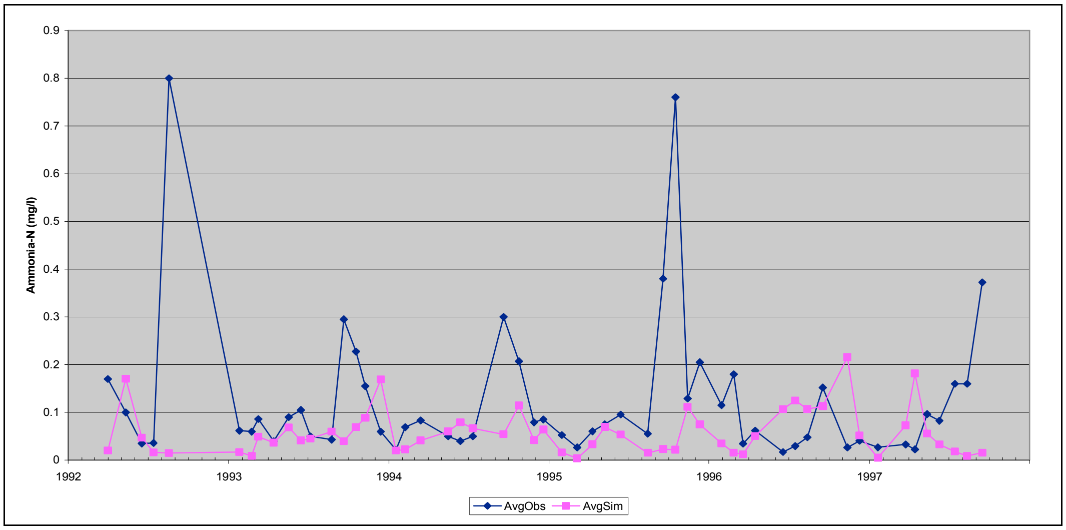

Figure 5.6.4-3. Observed and Simulated Average Surface Ammonia Concentrations, Lower Station, Calibration Scenario, Prettyboy Reservoir

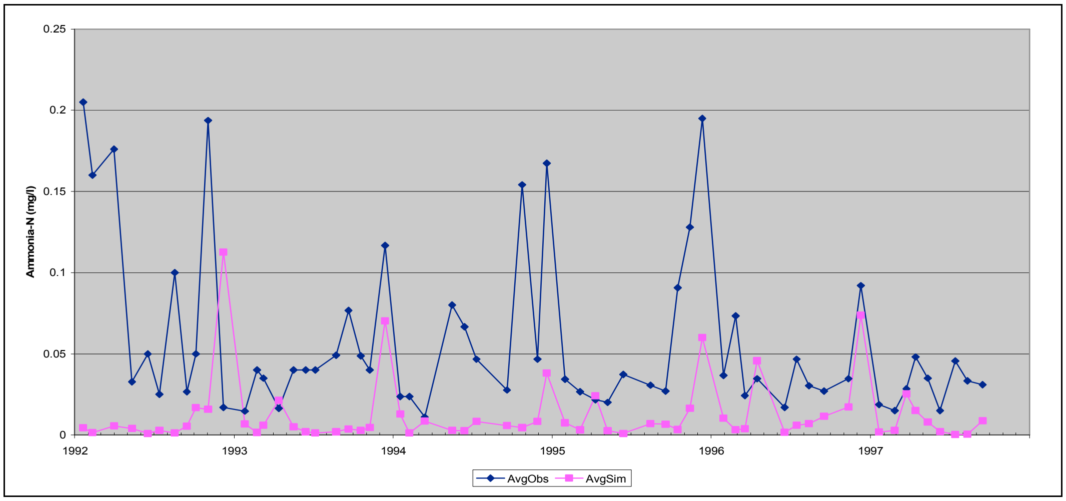

Figure 5.6.4-4. Observed and Simulated Average Bottom Ammonia Concentrations, Lower Station, Calibration Scenario, Prettyboy Reservoir

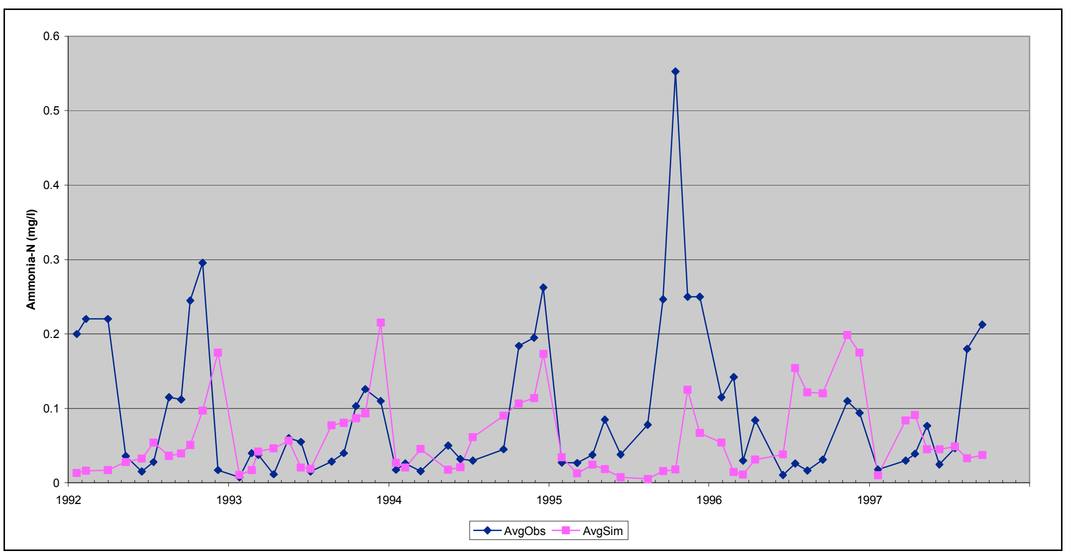

Figure 5.6.4-5. Observed and Simulated Average Surface Nitrate Concentrations, Middle Station, Calibration Scenario, Prettyboy Reservoir

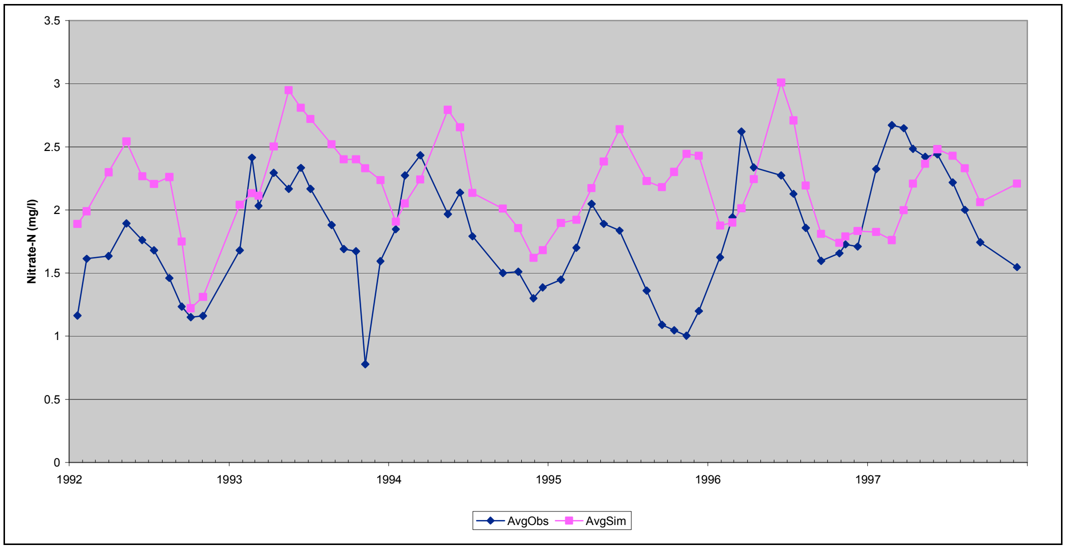

Figure 5.6.4-6. Observed and Simulated Average Bottom Nitrate Concentrations, Middle Station, Calibration Scenario, Prettyboy Reservoir

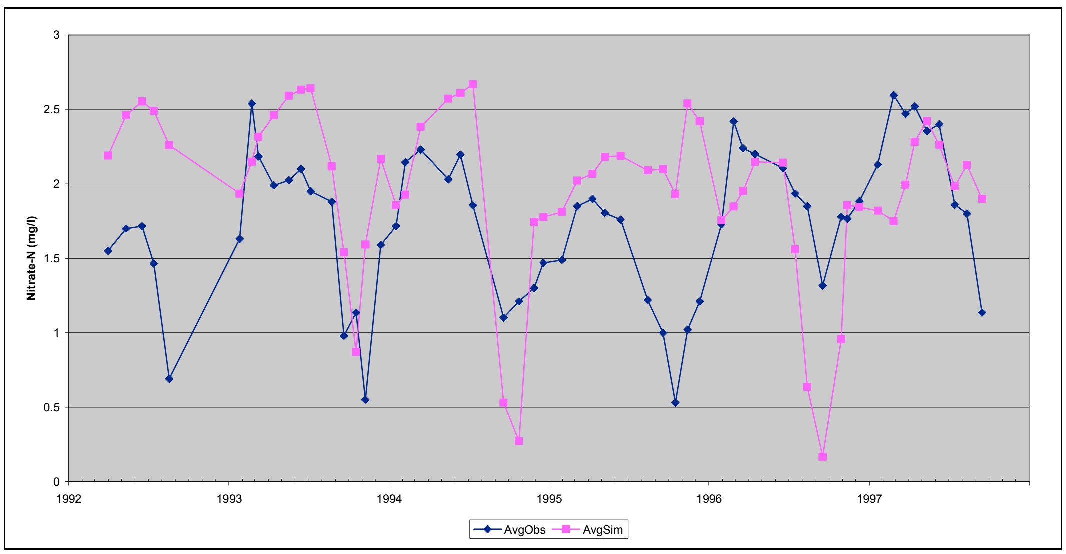

Figure 5.6.4-7. Observed and Simulated Average Surface Nitrate Concentrations, Lower Station, Calibration Scenario, Prettyboy Reservoir

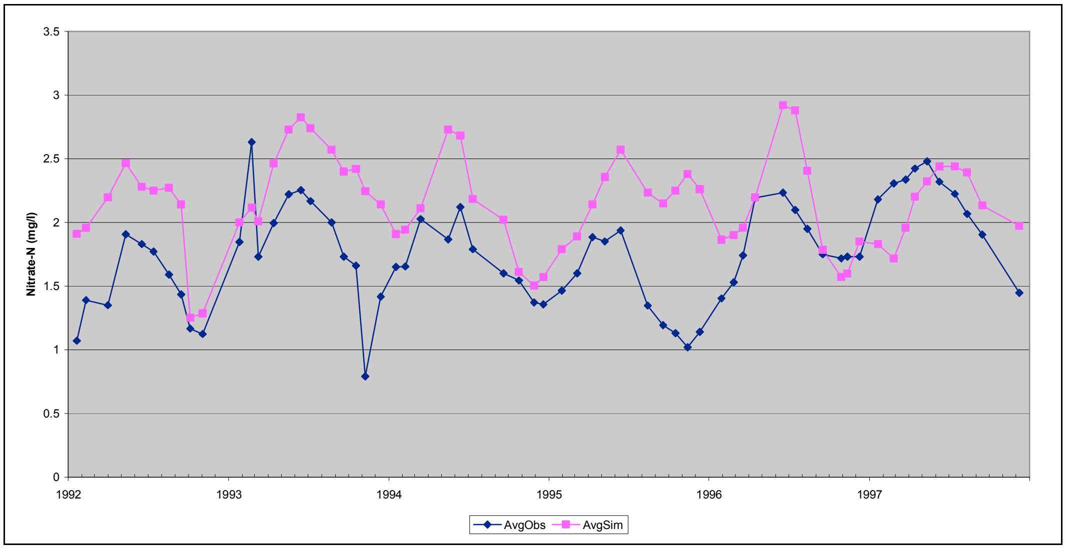

Figure 5.6.4-8. Observed and Simulated Average Bottom Nitrate Concentrations, Lower Station, Calibration Scenario, Prettyboy Reservoir

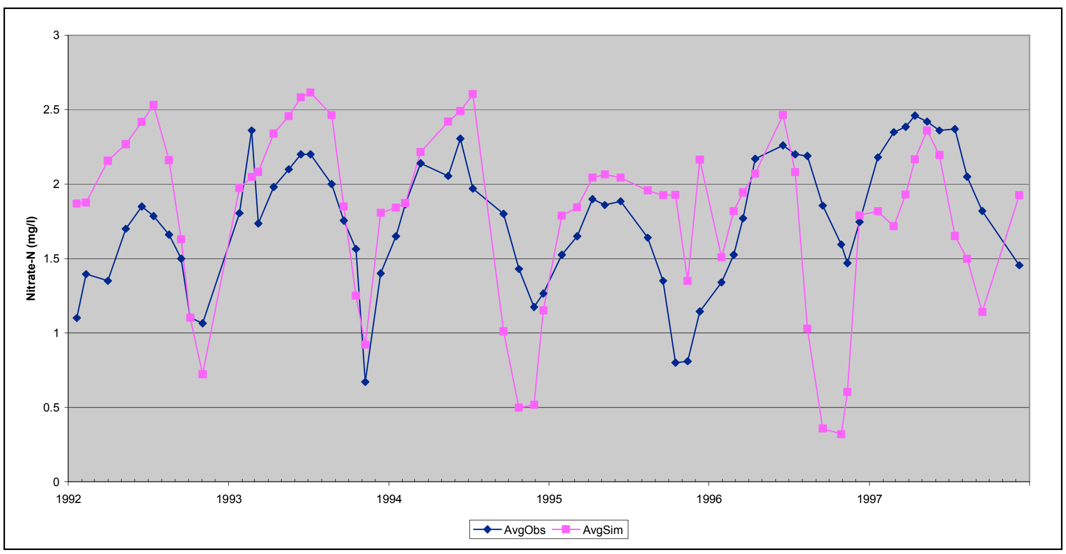

Figure 5.6.4-9. Observed and Simulated Average Surface Ammonia Concentrations, Upper Station, Calibration Scenario, Loch Raven Reservoir

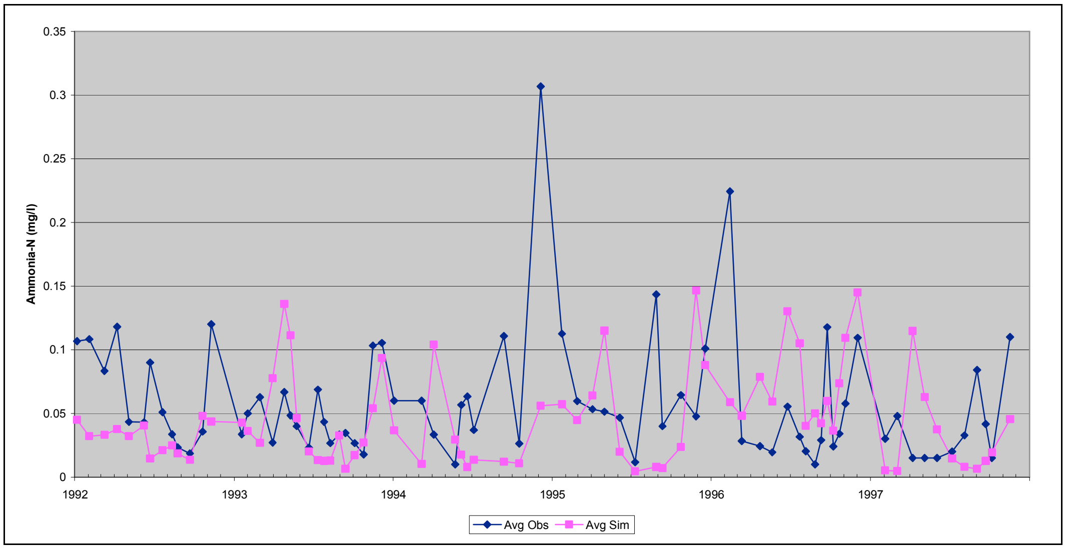

Figure 5.6.4-10. Observed and Simulated Average Bottom Ammonia Concentrations, Upper Station, Calibration Scenario, Loch Raven Reservoir

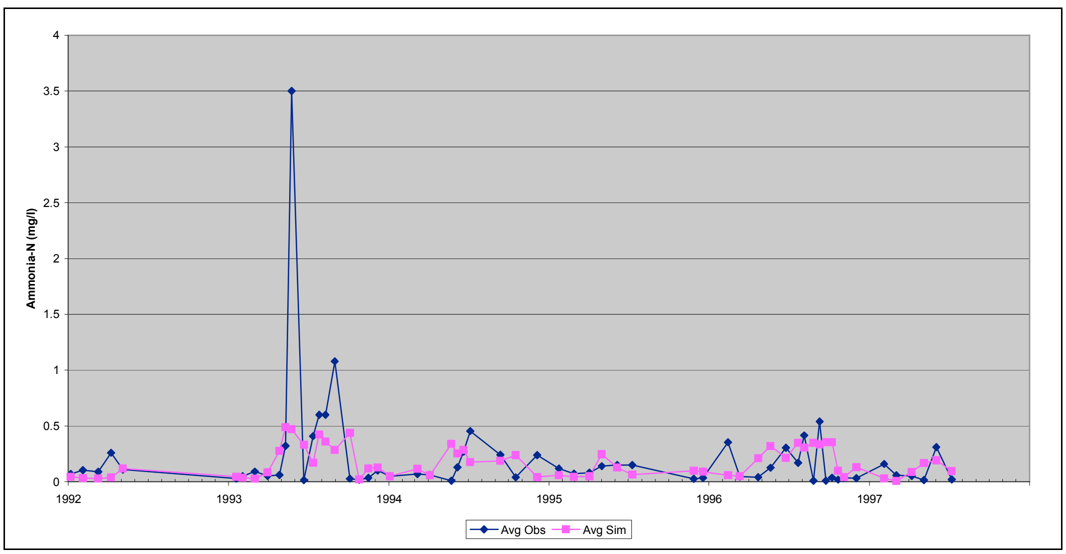

Figure 5.6.4-11. Observed and Simulated Average Surface Ammonia Concentrations, Middle Station, Calibration Scenario, Loch Raven Reservoir

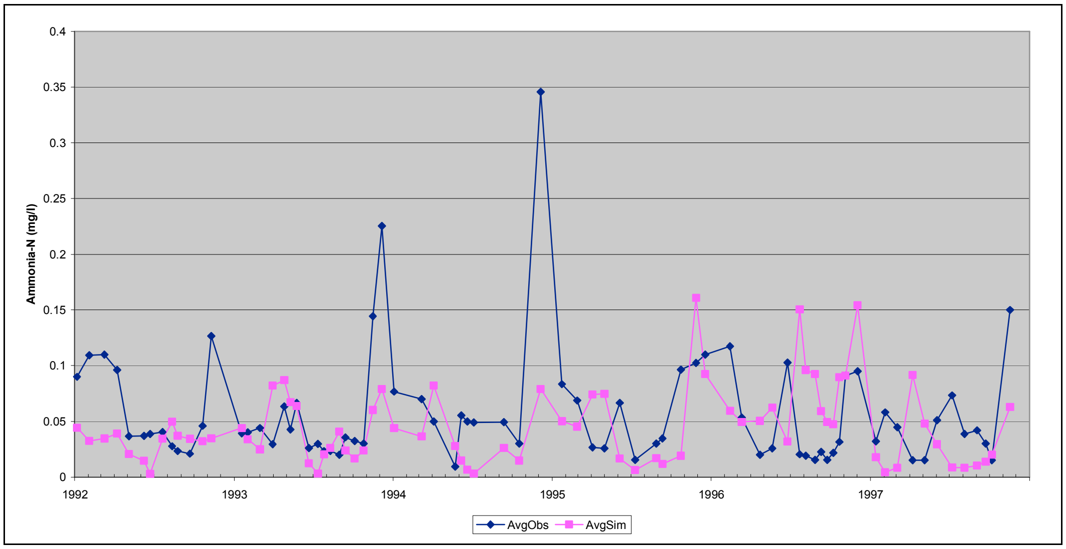

Figure 5.6.4-12. Observed and Simulated Average Bottom Ammonia Concentrations, Middle Station, Calibration Scenario, Loch Raven Reservoir

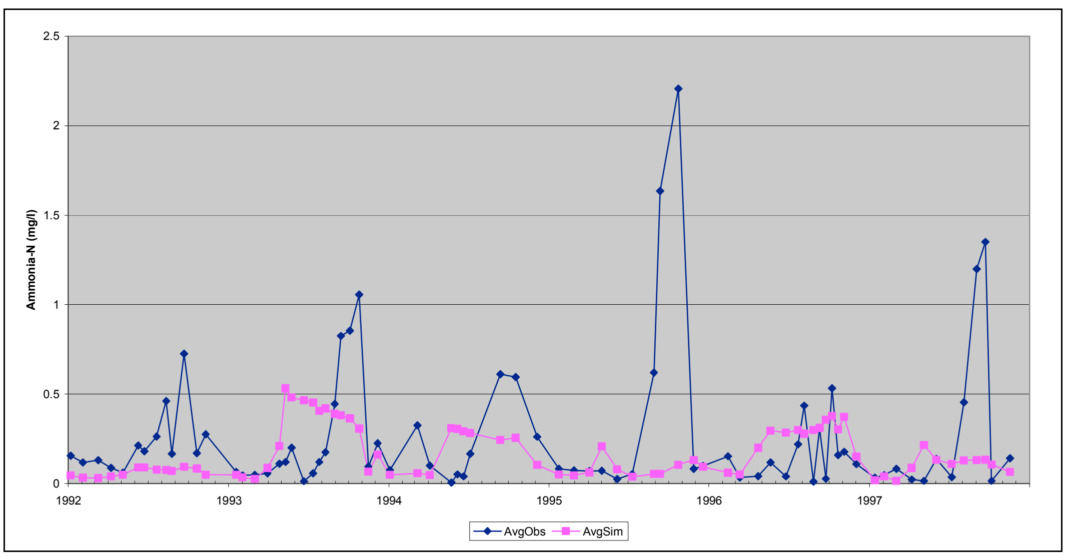

Figure 5.6.4-13. Observed and Simulated Average Surface Ammonia Concentrations, Lower Station, Calibration Scenario, Loch Raven Reservoir

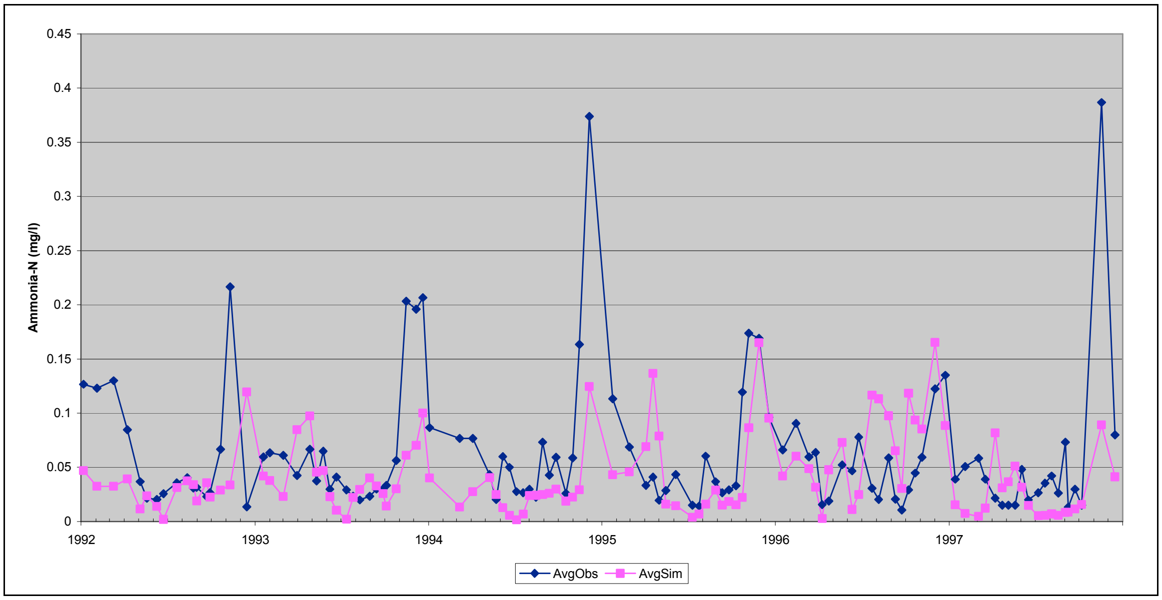

Figure 5.6.4-14. Observed and Simulated Average Bottom Ammonia Concentrations, Lower Station, Calibration Scenario, Loch Raven Reservoir

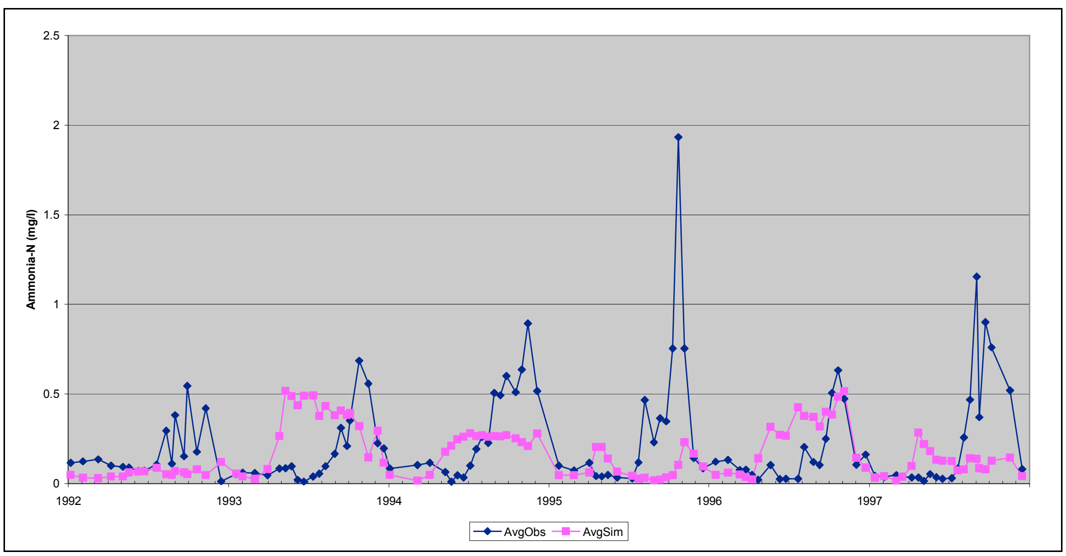

Figure 5.6.4-15. Observed and Simulated Average Surface Nitrate Concentrations, Upper Station, Calibration Scenario, Loch Raven Reservoir

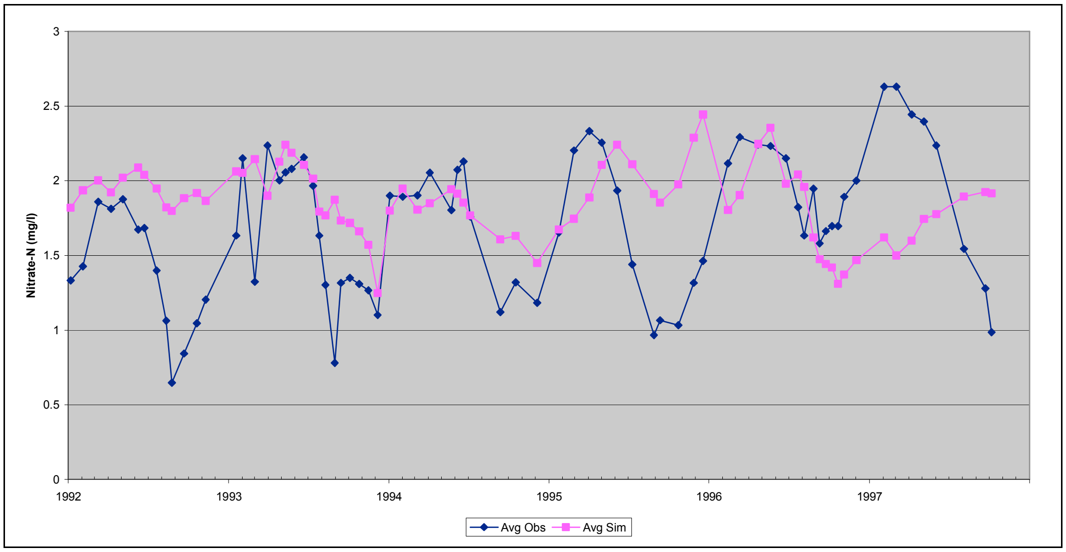

Figure 5.6.4-16. Observed and Simulated Average Bottom Nitrate Concentrations, Upper Station, Calibration Scenario, Loch Raven Reservoir.

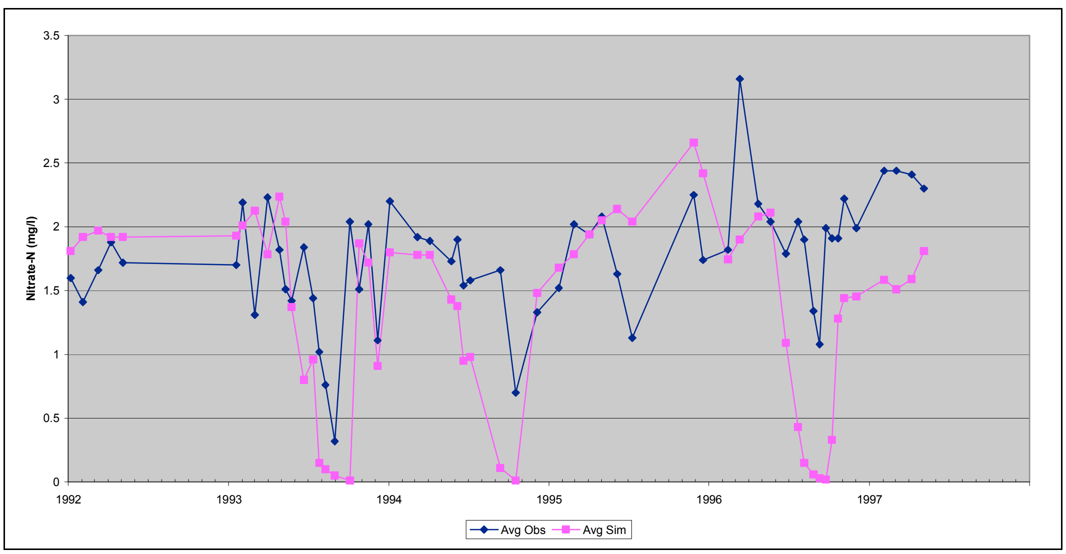

Figure 5.6.4-17. Observed and Simulated Average Surface Nitrate Concentrations, Middle Station, Calibration Scenario, Loch Raven Reservoir.

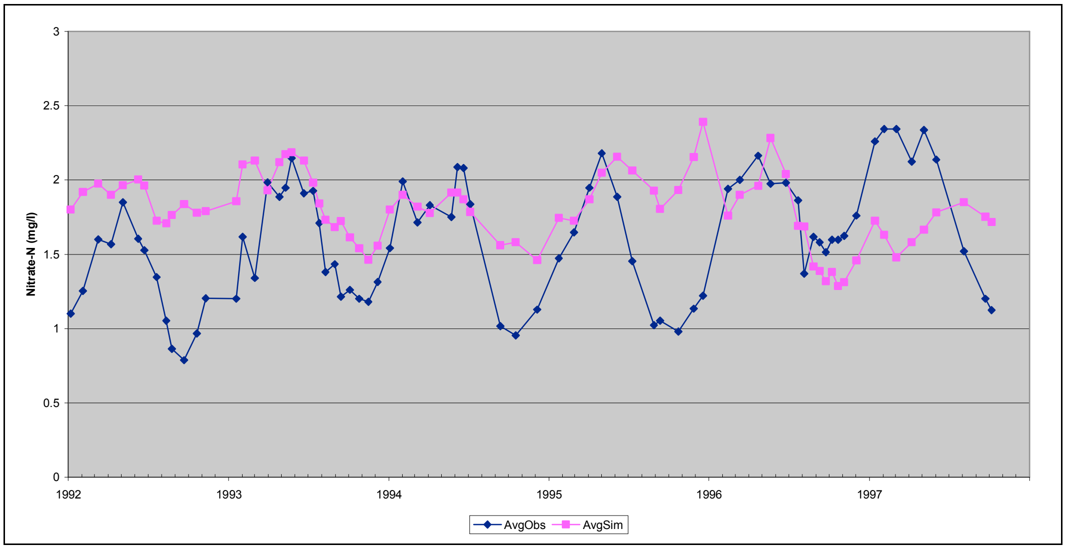

Figure 5.6.4-18. Observed and Simulated Average Bottom Nitrate Concentrations, Middle Station, Calibration Scenario, Loch Raven Reservoir

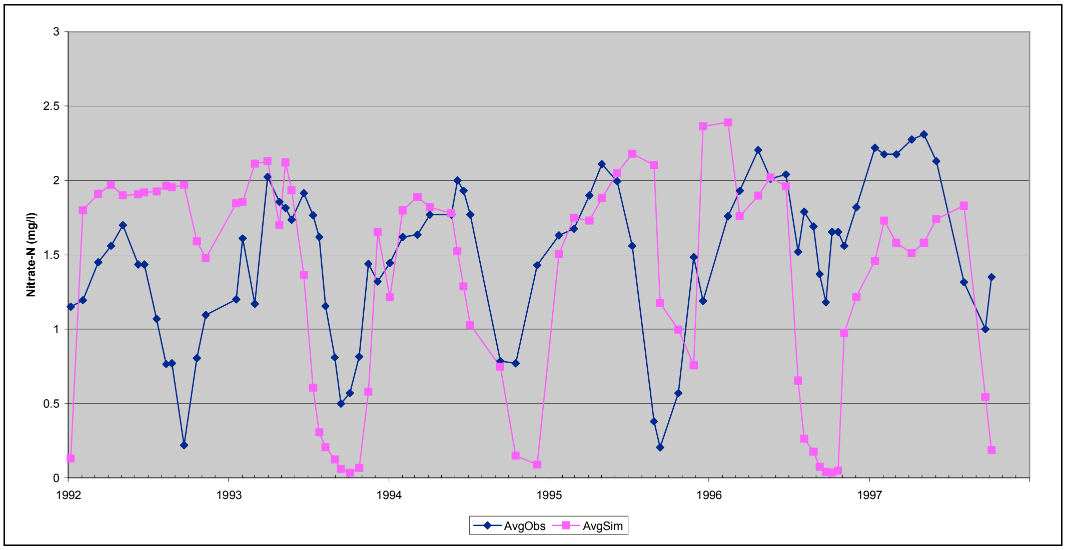

Figure 5.6.4-19. Observed and Simulated Average Surface Nitrate Concentrations, Lower Station, Calibration Scenario, Loch Raven Reservoir

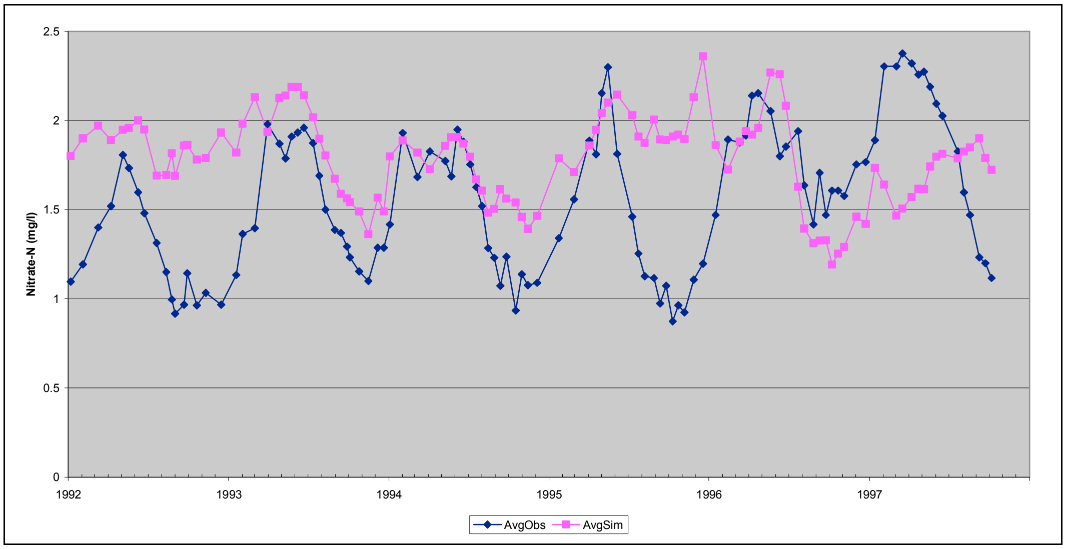

Figure 5.6.4-20. Observed and Simulated Average Bottom Nitrate Concentrations, Lower Station, Calibration Scenario, Loch Raven Reservoir

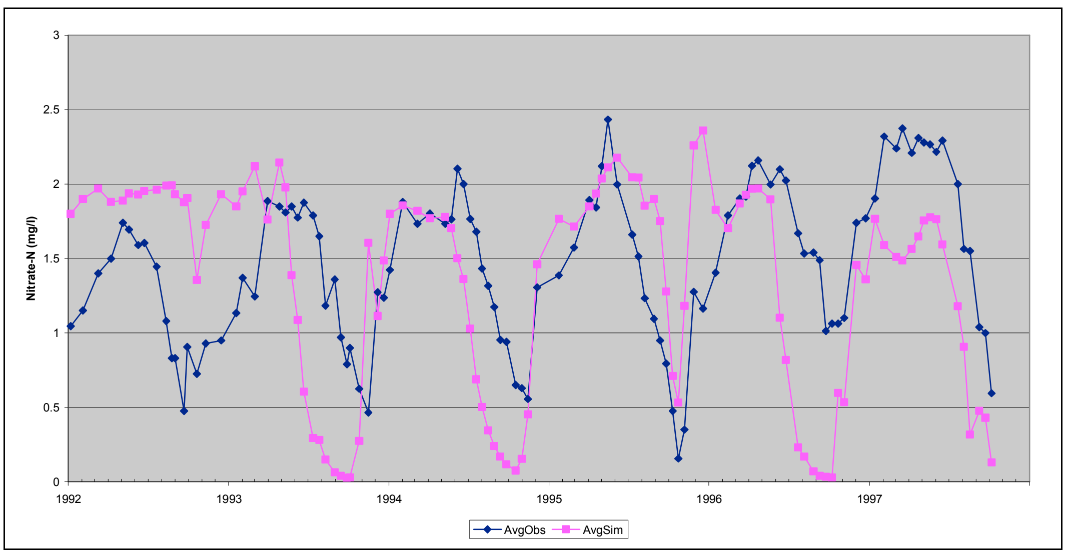

Section 6. LOAD REDUCTION SCENARIOS AND SENSITIVITY ANALYSIS

The primary purpose of the Gunpowder Falls modeling framework, including the W2 models of Prettyboy and Loch Raven Reservoirs, is to determine the maximum total phosphorus loads which allow the reservoirs to meet the TMDL endpoints for chlorophyll and dissolved oxygen described in section 5.1.1.

Using the calibrated reservoir models, phosphorus loads were reduced until a simulated load reduction achieved the desired TMDL endpoints. It was determined that a total phosphorus load reduction of 54% in Prettyboy Reservoir and 50% in Loch Raven Reservoir met the TMDL endpoints for chlorophyll. These TMDL Scenarios also met the dissolved oxygen endpoints in the well-mixed surface layer under stratified conditions; deviations from the endpoints only occurred when oxygen–poorer layers from the metalimnion were mixed into the surface layer. Hypoxia still occurred in the bottom layers even under reduced loading rates.

The interim DO criteria for reservoirs recognize that hypolimnetic hypoxia may be a natural condition determined by reservoir morphology and stratification. A scenario was developed which represented the loads that would occur if the watersheds draining to Perttyboy and Loch Raven Reservoirs were entirely forested. The All-Forest Scenario was used to test whether hypoxia would occur in the hypolimnion even under natural conditions. The scenario confirmed that hypoxia would occur even under all-forested conditions and that therefore, Prettyboy and Loch Raven Reservoirs would meet the interim DO criteria under the TMDL Scenarios.

The actual TMDLs for Prettyboy and Loch Raven Reservoirs, specified according to the provisions of the Clean Water Act, are described in the TMDL documentation (MDE, 2006). This chapter describes the TMDL Scenario and All-Forest Scenario in the context of model sensitivity analysis, after providing technical details on how the scenarios and other sensitivity analyses were implemented.

6.1. Scenario Descriptions

6.1.1. TMDL Scenario

The TMDL load reduction scenarios were taken equally across all species of phosphorus: dissolved phosphate, particulate organic and inorganic phosphorus, and the phosphorus in labile CBOD, dissolved labile organic matter.

6.1.2. All Forest Scenario

In the all-forest scenario, flows were taken from all land uses, but constituent EOS loads were determined as if all the land in each subwatershed was forested. The parameterization of all in-stream processes, including scour and phosphorus sorption dynamics, were taken from the calibration scenario. If the reservoir watersheds were truly all-forested, inflows to the reservoirs would be different, but different inflows would demand different outflows, and setting the outflows would require determining how the reservoirs would be operated under all-forested conditions. The All-Forest Scenario constructed here represents a controlled simulation experiment, in which only one set of factors, the loads of dissolved and labile particulate organic phosphorus, are changed from the Calibration Scenario. Under this scenario, all other factors, including reservoir stratification, remain unchanged, and are therefore comparable to the Calibration Scenario.

Sensitivity runs on the All-Forest Scenario were conducted by making an across-the-board cut in labile particulate organic phosphorus, which is the W2 state variable that represents particulate labile particulate organic matter.

6.1.3. Comparison of Scenario Loading Rates

Table 6.1-1 compares the loading rates of phosphorus species for the Calibration, TMDL, and All-Forest Scenarios. The Forest Scenario phosphorus loads are about half of the TMDL Scenario Loads, or in other words, the All-Forest Scenario represents about twice as great a reduction as the TMDL Scenario. Since the TMDL Scenario is an across-the-board reduction in TP (54% in Prettyboy and 50 % in Loch Raven) the relative fractions of each species in the TMDL Scenario is the same as the Calibration Scenario. The All-Forest Scenario has less PIP and more POP than the Calibration Scenario.

Table 6.1-1. Scenario Annual Phosphorus Load (lbs/yr) By Species and Forest Scenario Percent of Calibration Load

Phosphorus Species	Prettyboy Reservoir				Loch Raven Reservoir			
	Calibration	TMDL (46%)	Forest	Percent of Calibration	Calibration	TMDL (50%)	Forest	Percent of Calibration
DOP	3,520	1,619	1,108	31%	10,843	4,988	2,990	28%
DIP	13,458	6,191	2,235	17%	28,617	13,164	9,693	34%
PIP	12,266	5,642	892	7%	32,976	15,169	3,081	9%
POP	21,173	9,740	5,825	28%	37,759	17,369	15,572	41%
TP	50,417	23,192	10,060	20%	110,195	50,690	31,335	28%

6.2. Criteria Tests

Up to this point much of the evaluation of model performance focused on comparing simulated concentrations with their observed counterparts. In evaluating whether a scenario meets water quality standards, simulated concentrations must be evaluated everywhere in the reservoir in the reservoir where relevant, not just at the sampling locations and sampling depths. At their maximum surface water elevations, Prettyboy Reservoir contains 363 cells and Loch Raven Reservoir contains 274 cells. Advances in computer speed and memory has fortunately made processing the sheer amount of output to be evaluated a minor challenge. The primary challenge is determining, when applying the interim dissolved oxygen criteria, whether under stratified conditions a cell is the mixed surface layer.

6.2.1. Chlorophyll Tests

Each cell in the first 15 layers (15 meter depth) was tested to determine whether (1) the instantaneous concentration of chlorophyll was above 30 µg/l and (2) whether the 30-day moving average of the chlorophyll concentration was above 10 µg/l. Daily output was used to make the test. A cell's identify was fixed relative to the surface for the 30-day moving average. In other words, the average was made over the cell that was, for example six meters deep in segment four, even if a layer was added or subtracted during the 30-day period so that the cell's indices changed. Tracking cells relative to the surface better simulates how monitoring would actually be performed and can in many cases better track identify of the mass of material.

6.2.2. Dissolved Oxygen Tests

Determining whether the reservoirs meet the interim DO standards can be broken down into three steps. First, the DO concentrations in a cell must be checked to determine (1) if the concentration is below 5 mg/l and (2) if the daily average concentration is below 6 mg/l. If a cell fails either of these two conditions, it must be determined whether or not it is in the surface layer. If it fails either test and is in the surface layer it must be further determined whether or not it is impacted by the entrainment of low DO caused by the deepening of the surface layer or, as can also happen, the cell was itself previously below the well-mixed surface layer and has been recently mixed into the surface layer. Finally, it must be determined whether the low DO under stratified conditions is due primarily to constituent loads or is a naturally-occurring consequence of stratification and reservoir morphology.

The All-Forest Scenario and subsequent sensitivity analyses will demonstrate that hypoxia would occur even under the low constituent loading rates associated with an all-forested watershed. If the hypoxia in the reservoirs is a naturally-occurring condition, then the interim DO criteria would be violated if the all of the following conditions are met:

1. DO concentrations in a cell are below 5 mg/l or the daily average DO concentration is below 6 mg/l;
2. The cell is in the well-mixed surface layer or the reservoirs are unstratified; and
3. The low DO concentration in the cell is not explainable as a result the entrainment of low DO layers in the metalimnion such as occurs during the fall overturn.

To determine the instantaneous DO concentrations and daily average DO concentrations in a cell, DO concentrations for potential surface layer cells were output every tenth of a day. Each concentration was checked to determine whether it was below 5 mg/l. The ten concentrations in a calendar day were averaged to determine the daily average DO concentration for that day, which was checked against the 6 mg/l criterion.

6.2.2.1. Determination of the Position of the Surface Layer

The key difficulty is determining whether a cell is in the well-mixed surface layer. There are no agreed-upon numerical criteria for defining the boundaries of epilimnion, metalimnion, and hypolimnion. A temperature gradient of 1 ºC/m is often used as a rule-of-thumb to determine the location of the theormocline (Wetzel, 2005), but others reject that criteria (Hutchinson, 1967; Ford and Johnson, 1986). A glance at the Figure 5.1.3-1 or the temperature contours in Appendix C clearly show that temperature stratification regularly takes place in both Prettyboy and Loch Raven Reservoirs; it is difficult to determine a simple numerical criteria that captures the evident stratification. The temptation to paraphrase what one Supreme Court justice said in another context is strong: “I can’t define stratification but I know it when I see it.”

The following more-sophisticated procedure was used to determine the location of the surface layer on a daily basis:

1. A preliminary criterion is chosen which represents the temperature gradient that marks the boundary between the epilimnion and metalimnion.
2. On each day the average temperature in a layer was calculated for all model segments more than 15 meters deep.
3. The temperature difference between layers was calculated, starting from the surface layer. Since each layer except the surface layer is one meter thick, the temperature difference is easily translated into a temperature gradient.
4. Starting from the surface, the temperature differences are compared to the predetermined criterion. The bottom of the surface layer is the place where the temperature difference or gradient is larger than the criterion.

5. The location of the surface layer is checked for continuity. The reservoirs should be stratified between May and September. If there are days during that time when there was no temperature differences between layers greater than the criterion, then a smaller temperature gradient criterion was chosen and steps 3 and 4 were repeated.
6. Step 5 was repeated until there was continuous stratification from May into September.

The initial criterion chosen was the rule-of-thumb of 1 ºC/m. The final criterion used was 0.6 ºC/m. The average monthly temperature difference used to determine the surface layer remained approximately 1 ºC/m throughout the simulation. Table 6.2-1 and Table 6.2-2 show the monthly average of daily temperature difference used to determine the surface layer in Prettyboy and Loch Raven Reservoirs. The calculated surface layer is provisional in the following sense: Because it was calculated based on the average layer temperature in the deeper portion of the reservoir, it may not capture the stratification that occurs in the shallower segments, where the surface layer also tends to be less deep. Nevertheless, the identification of a daily location of the surface layer facilitated screening cells with low DO concentrations and there were only two cases in which a cell in the shallower segments with low DO was misclassified as a surface layer cell because the surface layer depth in the shallow segment was less than average depth over the reservoir.

Table 6.2-1 Monthly Average Daily Temperature Gradient (°C/m) Determining Relative Position of Epilimnion and Metalimnion in Prettyboy Reservoir

Year	May	June	July	August	September
1992	1.22	1.16	1.03	0.89	1.01
1993	1.30	1.18	1.30	0.98	1.25
1994	1.39	1.73	1.16	0.98	1.00
1995	0.99	1.21	1.15	0.91	0.92
1996	1.16	1.08	0.80	0.75	0.76
1997	0.86	1.37	1.21	0.88	0.83
Average	1.15	1.29	1.11	0.90	0.96

Table 6.2-2 Monthly Average Daily Temperature Gradient (°C/m) Determining Relative Position of Epilimnion and Metalimnion in Loch Raven Reservoir

Year	May	June	July	August	September
1992	1.04	1.10	1.04	0.90	0.81
1993	1.21	1.06	1.18	0.91	1.00
1994	1.08	1.32	1.13	0.98	0.74
1995	0.79	1.18	1.08	1.04	0.85
1996	1.12	1.15	1.14	0.82	0.82
1997	0.71	1.28	1.07	0.83	0.89
Average	0.99	1.18	1.11	0.91	0.85

Figures 6.2-1 and 6.2-2 show the position of the interface between epilimnion and metalimnion in Prettyboy and Loch Raven Reservoirs, May through September, for the simulation period. As the figures show, there is considerable fluctuation in the position of the layer. Fluctuations as much as five meters can occur in summer months.

Figure 6.2-1. Position of the Interface between Epilimnion and Metalimnion, Prettyboy Reservoir

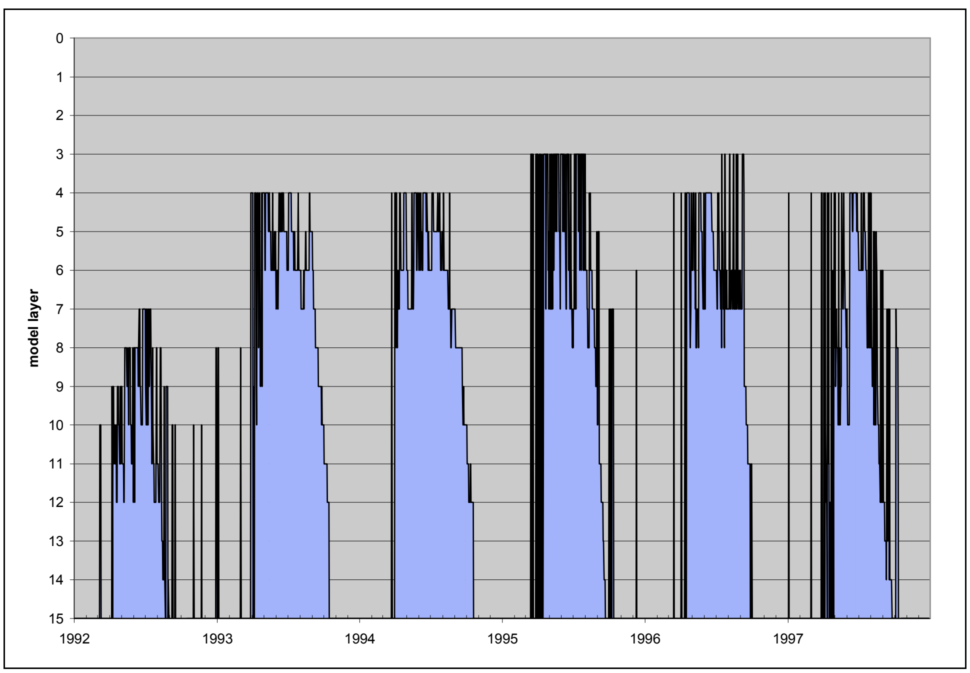

Figure 6.2-2. Position of the Interface Between Epilimnion and Metalimnion, Loch Raven Reservoir

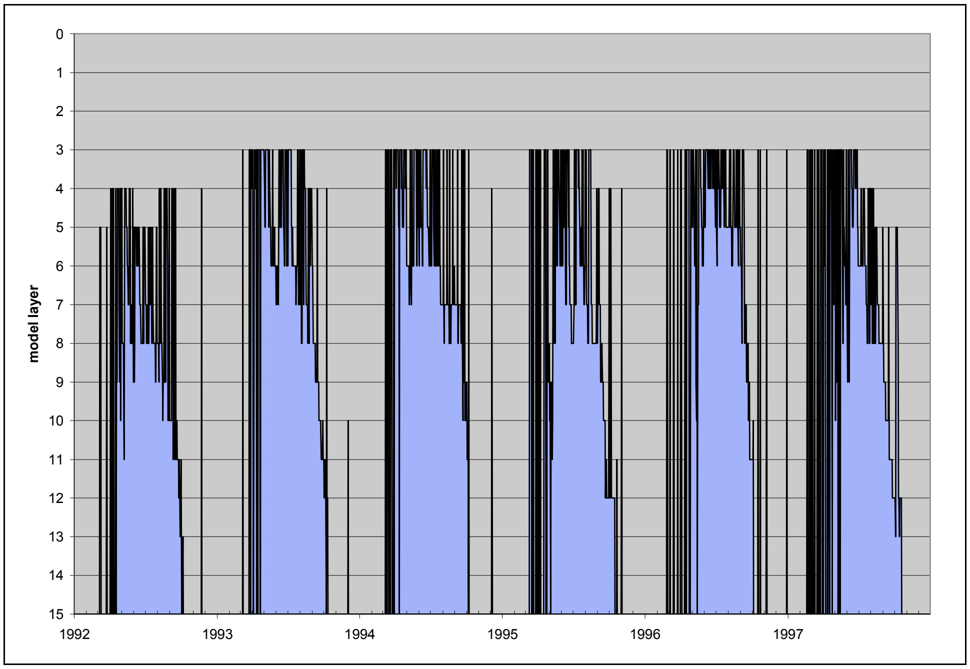

6.3. Response of Chlorophyll Concentrations to Reductions in Phosphorus Loads

As input loads to the reservoirs decrease, TP concentrations in the reservoirs decrease, although not linearly. Table 6.3-1 gives summary statistics for average surface TP concentrations in the reservoirs under the Calibration, TMDL, and All-Forest Scenarios.

The reservoir models are responsive to reductions in chlorophyll loads. Figures 6.3-1 and 6.3-2 show the maximum chlorophyll concentrations by sampling date in Prettyboy Reservoir and Loch Raven Reservoir under the TMDL Scenario and contrast them with the maximum observed concentrations and the maximum simulated concentrations under the Calibration Scenario. The total phosphorus load reduction is 54% in Prettyboy Reservoir and 50% in Loch Raven Reservoir under the TMDL Scenario.

Table 6.3-1. Scenario Summary Statistics for the Simulated Average Surface Concentrations (mg/l) of Total Phosphorus at Sampling Locations in Prettyboy and Loch Raven Reservoirs

Statistic	Prettyboy Reservoir			Loch Raven Reservoir		
	Calibration	TMDL	Forest	Calibration	TMDL	Forest
Minimum	0.022	0.011	0.008	0.025	0.01	0.006
1stQ	0.043	0.023	0.019	0.047	0.025	0.017
Median	0.054	0.029	0.024	0.055	0.029	0.021
3rdQ	0.067	0.034	0.028	0.063	0.035	0.025
Maximum	0.23	0.111	0.121	0.29	0.134	0.12
Average	0.057	0.03	0.025	0.058	0.031	0.025

Figures 6.3-3 and 6.3-4 show the daily maximum chlorophyll concentrations at sampling locations in Prettyboy Reservoir and Loch Raven Reservoir under the All-Forest Scenario and contrast them with the maximum concentrations under the Calibration Scenario and TMDL Scenario. Chlorophyll concentrations are minimal under the All-Forest Scenario. Lower primary productivity is a factor in the non-linear response of surface TP concentrations to input TP loads. For example, net algal uptake of DIP is approximately 30% of DIP input loads in winter and spring of 1992. This DIP leaves the surface when algae sink below the surface layer. As phosphorus concentrations decrease, algal growth is more limited and the net phosphorus uptake, as a percent of input loads, decreases.

Figure 6.3-1. Observed and Simulated Maximum Chlorophyll Concentrations by Date, TMDL Scenario, Prettyboy Reservoir

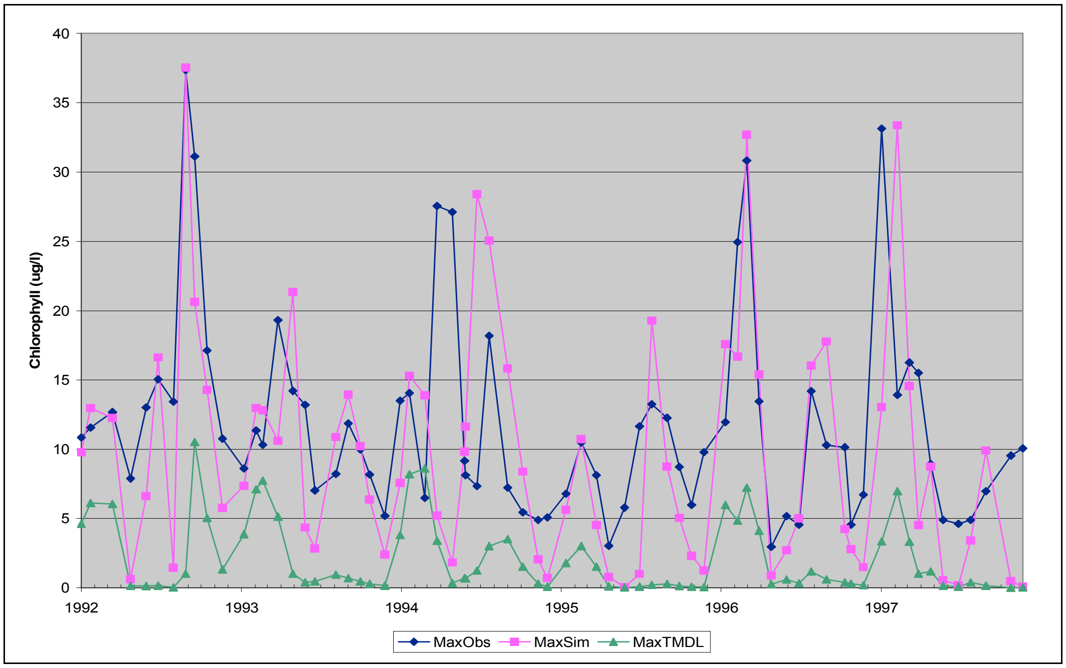

Figure 6.3-2. Observed and Simulated Maximum Chlorophyll Concentrations by Date, TMDL Scenario, Loch Raven Reservoir

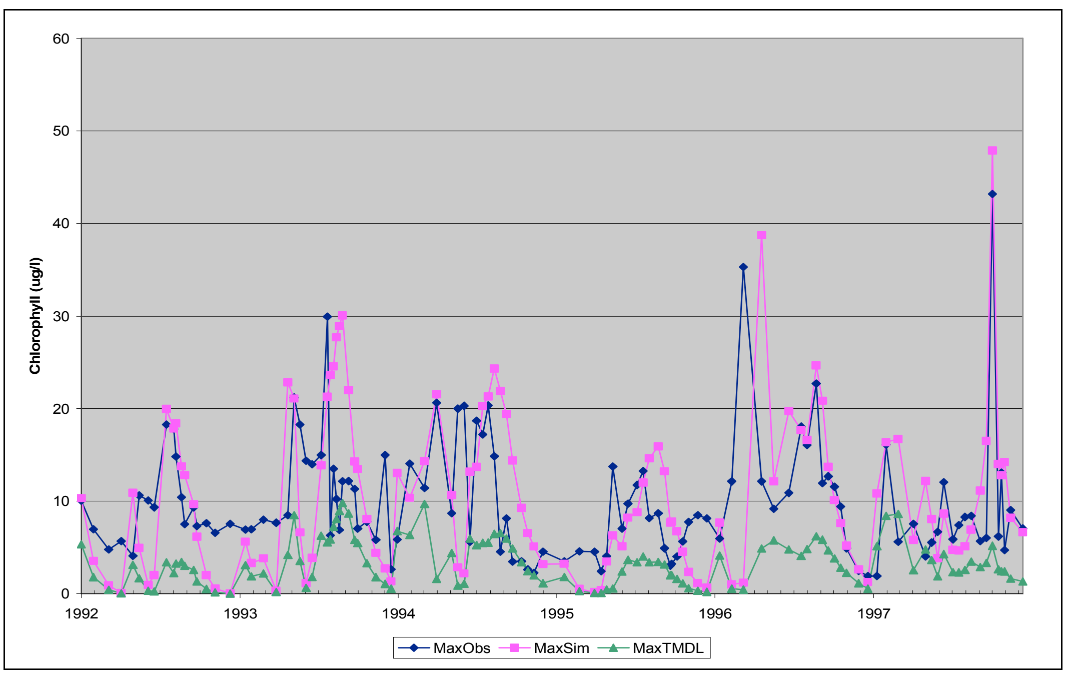

Figure 6.3-3. Simulated Maximum Chlorophyll Concentrations By Date, Calibration, TMDL, and Forest Scenarios, Prettyboy Reservoir

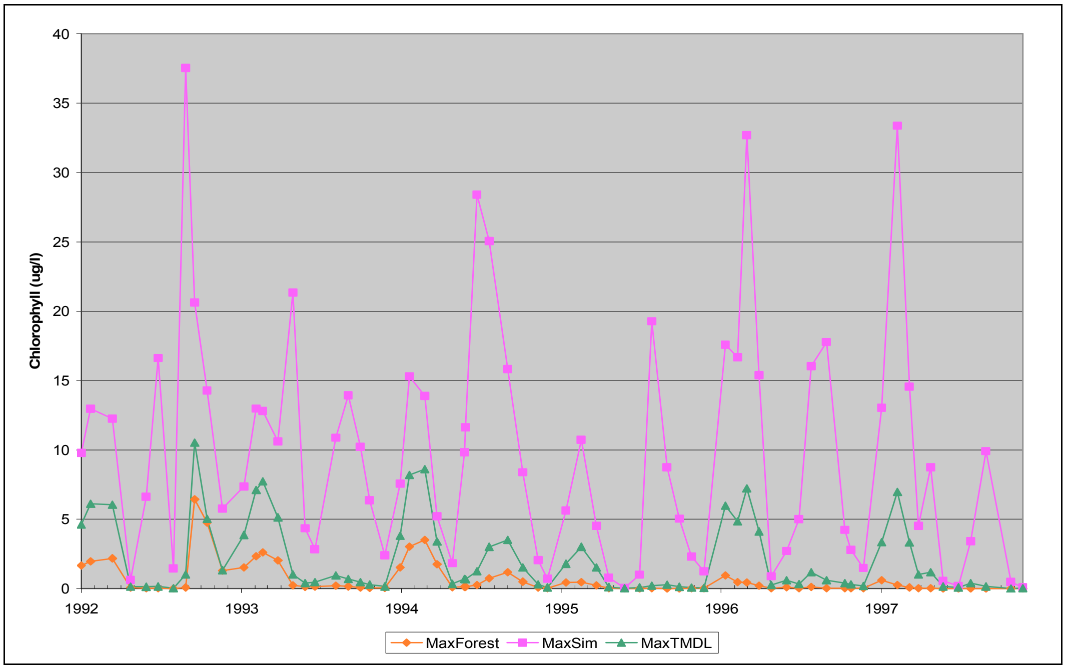

Figure 6.3-4. Simulated Maximum Chlorophyll Concentrations By Date, Calibration, TMDL, and Forest Scenarios, Loch Raven Reservoir.

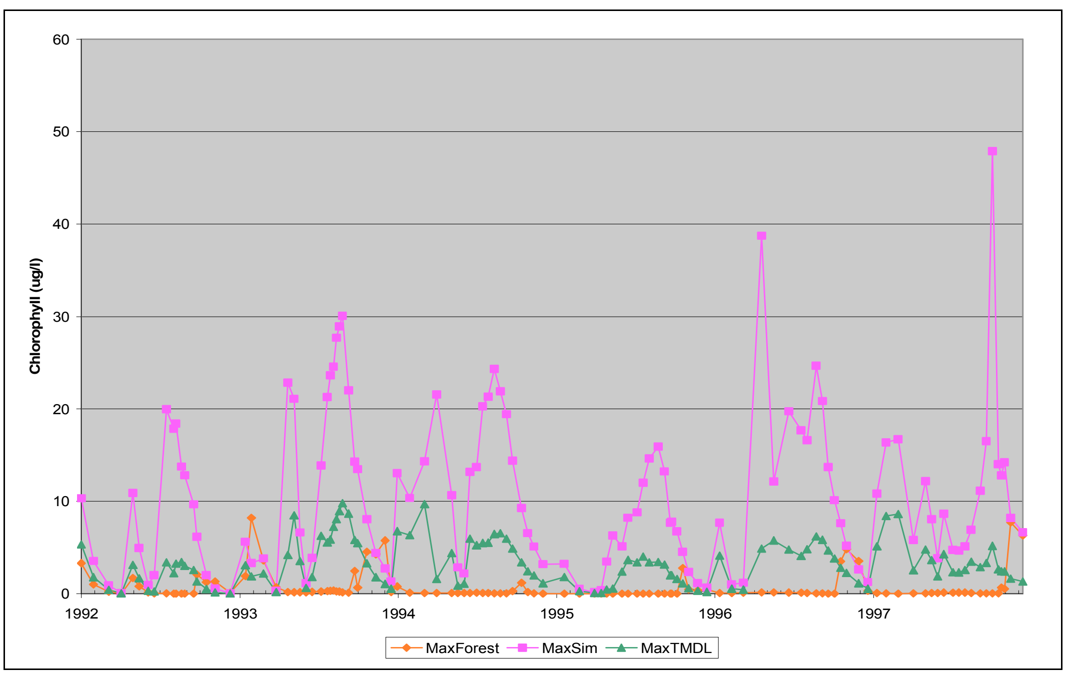

6.4. The Response of DO Concentrations to Load Reductions

Since the factors which determine DO concentrations in the surface layer and the bottom layer are different, and they are treated differently under the interim DO criteria, the simulated response of DO concentrations to load reductions will be discussed separately below.

6.4.1. The Response of Simulated Bottom DO Concentrations to Load Reductions

Figures 6.4-1 and 6.4-2 show the average bottom DO concentration for the Calibration Scenario and TMDL Scenario, at the middle and lower sampling locations in Prettyboy Reservoir. Figures 6.4-3 through 6.4-5 show the average bottom DO concentration for the Calibration Scenario and TMDL Scenario at the upper, middle, and lower sampling locations in Loch Raven Reservoir. The models respond to reductions in particulate organic phosphorus, but clearly do not meet the 5 mg/l DO criterion, even averaged over the bottom layers.

The All-Forest Scenario, as described in Section 6.1, was simulated to determine whether the source of the hypoxia in the hypolimnion is a natural consequence of stratification and would occur under the loading rates of an all-forested watershed. Figures 6.4-6 and 6.4-7 show the average bottom DO concentrations and the minimum DO concentrations for the All-Forest Scenario at the middle and lower sampling locations in Prettyboy Reservoir. Figures 6.4-8 through 6.4-10 show the average bottom DO concentrations and minimum DO concentrations for the All-Forest Scenario at the upper, middle, and lower sampling locations in Loch Raven Reservoir. In both reservoirs, average bottom DO concentrations improve significantly, but, as the plots of the minimum DO at the sampling locations show, hypoxia persists in both reservoirs in the summer of most of the years simulated. The hypoxia occurs primarily in the lowest depths of the segments of the reservoirs. At shallower depths within the hypolimnion the DO concentrations are greater, as demonstrated by the fact that average bottom DO concentrations are greater than the minimum concentrations. Generally, the hypoxia is more severe at the lower sampling stations at or just above the dams, but can occur in other portions of the reservoirs as well.

A sensitivity analysis was performed to reinforce the conclusion that hypoxia in the hypolimnion of both Prettyboy and Loch Raven Reservoirs is a natural condition due to thermal stratification. Given the low concentration of algal biomass in the All-Forest Scenario, the allochthonous sources of sediment oxygen demand, as represented by labile particulate organic phosphorus, are the primary cause of hypoxia in the hypolimnia of the reservoirs. The forest TP loading rates were based on available data, but some uncertainly may linger over (1) the fraction of phosphorus that is labile or (2) the oxygen equivalence of the organic material associated with organic phosphorus. These were calibrated in general but not specifically for forest loads. The loading rate of labile particulate phosphorus was reduced to 50%, 20%, and 10% of its value in the All-Forest Scenario in both reservoirs. Figure 6.4-11 shows the results, summarized as the percent of sampling dates under each sensitivity scenario in which the minimum DO concentration was less than 2 mg/l. The percent decreases with decreasing percentage of labile particulate phophorus in the Loch Raven Reservoir simulations, but remains around 15% even when loads are reduced to 10% of the original load in the All-Forest Scenario. In Prettyboy Reservoir, the percent of sampling dates with DO concentrations less than 2 mg/l remains above 25%. The All-Forest Scenario and the subsequent sensitivity analysis therefore demonstrate that hypoxia in the hypolimnion is a natural consequence of stratification.

Figure 6.4-1. Observed and Simulated Average Bottom DO Concentrations, Middle Station, TMDL Scenario, Prettyboy Reservoir

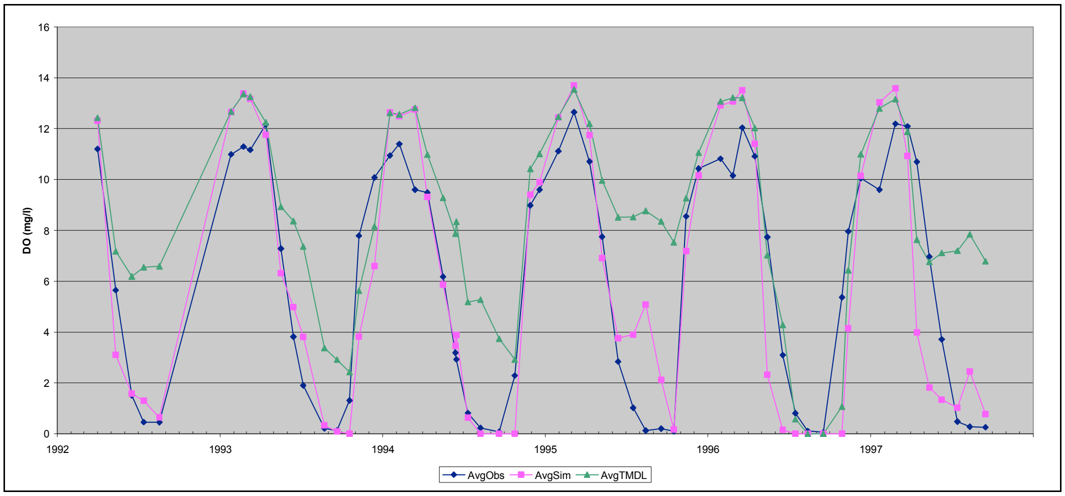

Figure 6.4-2. Observed and Simulated Average Bottom DO Concentrations, Lower Stations, TMDL Scenario, Prettyboy Reservoir

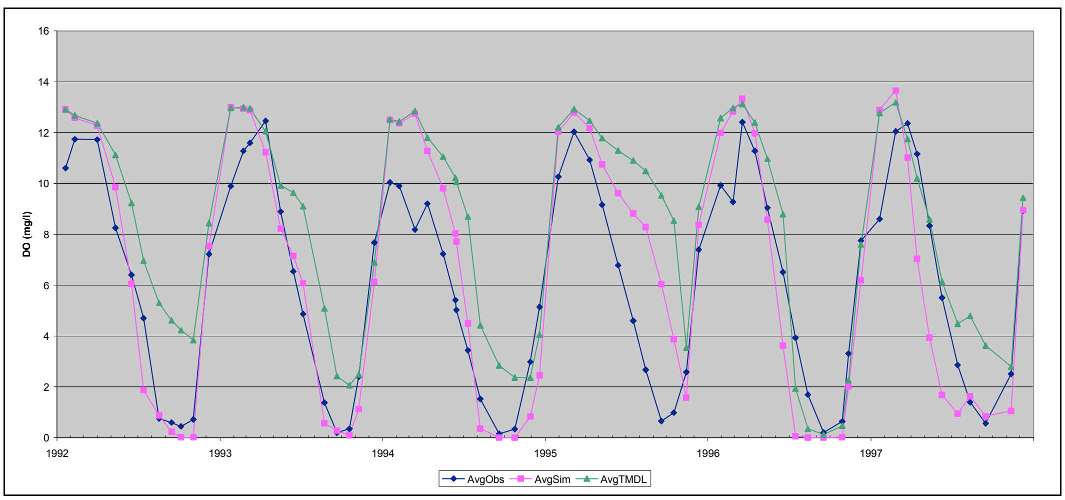

Figure 6.4-3. Observed and Simulated Average Bottom DO Concentrations, Upper Stations, TMDL Scenario, Loch Raven Reservoir

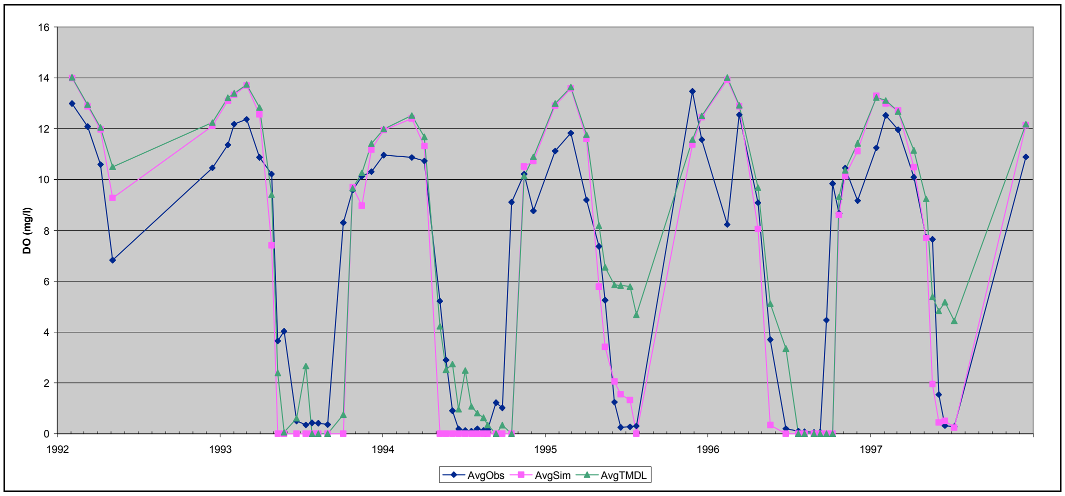

Figure 6.4-4. Observed and Simulated Average Bottom DO Concentrations, Middle Stations, TMDL Scenario, Loch Raven Reservoir

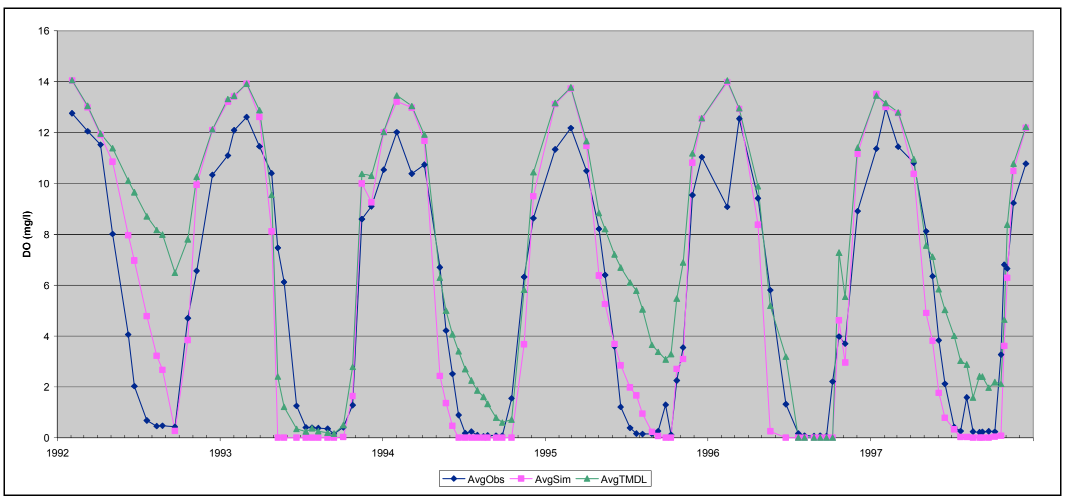

Figure 6.4-5. Observed and Simulated Average Bottom DO Concentrations, Lower Station, TMDL Scenario, Loch Raven Reservoir

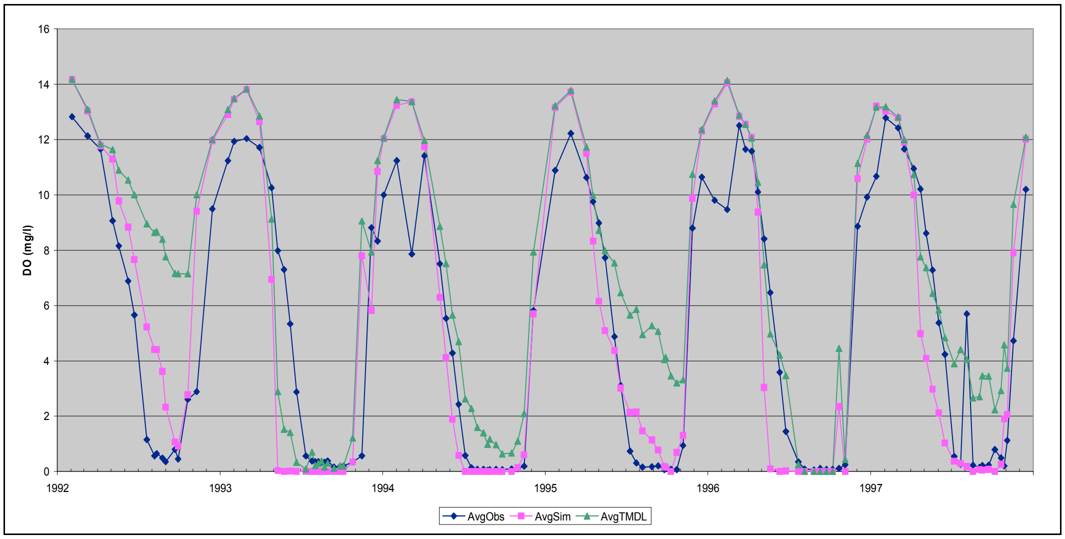

Figure 6.4-6. Observed and Simulated Average Bottom DO Concentrations, Middle Station, All-Forest Scenario, Prettyboy Reservoir

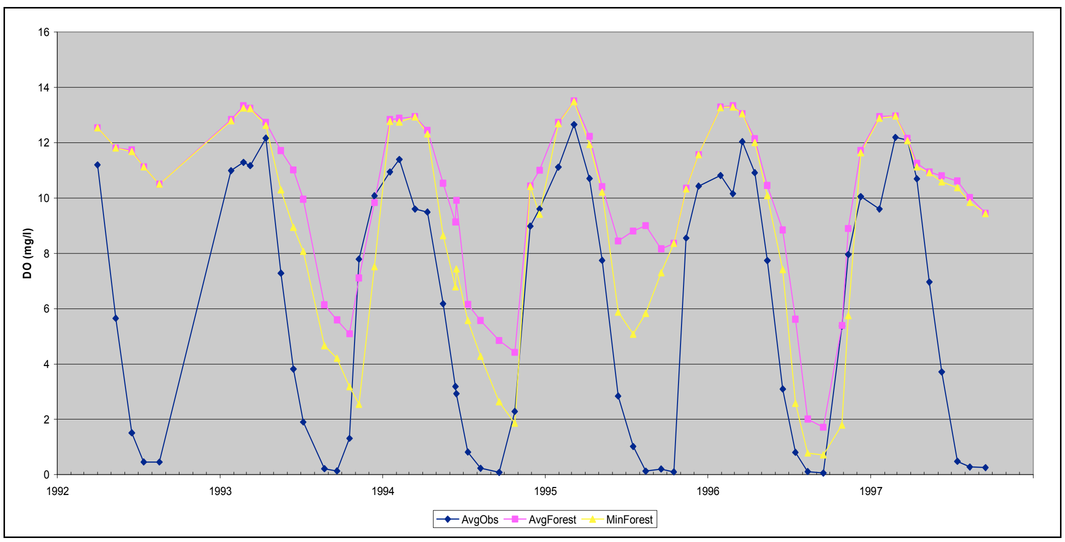

Figure 6.4-7. Observed and Simulated Average Bottom DO Concentrations, Lower Stations, All-Forest Scenario, Prettyboy Reservoir

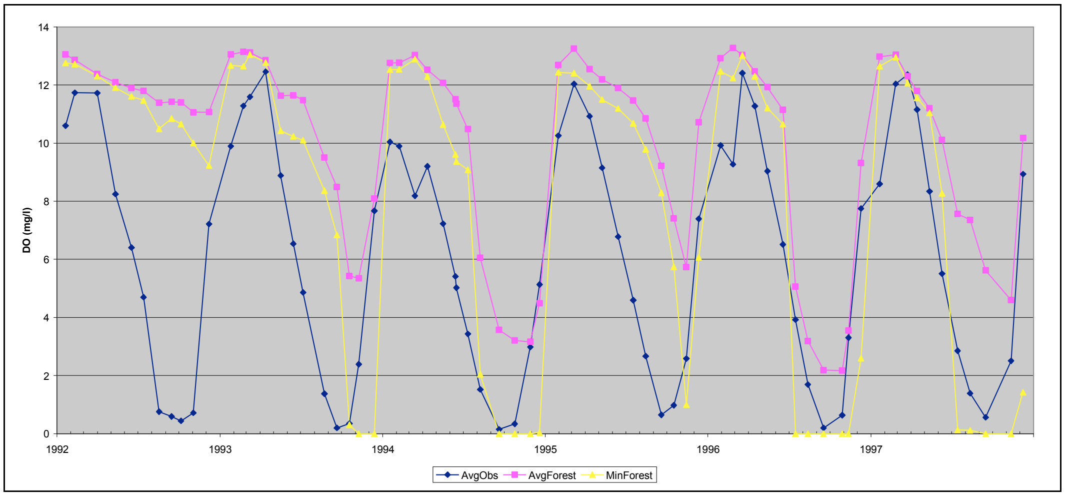

Figure 6.4-8. Observed and Simulated Average Bottom DO Concentrations, Upper Stations, All-Forest Scenario, Loch Raven Reservoir

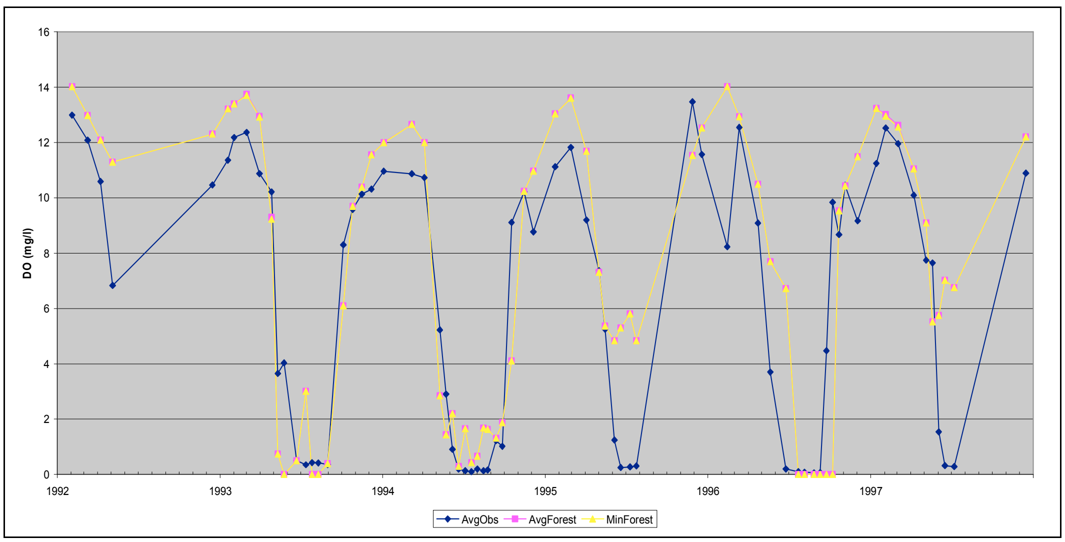

Figure 6.4-9. Observed and Simulated Average Bottom DO Concentrations, Middle Stations, All-Forest Scenario, Loch Raven Reservoir

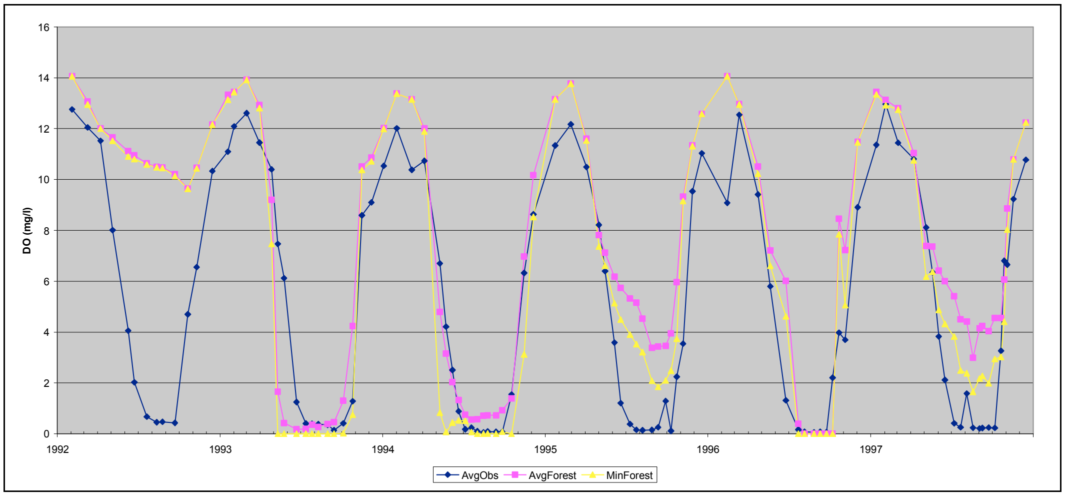

Figure 6.4-10. Observed and Simulated Average Bottom DO Concentrations, Lower Station, All-Forest Scenario, Loch Raven Reservoir

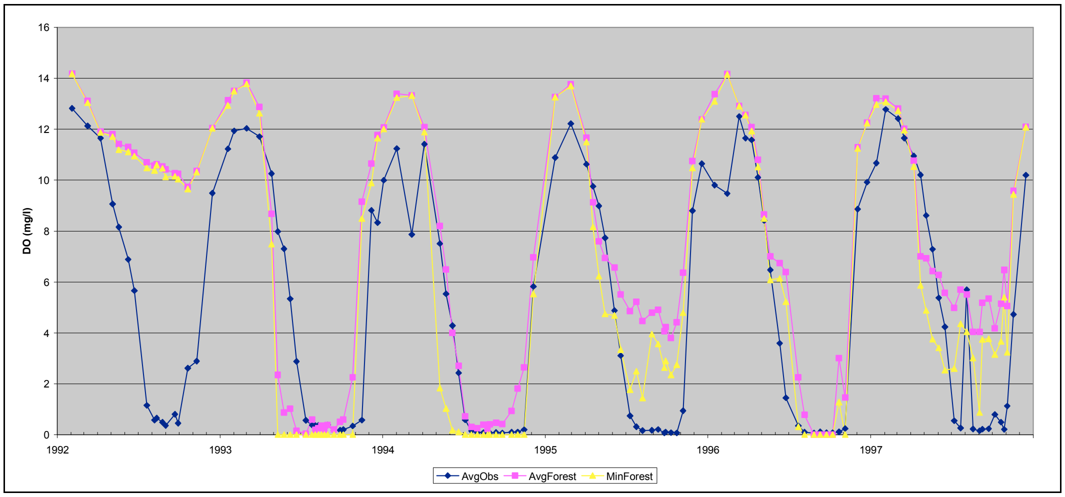

Figure 6.4-11. Percent of Sampling Dates on which DO < 2 mg/l at Sampling Locations as a function of Load Reductions from All-Forest Scenario

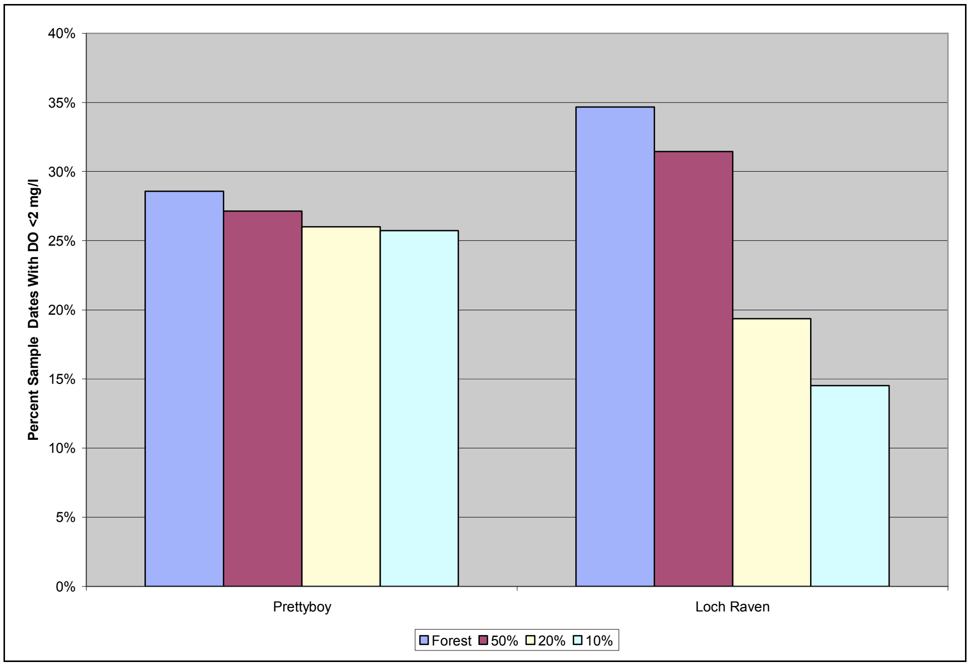

6.4.2. The Response of Simulated Surface DO Concentrations to Load Reductions

As discussed in Section 5.1.1, there is no evidence that DO concentrations fall below 5 mg/l in the surface layer except during periods of overturn or other fluctuations in the depth of the surface layer. Thus, there is no evidence that the instantaneous DO criterion of 5 mg/l is violated, provided that it can be shown that the low DO that occurs under stratification is a natural phenomenon. DPW does not collect multiple samples within a day and therefore does not provide the information necessary to evaluate whether the surface layer is maintaining a daily average DO concentration of 6 mg/l as specified for Use III waters.

Nonetheless, it is necessary to evaluate the simulation of DO in the TMDL Scenario to make sure that the scenario predicts that water quality standards for DO will be met under the TMDL loading rates. The procedures described in 6.2.2 were applied to the TMDL Scenario. All cells in the surface layers of Prettyboy and Loch Raven Reservoirs met both the 5 mg/l instantaneous DO criterion and the 6 mg/l daily average criterion with the following exceptions: (1) during the fall overturn in Prettyboy Reservoir in 1994 and

1996; (2) during the fall overturn in Loch Raven Reservoir in 1993, 1994, and 1996; and (3) on one day in Prettyboy Reservoir and three days in Loch Raven Reservoir when layers previously below the surface are entrained into the surface during fluctuations in the surface layers in the summer of 1996. Under the interim interpretation of DO criteria for stratified reservoirs, none of these cases counts as a violation of water quality standards for DO, because they are the effect of stratification-induced hypoxia in the layers below the surface.

In case of fluctuations in the surface layer in the summer of 1996, the concentration of DO in the newly incorporated layers, previously below the surface, do not immediately attain concentrations of 5 mg/l or a daily average of 6 mg/l within the same day that the surface layer deepens. Since the minimum depth of the surface layer at about two meters is attained in June, the fluctuations occurring throughout that summer can be considered part of a prolonged overturn that begins early with an unusually wet summer. It also must be admitted that surface DO is generally underpredicted in the summer of 1996 in both reservoirs, but particularly in Loch Raven, and that DO concentrations in the hypolimnion and metalimnion are underpredicted because SOD is probably oversimulated from material deposited during the January 1996 melt event. The underprediction of DO concentrations in the bottom layers makes it more difficult for layers entrained into the surface to quickly attain the surface DO concentration.

Figures 6.4-12 and 6.4-13 show the minimum surface DO concentration for the TMDL Scenario and All-Forest Scenario at the middle and lower sampling locations in Prettyboy Reservoir. In contrast to previous figures, the simulated daily average surface layer position was Figures 6.4-14 through 6.4-16 show the average surface DO concentration for the TMDL Scenario and All-Forest Scenario at the upper, middle, and lower sampling locations in Loch Raven Reservoir. There is little difference in minimum surface DO concentrations between the TMDL and All-Forest Scenarios. Loch Raven Reservoir show a minor increase in the minimum concentration during overturn, while in Prettyboy Reservoir, the TMDL Scenario has slightly higher DO in the summer and fall of 1996 than the All-Forest Scenario. This counterintuitive result is due to slight changes in stratification caused by lower sediment loads in the All-Forest Scenario, which facilitate the penetration of light and heat. The additional sensitivity simulations, in which labile particulate organic phosphorus was reduced to 50%, 20%, and 10% of its load in the All-Forest Scenario, confirm the insensitivity of simulated load reductions beyond the TMDL Scenario. Besides being relatively insensitive to load reductions beyond the TMDL Scenario, the simulation of surface DO is relatively insensitive to the choice of reaeration functions. Lowering the reaeration rate increases the number of cells with low DO concentrations in the surface layer, but does not induce any low DO concentrations which violate the interim DO standards.

Figure 6.4-12. Minimum DO Concentration at the Middle Sampling Location on Sampling Dates in the Simulated Surface Layer, Prettyboy Reservoir

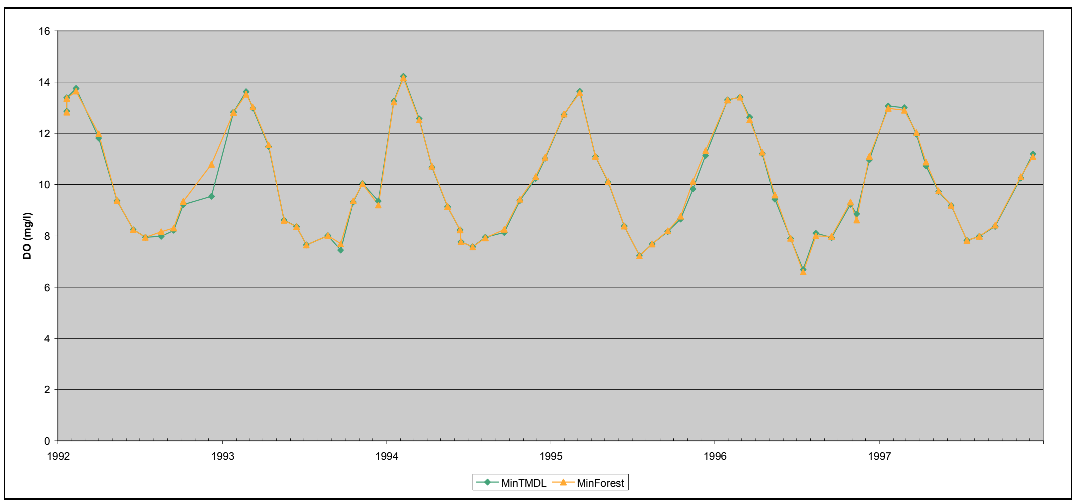

Figure 6.4-13. Minimum DO Concentration at the Lower Sampling Locations on Sampling Dates in the Simulated Surface Layer, Prettyboy Reservoir

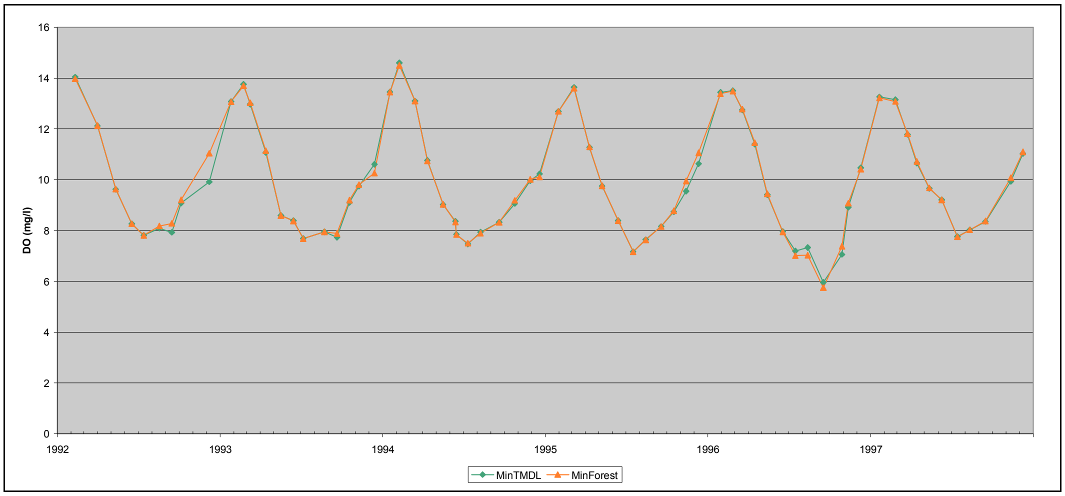

Figure 6.4-14. Minimum DO Concentration at the Upper Sampling Location on Sampling Dates in the Simulated Surface Layer, Loch Raven Reservoir

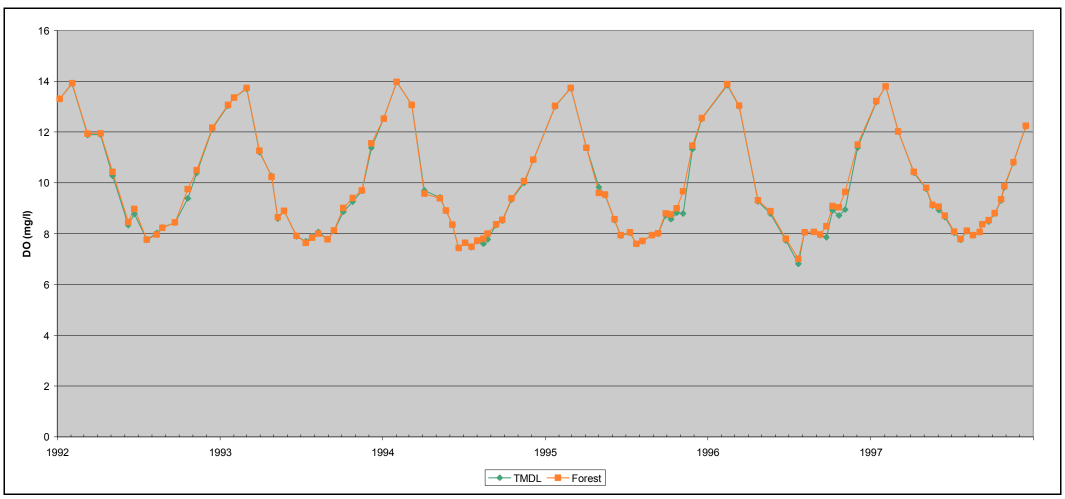

Figure 6.4-15. Minimum DO Concentration at the Middle Sampling Location on Sampling Dates in the Simulated Surface Layer, Loch Raven Reservoir

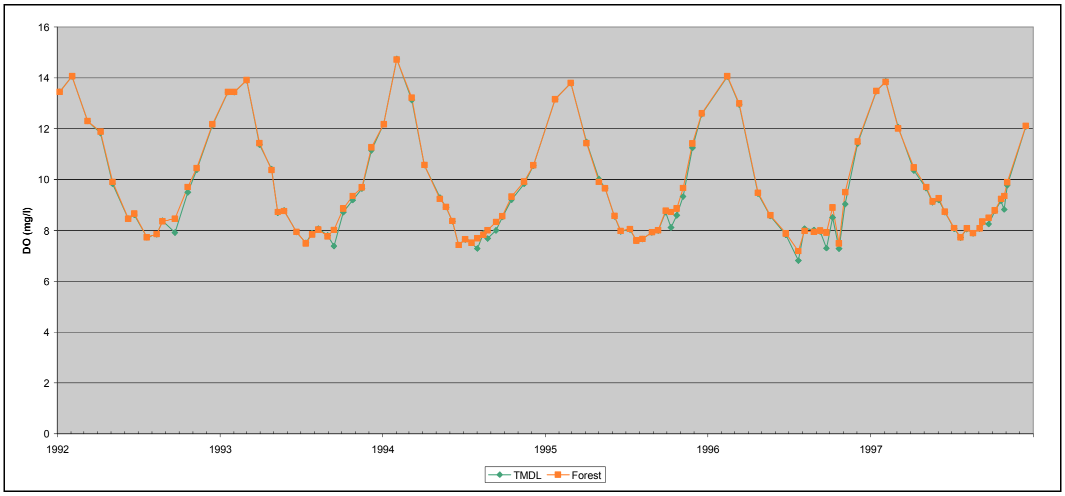

Figure 6.4-16. Minimum DO Concentration at the Lower Sampling Location on Sampling Dates in the Simulated Surface Layer, Loch Raven Reservoir

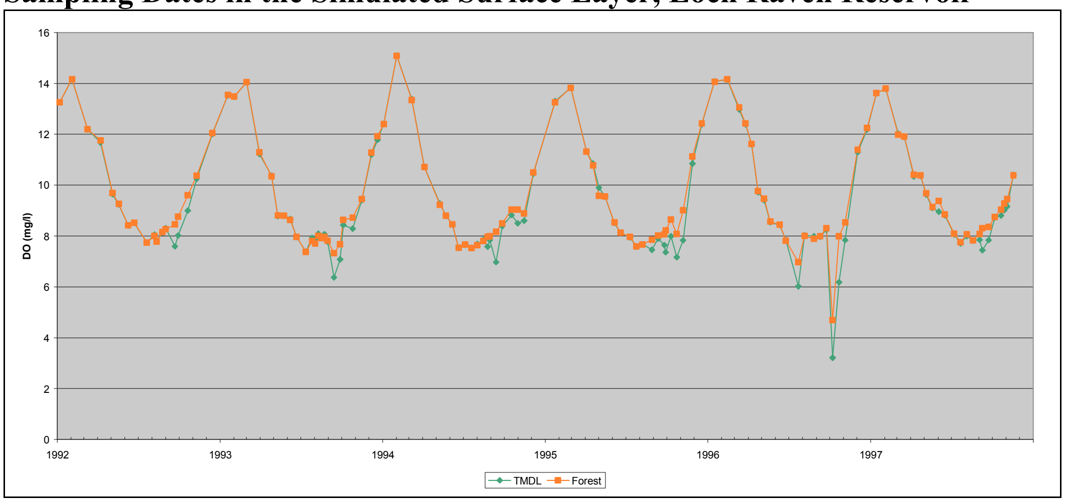

Section 7. CONCLUSIONS AND RECOMMENDATIONS

7.1. Summary and Conclusions

A modeling framework has been successfully developed to help establish TMDLs to address the nutrient impairments in Prettyboy and Loch Raven Reservoirs. The framework consists of an HSPF model of the Gunpowder Falls Watershed draining to the reservoirs and CE-QUAL-W2 models of each reservoir. The models have been successfully calibrated for the period 1992 to 1997. Load reduction scenarios have also been developed to determine the TMDLs and verify that the reservoirs meet water quality standards under the TMDLs.

The revised Gunpowder Falls HSPF Model updates the average annual loads of total phosphorus, sediment, ammonia, and nitrate entering Prettyboy and Loch Raven Reservoirs. Table 4.9-1 shows the average annual loads for these constituents. TP loads from agricultural sources account for over 80% of the load in Prettyboy Reservoir and over 50% of the load in Loch Raven Reservoir. TP loads from developed land, while accounting for less than 10% of the load in Prettyboy Reservoir, accounts for over 20% of the load in Loch Raven Reservoir.

The modeled loads incorporate available water quality monitoring data from 1985 to 2003 by establishing calibration targets with the help of the USGS's ESTIMATOR program. The model also incorporates information collected on animal populations, fertilizer usage, crop yields, and other aspects of agricultural practice specific to the Gunpowder Falls Watershed during the simulation period. The model uses statewide water quality monitoring data from the MS4 program to set calibration targets for developed land.

The CE-QUAL-W2 models successfully simulate the link between total phosphorus loads and algal growth. Each year of the simulation period is simulated individually. In each year, there are three seasonal algal groups. The models are calibrates such that (1) simulated peak chlorophyll *a* concentrations in an algal season as at least as large as the observed concentrations and (2) the distribution of simulated maximum chlorophyll **a** concentrations at sampling locations dominate the distribution of observed chlorophyll **a** concentrations. This calibration is conservative, in the sense that the simulated chlorophyll peaks are at least as large as their observed counterparts. Using the calibrated models, it was determined that, in order for the reservoirs to meet water quality standards, a 54% reduction in average annual total phosphorus load would be required in Prettyboy Reservoir and a 50% reduction would be required in Loch Raven Reservoir.

The models also demonstrate that under TMDL loading rates, both reservoirs would meet Maryland's interim interpretation of water quality standards for dissolved oxygen. In particular, the models were used to demonstrate that the hypolimnetic hypoxia observed in both reservoirs is a natural condition, a result of the degree of temperature stratification and morphology of the reservoirs. This was shown by simulating the water quality response of the reservoirs to the constituent loads that would occur if the reservoir watersheds were all-forested. Even under all-forested conditions, significant hypolimnetic hypoxia would still occur.

7.2. Recommendations

While the models are more than adequate to develop TMDLs for the reservoirs and determine whether they are meeting water quality standards, they could possibly be improved at a later date by: (1) the collection of additional monitoring data, and (2) the development of a more sophisticated model of the sediment diagenesis.

7.2.1. Additional Monitoring Data

There is no model which could not be improved if additional monitoring data were available, and these models are no exception. Additional water quality monitoring could reduce some of the uncertainty associated with constituent load and the reservoirs' response to those loads.

The following list indicates where existing tributary monitoring programs could be improved:

- Additional storm sampling on the tributaries to Prettyboy Reservoir;
- Additional CBOD, TOC, and COD monitoring in tributary storm samples; and
- Analysis of water quality samples for TKN, DIP, and other nutrient species in both the tributaries.

Baltimore County has initiated storm water monitoring in the Prettyboy Reservoir tributaries, but it will be several years before enough data is collected to provide meaningful load estimates. DEPRM (2000) expanded the range of constituents analyzed in the water quality monitoring program, but seems to have been discontinued. That study also collected data from smaller, more homogeneous watersheds, that, in sufficient quantity, coud be used to better calibrate loads from individual land uses.

From the modeling point-of-view, the reservoir monitoring program could be improved by analyzing samples for (1) DIP, (2) TKN, and (3) some measures of oxygen-demanding material and organic carbon, such as CBOD, TOC, or COD. The first is important for determining how much phosphorus is bioavailable, the second for better understanding the nitrogen cycle in the reservoirs, and the last for quantifying water column oxygen demand and potential contributors to sediment oxygen demand.

7.2.2. Enhancements to the Simulation of Sediment Diagenesis

The current sediment diagenesis component of the W2 model represents one state variable, organic matter in the sediments, with a single temperature-dependent decay rate that generates sediment oxygen demand. Ammonia and phosphorus releases are determined as a fraction of sediment oxygen demand. This model is indeed adequate to represent the link between deposited organic material, sediment oxygen demand, and hypoxia in the hypolimnia of the reservoirs. The rate and timing of sediment oxygen demand is reasonably represented in the model with the possible exception of 1996, where the January melt event causes the simulation of hypoxia to lead the observed concentrations.

The sediment diagenesis component of the W2 model could be improved by establishing a separate sediment state variable for different sources or types of organic material, each with their own decay rates and temperature adjustments. The ability to discriminate between different types of organic material in the sediment could help improve the timing of SOD in the face of large events like the 1996 event. The rate and timing of ammonia fluxes, which is a weakness of the current models, could then possibly be improved by determining a separate stoichiometric ratio for each type of organic material in the sediment.

Under the current monitoring program, a more sophisticated diagenesis model would outstrip available data. If the additional information described in Section 7.2.1 were collected, however, it might be possible to gain a better understanding of interactions between the sediment and the water column.

REFERENCES

Bahr, R. P. 1997. Maryland's National Pollutant Discharge Elimination System Municipal Stormwater Monitoring. Maryland Department of the Environment. Baltimore, MD.

Beaulac, M. N., and K. H. Reckhow. 1982. An Examination of Land Use—Nutrient Export Relationships. Water Resources Bulletin18. pp. 1013-1022.

Bicknell, B. R., Donigian, A. S., and Jobes, T.H. 1996. "Modeling Nitrogen Cycling and Export in Forested Watersheds Using HSPF." U.S. EPA, Athens, GA.

City of Baltimore Department of Public Works. 1981. The Story of Baltimore's Water Supply. Baltimore, MD.

City of Baltimore Department of Public Works.2005. Reservoir Water Quality Assessment for Loch Raven, Prettyboy, and Liberty Reservoirs. Interin Report. Baltimore, MD.

City of Baltimore Department of Public Works.1996. Reservoir Watershed Management Report. Volume I. Selected Graphics, Report Conclusions, and Discussion. In 1995 Action Report for The Reservoir Watersheds. Reservoir Watershed Protection Committee. Baltimore Metropolitan Council. Baltimore, MD.

Baltimore County Department of Environmental Protection and Resource Management. Gunpowder Watershed Study Monitoring Results. 2000.

Chiandani, G. and M. Vighi.1974. "The N:P Ratio and Tests with *Selanastrum* to Predict Eutrophication in Lakes," Water Research, Vol. 8, pp. 1063-1069.

Code of Maryland Regulations, 26.08.02.03, 26.08.02.08

Cole, T. M. and E. M. Buchak. 1995. CE-QUAL-W2: A Two-Dimensional Laterally Averaged, Hydrodynamic and Water Quality Model, Version 2.0. User Manual. Washington, DC. U.S. Army Corps of Engineers. Instruction Report EL-95-1.

Cole, T. M. and S. A. Wells. 2003. CE-QUAL-W2: A Two-Dimensional Laterally Averaged, Hydrodynamic and Water Quality Model, Version 3.2. User Manual. Washington, DC. U.S. Army Corps of Engineers. Instruction Report EL-03-1.

Cohn, T. A. , L. L. Delong, E. J. Gilroy, R. M. Hirsch, and D. Wells. 1989. Estimating Constituent Loads. Water Resources Research 28. pp.937-942.

Cohn, T. A., D. L. Caulder, E. J. Gilroy, L. D. Zynjuk, and R. M. Summers. 1992. The Validity of a Simple Log-linear Model for Estimating Fluvial Constituent Loads. Water Resources Research 28. pp. 2353-2364.

Donigian, A.S., Imhoff, J. C., and Bicknell, B. R.1983. "Modeling Water Quality and the Effects of Agricultural Best Management Practices in Four Mile Creek.", U.S. EPA, Athens, GA.

Edinger, J. E. and E. M. Buchak. 1975. A Hydrodynamic, Two-Dimensional Reservoir Model: The Computational Basis. U. S. Army Engineer Division, Ohio River. Cincinnati, OH.

Ford, D. E. and L. S. Johnson. 1986. An Assessment of Reservoir Mixing Processes. U. S. Army Corps of Engineers Waterways Experimental Station. Vicksburg, MS. Technical Report E-86-7.

Hutchinson, G. E. 1967. A Treatise on Limnology. 3 volumes. John Wiley and Sons. New York.

Langland, M.J., R. E. Edwards, L. A. Sprague, and S. E. Yochum, 2001. Summary of Trends and Status Analysis for Flow, Nutrients, and Sediments at Selected Nontidal Sites, Chesapeake Bay Basin, 1985-99: U.S. Geological Survey Open File Report 01-73.

Langland, M.J., S. W. Phillips, J. P. Raffensperger, and D. L. Moyer. 2005. Changes in streamflow and water quality in selected nontidal sites in the Chesapeake Bay Basin, 1985-2003: U.S. Geological Survey Scientific Investigations Report 2004-5259.

Leung , W. and R. Zou. 2000. Water Quality Modeling of the Loch Raven and Prettyboy Reservoirs. Department of Civil Engineering. University of Virginia. Charlottesville, VA.

Preston, S. D. 1990. "Estimation of Discharge, Runoff and Baseflow in Ungauged Basins of the Maryland Piedmont." Unpublished., Baltimore, MD.

Maryland Department of the Environment. 2005. Source Water Assessment for Loch Raven Reservoir Watershed. Baltimore, MD.

Matthews, E. D. 1969. Soil Survey of Carroll County, Maryland. Soil Conservation Service. Washington, DC.

Ortt, R. A. Jr., R. T. Kerhin, D. Wells and J. Cornwell. 2000. Bathymetric Survey and Sedimentation Analysis of Loch Raven and Prettyboy Reservoirs. Maryland Geological Survey. Coastal and Estuarine Geology File Report 99-4.

Reservoir Technical Group. Baltimore Reservoir Watershed Management Program. 2004. Reservoir Program Technical Report: Water Quality Assessment, Targeted Studies, and

Ongoing Water Quality Issues in the Baltimore Metropolitan Water Suppliy Reservoirs and Their Watersheds. Baltimore Metropolitan Council. Baltimore, MD.

Reybold, W. U. and E. D. Matthews. 1976. Soil Survey of Baltimore County, Maryland. Soil Conservation Service. Washington, DC.

Stack, W. P. and K. T. Belt.1989. The Selection of Appropriate Flow Averaging Periods in Evaluating Pollutant Loads Using the Flow Interval Method. Lake and Reservoir Mangagement 5.2: 67-73.

Tetra Tech. 1997. Water Quality Management Plan for Loch Raven Watershed. Fairfax, VA.

Walker, William, Jr. 1988. Evaluating Watershed Monitoring Programs. Concord, MA.

Walker, William, Jr. 1999. Simplified Procesures for Eutrophication Assessment and Prediction: User Manual. Instruction Report W-96-2. Waterways Experiment Station, U.S. Corps of Engineers. Washington, DC.

Weisberg, S. B. , K. A. Rose, B. S. Clevenger, and J. O. Smith. 1985. Inventory of Maryland Dams and Assessment of Hydropower Resources. Martin Marietta Environmental Systems. Columbia, Maryland.

LIST OF ABBREVIATIONS

BMP	Best Management Practice
BOD	Biological Oxygen Demand
CBOD	Carbonaceous Biochemical Oxygen Demand
CE-QUAL-W2	U.S. Army Corps of Engineers Water Quality and Hydrodynamic Model, Version 3
Chla	Active Chlorophyll *a*
COMAR	Code of Maryland Regulations
CWA	Clean Water Act
CWAP	Clean Water Action Plan
DEPRM	Baltimore County Department of Environmental Protection and Resource Management
DO	Dissolved Oxygen
DPW	Baltimore City Department of Public Works
EPA	Environmental Protection Agency
FSA	Farm Service Administration
HSPF	Hydrological Simulation Program Fortran
ICPRB	Interstate Commission on the Potomac River Basin
LA	Load Allocation
lbs/yr	Pounds per Year
MD	Maryland
MDA	Maryland Department of Agriculture
MDE	Maryland Department of the Environment
MDP	Maryland Department of Planning
MGS	Maryland Geological Survey
mg/l	Milligrams per Liter
MGD	Million Gallons per Day
MOS	Margin of Safety
MS4	Municipal Separate Storm Sewer System
NBOD	Nitrogenous Biochemical Oxygen Demand
NMP	Nutrient Management Plan
NOAA	National Oceanic and Atmospheric Administration
NPDES	National Pollutant Discharge Elimination System
NPS	Nonpoint Source
POM	Particulate Organic Matter
PO4	Phosphate
RTG	Reservoir Technical Group
SCWQP	Soil Conservation and Water Quality Plan

SOD	Sediment Oxygen Demand
TMDL	Total Maximum Daily Load
TN	Total Nitrogen
TP	Total Phosphorus
TSI	Trophic State Index
TSS	Total Suspended Solids
W2	CE-QUAL-W2
WLA	Wasteload Allocation
WQIA	Water Quality Improvement Act
WQLS	Water Quality Limited Segment
WWTP	Waste Water Treatment Plant
μg/l	Micrograms per Liter

APPENDIX A

Table A.1 Agricultural Land Use Classification

AGRICULTURAL LAND USE CLASSIFICATION		
1997	**ADJUSTED_CENSUS_CTIC**	**HSPF Watershed Model**
1997 CENSUS CATEGORY	**CROP_CATG AND SEASONAL ROTATIONS**	**CROP_Category**
BARLEY_GRAIN	NO-TILL BARLEY_GRAIN	DOUBLE CROP
BARLEY_GRAIN	FLSD RIDGE-TILL BARLEY	DOUBLE CROP
BARLEY_GRAIN	FLSD MULCH-TILL BARLEY	DOUBLE CROP
BARLEY_GRAIN	15-30% RESIDUE TO FLSD BARLEY	DOUBLE CROP
BARLEY_GRAIN	<15% RESIDUE TO FLSD BARLEY	DOUBLE CROP
OATS_GRAIN	NO-TILL OATS_GRAIN	DOUBLE CROP
OATS_GRAIN	SPSD RIDGE-TILL OATS	DOUBLE CROP
OATS_GRAIN	SPSD MULCH-TILL OATS	DOUBLE CROP
OATS_GRAIN	15-30% RESIDUE TO SPSD OATS	DOUBLE CROP
OATS_GRAIN	<15% RESIDUE TO SPSD OATS	DOUBLE CROP
RYE_GRAIN	NO-TILL RYE_GRAIN	DOUBLE CROP
RYE_GRAIN	FLSD RIDGE-TILL RYE	DOUBLE CROP
RYE_GRAIN	FLSD MULCH-TILL RYE	DOUBLE CROP
RYE_GRAIN	15-30% RESIDUE TO FLSD RYE	DOUBLE CROP
RYE_GRAIN	<15% RESIDUE TO FLSD RYE	DOUBLE CROP
SOYBEANS_BEANS	DC WHEAT TO RIDGE-TILL SOYBEANS	DOUBLE CROP
SOYBEANS_BEANS	DC WHEAT TO MULCH-TILL SOYBEANS	DOUBLE CROP
SOYBEANS_BEANS	DC BARLEY TO RIDGE-TILL SOYBEANS	DOUBLE CROP
SOYBEANS_BEANS	DC BARLEY TO MULCH-TILL SOYBEANS	DOUBLE CROP
SOYBEANS_BEANS	DC RYE TO RIDGE-TILL SOYBEANS	DOUBLE CROP
SOYBEANS_BEANS	DC RYE TO MULCH-TILL SOYBEANS	DOUBLE CROP
WHEAT_GRAIN	NO-TILL WHEAT_GRAIN	DOUBLE CROP
WHEAT_GRAIN	FLSD RIDGE-TILL WHEAT	DOUBLE CROP
WHEAT_GRAIN	FLSD MULCH-TILL WHEAT	DOUBLE CROP
WHEAT_GRAIN	15-30% RESIDUE TO FLSD WHEAT	DOUBLE CROP
WHEAT_GRAIN	<15% RESIDUE TO FLSD WHEAT	DOUBLE CROP
SOYBEANS_BEANS	NO-TILL SOYBEANS_BEANS	FULL SEASON BEANS
SOYBEANS_BEANS	FS RIDGE-TILL SOYBEANS	FULL SEASON BEANS
SOYBEANS_BEANS	FS MULCH-TILL SOYBEANS	FULL SEASON BEANS
SOYBEANS_BEANS	15-30% RESIDUE TO FS SOYBEANS	FULL SEASON BEANS
SOYBEANS_BEANS	<15% RESIDUE TO FS SOYBEANS	FULL SEASON BEANS
SOYBEANS_BEANS	NO-TILL SOYBEANS_BEANS	FULL SEASON BEANS
SOYBEANS_BEANS	15-30% RESIDUE TO DC SOYBEANS	FULL SEASON BEANS
SOYBEANS_BEANS	<15% RESIDUE TO DC SOYBEANS	FULL SEASON BEANS
SOYBEANS_BEANS	NO-TILL DC BARLEY TO NO-TILL SOYBEANS	FULL SEASON BEANS
SOYBEANS_BEANS	15-30% RESIDUE TO DC SOYBEANS	FULL SEASON BEANS
SOYBEANS_BEANS	<15% RESIDUE TO DC SOYBEANS	FULL SEASON BEANS
SOYBEANS_BEANS	NO-TILL DC RYE TO NO-TILL SOYBEANS	FULL SEASON BEANS

SOYBEANS_BEANS	15-30% RESIDUE TO DC SOYBEANS	FULL SEASON BEANS
SOYBEANS_BEANS	<15% RESIDUE TO DC SOYBEANS	FULL SEASON BEANS
ALFALFA_HAY	NO-TILL ALFALFA_HAY	HAY
ALFALFA_HAY	RIDGE-TILL ALFALFA	HAY
ALFALFA_HAY	MULCH-TILL ALFALFA	HAY
ALFALFA_HAY	15-30% RESIDUE TO ALFALFA	HAY
ALFALFA_HAY	<15% RESIDUE TO ALFALFA	HAY
GRASS_HAYLAGE	RIDGE-TILL GRASS HAYLAGE	HAY
GRASS_HAYLAGE	MULCH-TILL GRASS HAYLAGE	HAY
GRASS_HAYLAGE	15-30% RESIDUE TO GRASS HAYLAGE	HAY
GRASS_HAYLAGE	<15% RESIDUE TO GRASS HAYLAGE	HAY
GRASS_HAYLAGE	NO-TILL GRASS_HAYLAGE	HAY
SMALL_GRAIN_HAY	NO-TILL SMALL_GRAIN_HAY	HAY
SMALL_GRAIN_HAY	RIDGE-TILL SMALL GRAIN HAY	HAY
SMALL_GRAIN_HAY	MULCH-TILL SMALL GRAIN HAY	HAY
SMALL_GRAIN_HAY	15-30% RESIDUE TO SMALL GRAIN HAY	HAY
SMALL_GRAIN_HAY	<15% RESIDUE TO SMALL GRAIN HAY	HAY
SOD	SOD	HAY
SOD	SOD	HAY
SOD	SOD	HAY
SOD	SOD	HAY
SOD	NO-TILL SOD	HAY
SORGHUM_SILAGE	NO-TILL SORGHUM_SILAGE	HAY
SORGHUM_SILAGE	FS RIDGE-TILL SORGHUM	HAY
SORGHUM_SILAGE	FS MULCH-TILL SORGHUM	HAY
SORGHUM_SILAGE	15-30% RESIDUE TO FS SORGHUM	HAY
SORGHUM_SILAGE	<15% RESIDUE TO FS SORGHUM	HAY
TAME_HAY	RIDGE-TILL TAME HAY	HAY
TAME_HAY	MULCH-TILL TAME HAY	HAY
TAME_HAY	15-30% RESIDUE TO TAME HAY	HAY
TAME_HAY	<15% RESIDUE TO TAME HAY	HAY
TAME_HAY	NO-TILL TAME_HAY	HAY
TIMOTHY_SEED	RIDGE-TILL TIMOTHY	HAY
TIMOTHY_SEED	MULCH-TILL TIMOTHY	HAY
TIMOTHY_SEED	15-30% RESIDUE TO TIMOTHY	HAY
TIMOTHY_SEED	<15% RESIDUE TO TIMOTHY	HAY
TIMOTHY_SEED	NO-TILL TIMOTHY_SEED	HAY
WILD_HAY	RIDGE-TILL WILD HAY	HAY
WILD_HAY	MULCH-TILL WILD HAY	HAY
WILD_HAY	15-30% RESIDUE TO WILD HAY	HAY
WILD_HAY	<15% RESIDUE TO WILD HAY	HAY
WILD_HAY	NO-TILL WILD_HAY	HAY
CORN_GRAIN	15-30% RESIDUE TO FS CORN_GRAIN	HI-TILL CORN
CORN_GRAIN	<15% RESIDUE TO FS CORN_GRAIN	HI-TILL CORN
CORN_GRAIN	15-30% RESIDUE TO DC CORN_GRAIN	HI-TILL CORN
CORN_GRAIN	<30% RESIDUE TO DC CORN_GRAIN	HI-TILL CORN
CORN_SILAGE	15-30% RESIDUE TO FS CORN_SILAGE	HI-TILL CORN
CORN_SILAGE	<15% RESIDUE TO FS CORN_SILAGE	HI-TILL CORN

CORN_SILAGE	15-30% RESIDUE TO DC CORN_SILAGE	HI-TILL CORN
CORN_SILAGE	<15% RESIDUE TO DC CORN_SILAGE	HI-TILL CORN
CORN_GRAIN	NO-TILL CORN_GRAIN	LO-TILL CORN
CORN_GRAIN	FS RIDGE-TILL CORN_GRAIN	LO-TILL CORN
CORN_GRAIN	FS MULCH-TILL CORN_GRAIN	LO-TILL CORN
CORN_GRAIN	NO-TILL CORN_GRAIN	LO-TILL CORN
CORN_GRAIN	DC RIDGE-TILL CORN_GRAIN	LO-TILL CORN
CORN_GRAIN	DC MULCH-TILL CORN_GRAIN	LO-TILL CORN
CORN_SILAGE	NO-TILL CORN_SILAGE	LO-TILL CORN
CORN_SILAGE	FS RIDGE-TILL CORN_SILAGE	LO-TILL CORN
CORN_SILAGE	FS MULCH-TILL CORN_SILAGE	LO-TILL CORN
CORN_SILAGE	NO-TILL CORN_SILAGE	LO-TILL CORN
CORN_SILAGE	DC RIDGE-TILL CORN_SILAGE	LO-TILL CORN
CORN_SILAGE	DC MULCH-TILL CORN_SILAGE	LO-TILL CORN
CONSERVATION RESERVE PROGRAM	CONSERVATION RESERVE PROGRAM	PASTURE
COVER_CROP_ACREAGE	COVER_CROP_ACREAGE	PASTURE
FAILED_CROP_ACREAGE	FAILED_CROP_ACREAGE	PASTURE
IDLELAND	IDLELAND	PASTURE
PASTURE_ET_RANGELAND	PASTURE_ET_RANGELAND	PASTURE
PASTURE_OR_GRAZING	RIDGE-TILL NEW PERMANENT PASTURE	PASTURE
PASTURE_OR_GRAZING	MULCH-TILL NEW PERMANENT PASTURE	PASTURE
PASTURE_OR_GRAZING	15-30% RESIDUE TO NEW PERMANENT PASTURE	PASTURE
PASTURE_OR_GRAZING	<15% RESIDUE TO NEW PERMANENT PAST	PASTURE
PASTURE_OR_GRAZING	NO-TILL PASTURE_OR_GRAZING	PASTURE
SUMMER_FALLOW_ACREAGE	SUMMER_FALLOWED_ACREAGE	PASTURE
APPLES	RIDGE_TILL APPLES	VEGETABLES
APPLES	MULCH_TILL APPLES	VEGETABLES
APPLES	15-30% RESIDUE TO APPLES	VEGETABLES
APPLES	<15% RESIDUE TO APPLES	VEGETABLES
APPLES	NO-TILL APPLES	VEGETABLES
ASPARAGUS	RIDGE_TILL ASPARAGUS	VEGETABLES
ASPARAGUS	MULCH_TILL ASPARAGUS	VEGETABLES
ASPARAGUS	15-30% RESIDUE TO ASPARAGUS	VEGETABLES
ASPARAGUS	<15% RESIDUE TO ASPARAGUS	VEGETABLES
ASPARAGUS	NO-TILL ASPARAGUS	VEGETABLES
BEDDING_PLANTS	BEDDING PLANTS	VEGETABLES
BEDDING_PLANTS	BEDDING PLANTS	VEGETABLES
BEDDING_PLANTS	BEDDING PLANTS	VEGETABLES
BEDDING_PLANTS	BEDDING PLANTS	VEGETABLES
BEDDING_PLANTS	NO-TILL BEDDING_PLANTS	VEGETABLES
BEET	RIDGE_TILL BEETS	VEGETABLES
BEET	MULCH_TILL BEETS	VEGETABLES
BEET	15-30% RESIDUE TO BEETS	VEGETABLES
BEET	<15% RESIDUE TO BEETS	VEGETABLES
BEET	NO-TILL BEETS	VEGETABLES
BLACKBERRIES	RIDGE_TILL BLACKBERRIES	VEGETABLES

BLACKBERRIES	MULCH_TILL BLACKBERRIES	VEGETABLES
BLACKBERRIES	15-30% RESIDUE TO BLACKBERRIES	VEGETABLES
BLACKBERRIES	<15% RESIDUE TO BLACKBERRIES	VEGETABLES
BLACKBERRIES	NO-TILL BLACKBERRIES	VEGETABLES
BROCCOLI	RIDGE_TILL BROCCOLI	VEGETABLES
BROCCOLI	MULCH_TILL BROCCOLI	VEGETABLES
BROCCOLI	15-30% RESIDUE TO BROCCOLI	VEGETABLES
BROCCOLI	<15% RESIDUE TO BROCCOLI	VEGETABLES
BROCCOLI	NO-TILL BROCCOLI	VEGETABLES
CABBAGE	RIDGE_TILL CABBAGE	VEGETABLES
CABBAGE	MULCH_TILL CABBAGE	VEGETABLES
CABBAGE	15-30% RESIDUE TO CABBAGE	VEGETABLES
CABBAGE	<15% RESIDUE TO CABBAGE	VEGETABLES
CABBAGE	NO-TILL CABBAGE	VEGETABLES
CANTALOUPES	RIDGE_TILL CANTALOUPES	VEGETABLES
CANTALOUPES	RIDGE_TILL CANTALOUPES	VEGETABLES
CANTALOUPES	15-30% RESIDUE TO CANTALOUPES	VEGETABLES
CANTALOUPES	<15% RESIDUE TO CANTALOUPES	VEGETABLES
CANTALOUPES	NO-TILL CANTALOUPES	VEGETABLES
COLLARDS	RIDGE_TILL COLLARDS	VEGETABLES
COLLARDS	MULCH_TILL COLLARDS	VEGETABLES
COLLARDS	15-30% RESIDUE TO COLLARDS	VEGETABLES
COLLARDS	<15% RESIDUE TO COLLARDS	VEGETABLES
COLLARDS	NO-TILL COLLARDS	VEGETABLES
CUCUMBERS	RIDGE_TILL CUCUMBERS	VEGETABLES
CUCUMBERS	MULCH_TILL CUCUMBERS	VEGETABLES
CUCUMBERS	15-30% RESIDUE TO CUCUMBERS	VEGETABLES
CUCUMBERS	<15% RESIDUE TO CUCUMBERS	VEGETABLES
CUCUMBERS	NO-TILL CUCUMBERS	VEGETABLES
CUT_FLOWERS	CUT FLOWERS	VEGETABLES
CUT_FLOWERS	CUT FLOWERS	VEGETABLES
CUT_FLOWERS	CUT FLOWERS	VEGETABLES
CUT_FLOWERS	CUT FLOWERS	VEGETABLES
CUT_FLOWERS	NO-TILL CUT_FLOWERS	VEGETABLES
EGGPLANT	RIDGE_TILL EGGPLANT	VEGETABLES
EGGPLANT	MULCH_TILL EGGPLANT	VEGETABLES
EGGPLANT	15-30% RESIDUE TO EGGPLANT	VEGETABLES
EGGPLANT	<15% RESIDUE TO EGGPLANT	VEGETABLES
EGGPLANT	NO-TILL EGGPLANT	VEGETABLES
GRAPES	RIDGE_TILL GRAPES	VEGETABLES
GRAPES	MULCH_TILL GRAPES	VEGETABLES
GRAPES	15-30% RESIDUE TO GRAPES	VEGETABLES
GRAPES	<15% RESIDUE TO GRAPES	VEGETABLES
GRAPES	NO-TILL GRAPES	VEGETABLES
GREEN_LIMA_BEANS	RIDGE_TILL GREEN LIMA BEANS	VEGETABLES
GREEN_LIMA_BEANS	MULCH_TILL GREEN LIMA BEANS	VEGETABLES
GREEN_LIMA_BEANS	15-30% RESIDUE TO GREEN LIMA BEANS	VEGETABLES
GREEN_LIMA_BEANS	<15% RESIDUE TO GREEN LIMA BEANS	VEGETABLES

GREEN_LIMA_BEANS	NO-TILL GREEN_LIMA_BEANS	VEGETABLES
GREEN_ONIONS	RIDGE_TILL GREEN ONIONS	VEGETABLES
GREEN_ONIONS	MULCH_TILL GREEN ONIONS	VEGETABLES
GREEN_ONIONS	15-30% RESIDUE TO GREEN ONIONS	VEGETABLES
GREEN_ONIONS	<15% RESIDUE TO GREEN ONIONS	VEGETABLES
GREEN_ONIONS	NO-TILL GREEN_ONIONS	VEGETABLES
GREEN_PEAS	RIDGE_TILL GREEN PEAS	VEGETABLES
GREEN_PEAS	MULCH_TILL GREEN PEAS	VEGETABLES
GREEN_PEAS	15-30% RESIDUE TO GREEN PEAS	VEGETABLES
GREEN_PEAS	<15% RESIDUE TO GREEN PEAS	VEGETABLES
GREEN_PEAS	NO-TILL GREEN_PEAS	VEGETABLES
HERBS	RIDGE_TILL HERBS	VEGETABLES
HERBS	MULCH_TILL HERBS	VEGETABLES
HERBS	15-30% RESIDUE TO HERBS	VEGETABLES
HERBS	<15% RESIDUE TO HERBS	VEGETABLES
HERBS	NO-TILL HERBS	VEGETABLES
HOT_PEPPERS	RIDGE_TILL HOT PEPPERS	VEGETABLES
HOT_PEPPERS	RIDGE_TILL HOT PEPPERS	VEGETABLES
HOT_PEPPERS	15-30% RESIDUE TO HOT PEPPERS	VEGETABLES
HOT_PEPPERS	<15% RESIDUE TO HOT PEPPERS	VEGETABLES
HOT_PEPPERS	NO-TILL HOT_PEPPERS	VEGETABLES
KALE	RIDGE_TILL KALE	VEGETABLES
KALE	MULCH_TILL KALE	VEGETABLES
KALE	15-30% RESIDUE TO KALE	VEGETABLES
KALE	<15% RESIDUE TO KALE	VEGETABLES
KALE	NO-TILL KALE	VEGETABLES
LETTUCE	RIDGE_TILL LETTUCE	VEGETABLES
LETTUCE	MULCH_TILL LETTUCE	VEGETABLES
LETTUCE	15-30% RESIDUE TO LETTUCE	VEGETABLES
LETTUCE	<15% RESIDUE TO LETTUCE	VEGETABLES
LETTUCE	NO-TILL LETTUCE	VEGETABLES
MIXED_VEGETABLES	RIDGE_TILL MIXED VEGETABLES	VEGETABLES
MIXED_VEGETABLES	MULCH_TILL MIXED VEGETABLES	VEGETABLES
MIXED_VEGETABLES	15-30% RESIDUE TO MIXED VEGETABLES	VEGETABLES
MIXED_VEGETABLES	<15% RESIDUE TO MIXED VEGETABLES	VEGETABLES
MIXED_VEGETABLES	NO-TILL MIXED_VEGETABLES	VEGETABLES
MUSTARD_GREENS	RIDGE_TILL MUSTARD GREENS	VEGETABLES
MUSTARD_GREENS	MULCH_TILL MUSTARD GREENS	VEGETABLES
MUSTARD_GREENS	15-30% RESIDUE TO MUSTARD GREENS	VEGETABLES
MUSTARD_GREENS	<15% RESIDUE TO MUSTARD GREENS	VEGETABLES
MUSTARD_GREENS	NO-TILL MUSTARD_GREENS	VEGETABLES
NURSERY_ET_FLORICULTURE	NURSERY ET FLORICULTURE	VEGETABLES
NURSERY_ET_FLORICULTURE	NURSERY ET FLORICULTURE	VEGETABLES
NURSERY_ET_FLORICULTURE	NURSERY ET FLORICULTURE	VEGETABLES
NURSERY_ET_FLORICULTURE	NURSERY ET FLORICULTURE	VEGETABLES
NURSERY_ET_FLORICULTURE	NO-TILL NURSERY_ET_FLORICULTURE	VEGETABLES
NURSEY_CROPS	NURSERY CROPS	VEGETABLES
NURSEY_CROPS	NURSERY CROPS	VEGETABLES

NURSEY_CROPS	NURSERY CROPS	VEGETABLES
NURSEY_CROPS	NURSERY CROPS	VEGETABLES
NURSEY_CROPS	NO-TILL NURSERY_CROPS	VEGETABLES
OKRA	RIDGE_TILL OKRA	VEGETABLES
OKRA	MULCH_TILL OKRA	VEGETABLES
OKRA	15-30% RESIDUE TO OKRA	VEGETABLES
OKRA	<15% RESIDUE TO OKRA	VEGETABLES
OKRA	NO-TILL OKRA	VEGETABLES
OTHER_CROPS	OTHER CROPS	VEGETABLES
OTHER_CROPS	OTHER CROPS	VEGETABLES
OTHER_CROPS	OTHER CROPS	VEGETABLES
OTHER_CROPS	OTHER CROPS	VEGETABLES
OTHER_CROPS	NO-TILL OTHER_CROPS	VEGETABLES
OTHER_FRUITS	RIDGE_TILL OTHER FRUITS	VEGETABLES
OTHER_FRUITS	MULCH_TILL OTHER FRUITS	VEGETABLES
OTHER_FRUITS	15-30% RESIDUE TO OTHER FRUITS	VEGETABLES
OTHER_FRUITS	<15% RESIDUE TO OTHER FRUITS	VEGETABLES
OTHER_FRUITS	NO-TILL OTHER_FRUITS	VEGETABLES
OTHER_NURSERY	OTHER NURSERY	VEGETABLES
OTHER_NURSERY	OTHER NURSERY	VEGETABLES
OTHER_NURSERY	OTHER NURSERY	VEGETABLES
OTHER_NURSERY	OTHER NURSERY	VEGETABLES
OTHER_NURSERY	NO-TILL OTHER_NURSERY	VEGETABLES
OTHER_VEGETABLES	RIDGE_TILL OTHER VEGETABLES	VEGETABLES
OTHER_VEGETABLES	MULCH_TILL OTHER VEGETABLES	VEGETABLES
OTHER_VEGETABLES	15-30% RESIDUE TO OTHER VEGETABLES	VEGETABLES
OTHER_VEGETABLES	<15% RESIDUE TO OTHER VEGETABLES	VEGETABLES
OTHER_VEGETABLES	NO-TILL OTHER_VEGETABLES	VEGETABLES
PARSLEY	RIDGE_TILL PARSLEY	VEGETABLES
PARSLEY	MULCH_TILL PARSLEY	VEGETABLES
PARSLEY	15-30% RESIDUE TO PARSLEY	VEGETABLES
PARSLEY	<15% RESIDUE TO PARSLEY	VEGETABLES
PARSLEY	NO-TILL PARSLEY	VEGETABLES
PEACHES	RIDGE_TILL PEACHES	VEGETABLES
PEACHES	MULCH_TILL PEACHES	VEGETABLES
PEACHES	15-30% RESIDUE TO PEACHES	VEGETABLES
PEACHES	<15% RESIDUE TO PEACHES	VEGETABLES
PEACHES	NO-TILL PEACHES	VEGETABLES
PEARS	RIDGE_TILL PEARS	VEGETABLES
PEARS	MULCH_TILL PEARS	VEGETABLES
PEARS	15-30% RESIDUE TO PEARS	VEGETABLES
PEARS	<15% RESIDUE TO PEARS	VEGETABLES
PEARS	NO-TILL PEARS	VEGETABLES
PLUMS	RIDGE_TILL PLUMS	VEGETABLES
PLUMS	MULCH_TILL PLUMS	VEGETABLES
PLUMS	15-30% RESIDUE TO PLUMS	VEGETABLES
PLUMS	<15% RESIDUE TO PLUMS	VEGETABLES
PLUMS	NO-TILL PLUMS	VEGETABLES

POTATOES	NO-TILL POTATOES	VEGETABLES
POTATOES	RIDGE_TILL POTATOES	VEGETABLES
POTATOES	MULCH_TILL POTATOES	VEGETABLES
POTATOES	15-30% RESIDUE TO POTATOES	VEGETABLES
POTATOES	<15% RESIDUE TO POTATOES	VEGETABLES
PUMPKINS	RIDGE-TILL PUMPKINS	VEGETABLES
PUMPKINS	MULCH-TILL PUMPKINS	VEGETABLES
PUMPKINS	15-30% RESIDUE TO PUMPKINS	VEGETABLES
PUMPKINS	<15% RESIDUE TO PUMPKINS	VEGETABLES
PUMPKINS	NO-TILL PUMPKINS	VEGETABLES
RADISHES	RIDGE-TILL RADISHES	VEGETABLES
RADISHES	MULCH-TILL RADISHES	VEGETABLES
RADISHES	15-30% RESIDUE TO RADISHES	VEGETABLES
RADISHES	<15% RESIDUE RADISHES	VEGETABLES
RADISHES	NO-TILL RADISHES	VEGETABLES
RASPBERRIES	RIDGE_TILL RASPBERRIES	VEGETABLES
RASPBERRIES	MULCH_TILL RASPBERRIES	VEGETABLES
RASPBERRIES	15-30% RESIDUE TO RASPBERRIES	VEGETABLES
RASPBERRIES	<15% RESIDUE TO RASPBERRIES	VEGETABLES
RASPBERRIES	NO-TILL RASPBERRIES	VEGETABLES
SNAP_BEANS	RIDGE_TILL SNAP BEANS	VEGETABLES
SNAP_BEANS	MULCH_TILL SNAP BEANS	VEGETABLES
SNAP_BEANS	15-30% RESIDUE TO SNAP BEANS	VEGETABLES
SNAP_BEANS	<15% RESIDUE TO SNAP BEANS	VEGETABLES
SNAP_BEANS	NO-TILL SNAP_BEANS	VEGETABLES
SPINACH	RIDGE_TILL SPINACH	VEGETABLES
SPINACH	MULCH_TILL SPINACH	VEGETABLES
SPINACH	15-30% RESIDUE TO SPINACH	VEGETABLES
SPINACH	<15% RESIDUE TO SPINACH	VEGETABLES
SPINACH	NO-TILL SPINACH	VEGETABLES
SQUASH	RIDGE_TILL SQUASH	VEGETABLES
SQUASH	MULCH_TILL SQUASH	VEGETABLES
SQUASH	15-30% RESIDUE TO SQUASH	VEGETABLES
SQUASH	<15% RESIDUE TO SQUASH	VEGETABLES
SQUASH	NO-TILL SQUASH	VEGETABLES
STRAWBERRIES	RIDGE_TILL STRAWBERRIES	VEGETABLES
STRAWBERRIES	MULCH_TILL STRAWBERRIES	VEGETABLES
STRAWBERRIES	15-30% RESIDUE TO STRAWBERRIES	VEGETABLES
STRAWBERRIES	<15% RESIDUE TO STRAWBERRIES	VEGETABLES
STRAWBERRIES	NO-TILL STRAWBERRIES	VEGETABLES
SWEET_CHERRIES	RIDGE_TILL SWEET CHERRIES	VEGETABLES
SWEET_CHERRIES	MULCH_TILL SWEET CHERRIES	VEGETABLES
SWEET_CHERRIES	15-30% RESIDUE TO SWEET CHERRIES	VEGETABLES
SWEET_CHERRIES	<15% RESIDUE TO SWEET CHERRIES	VEGETABLES
SWEET_CHERRIES	NO-TILL SWEET_CHERRIES	VEGETABLES
SWEET_CORN	RIDGE_TILL SWEET CORN	VEGETABLES
SWEET_CORN	MULCH_TILL SWEET CORN	VEGETABLES
SWEET_CORN	15-30% RESIDUE TO SWEET CORN	VEGETABLES

SWEET_CORN	<15% RESIDUE TO SWEET CORN	VEGETABLES
SWEET_CORN	NO-TILL SWEET_CORN	VEGETABLES
SWEET_PEPPERS	RIDGE_TILL SWEET PEPPERS	VEGETABLES
SWEET_PEPPERS	MULCH_TILL SWEET PEPPERS	VEGETABLES
SWEET_PEPPERS	15-30% RESIDUE TO SWEET PEPPERS	VEGETABLES
SWEET_PEPPERS	<15% RESIDUE TO SWEET PEPPERS	VEGETABLES
SWEET_PEPPERS	NO-TILL SWEET_PEPPERS	VEGETABLES
TAME_BLUEBERRIES	RIDGE_TILL TAME BLUEBERRIES	VEGETABLES
TAME_BLUEBERRIES	MULCH_TILL TAME BLUEBERRIES	VEGETABLES
TAME_BLUEBERRIES	15-30% RESIDUE TO TAME BLUEBERRIES	VEGETABLES
TAME_BLUEBERRIES	<15% RESIDUE TO TAME BLUEBERRIES	VEGETABLES
TAME_BLUEBERRIES	NO-TILL TAME_BLUEBERRIES	VEGETABLES
TOMATOES	RIDGE_TILL TOMATOES	VEGETABLES
TOMATOES	MULCH_TILL TOMATOES	VEGETABLES
TOMATOES	15-30% RESIDUE TO TOMATOES	VEGETABLES
TOMATOES	<15% RESIDUE TO TOMATOES	VEGETABLES
TOMATOES	NO-TILL TOMATOES	VEGETABLES
TURNIPS	RIDGE_TILL TURNIPS	VEGETABLES
TURNIPS	MULCH_TILL TURNIPS	VEGETABLES
TURNIPS	15-30% RESIDUE TO TURNIPS	VEGETABLES
TURNIPS	<15% RESIDUE TO TURNIPS	VEGETABLES
TURNIPS	NO-TILL TURNIPS	VEGETABLES
TURNIPS_GREENS	RIDGE_TILL TURNIP GREENS	VEGETABLES
TURNIPS_GREENS	MULCH_TILL TURNIP GREENS	VEGETABLES
TURNIPS_GREENS	15-30% RESIDUE TO TURNIP GREENS	VEGETABLES
TURNIPS_GREENS	<15% RESIDUE TO TURNIP GREENS	VEGETABLES
TURNIPS_GREENS	NO-TILL TURNIP_GREENS	VEGETABLES
WATERMELONS	RIDGE_TILL WATERMELONS	VEGETABLES
WATERMELONS	MULCH_TILL WATERMELONS	VEGETABLES
WATERMELONS	15-30% RESIDUE TO WATERMELONS	VEGETABLES
WATERMELONS	<15% RESIDUE TO WATERMELONS	VEGETABLES
WATERMELONS	NO-TILL WATERMELONS	VEGETABLES

APPENDIX B

B.1 Time Series. Simulated and Observed Daily Average Flow. Segment 10

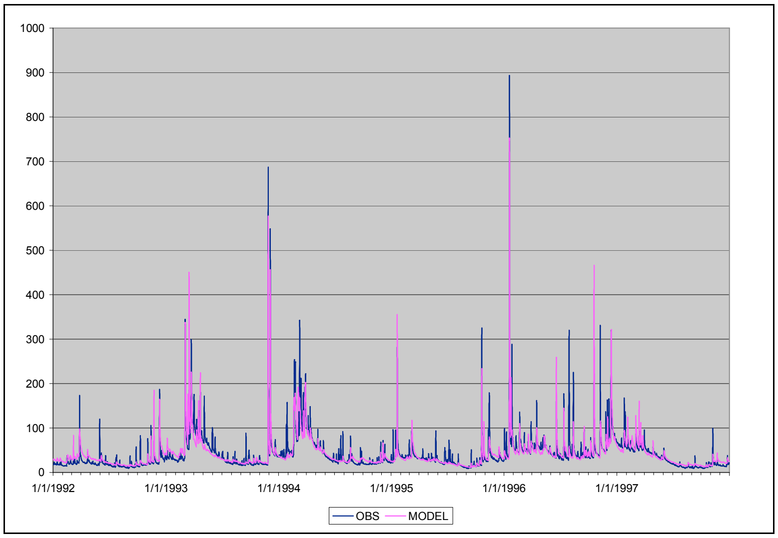

B.2 Scatter Plot. Simulated and Observed Daily Average Flow. Segment 10

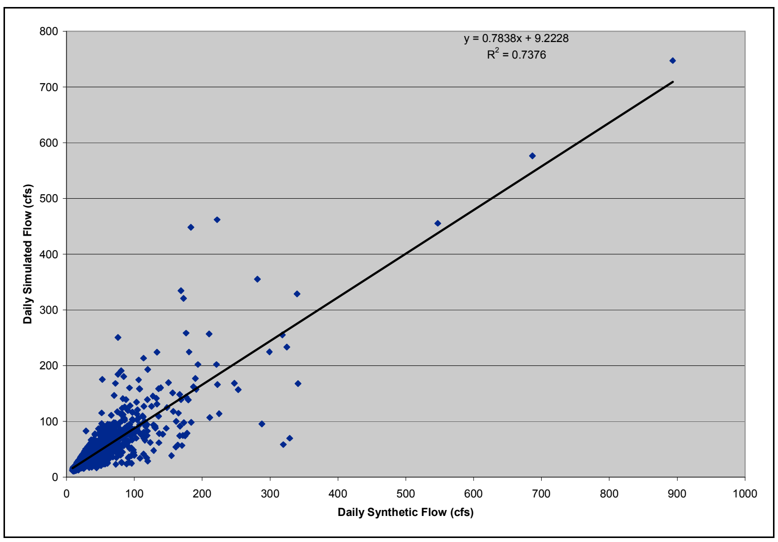

B.3 Cumulative Distribution Function. Simulated and Observed Daily Average Flow. Segment 10

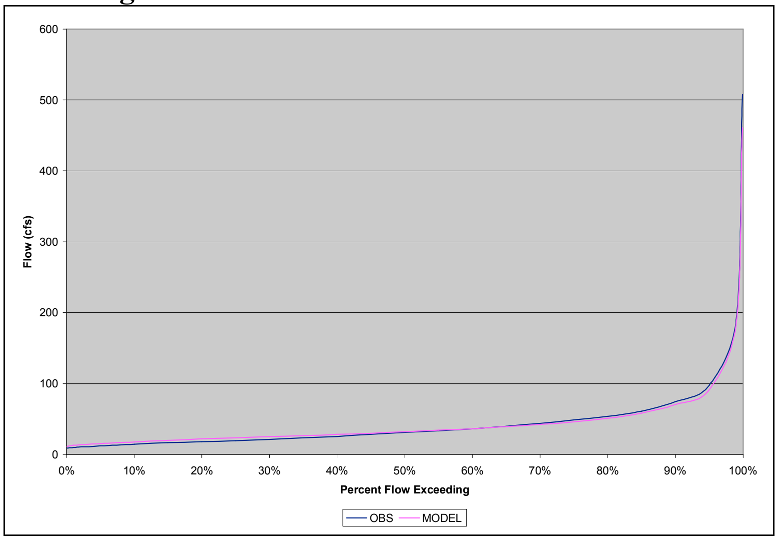

B.4 Scatter Plot. Simulated and Observed Monthly Average Flow. Segment 10

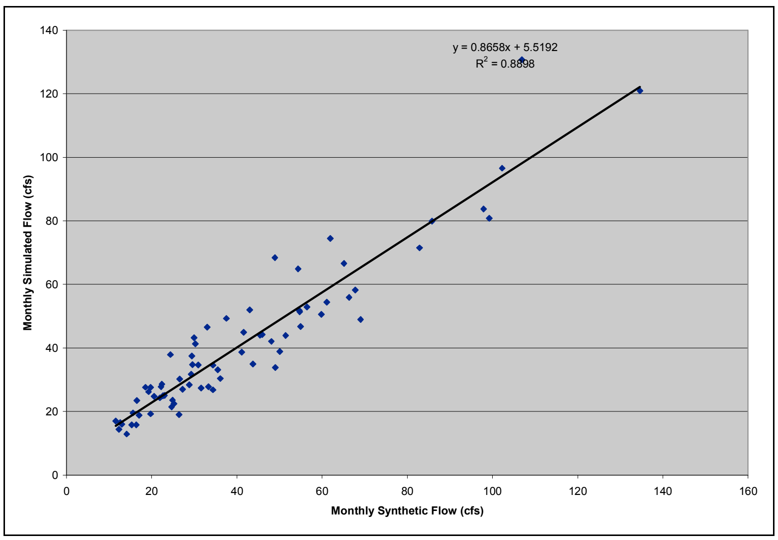

B.5 Time Series. Simulated and Observed Daily Average Flow. Segment 20

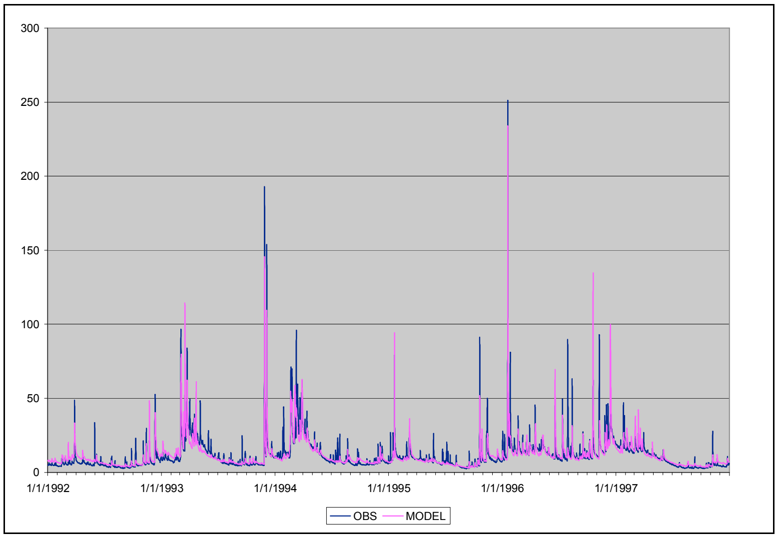

B.6 Scatter Plot. Simulated and Observed Daily Average Flow. Segment 20

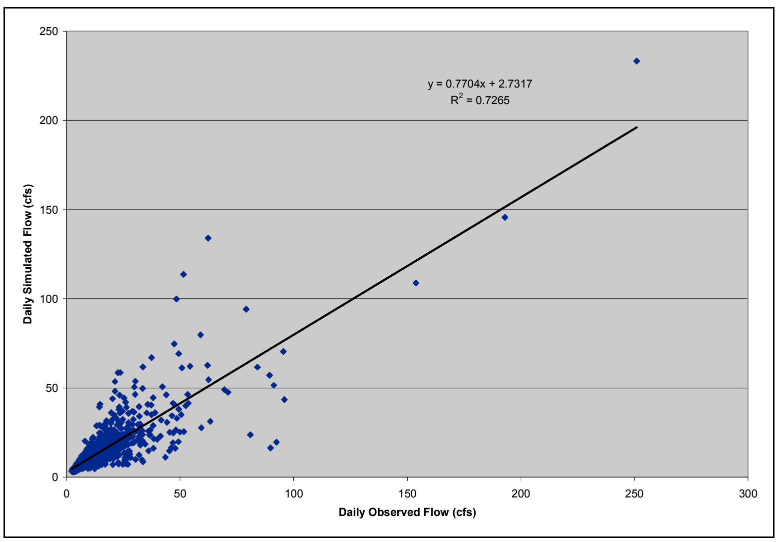

B.7 Cumulative Distribution Function. Simulated and Observed Daily Average Flow. Segment 20

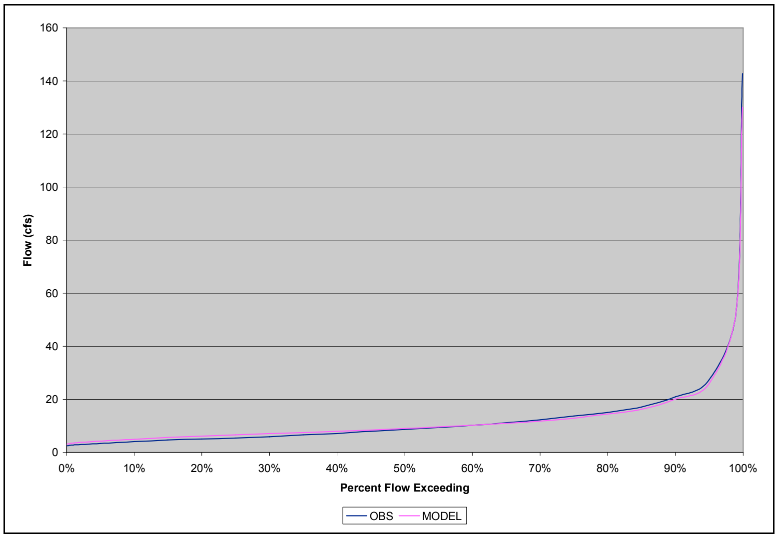

B.8 Scatter Plot. Simulated and Observed Monthly Average Flow. Segment 20

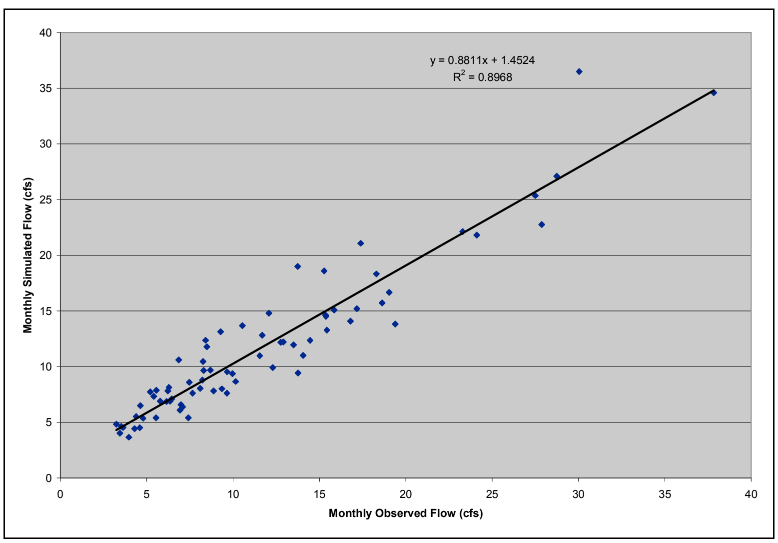

B.9 Time Series. Simulated and Observed Daily Average Flow. Segment 30

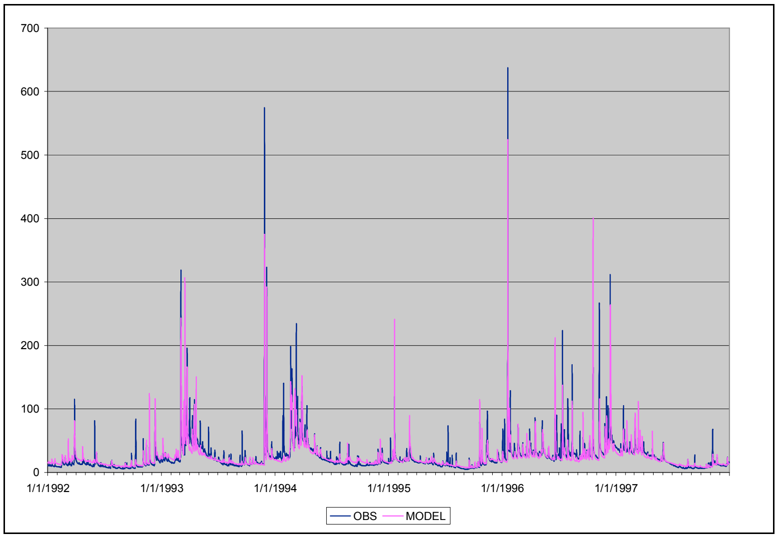

B.10 Scatter Plot. Simulated and Observed Daily Average Flow. Segment 30

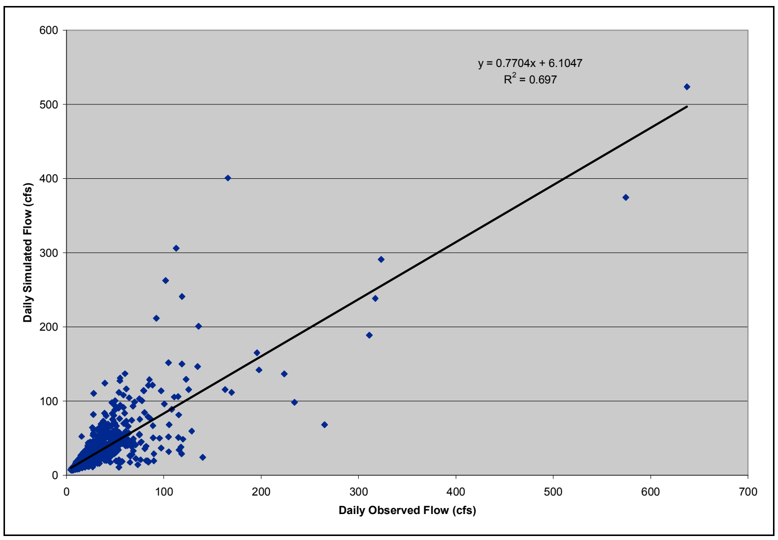

B.11 Cumulative Distribution Function. Simulated and Observed Daily Average Flow. Segment 30

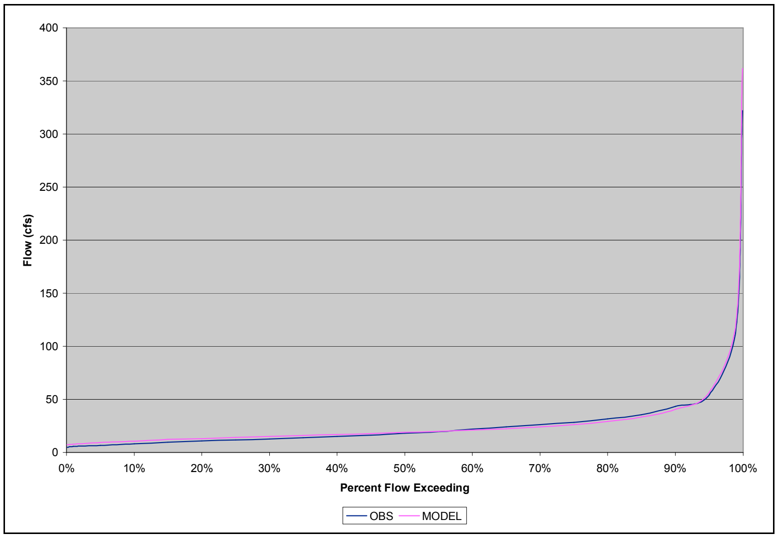

B.12 Scatter Plot. Simulated and Observed Monthly Average Flow. Segment 30

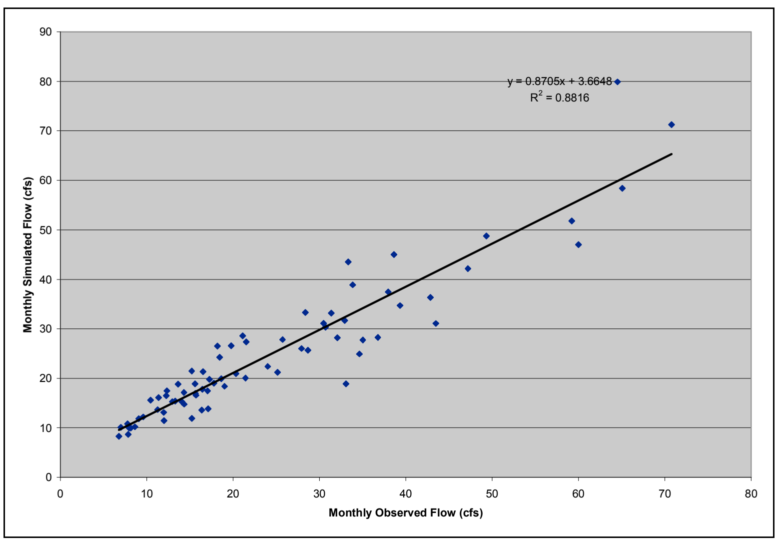

B.13 Time Series. Simulated and Observed Daily Average Flow. Segment 50

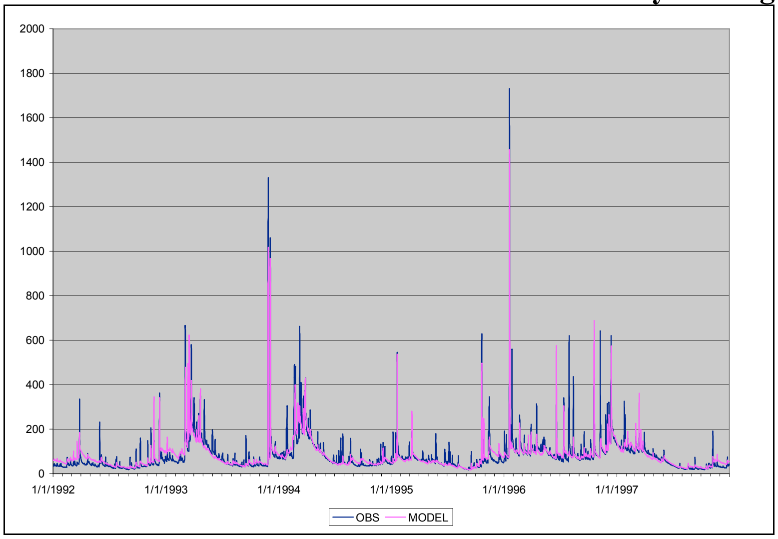

B.14 Scatter Plot. Simulated and Observed Daily Average Flow. Segment 50

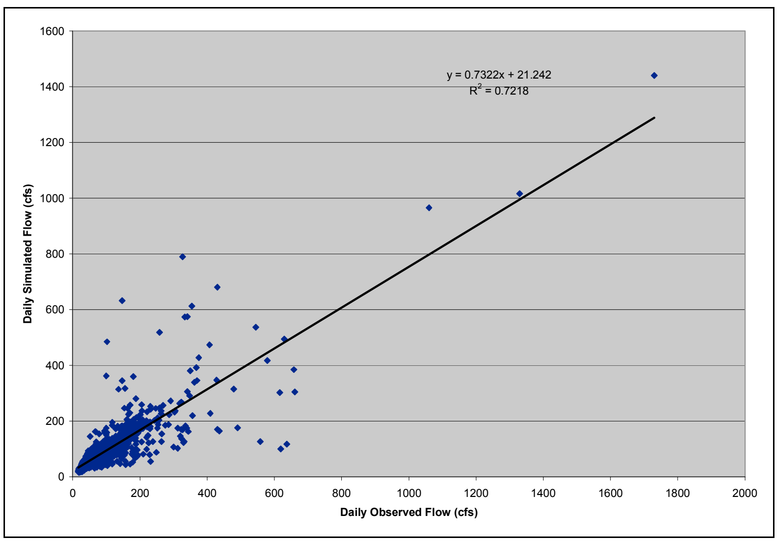

B.15 Cumulative Distribution Function. Simulated and Observed Daily Average Flow. Segment 50

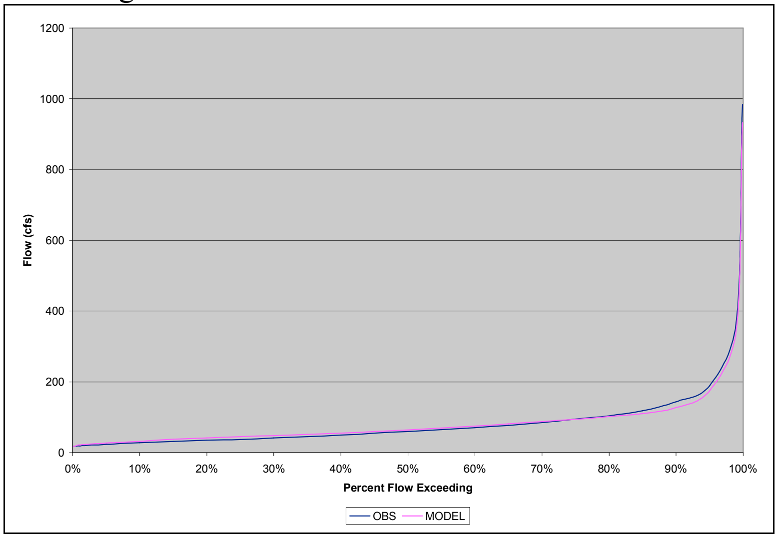

B.16 Scatter Plot. Simulated and Observed Monthly Average Flow. Segment 50

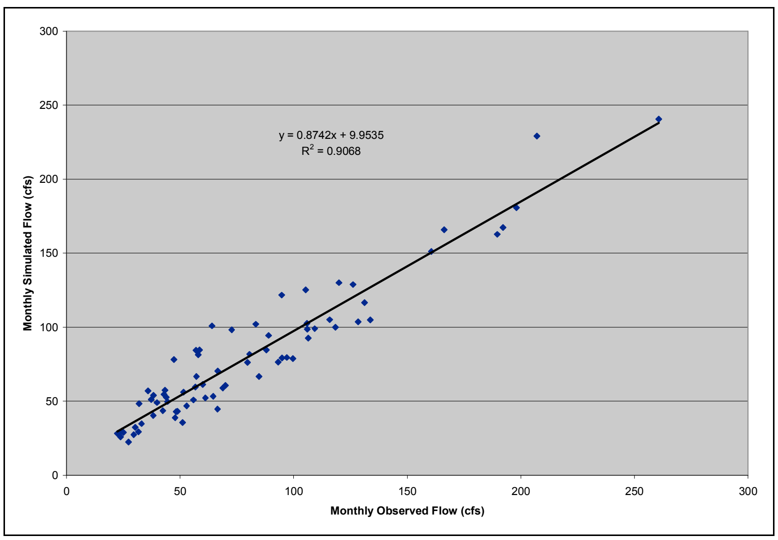

B.17 Time Series. Simulated and Observed Daily Average Flow. Segment 90

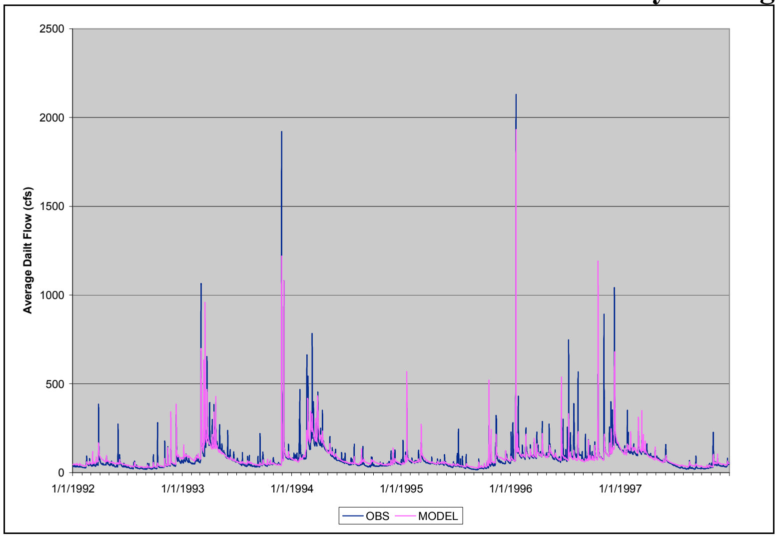

B.18 Scatter Plot. Simulated and Observed Daily Average Flow. Segment 90

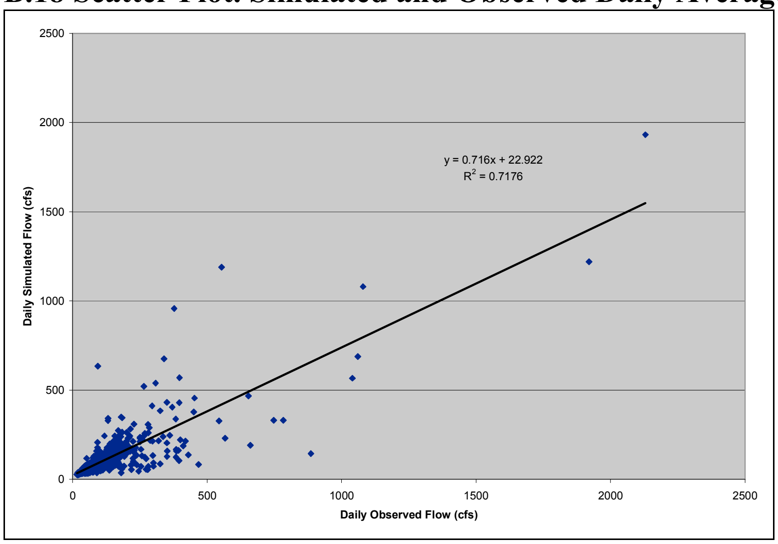

B.19 Cumulative Distribution Function. Simulated and Observed Daily Average Flow. Segment 90

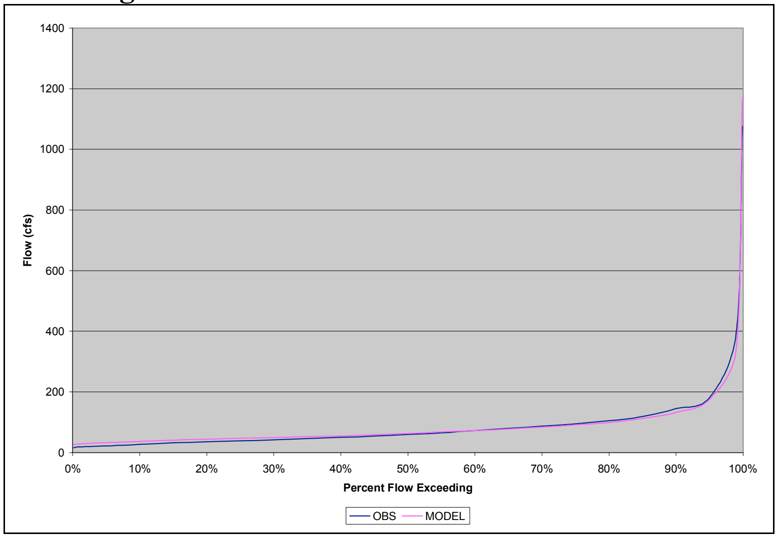

B.20 Scatter Plot. Simulated and Observed Monthly Average Flow. Segment 90

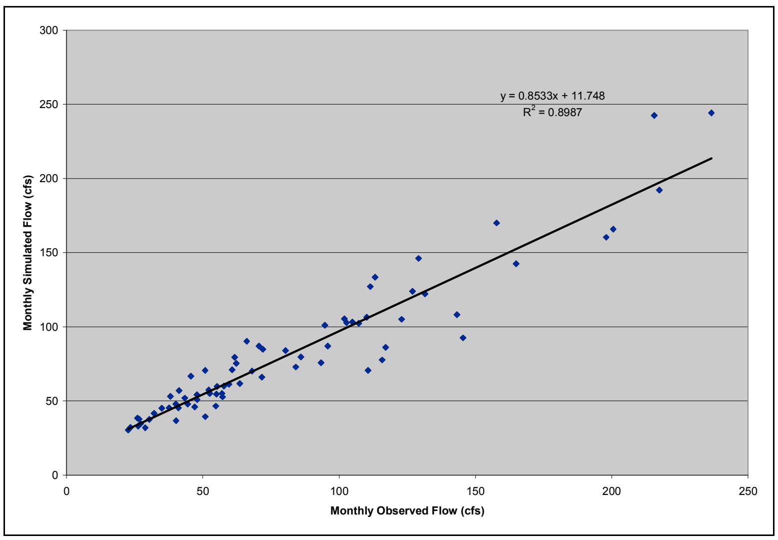

B.21 Time Series. Simulated and Observed Daily Average Flow. Segment 100

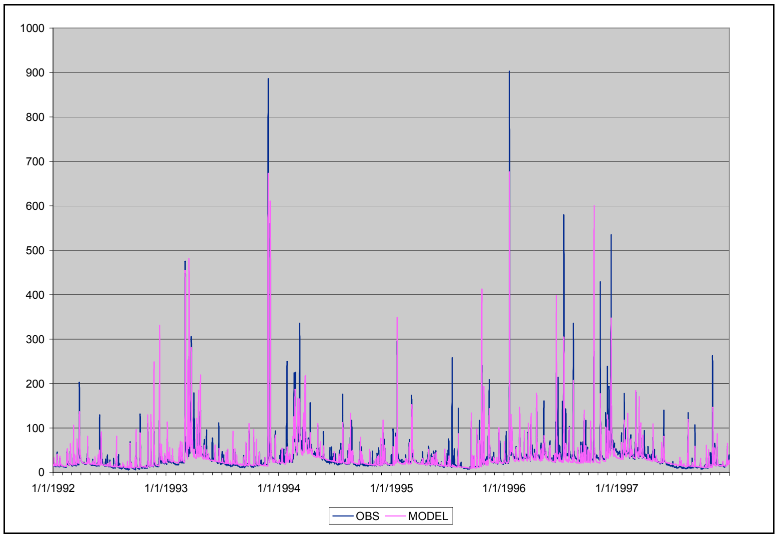

B.22 Scatter Plot. Simulated and Observed Daily Average Flow. Segment 100

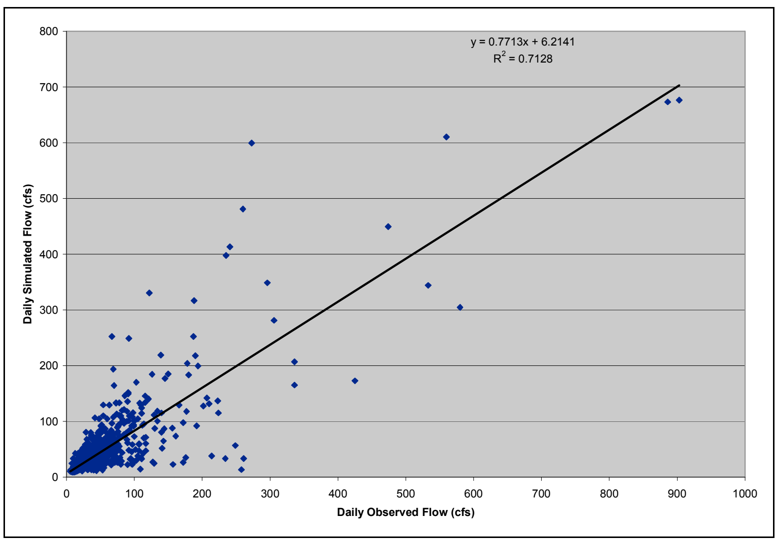

B.23 Cumulative Distribution Function. Simulated and Observed Daily Average Flow. Segment 100

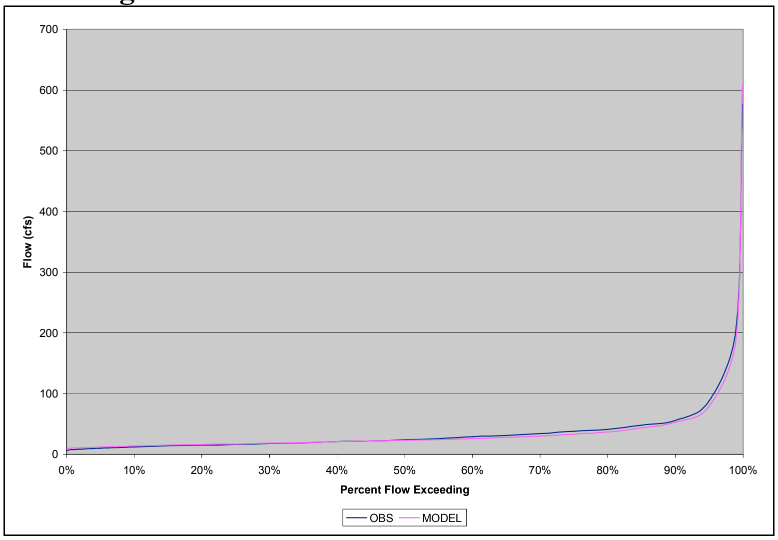

B.24 Scatter Plot. Simulated and Observed Monthly Average Flow. Segment 100

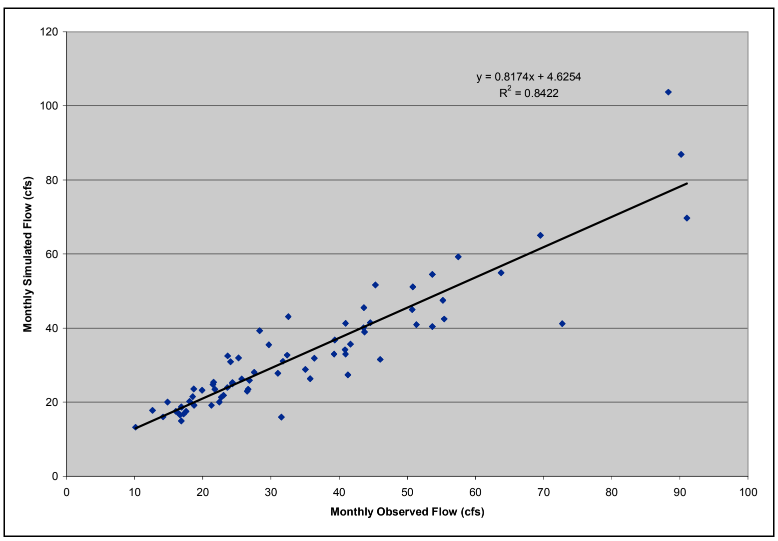

B.25 Time Series. Simulated and Observed Daily Average Flow. Segment 60

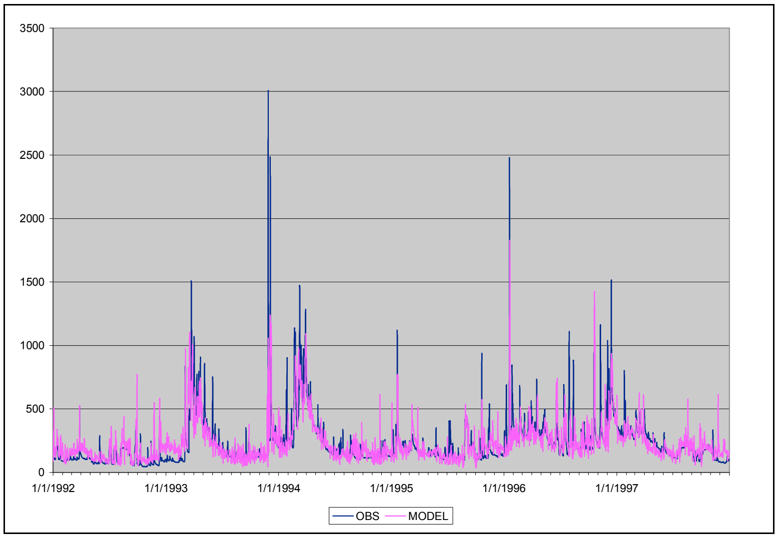

B.26 Scatter Plot. Simulated and Observed Daily Average Flow. Segment 60

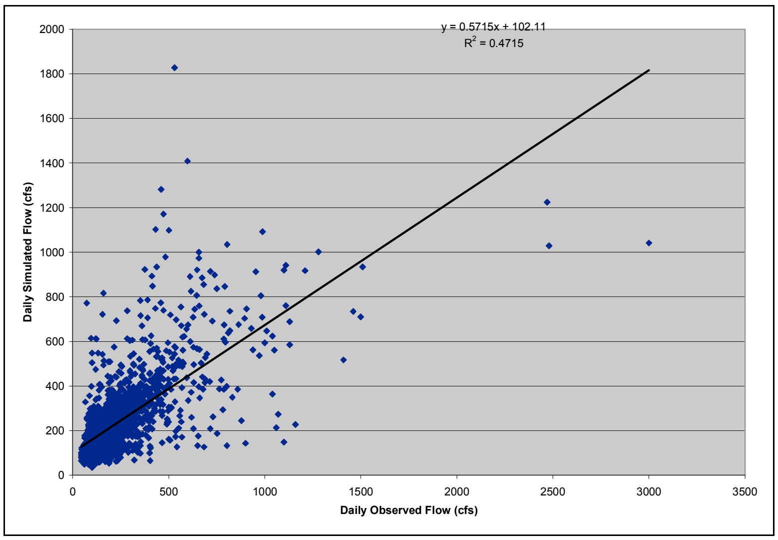

B.27 Cumulative Distribution Function. Simulated and Observed Daily Average Flow. Segment 60

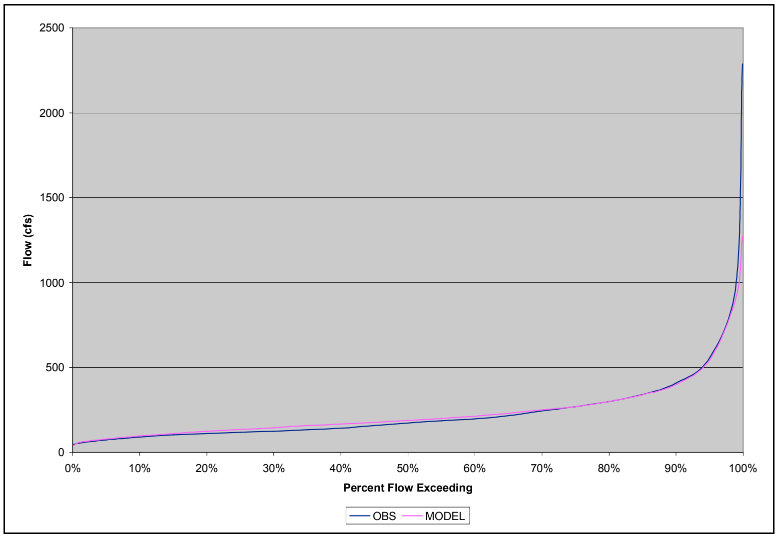

B.28 Scatter Plot. Simulated and Observed Monthly Average Flow. Segment 60

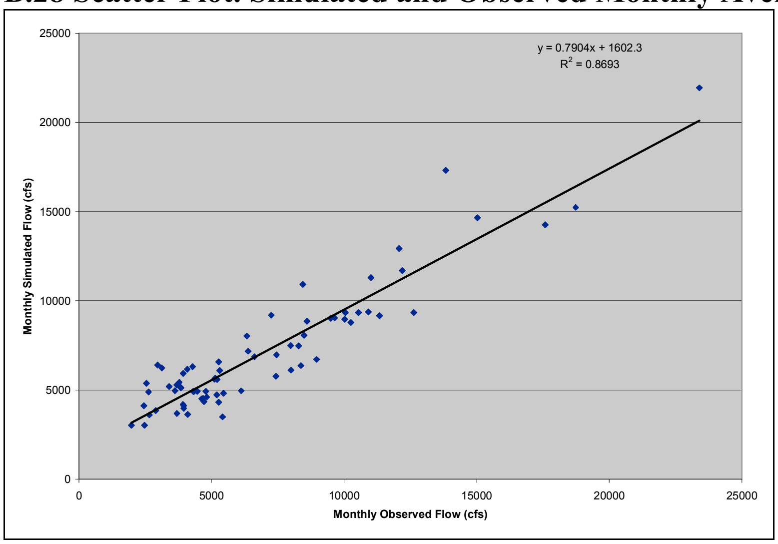

APPENDIX C

Figure C.1. Isothemal Contours, Prettyboy Reservoir, Lower Sampling Locations, 1992-1995

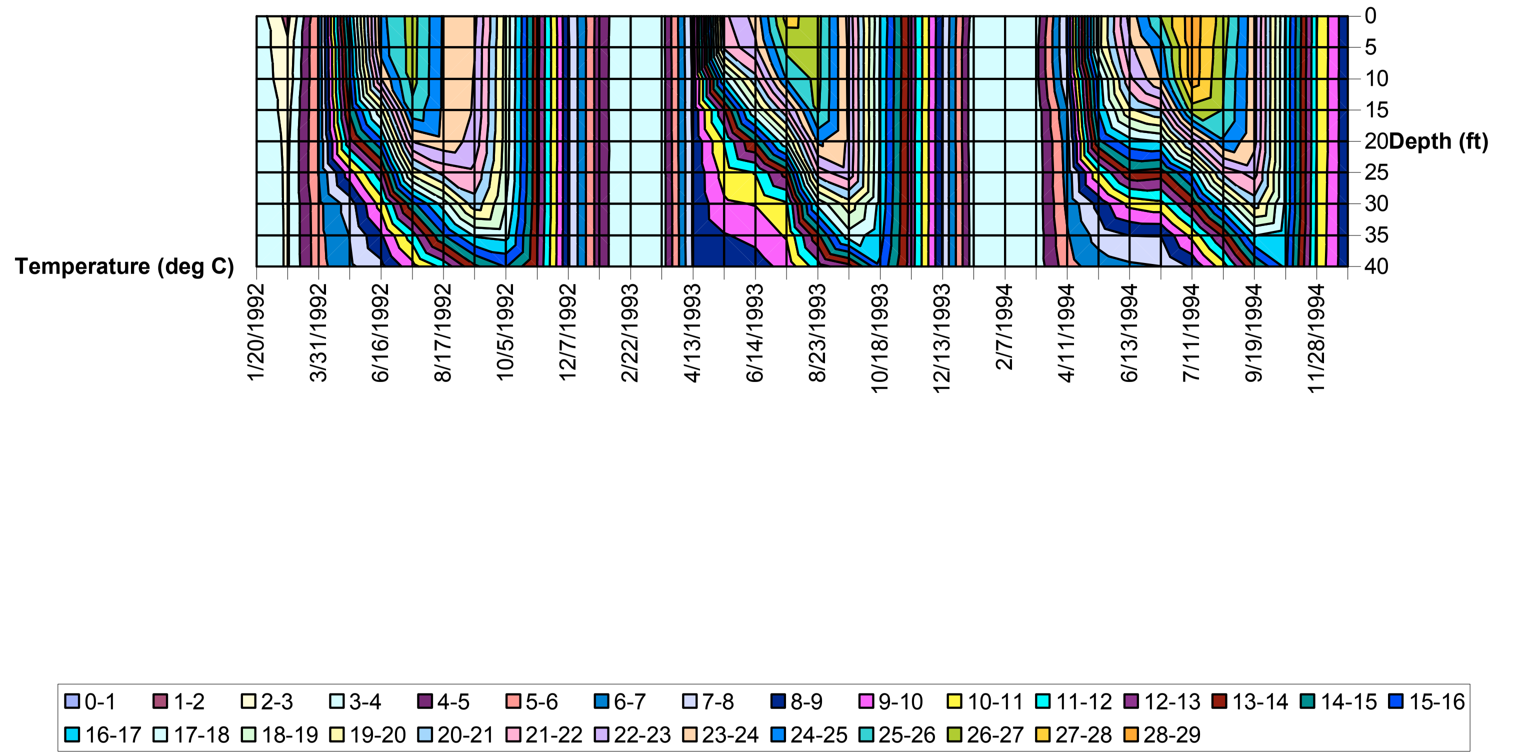

Figure C.2. Isothemal Contours, Prettyboy Reservoir, Lower Sampling Locations, 1996-1998

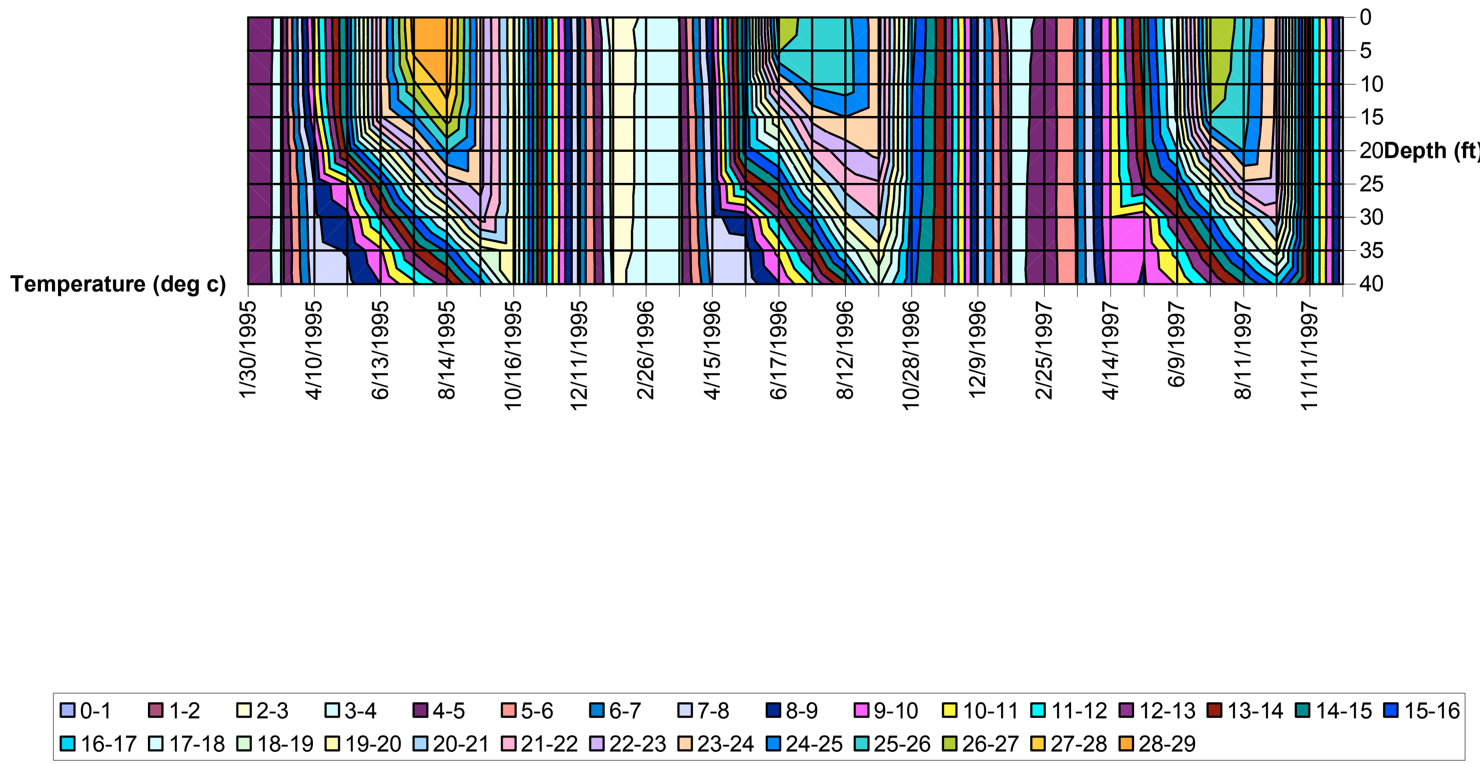

Figure C.3. Isothermal Contours, Prettyboy Reservoir, Lower Sampling Locations, 1999-2001

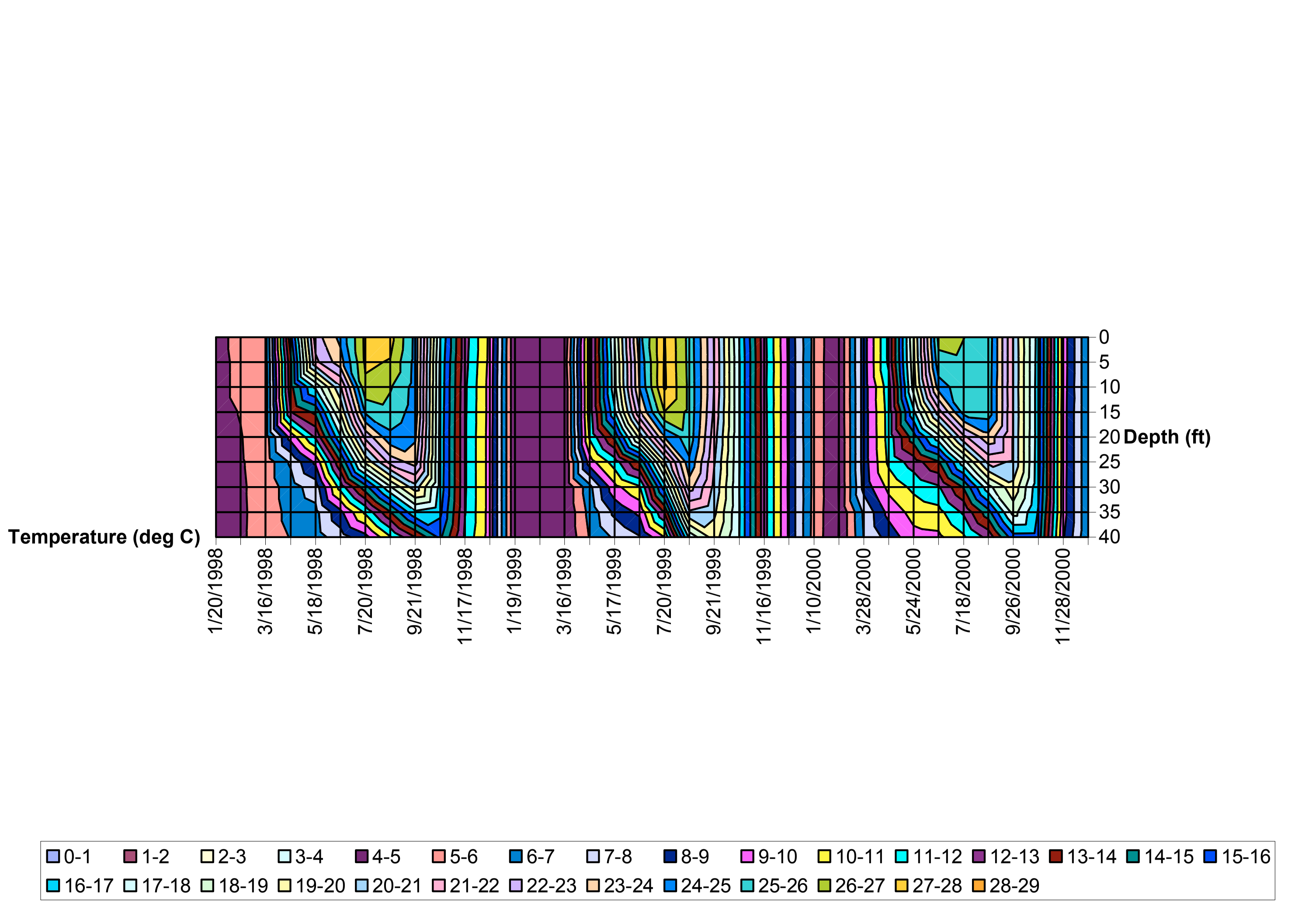

Figure C.4. Isothermal Contours, Prettyboy Reservoir, Lower Sampling Locations, 2002-2004

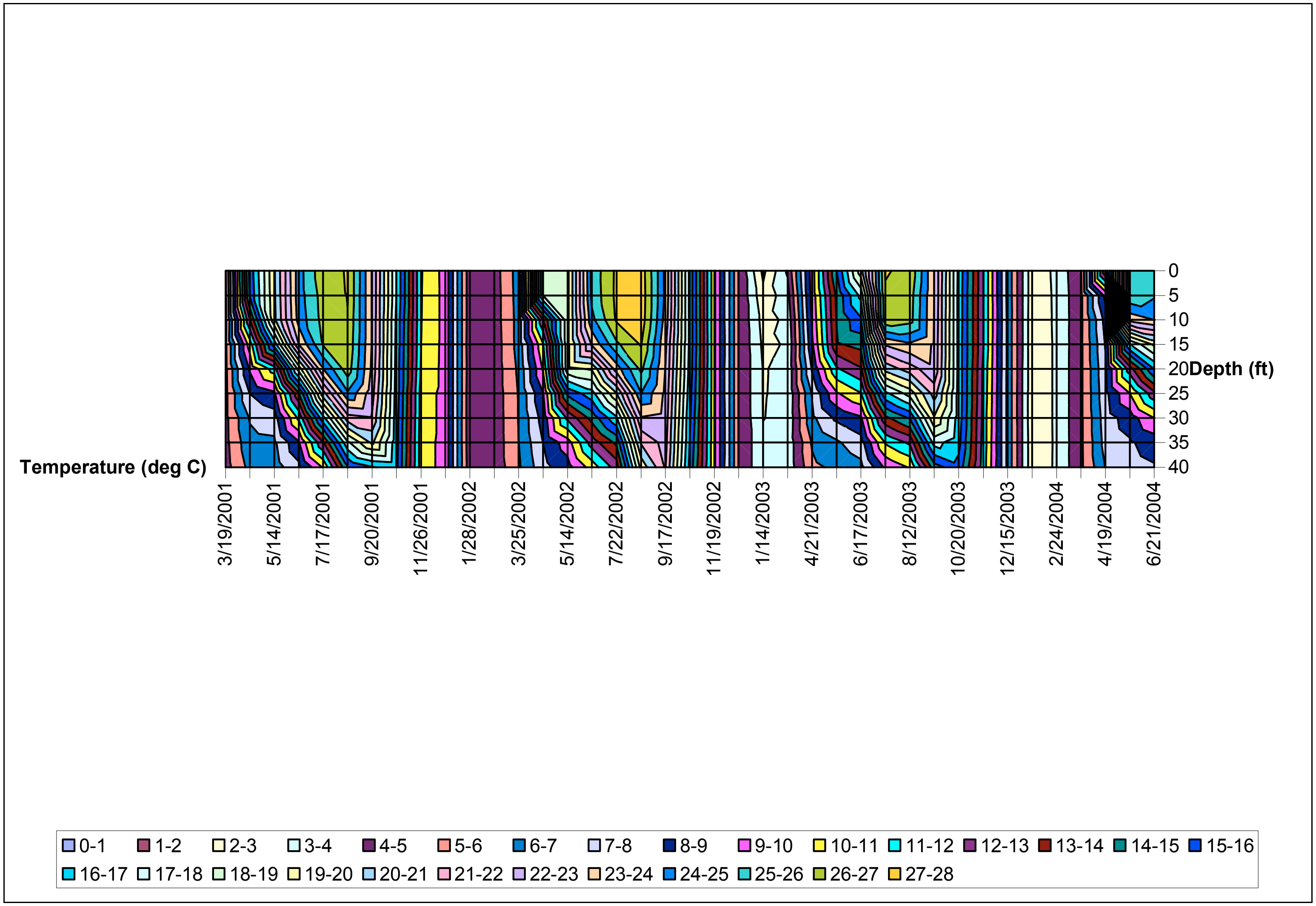

Figure C.5. Isothermal Contours, Prettyboy Reservoir, Middle Sampling Location, 1992-1994

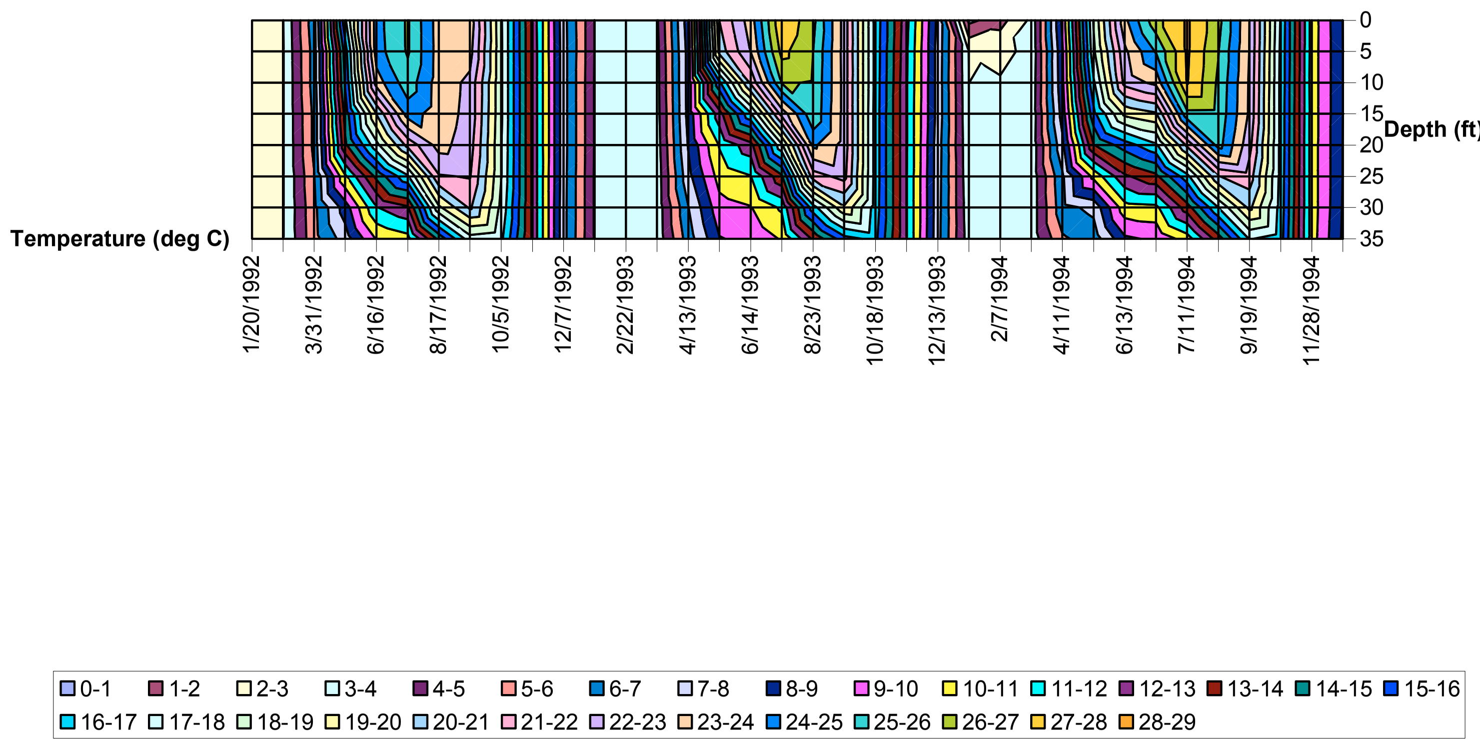

Figure C.6. Isothermal Contours, Prettyboy Reservoir, Middle Sampling Location, 1995-1997

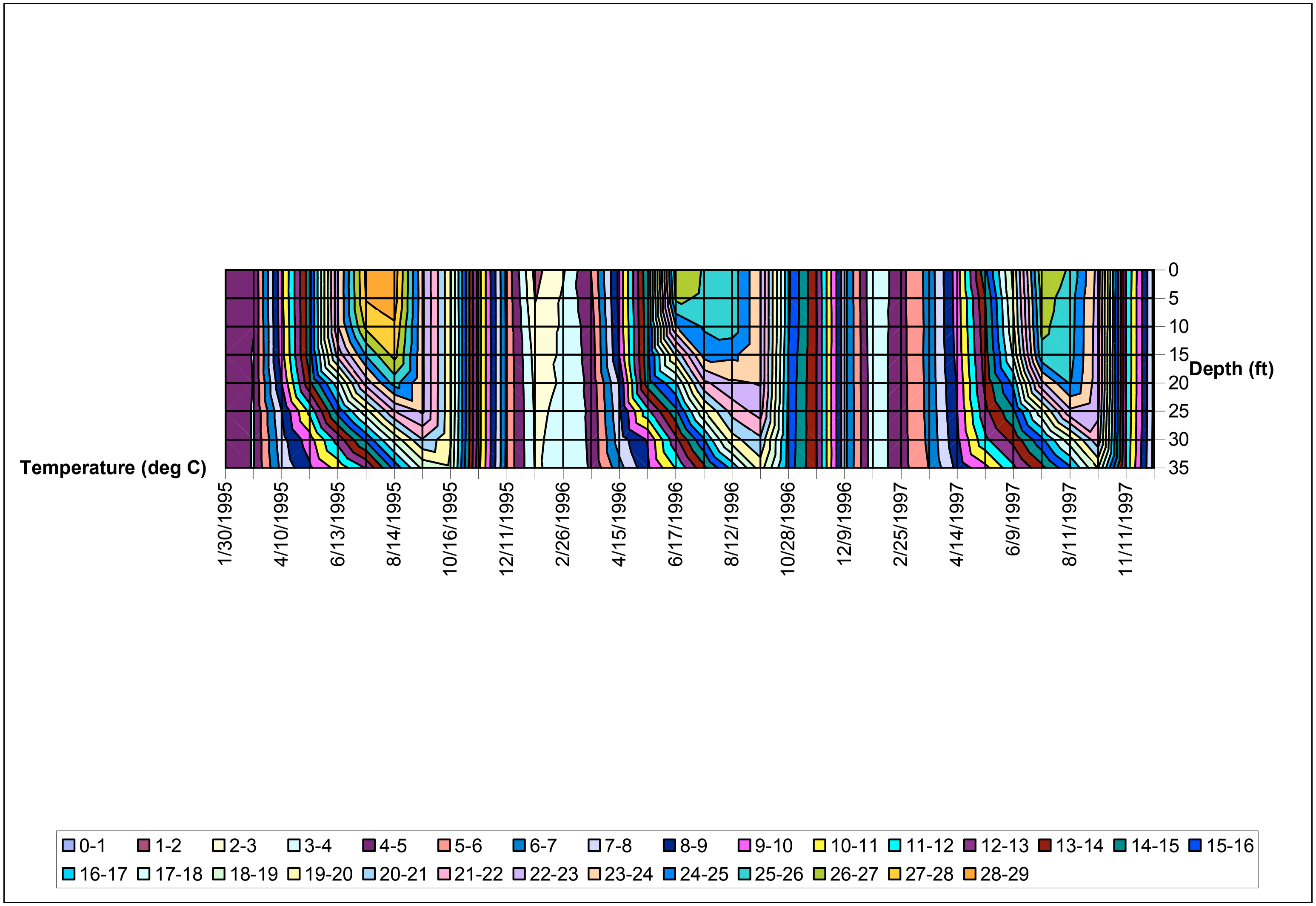

Figure C.7. Isothermal Contours, Prettyboy Reservoir, Middle Sampling Location, 1998-2000

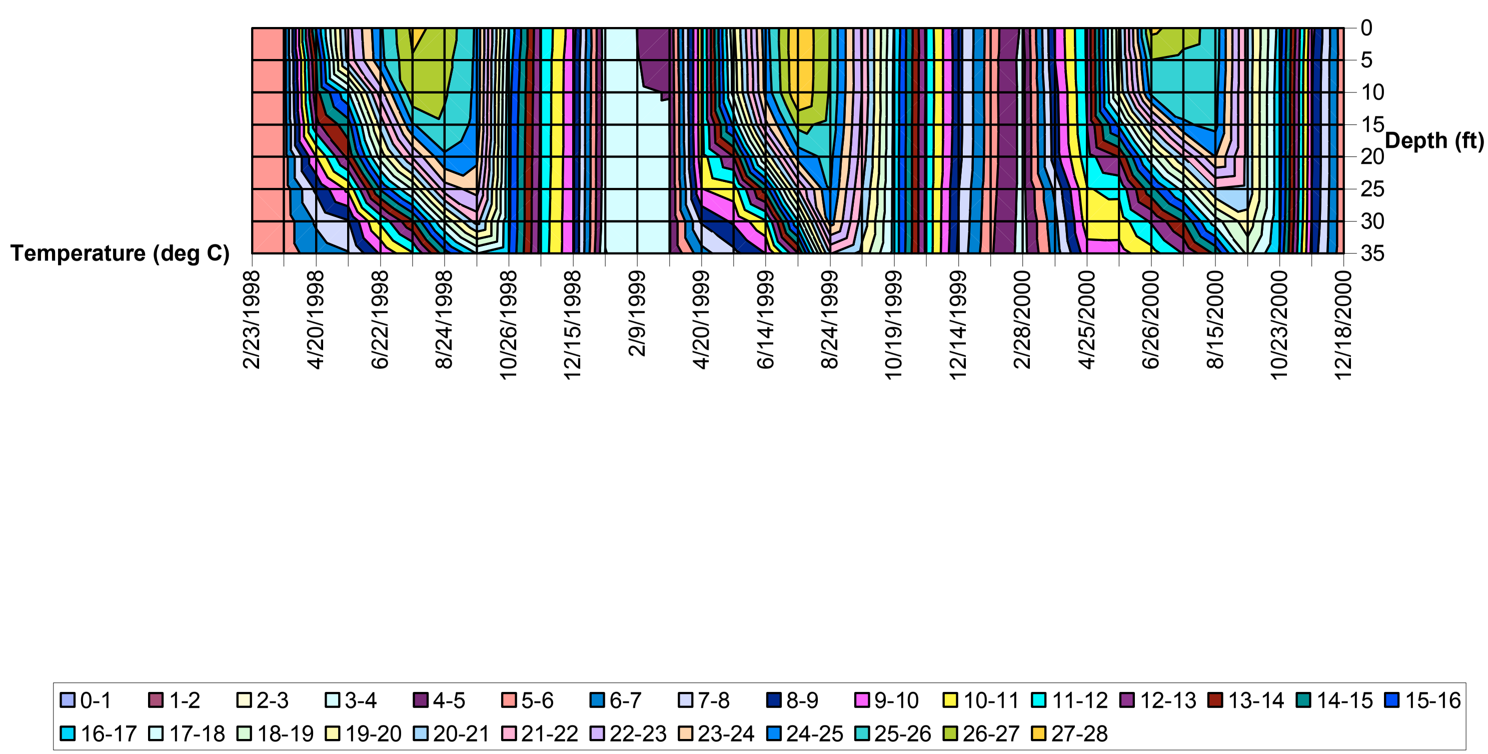

Figure C.8. Isothermal Contours, Prettyboy Reservoir, Middle Sampling Location, 2001-2004

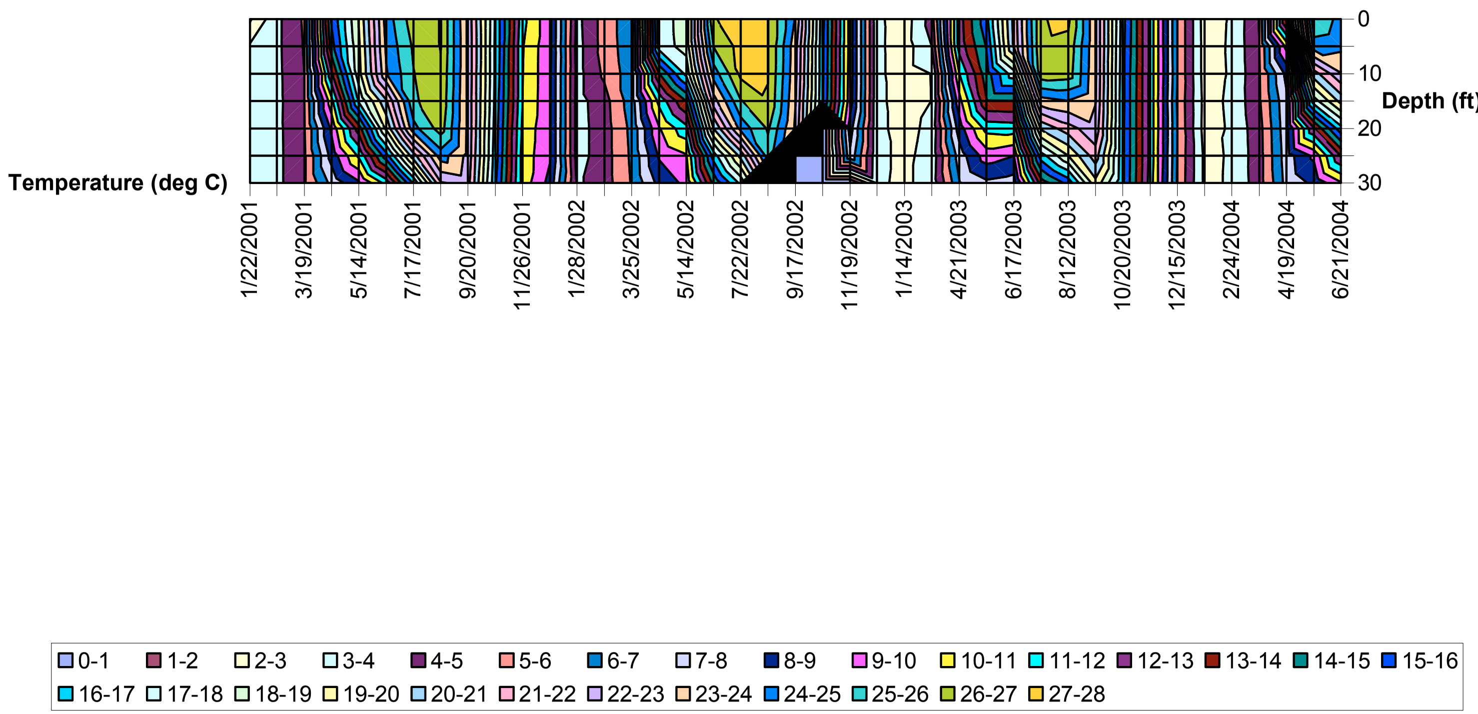

Figure C.9. Isothermal Contours, Loch Raven Reservoir, Lower Sampling Locations, 1992-1994

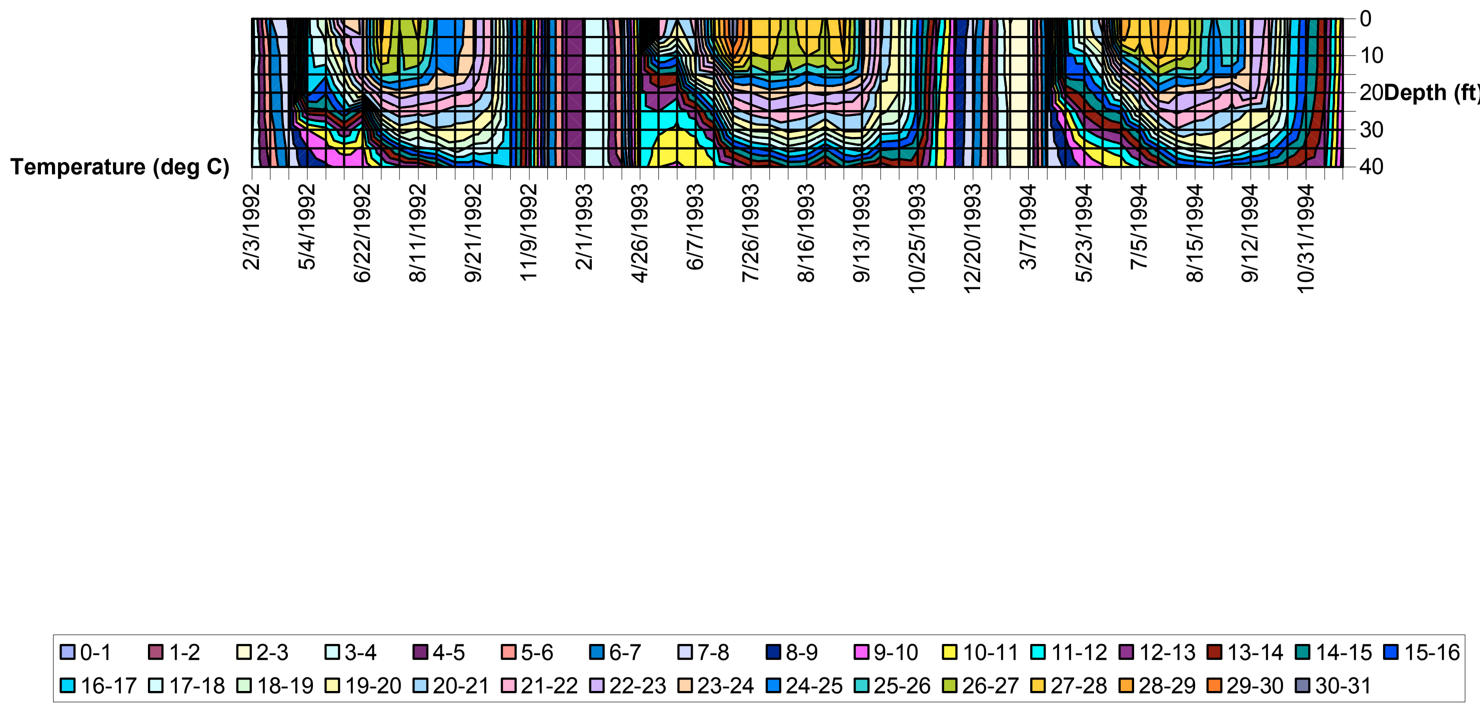

Figure C.10. Isothermal Contours, Loch Raven Reservoir, Lower Sampling Locations, 1995-1997

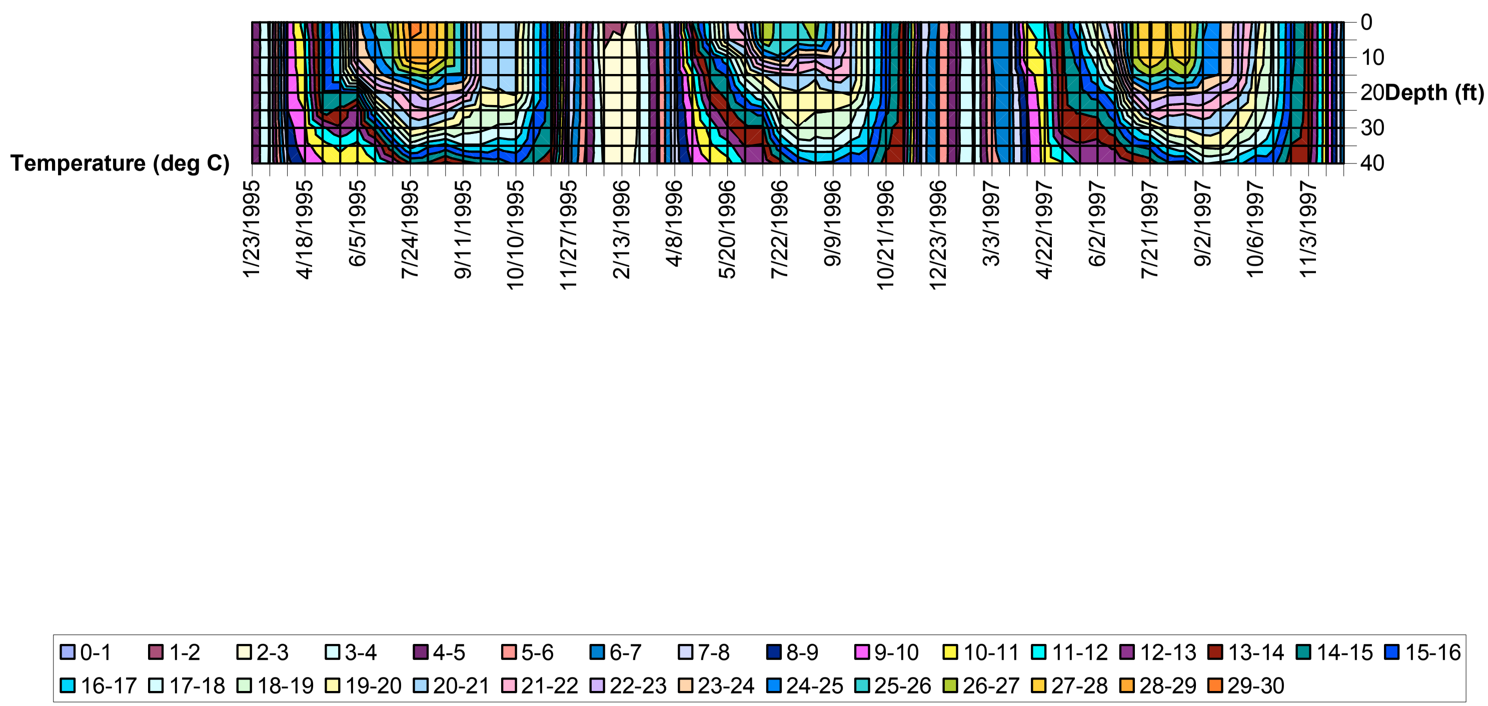

Figure C.11. Isothermal Contours, Loch Raven Reservoir, Lower Sampling Locations, 1998-2000

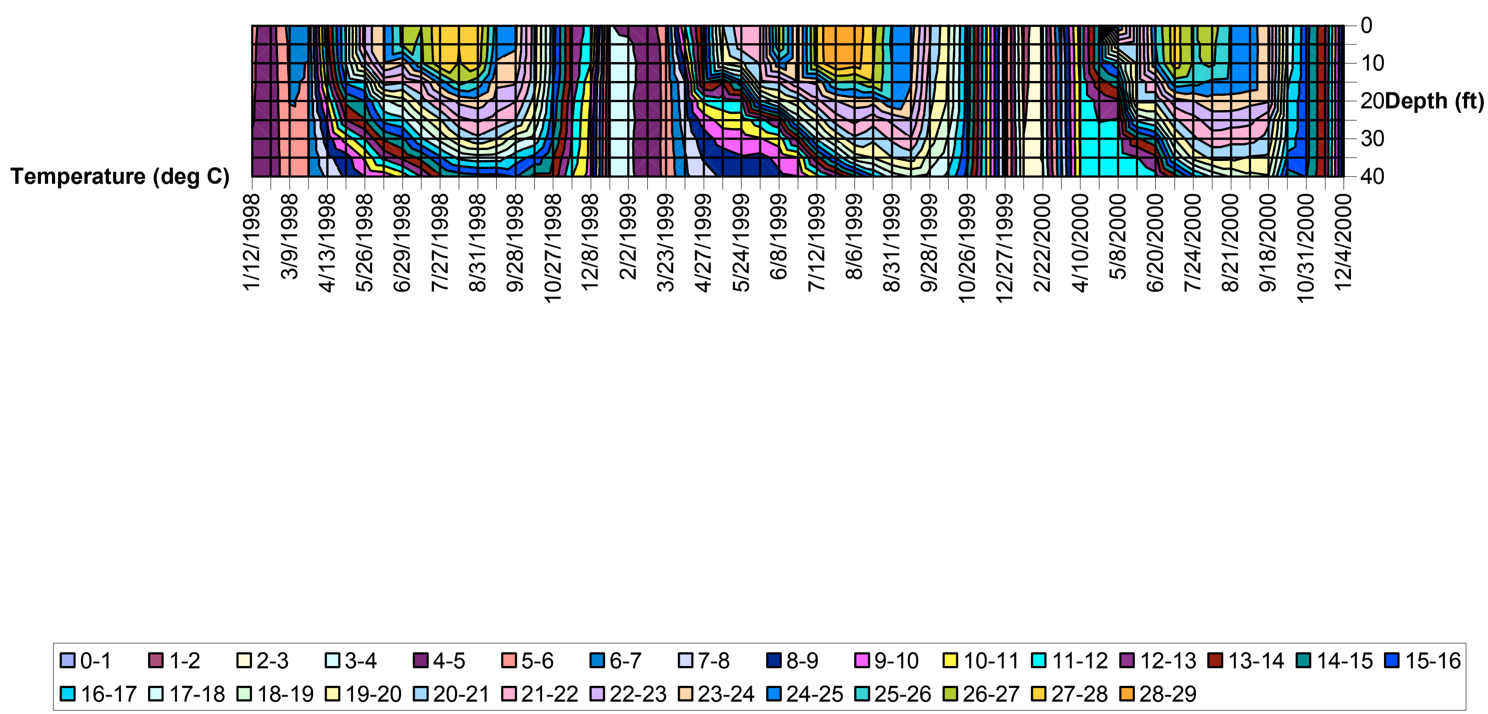

Figure C.12. Isothermal Contours, Loch Raven Reservoir, Lower Sampling Locations, 2001-2004

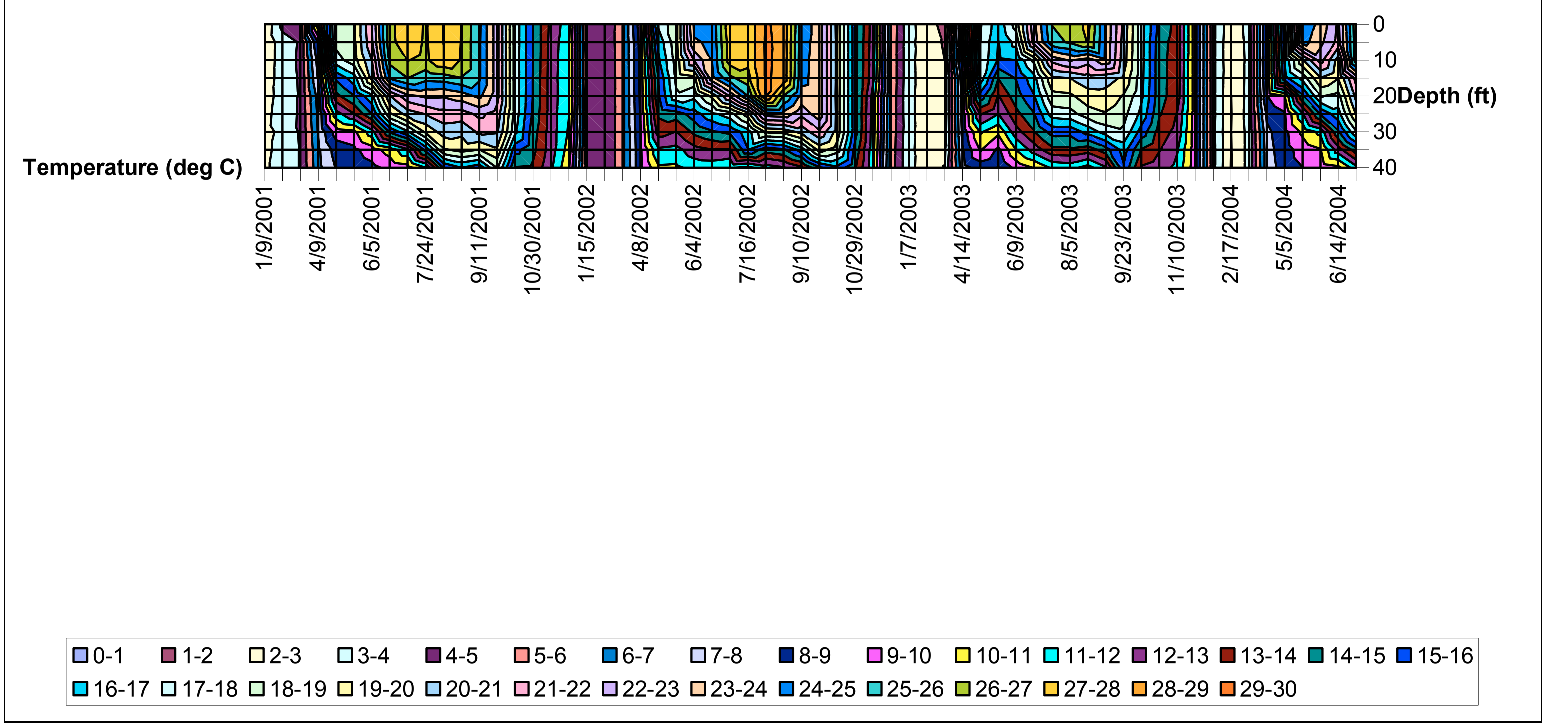

Figure C.13. Isothermal Contours, Loch Raven Reservoir, Middle Sampling Locations, 1992-1994

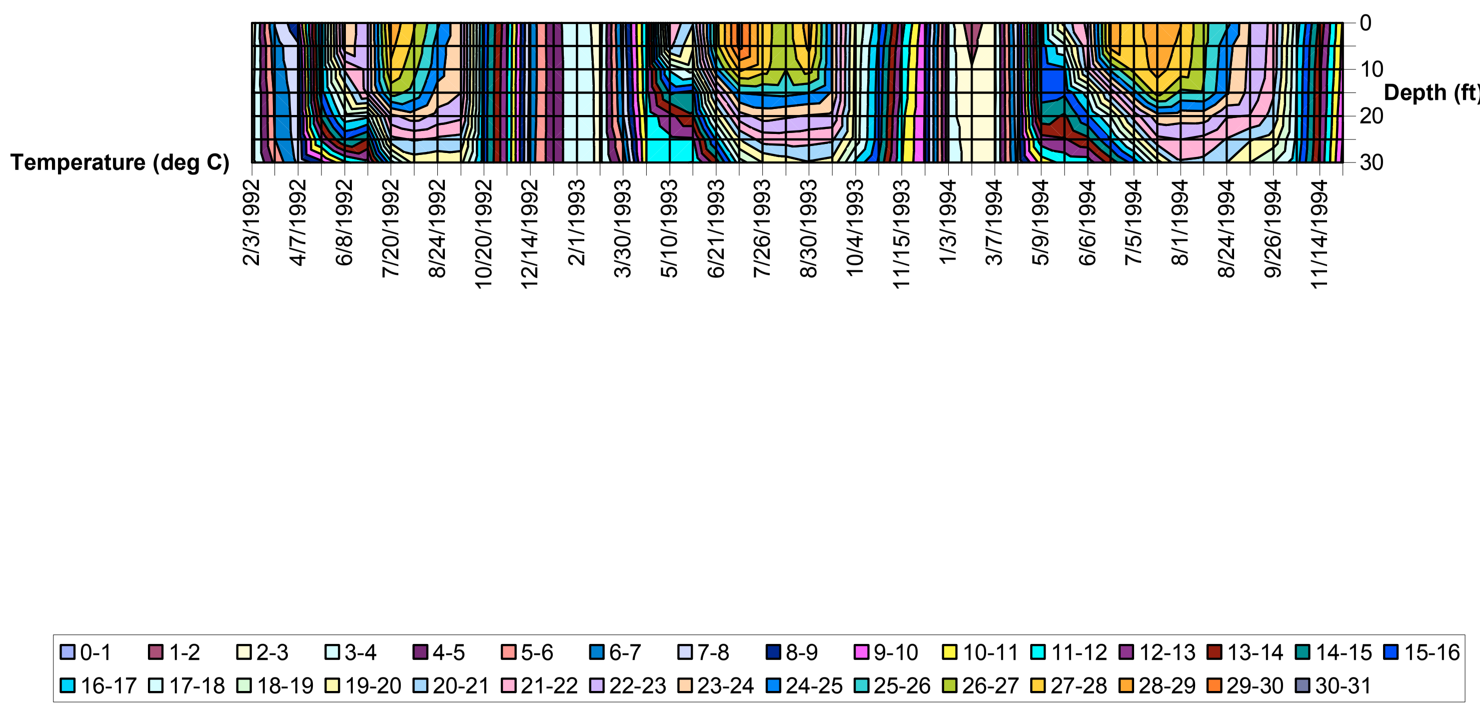

Figure C.14. Isothermal Contours, Loch Raven Reservoir, Middle Sampling Locations, 1995-1997

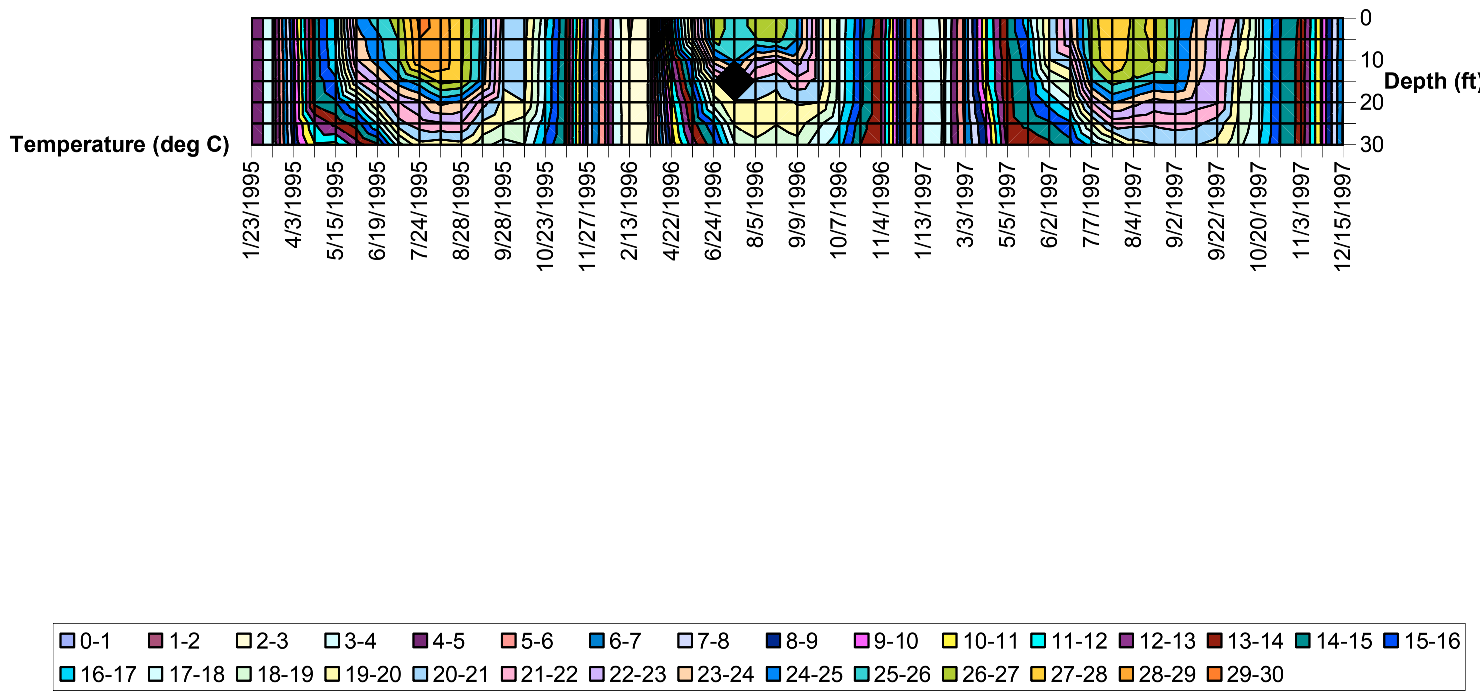

Figure C.15. Isothermal Contours, Loch Raven Reservoir, Middle Sampling Location, 1998-2000

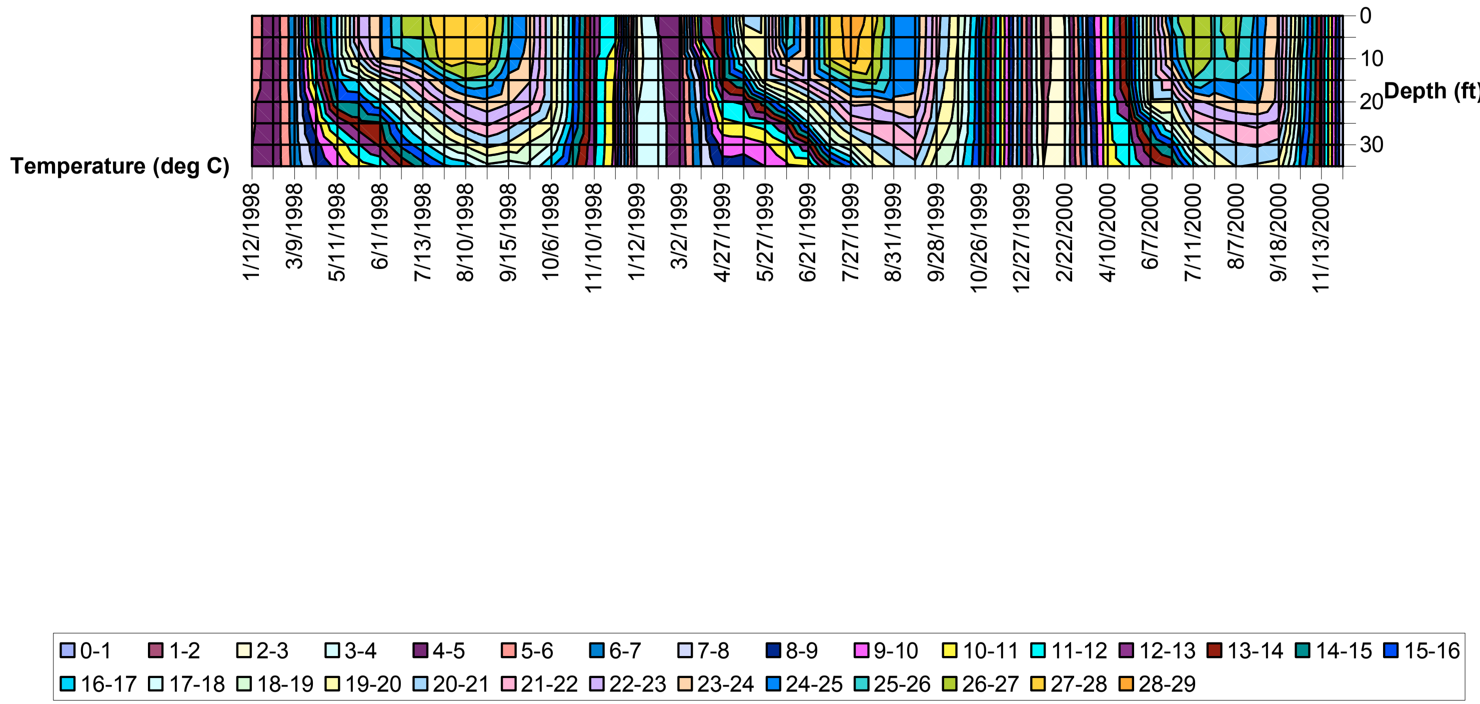

Figure C.16. Isothermal Contours, Loch Raven Reservoir, Middle Sampling Location, 2001-2004

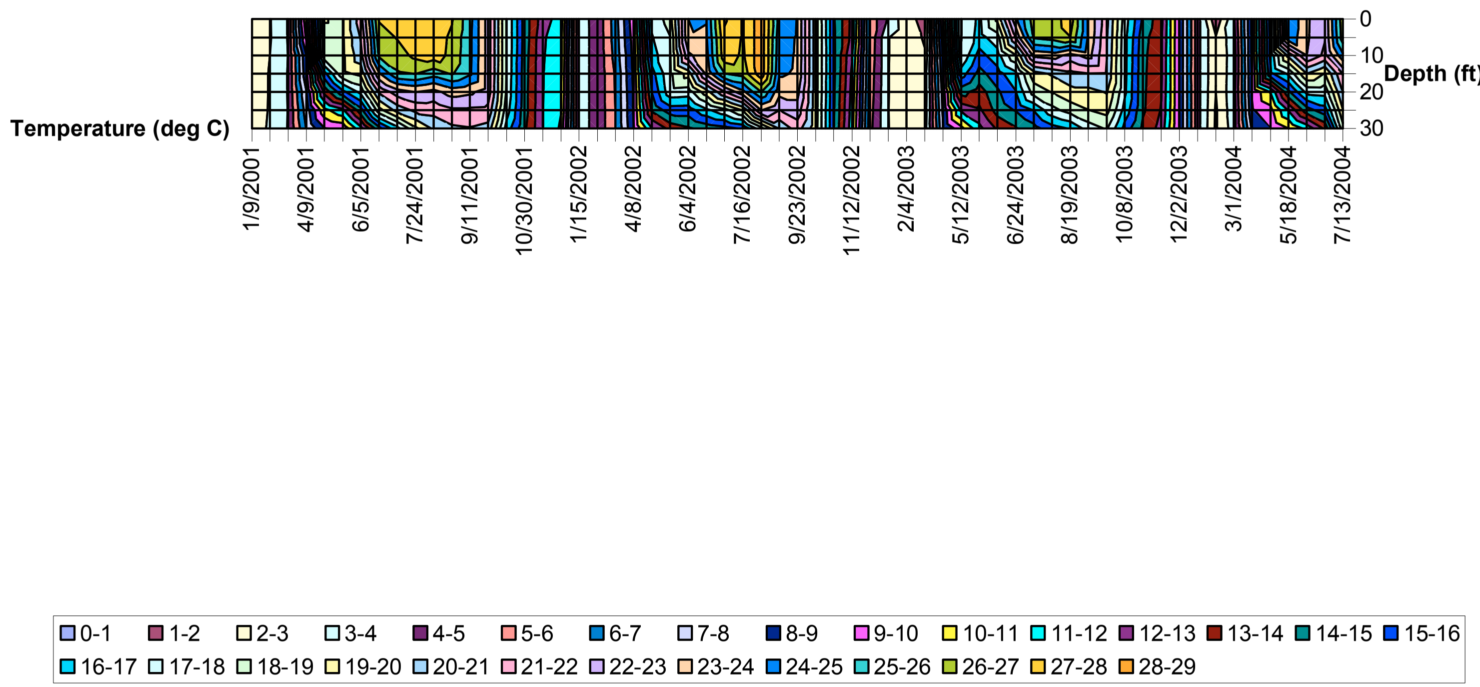

Figure C.17. Isothermal Contours, Loch Raven Reservoir, Upper Sampling Location, 1992-1994

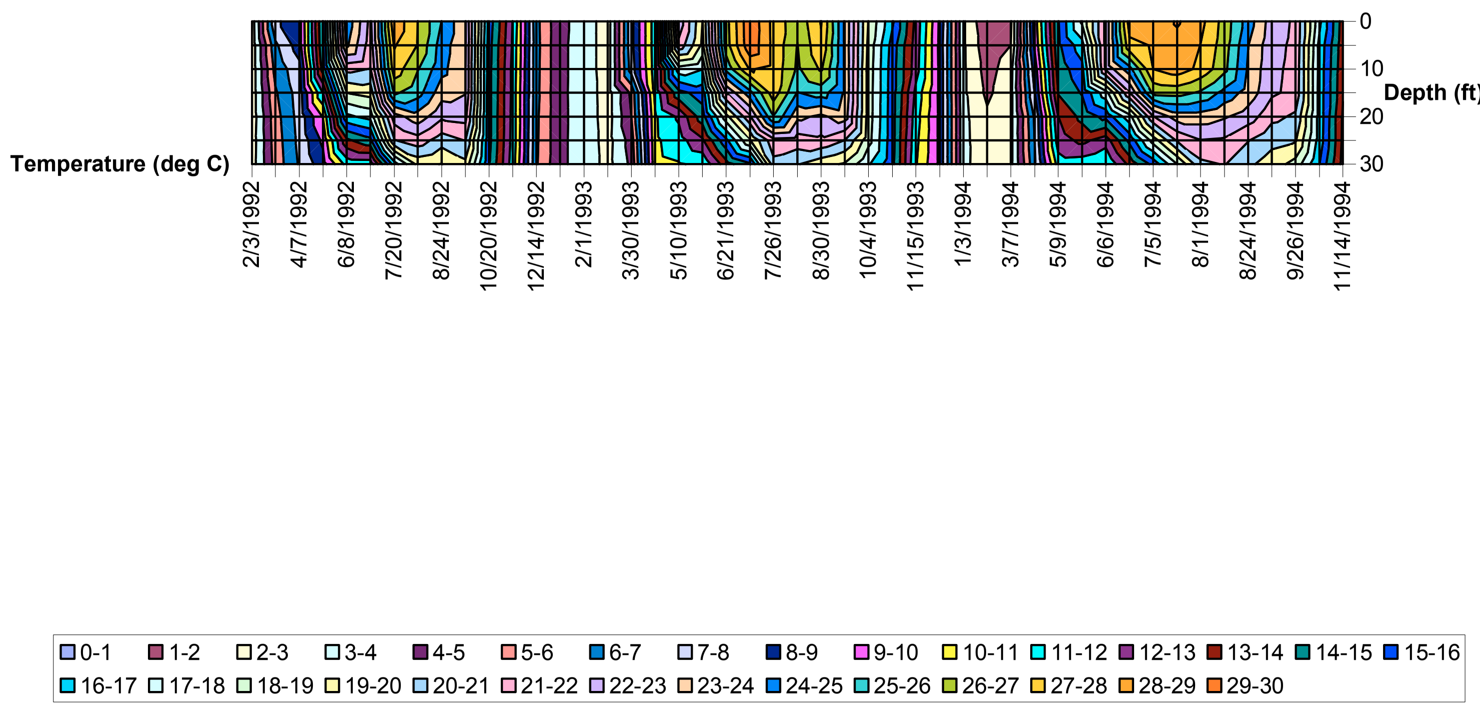

Figure C.18. Isothermal Contours, Loch Raven Reservoir, Upper Sampling Location, 1995-1997

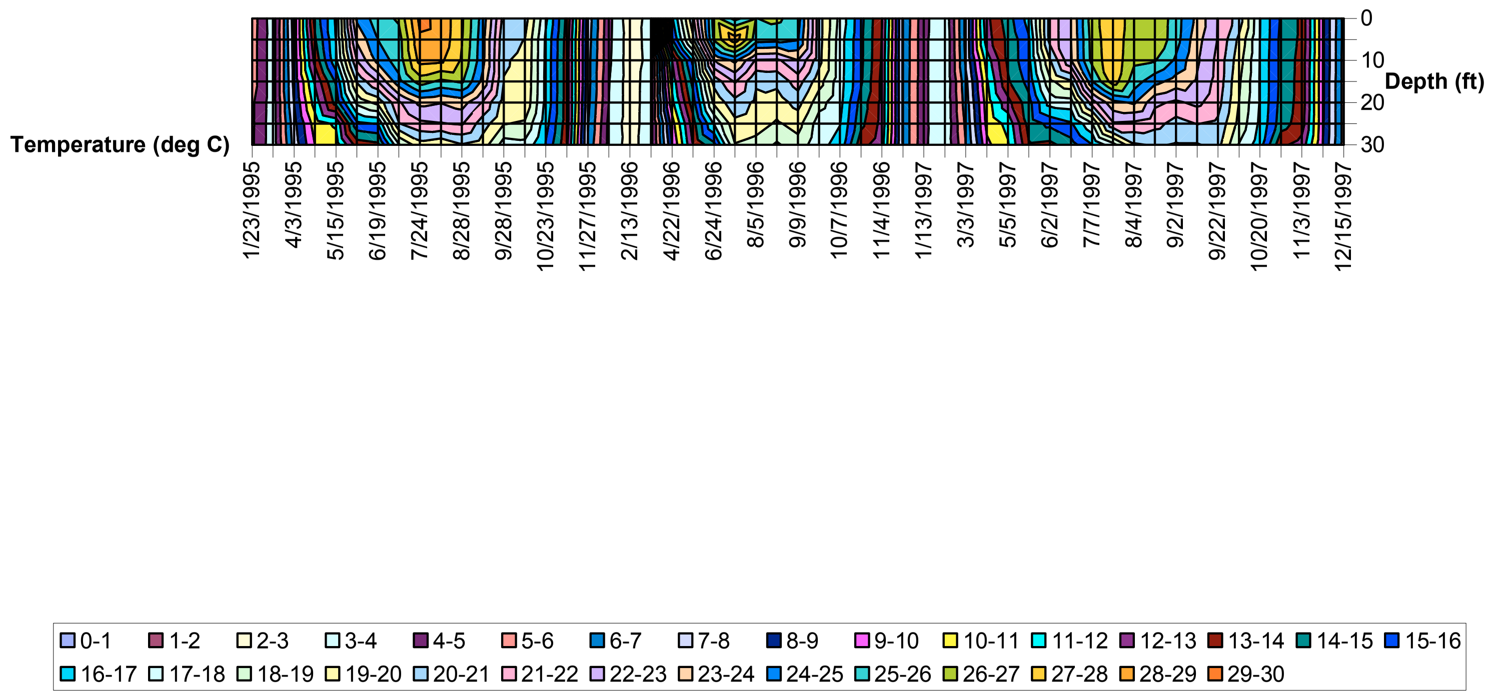

Figure C.19. Isothermal Contours, Loch Raven Reservoir, Upper Sampling Location, 1998-2000

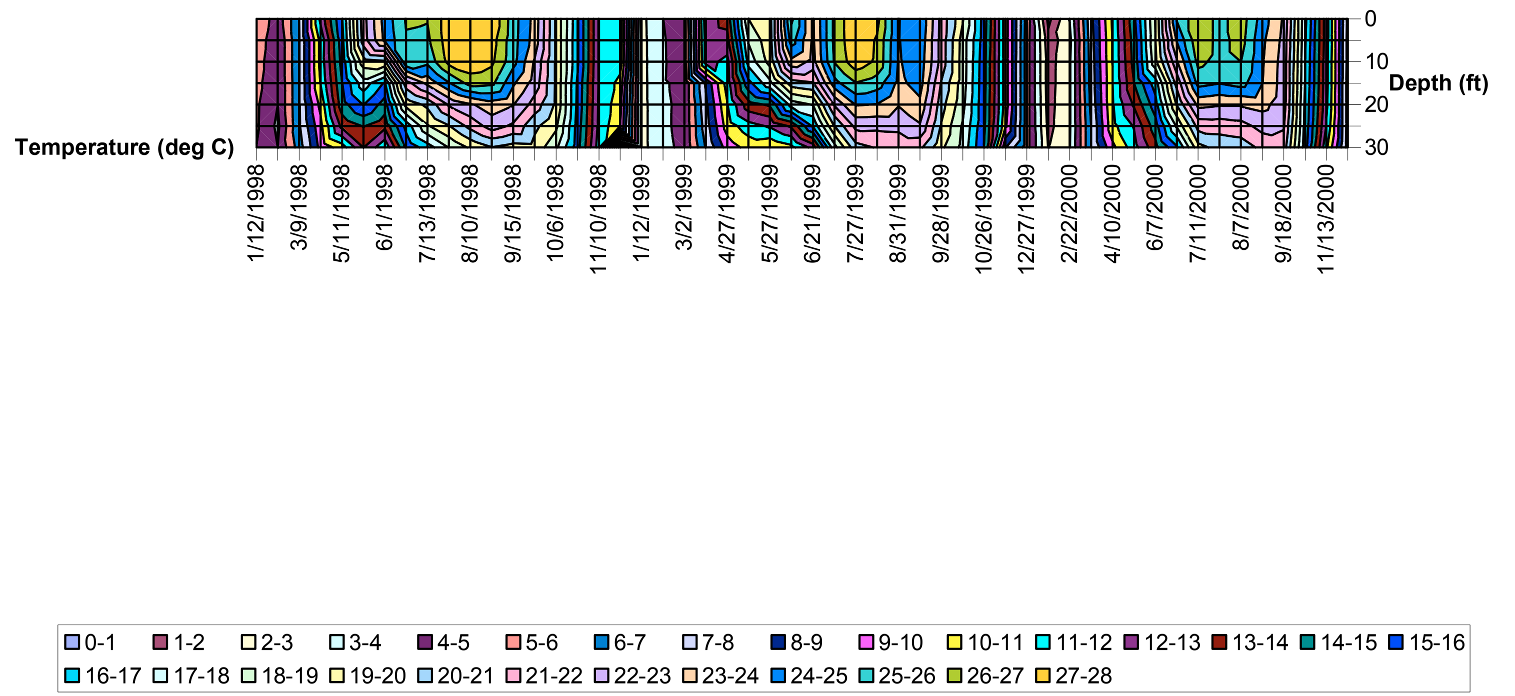

Figure C.20. Isothermal Contours, Loch Raven Reservoir, Upper Sampling Location, 2001-2004

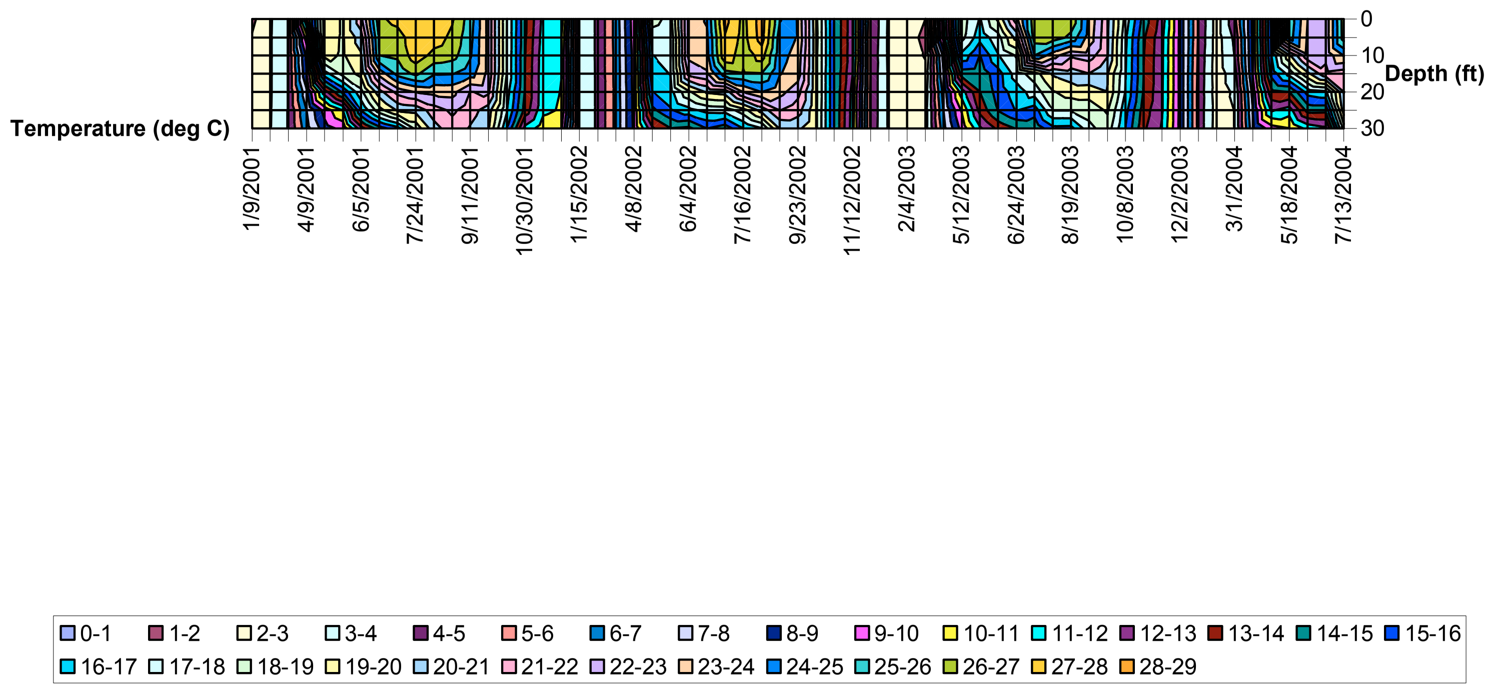

Figure C.21. Average Bottom Dissolved Oxygen. Lower Sampling Locations, Prettyboy Reservoir

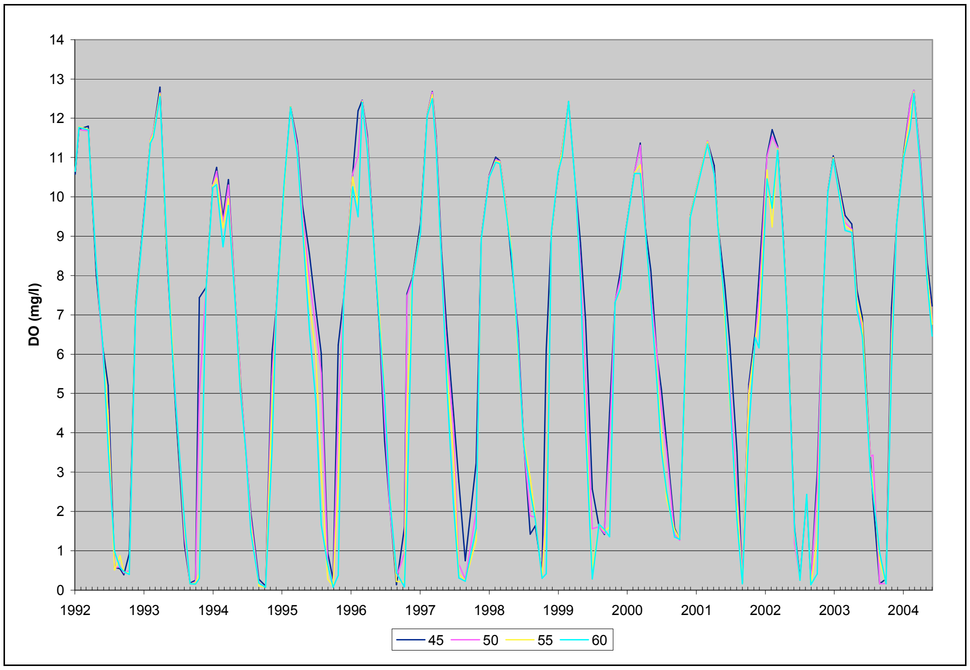

Figure C.22. Average Bottom Dissolved Oxygen. Middle Sampling Location, Prettyboy Reservoir

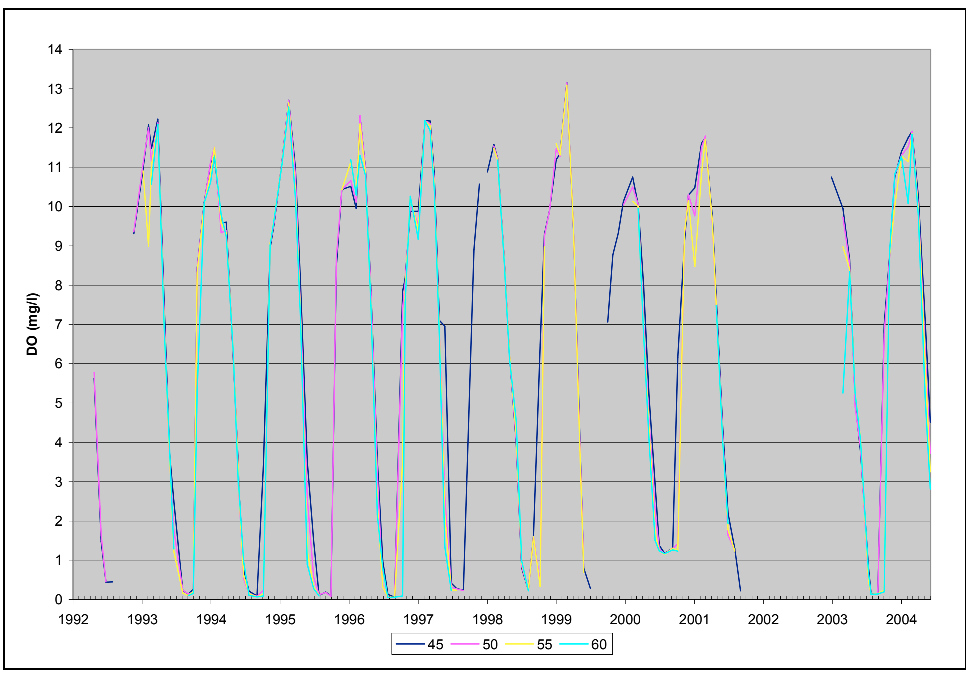

Figure C.23. Average Bottom Dissolved Oxygen. Lower Sampling Location, Loch Raven Reservoir

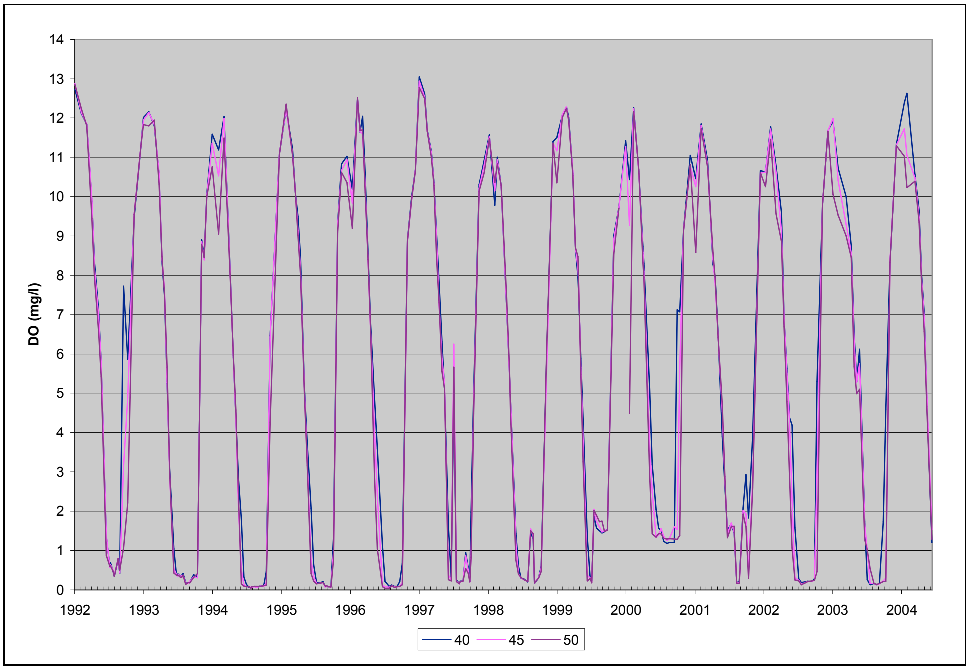

Figure C.24. Average Bottom Dissolved Oxygen. Middle Sampling Locations, Loch Raven Reservoir

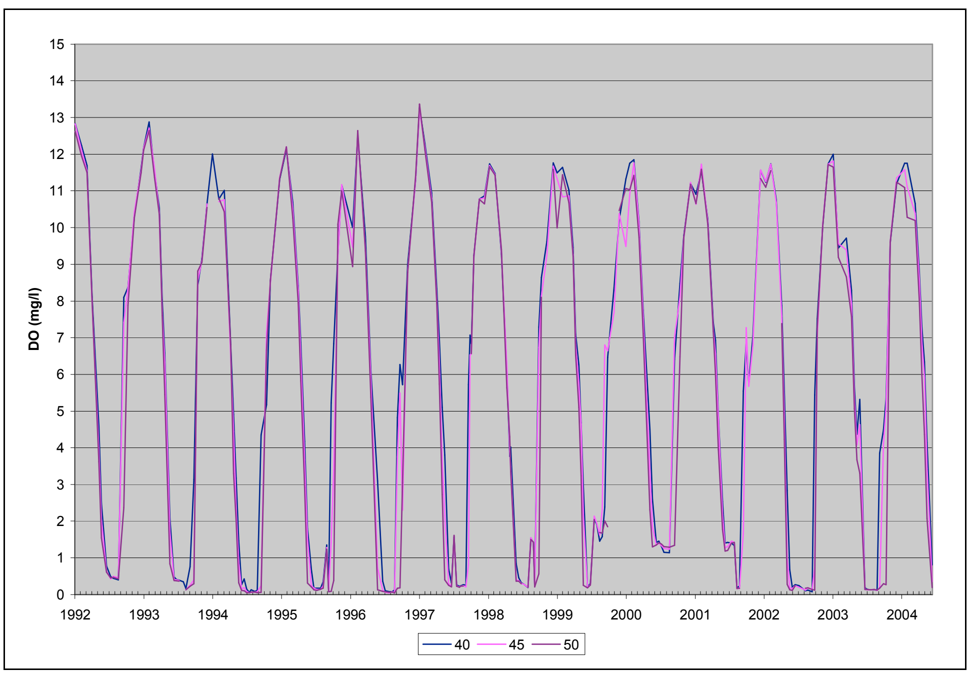

Figure C.25. Average Bottom Dissolved Oxygen. Upper Sampling Locations, Loch Raven Reservoir

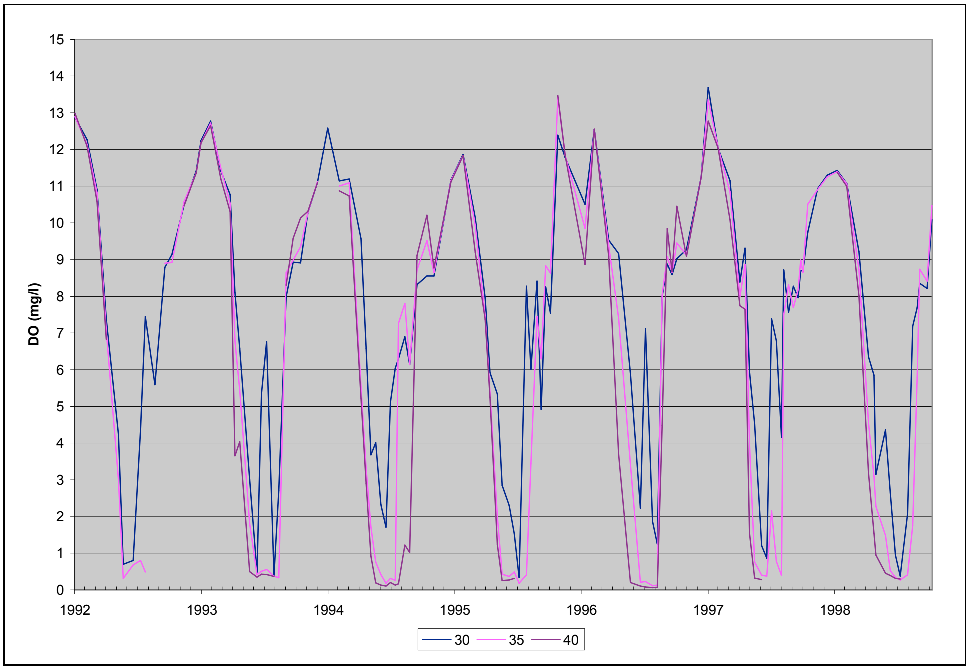

Figure C.26. Average Surface Dissolved Oxygen. Lower Sampling Locations, Prettyboy Reservoir

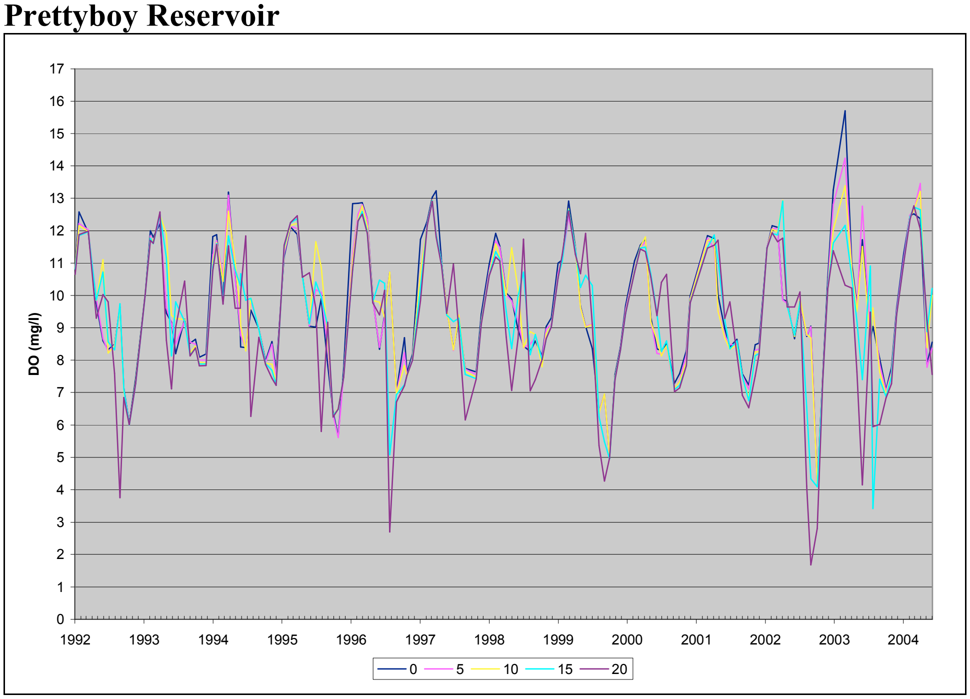

Figure C.27. Average Surface Dissolved Oxygen. Middle Sampling Location, Prettyboy Reservoir

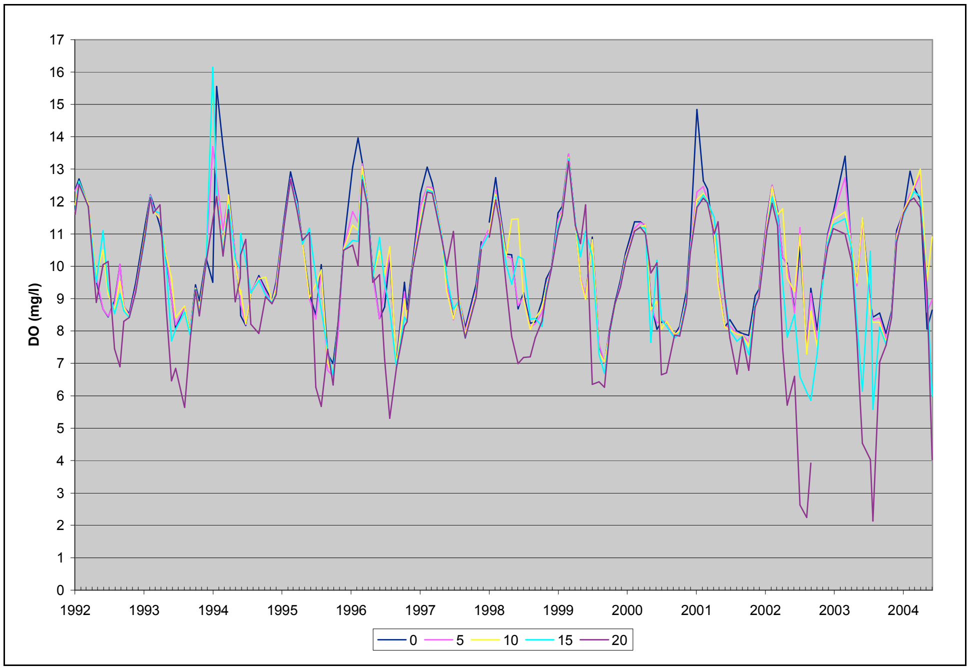

Figure C.28. Average Surface Dissolved Oxygen. Lower Sampling Location, Loch Raven Reservoir

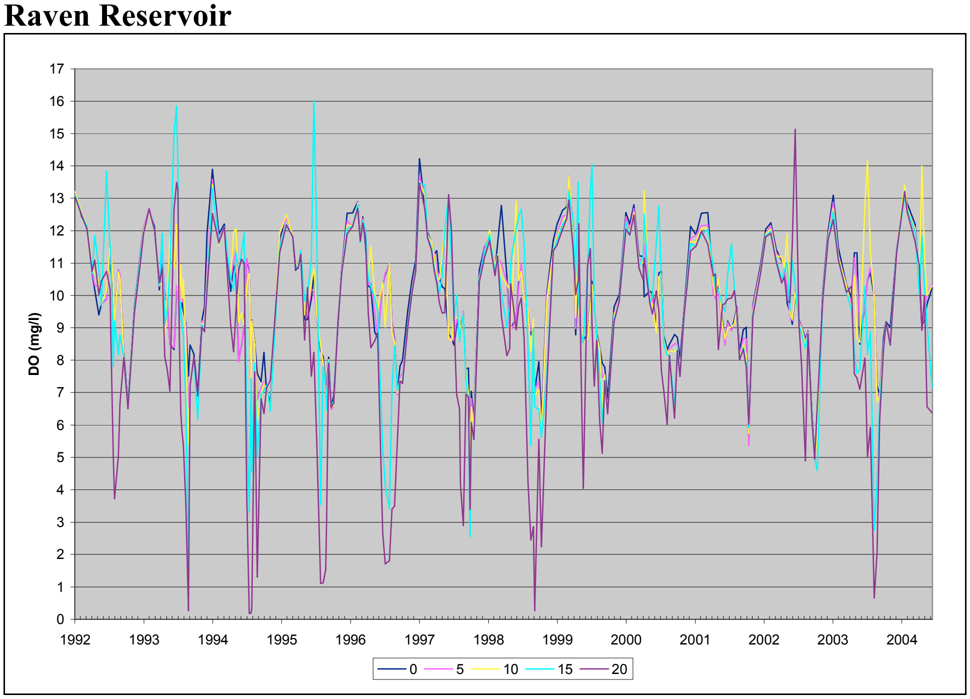

Figure C.29. Average Surface Dissolved Oxygen. Middle Sampling Locations, Loch Raven Reservoir

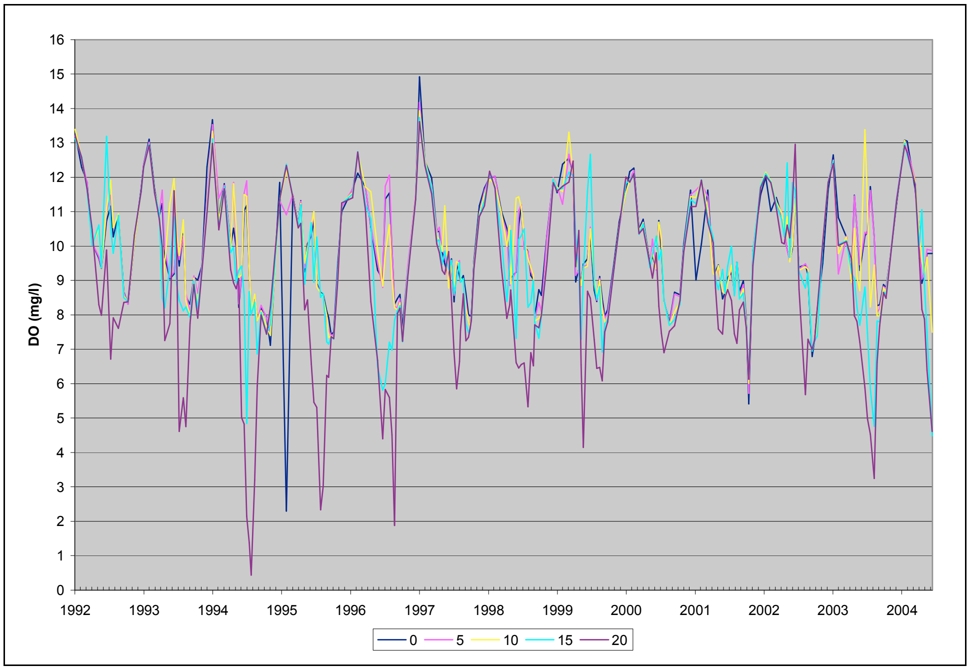

Figure C.30. Average Surface Dissolved Oxygen. Upper Sampling Locations, Loch Raven Reservoir

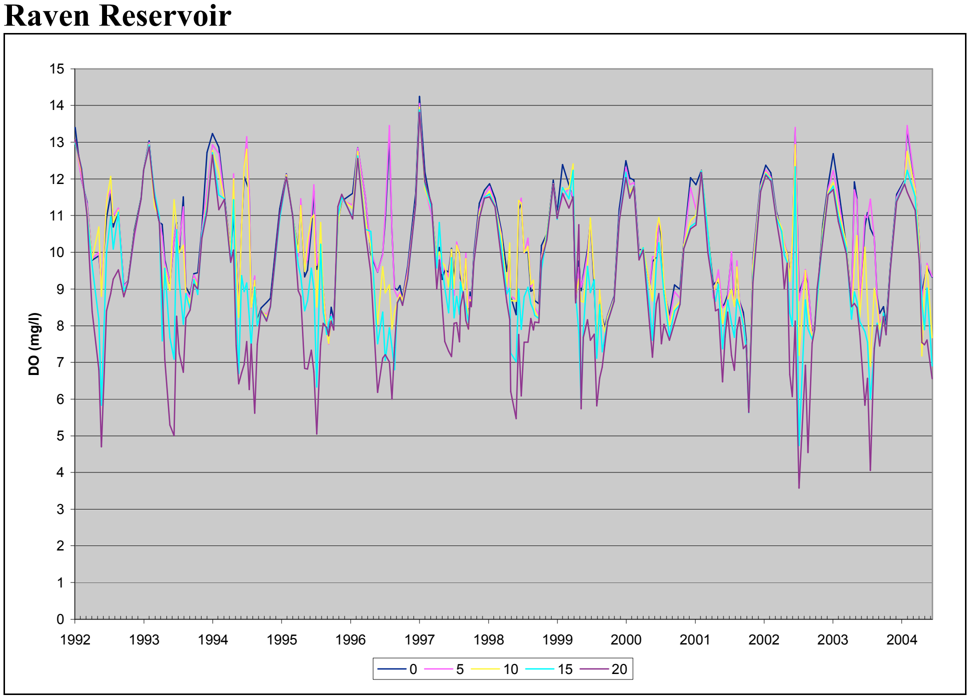

Figure C.31. Average Total Phosphorus. Lower Sampling Locations, Prettyboy Reservoir

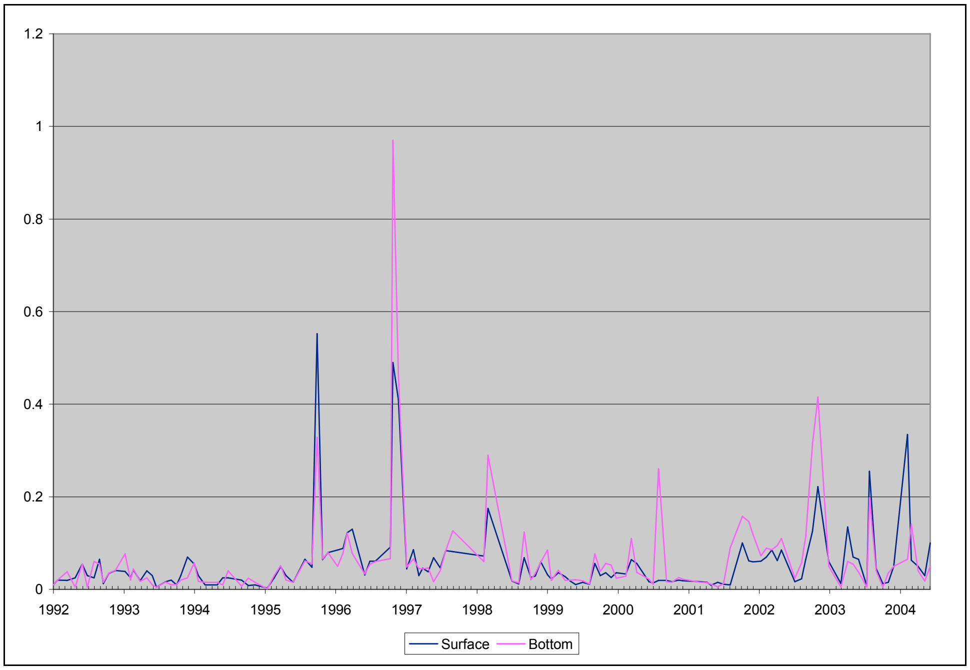

Figure C.32. Average Total Phosphorus. Middle Sampling Location, Prettyboy Reservoir

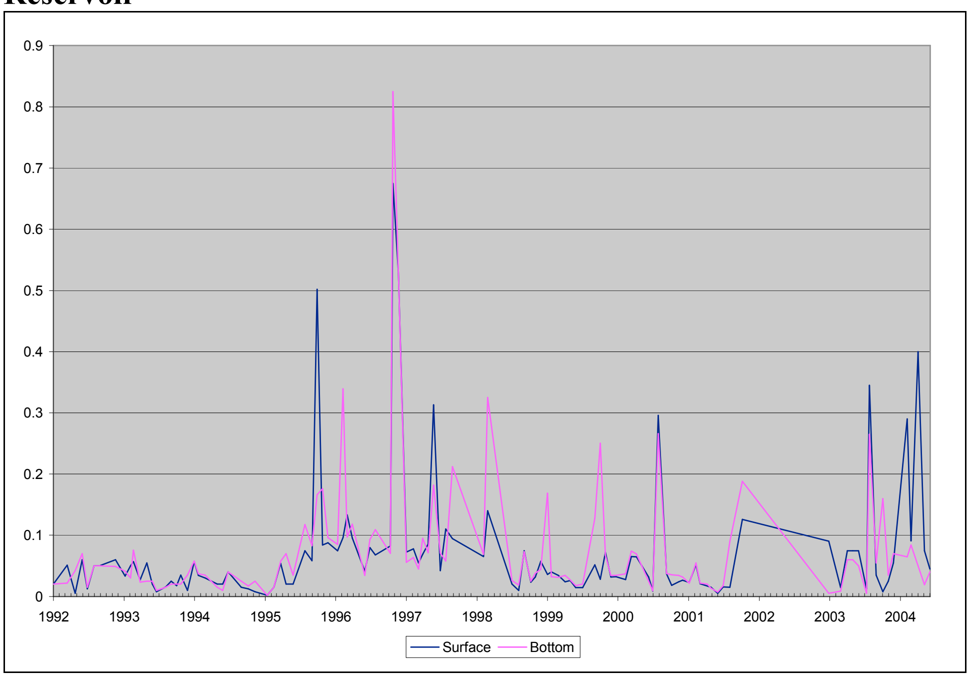

Figure C.33. Average Total Phosphorus. Lower Sampling Location, Loch Raven Reservoir

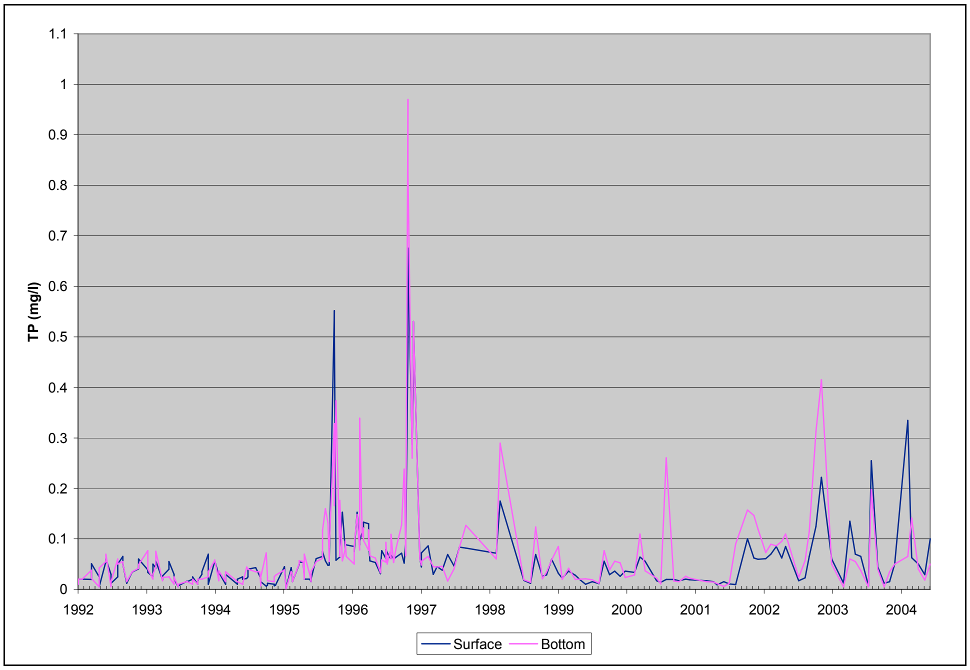

Figure C.34. Average Total Phosphorus. Middle Sampling Locations, Loch Raven Reservoir

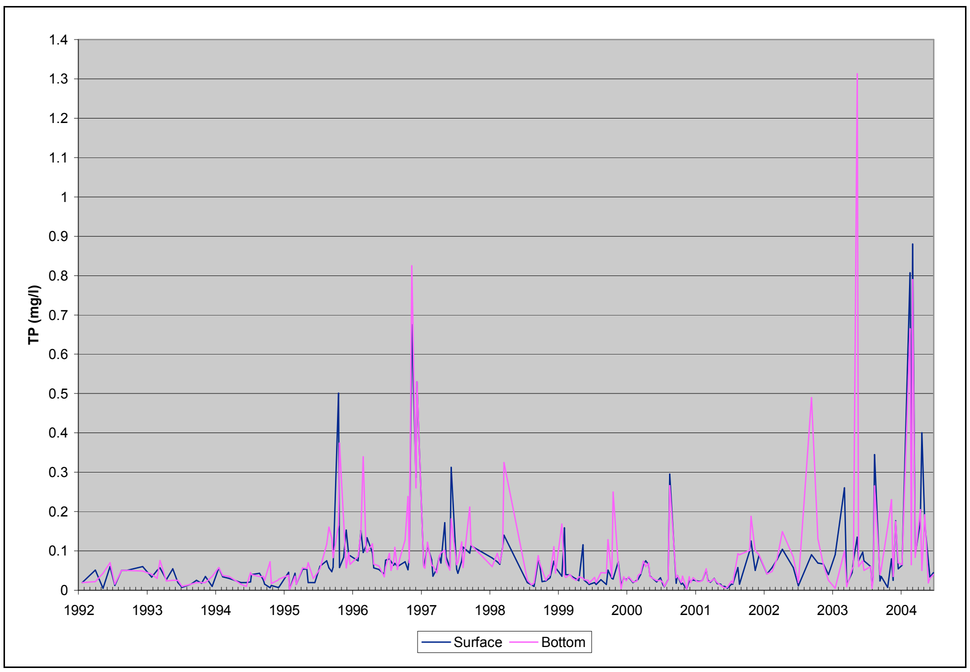

Figure C.35. Average Total Phosphorus. Upper Sampling Locations, Loch Raven Reservoir

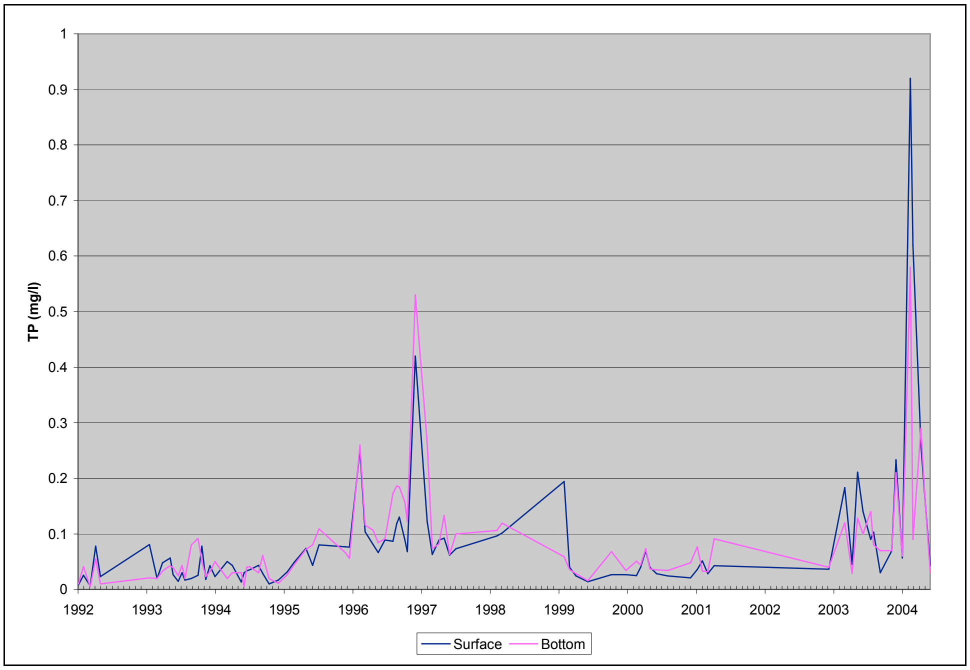

Figure C.36. Average Ammonia Nitrogen. Lower Sampling Locations, Prettyboy Reservoir

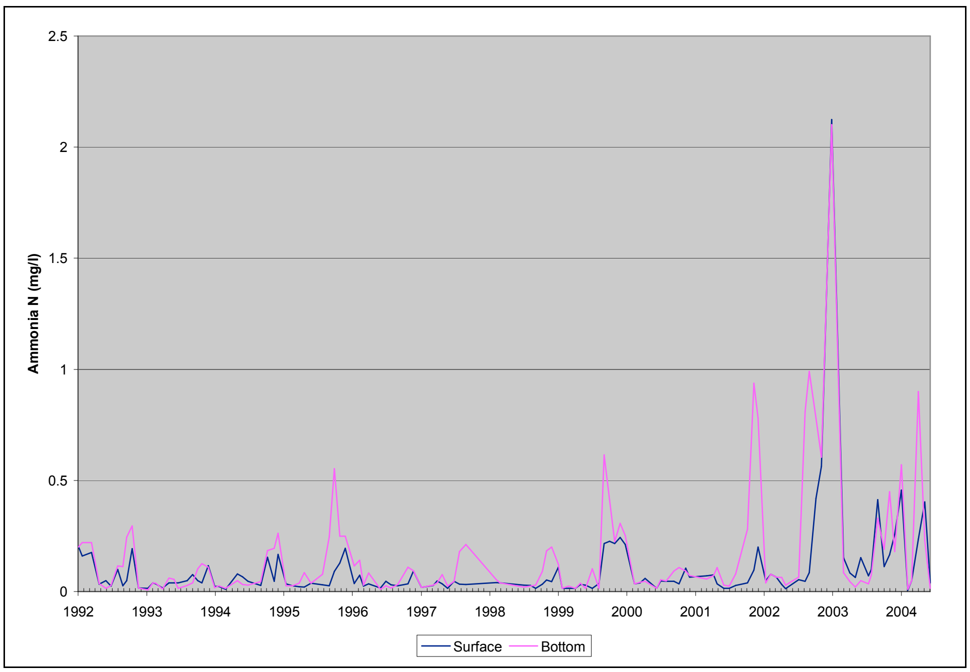

Figure C.37. Average Ammonia Nitrogen. Middle Sampling Location, Prettyboy Reservoir

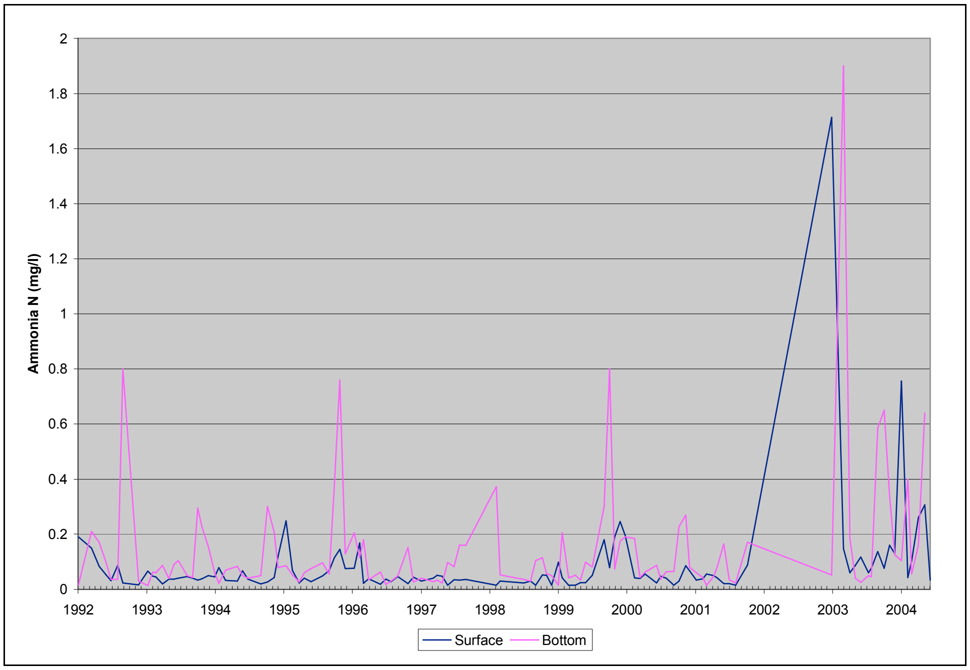

Figure C.38. Average Ammonia Nitrogen. Lower Sampling Location, Loch Raven Reservoir

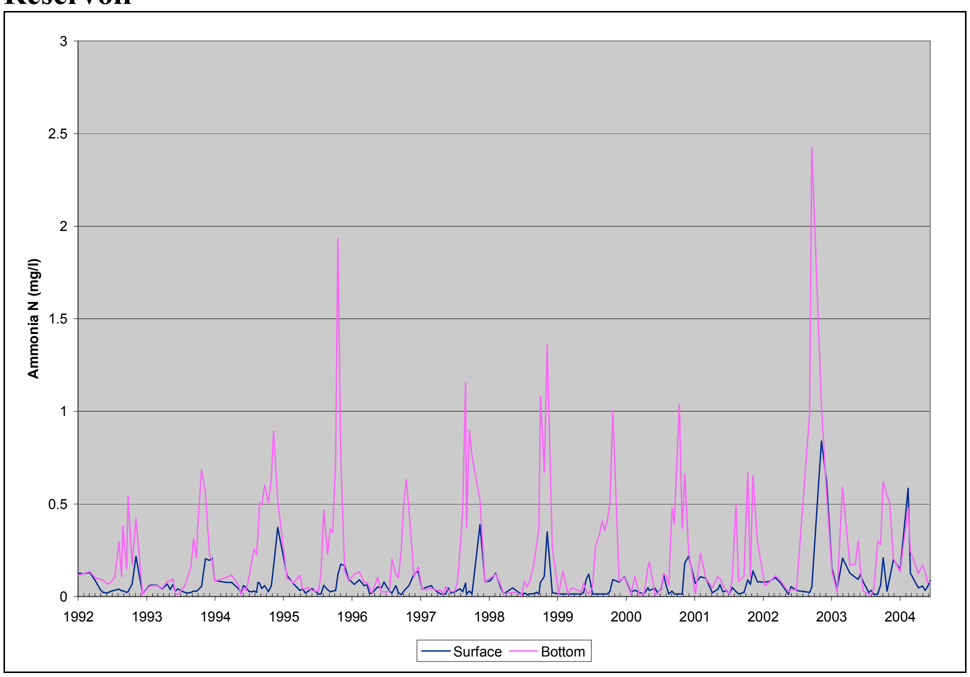

Figure C.39. Average Ammonia Nitrogen. Middle Sampling Locations, Loch Raven Reservoir

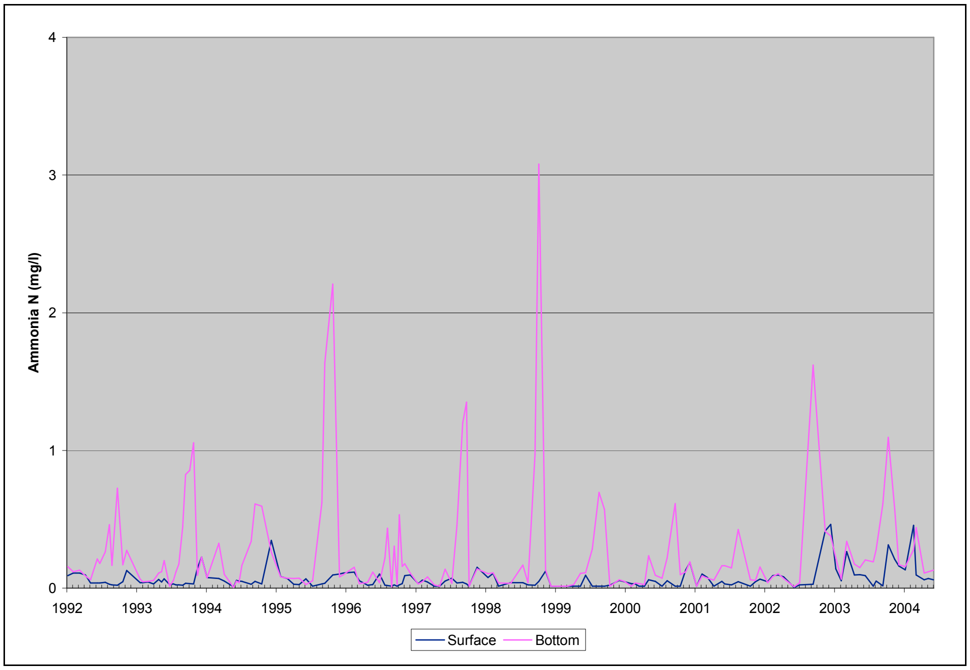

Figure C.40. Average Ammonia Nitrogen. Upper Sampling Locations, Loch Raven Reservoir

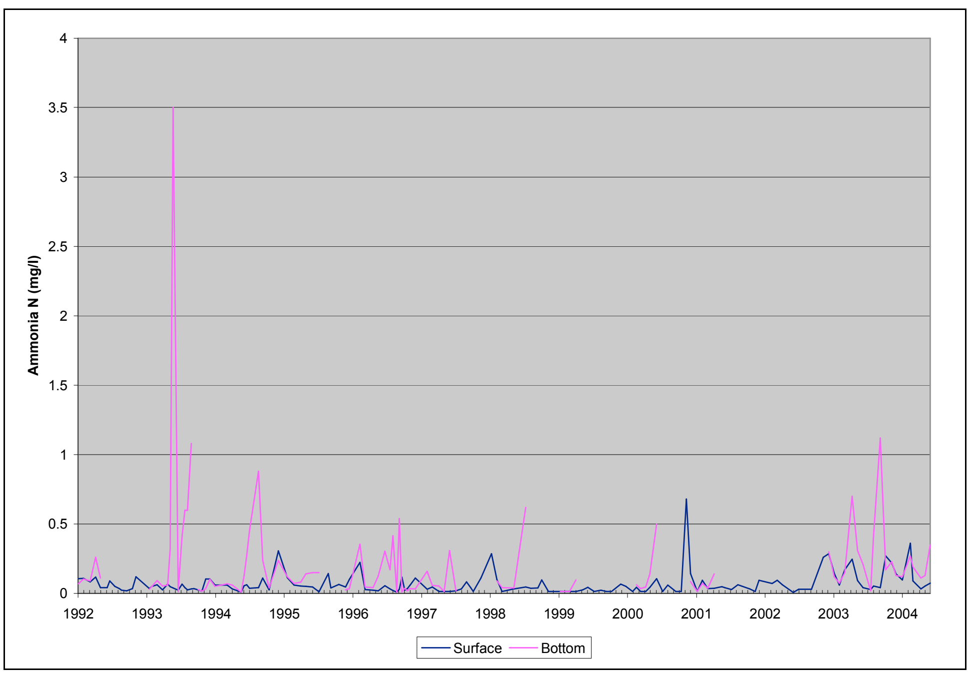

Figure C.41. Average Nitrate Nitrogen. Lower Sampling Locations, Prettyboy Reservoir

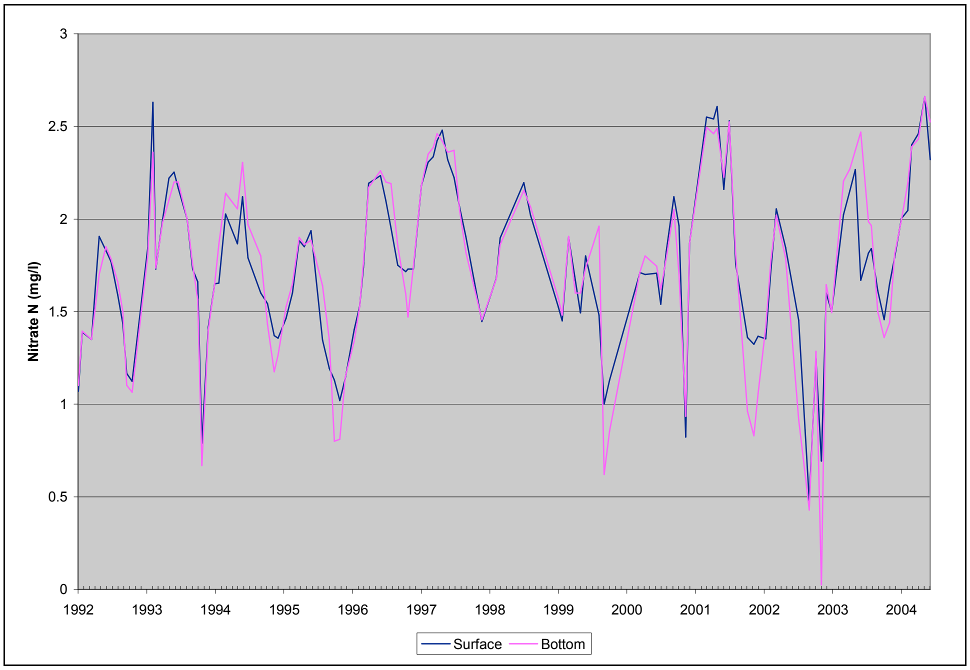

Figure C.42. Average Nitrate Nitrogen. Middle Sampling Location, Prettyboy Reservoir

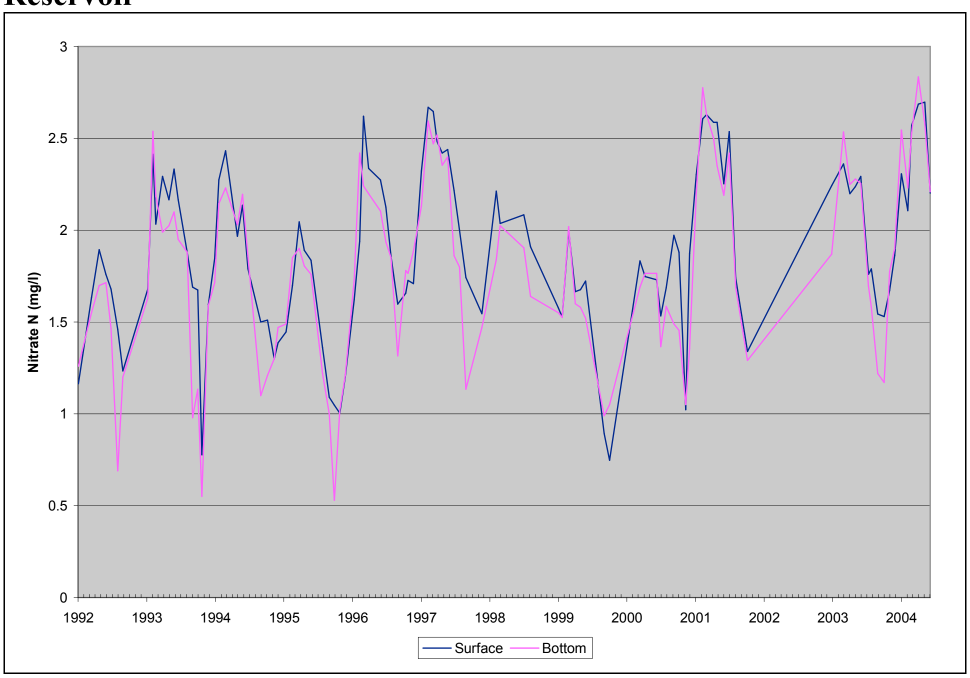

Figure C.43. Average Nitrate Nitrogen. Lower Sampling Location, Loch Raven Reservoir

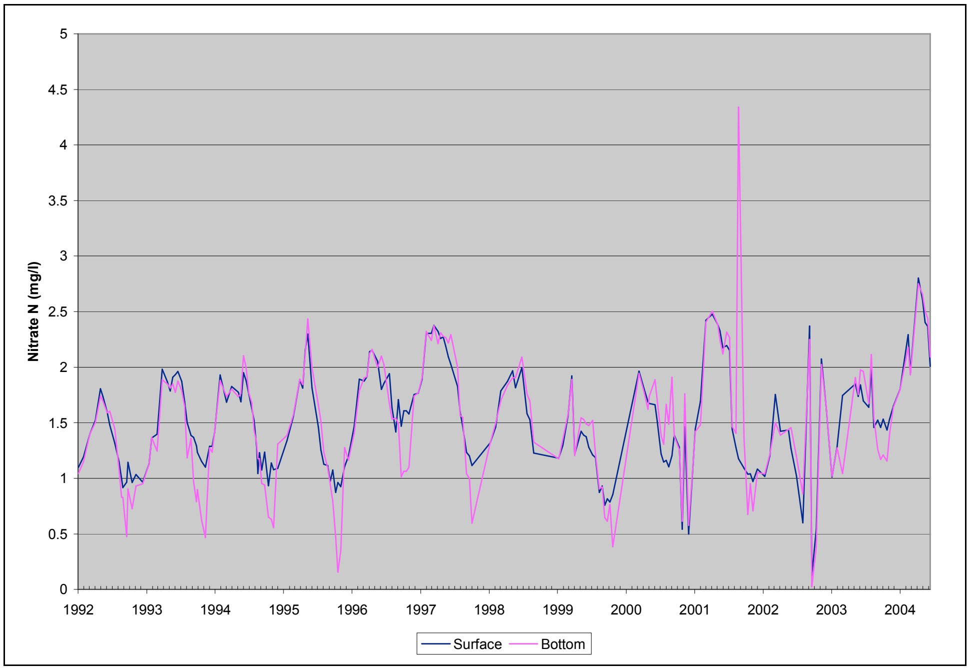

Figure C.44. Average Nitrate Nitrogen. Middle Sampling Locations, Loch Raven Reservoir

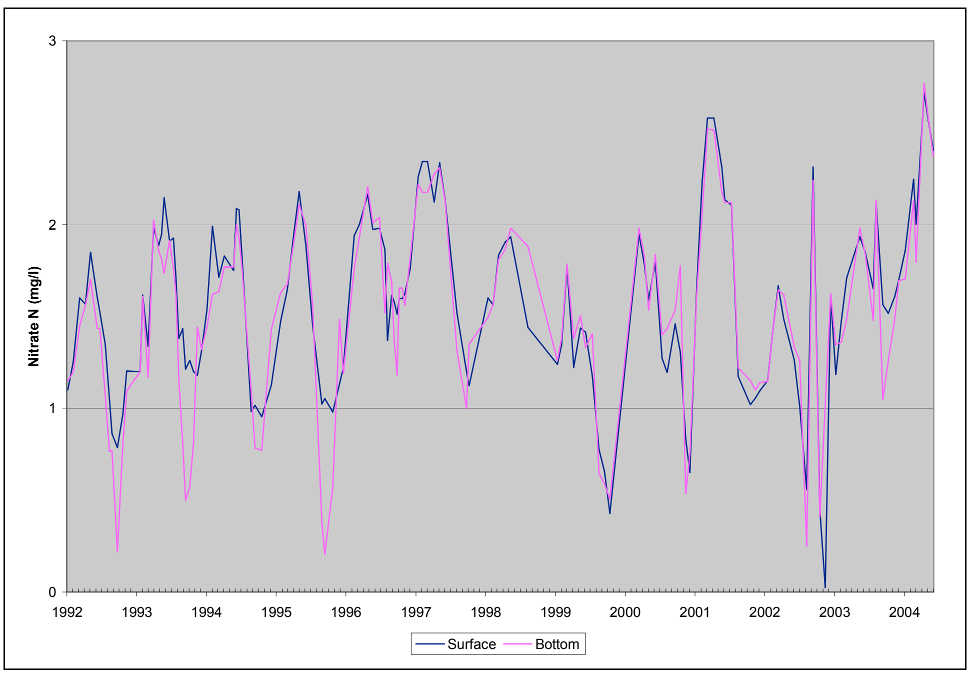

Figure C.45. Average Nitrate Nitrogen. Upper Sampling Locations, Loch Raven Reservoir

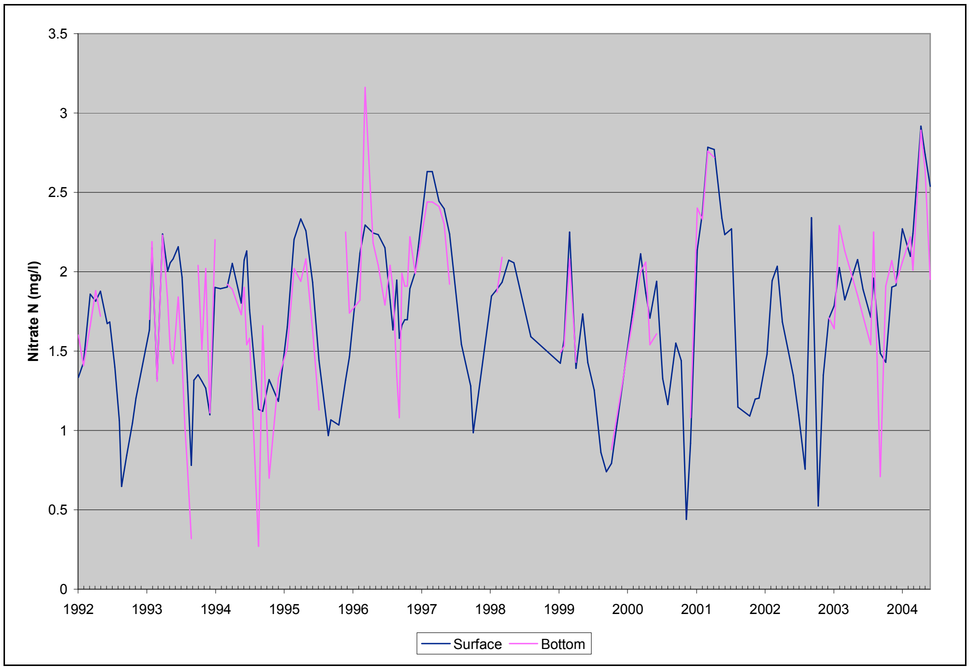

Figure C.36. Average Secchi Depth. Lower Sampling Locations, Prettyboy Reservoir

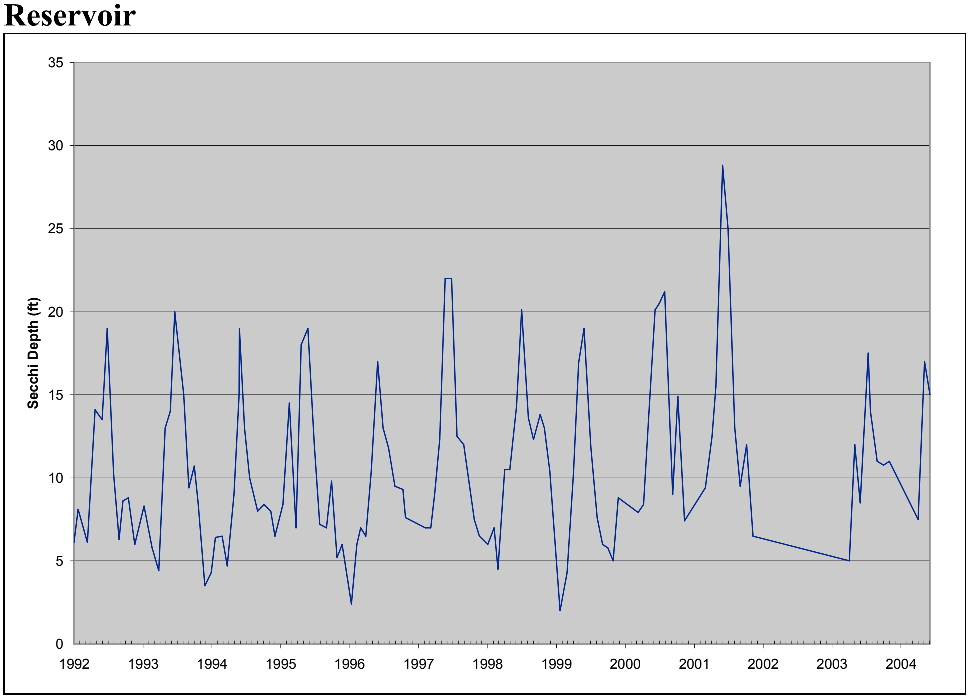

Figure C.37. Average Secchi Depth. Middle Sampling Location, Prettyboy Reservoir

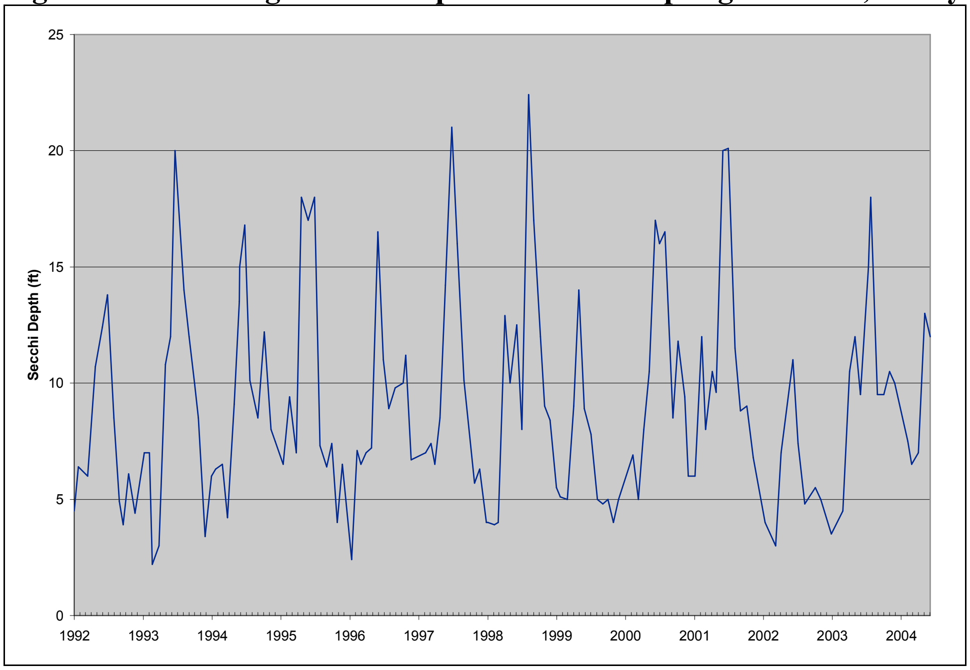

Figure C.38. Average Secchi Depth. Lower Sampling Location, Loch Raven Reservoir

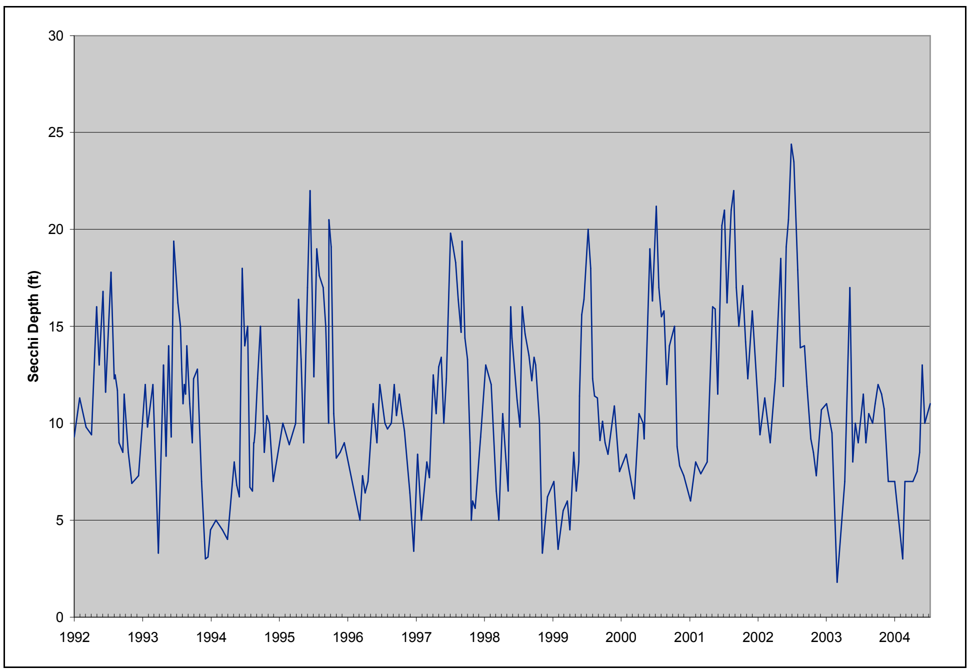

Figure C.39. Average Secchi Depth. Middle Sampling Locations, Loch Raven Reservoir

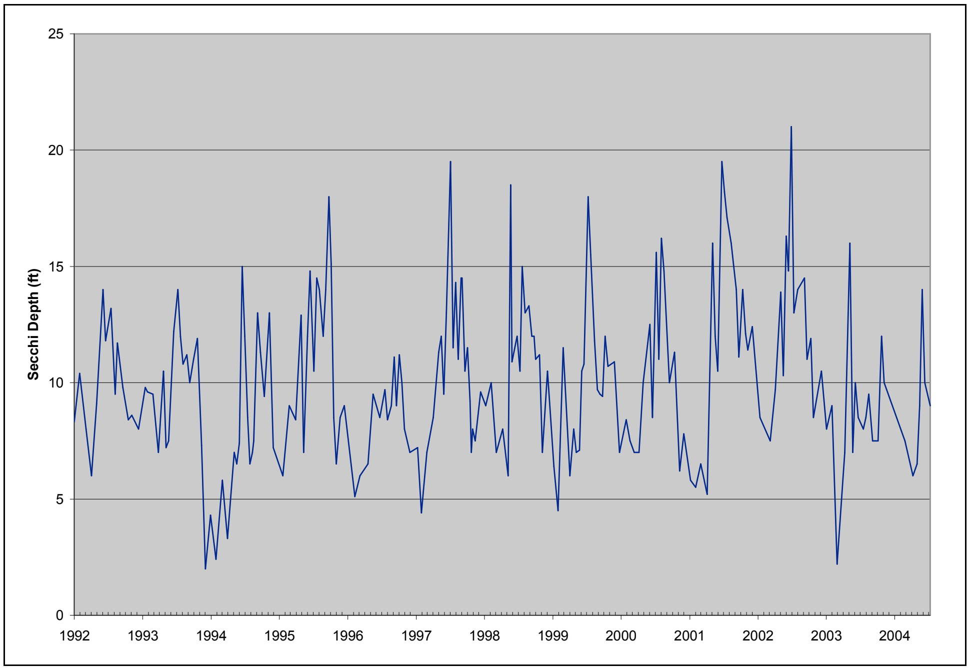

Figure C.40. Average Secchi Depth. Upper Sampling Locations, Loch Raven Reservoir

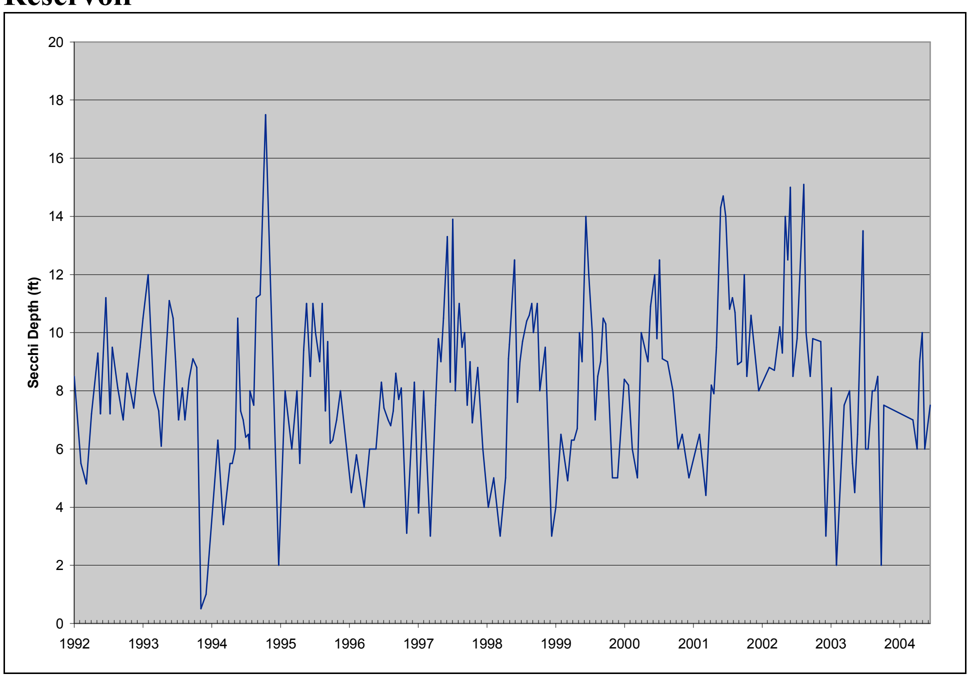

Figure C.51. Surface Chlorophyll a. Lower Sampling Locations, Prettyboy Reservoir

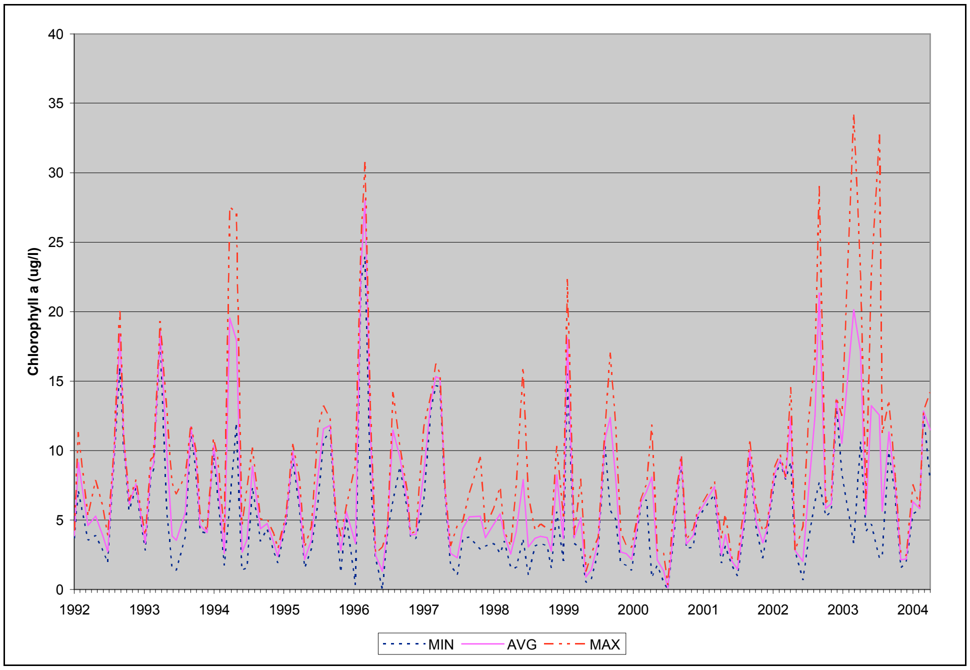

Figure C.52. Surface Chlorophyll a. Middle Sampling Location, Prettyboy Reservoir

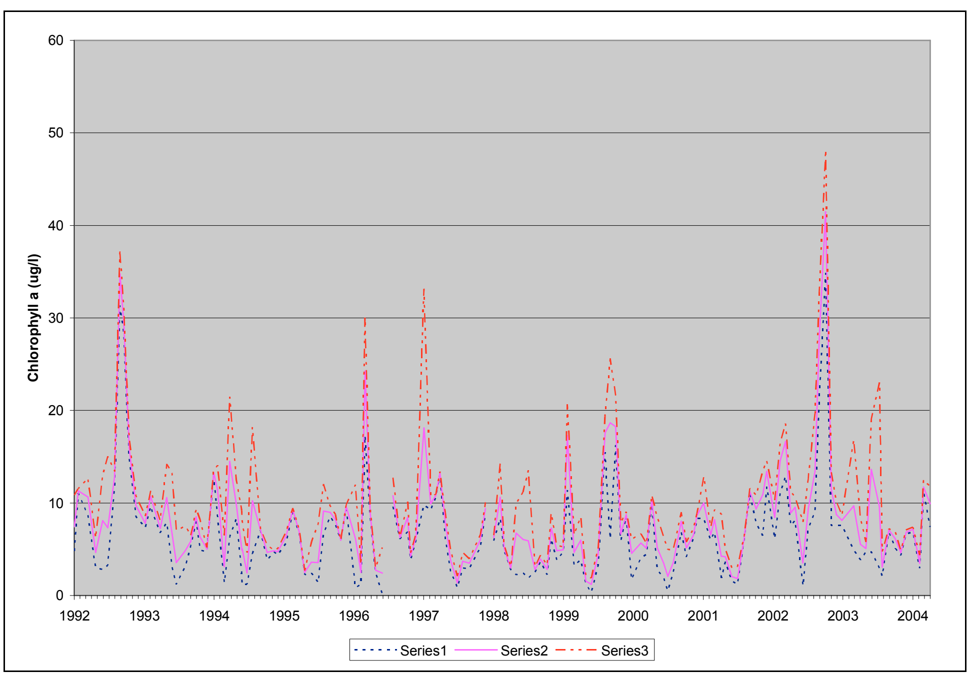

Figure C.53. Surface Chlorophyll a. Lower Sampling Location, Loch Raven Reservoir

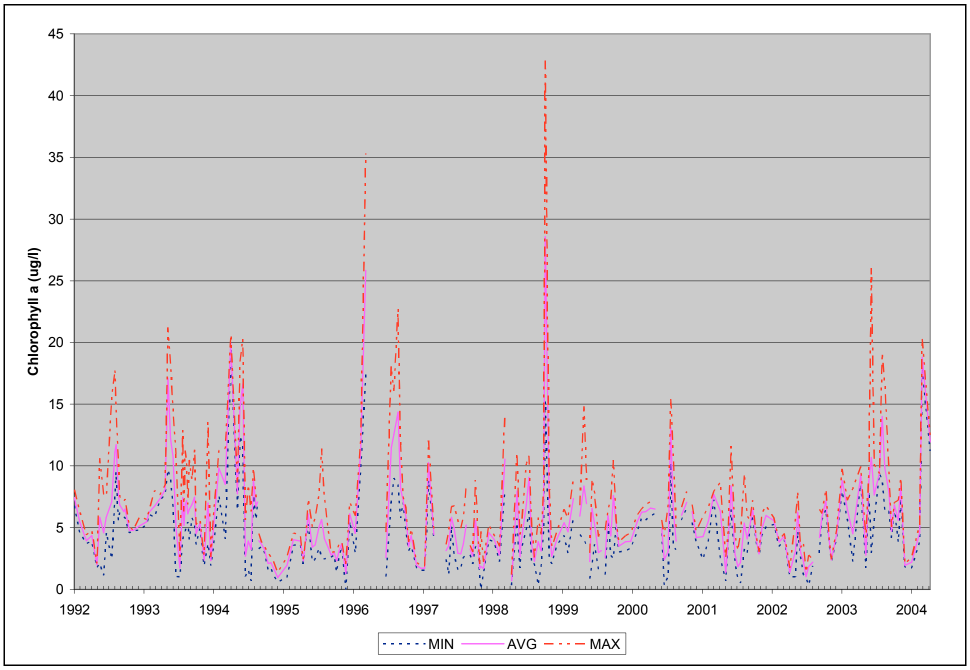

Figure C.54. Surface Chlorophyll a. Middle Sampling Locations, Loch Raven Reservoir

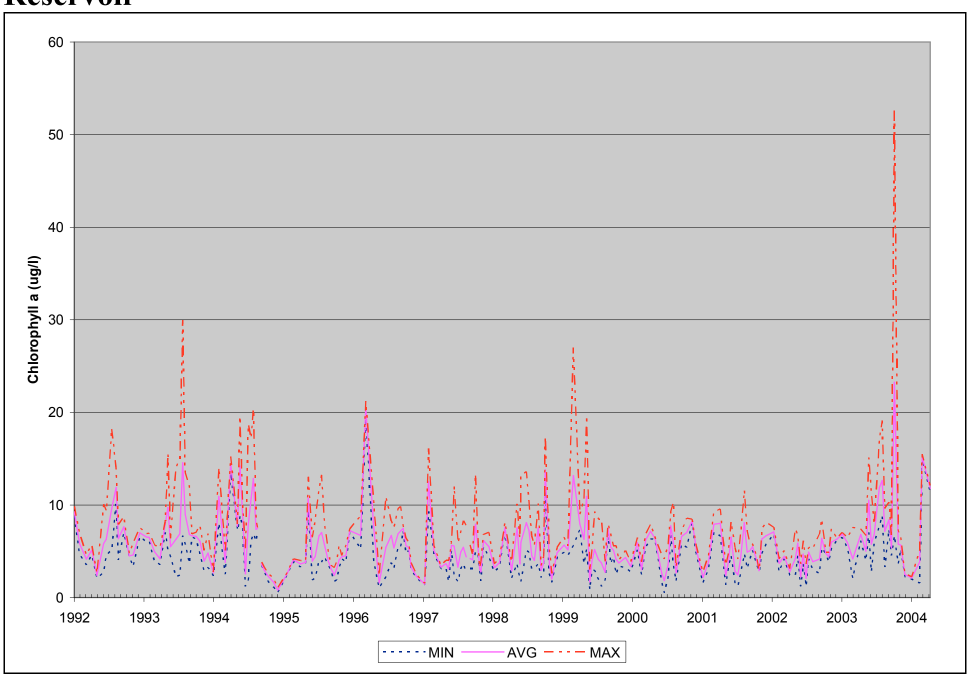

Figure C.55. Surface Chlorophyll a. Upper Sampling Locations, Loch Raven Reservoir

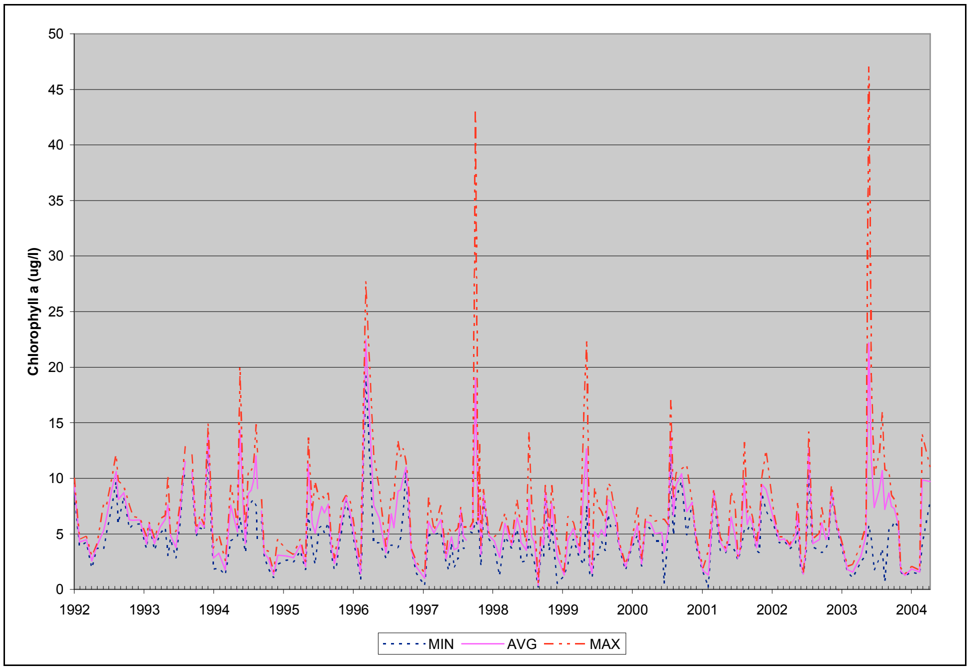

APPENDIX D

Figure D.1. Observed and Simulated Water Surface Elevations, 1992, Prettyboy Reservoir

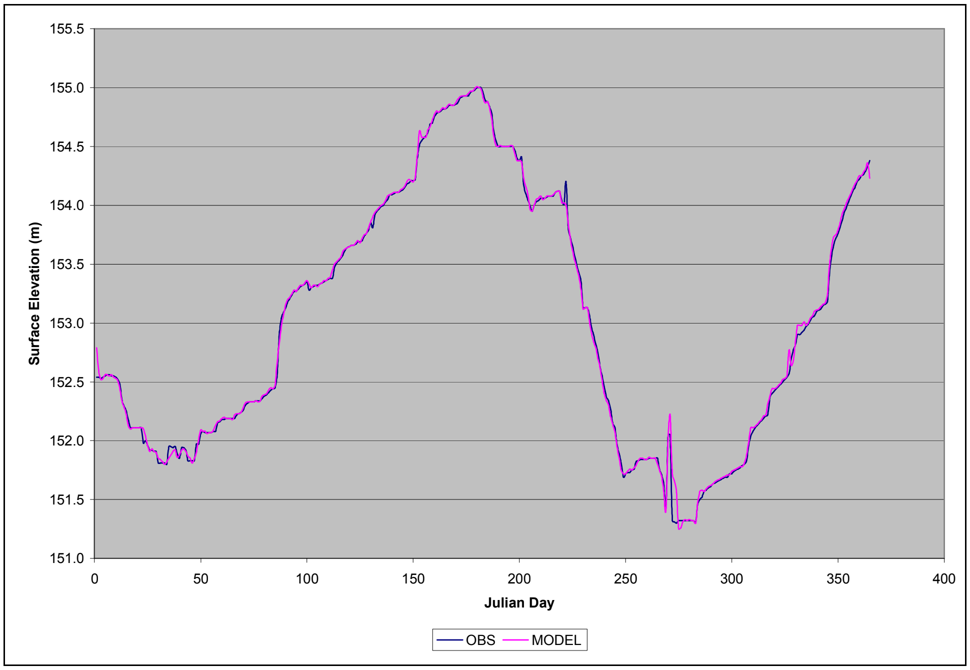

Figure D.2. Observed and Simulated Water Surface Elevations, 1993, Prettyboy Reservoir

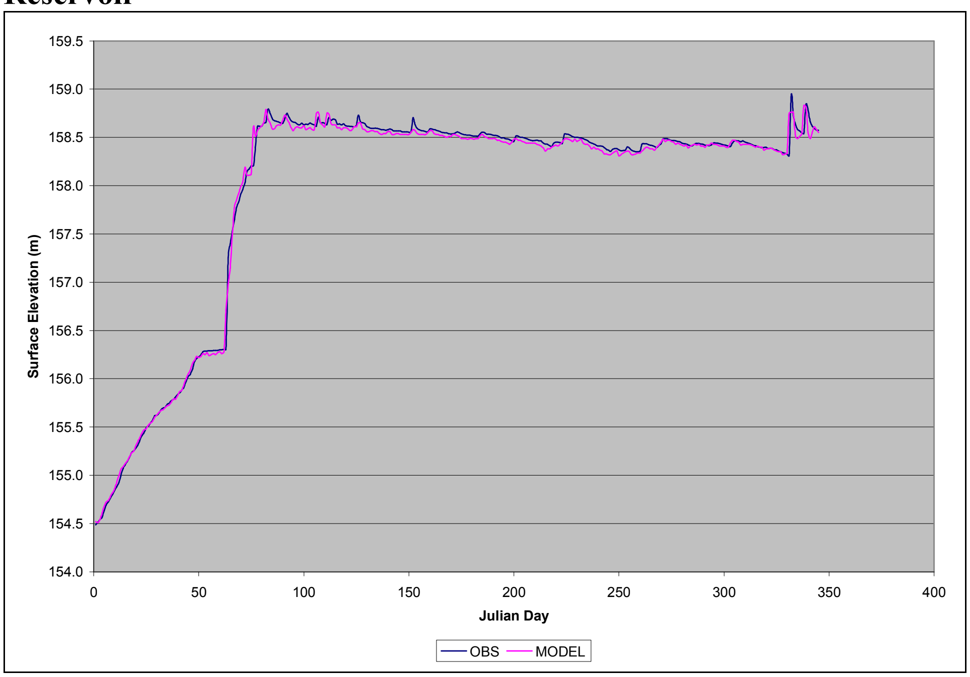

Figure D.3. Observed and Simulated Water Surface Elevations, 1994, Prettyboy Reservoir

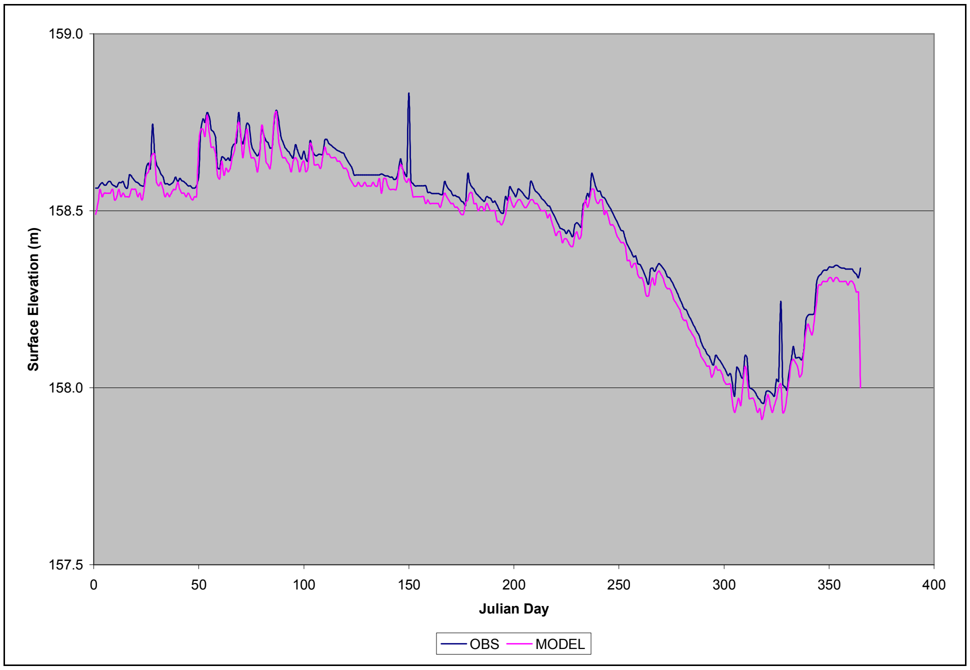

Figure D.4. Observed and Simulated Water Surface Elevations, 1995, Prettyboy Reservoir

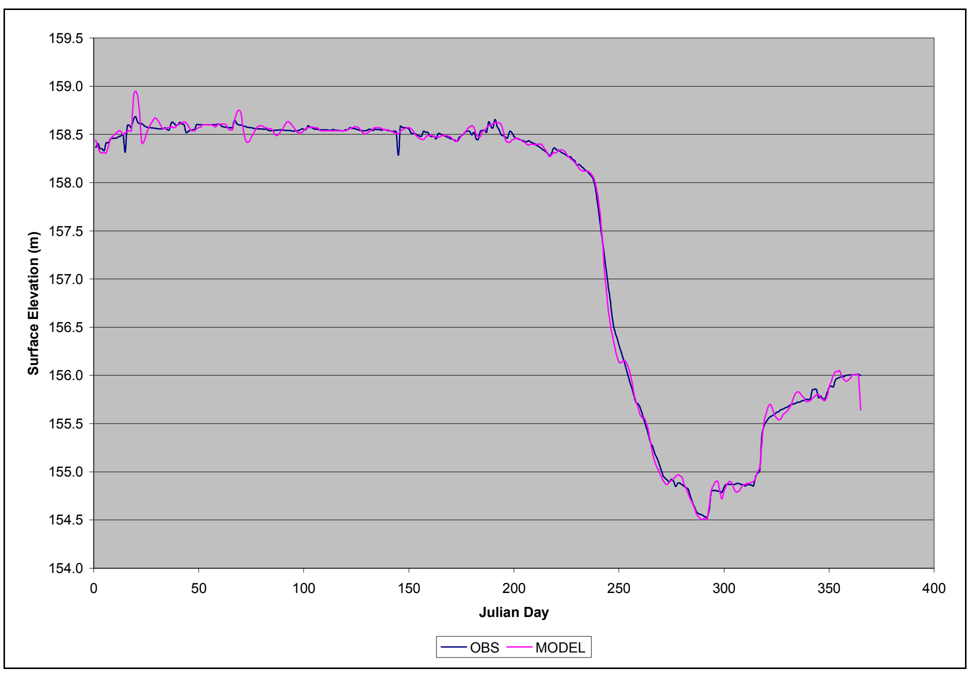

Figure D.5. Observed and Simulated Water Surface Elevations, 1996, Prettyboy Reservoir

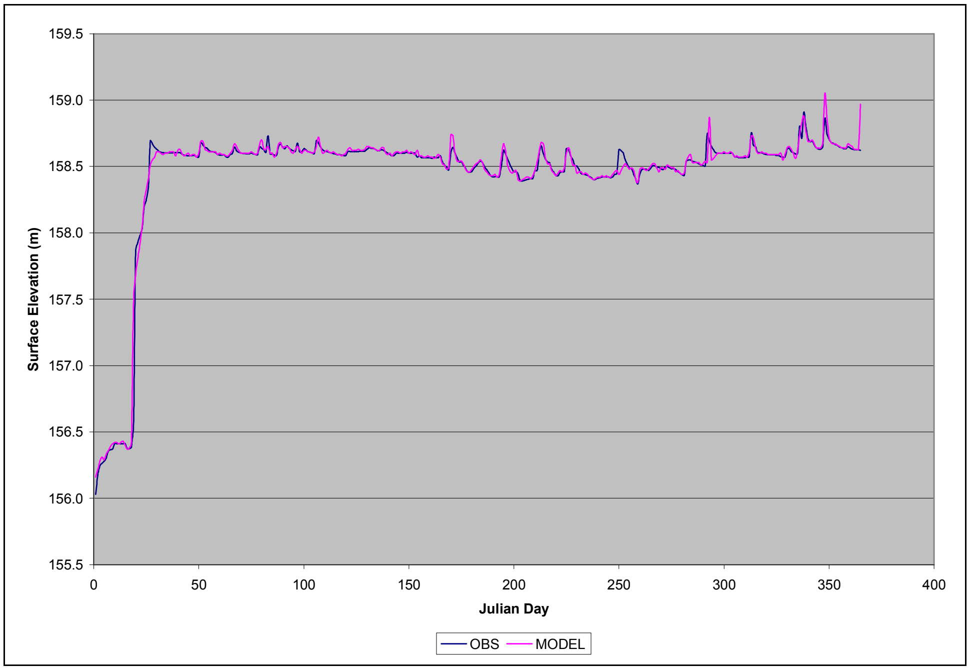

Figure D.6. Observed and Simulated Water Surface Elevations, 1997, Prettyboy Reservoir

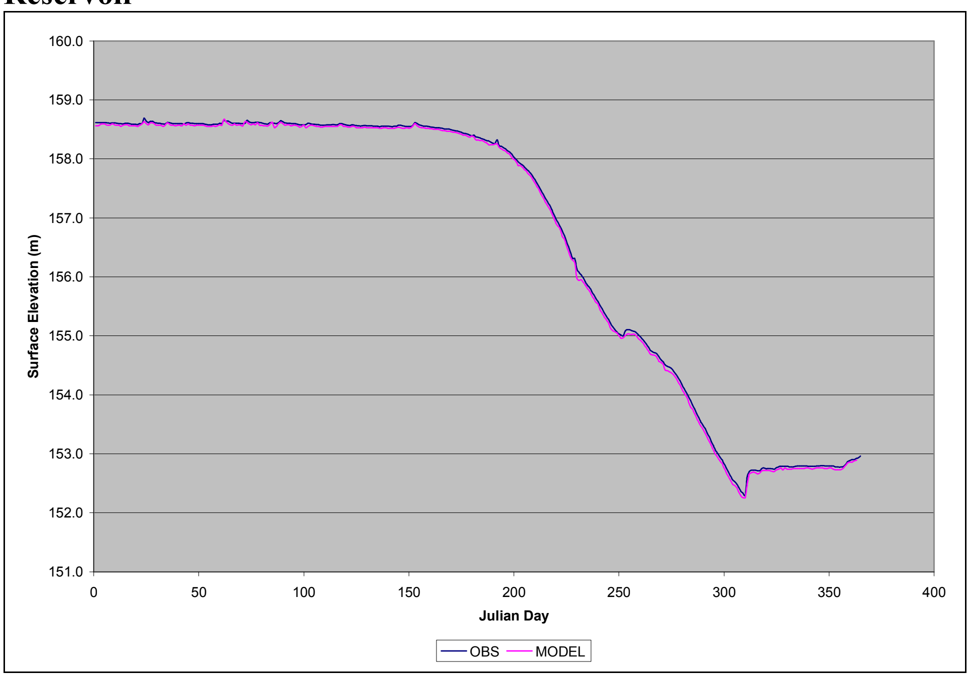

Figure D.7. Observed and Simulated Water Surface Elevations, 1992, Loch Raven Reservoir

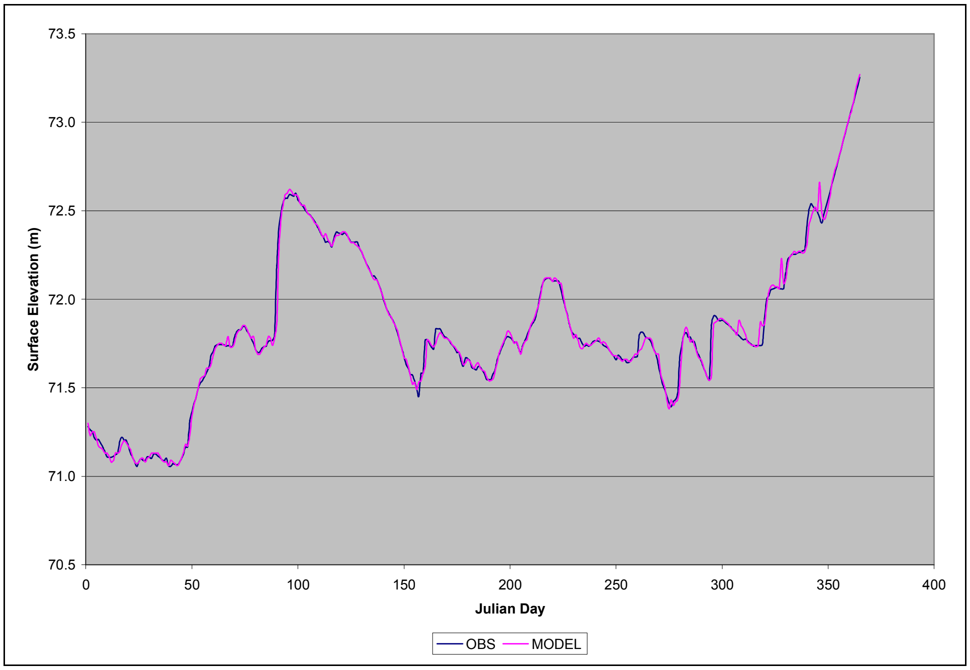

Figure D.8. Observed and Simulated Water Surface Elevations, 1993, Loch Raven Reservoir

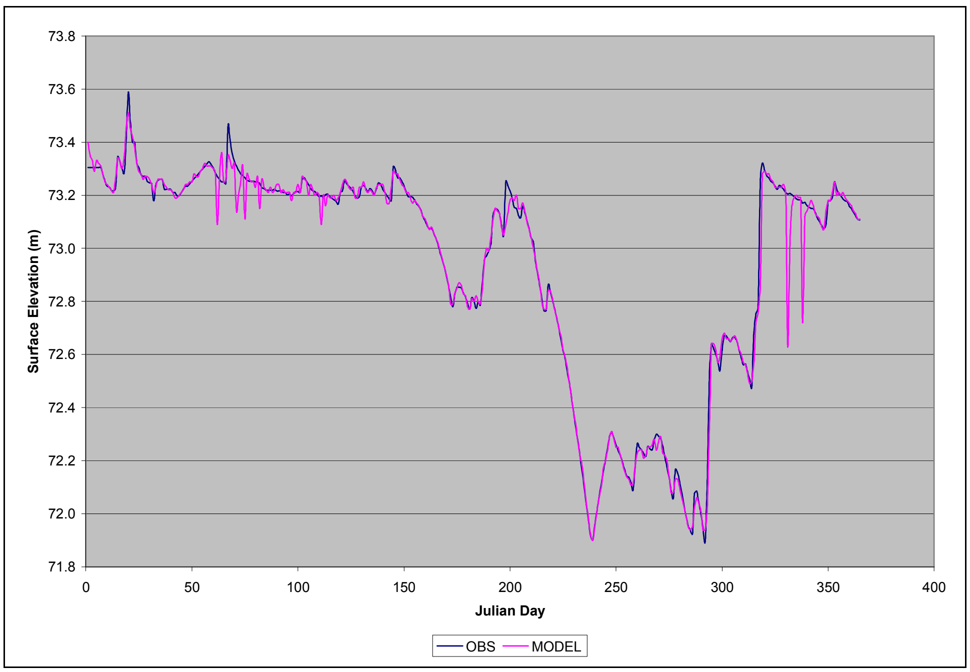

Figure D.9. Observed and Simulated Water Surface Elevations, 1994, Loch Raven Reservoir

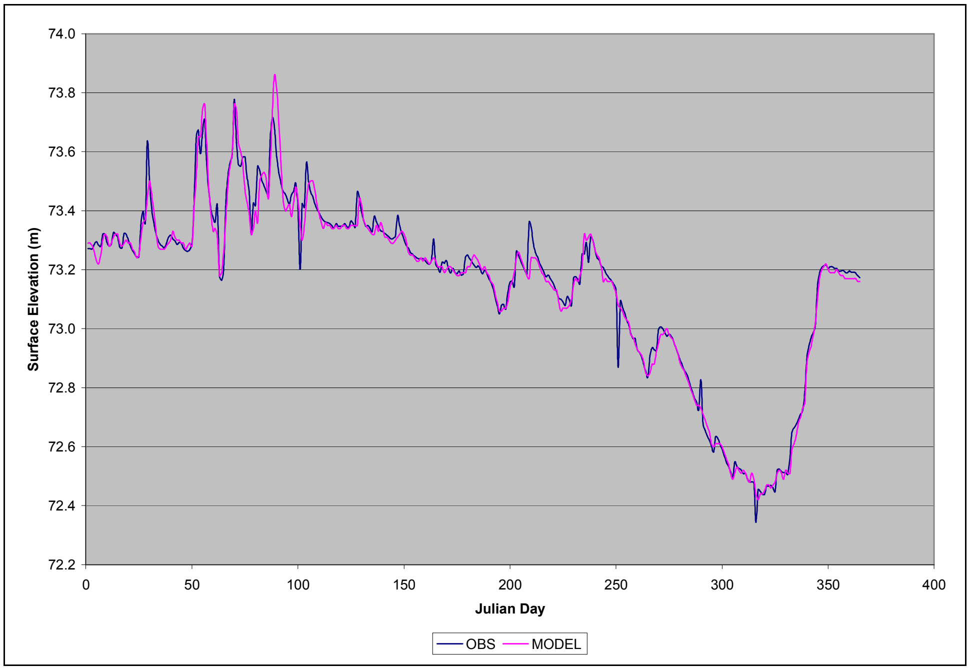

Figure D.10. Observed and Simulated Water Surface Elevations, 1995, Loch Raven Reservoir

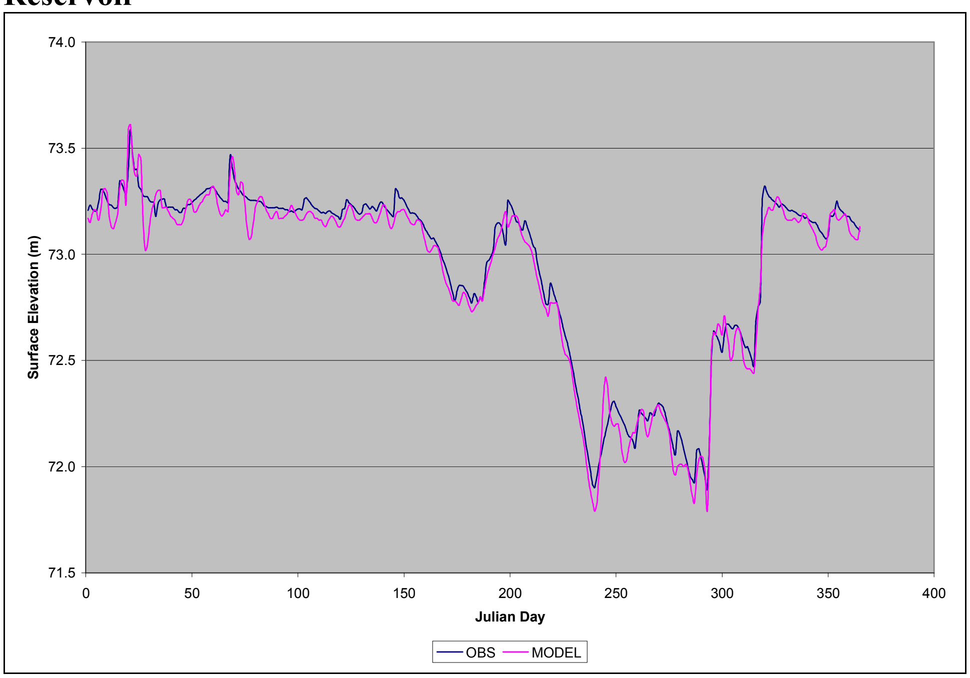

Figure D.11. Observed and Simulated Water Surface Elevations, 1996, Loch Raven Reservoir

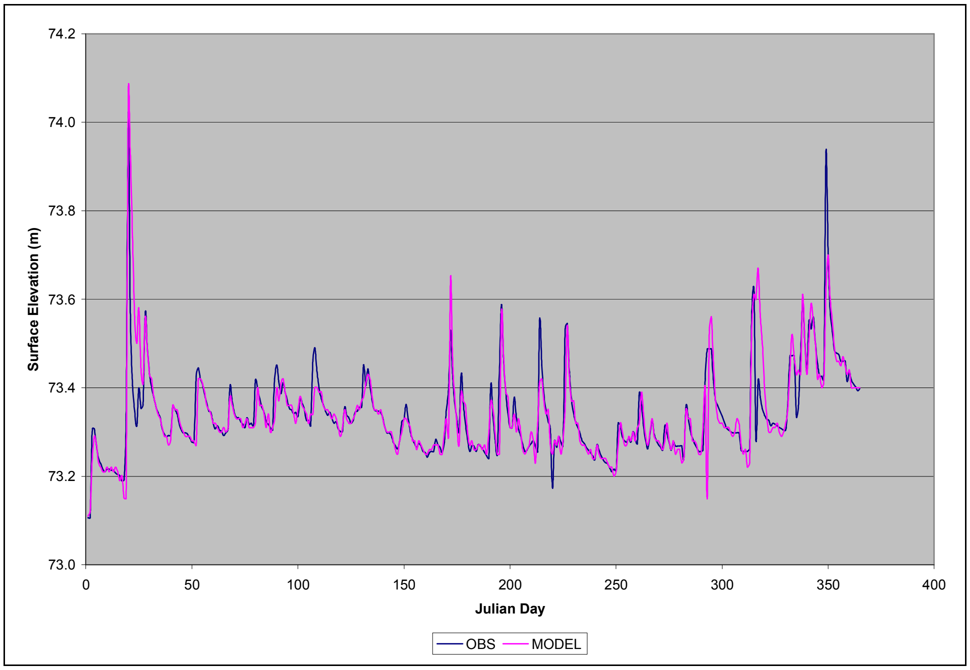

Figure D.12. Observed and Simulated Water Surface Elevations, 1997, Loch Raven Reservoir